Evaluation of the Effectiveness of a Desulphurized Tailings Cover at Detour Lake Mine

A Thesis Submitted to the College of
Graduate Studies and Research
in Partial Fulfillment of the Requirements
for the Degree of Master of Science
in the Division of Environmental Engineering
University of Saskatchewan
Saskatoon

By
Bonnie Sjoberg Dobchuk
Spring 2002

Permission to Use

In presenting this thesis in partial fulfillment of the requirements for a Postgraduate degree from the University of Saskatchewan, I agree that the Libraries of this University may make it freely available for inspection. I further agree that permission for copying of this thesis in any manner, in whole or in part, for scholarly purposes may be granted by the professor or professors who supervised my thesis work or, in their absence, by the Head of the Department or the Dean of the College in which my thesis work was done. It is understood that any copying or publication or use of this thesis or parts thereof for financial gain shall not be allowed without my written permission. It is also understood that due recognition shall be given to me and to the University of Saskatchewan, Saskatoon in any scholarly use which may be made of any material in my thesis.

Requests for permission to copy or to make other use of material in this thesis in whole or part should be addressed to:

Head, Division of Environmental Engineering
University of Saskatchewan
Saskatoon, SK, Canada
S7N 5A9

ABSTRACT

Cover technology has developed over the last decade as a remediation option to reduce acid rock drainage from mine tailings. Desulphurized tailings have been investigated as a cover material due to their potential to consume oxygen, hydraulic properties and relative abundance at mine sites. A desulphurized tailings cover was installed at the Detour Lake Mine to cover a portion of the tailings impoundment. The desulphurized tailings cover was intended to reduce oxygen penetration into the sulphidic tailings by maintaining saturation to reduce oxygen diffusion and by consuming oxygen by oxidation of the remaining sulphide minerals. A research study was initiated to evaluate the effectiveness of this cover at reducing oxygen penetration into the sulphidic tailings.

The scope of the research involved a field investigation, laboratory analysis and numerical modeling. The field investigation involved instrumenting the tailings impoundment to measure weather data, water levels and water content. Tailings samples were evaluated in the laboratory investigation for geotechnical and geochemical characteristics.

The purpose of the field and laboratory investigation was to satisfy two objectives: to yield qualitative conclusions regarding the effectiveness of the desulphurized tailings cover and to establish representative profiles for the numerical modeling.

The purpose of the numerical modeling was to evaluate the oxygen concentration through various tailings profiles to determine the relative effect of weather, vegetation

and water table depth. The program SoilCover and a finite difference program were used for this evaluation.

The general conclusion from this research was that the desulphurized tailings cover is likely not reducing oxygen penetration into the sulphidic tailings to very low levels over the entire tailings surface. The factors acting to reduce the oxygen penetration are the ability of the sulphidic tailings to remain saturated well above the water table, the consumption of a portion of the oxygen by kinetic oxidation and the potential, based on field observations, for fine tailings layers within the tailings profiles to act as oxygen barriers.

ACKNOWLEDGEMENTS

I would first like to acknowledge the support given to me by my supervisor, Dr. Ward Wilson. I feel honoured to have had his guidance and friendship over the last few years. I would also like to thank Dale Pavier for his assistance with the field and laboratory program and Keith Ferguson of Placer Dome Inc. and Michel Aubertin of École Polytechnique for their technical assistance.

The Natural Sciences and Engineering Research Council provided funding for this research along with assistance from Dr. Ward Wilson and Placer Dome Inc.

Lastly, I would like to thank my husband, Jeff Dobchuk, for his love and support.

TABLE OF CONTENTS

LIST OF FIGURES

LIST OF TABLES

q = mass flux of oxygen ($kg/m^2/s$).
D = diffusion coefficient (m^2/s).
C = oxygen concentration (kg/m^3).
x = depth (m).
n_{eq} = equivalent porosity (m^3/m^3).
n_a = air-filled porosity (m^3/m^3).
n_w = water-filled porosity (m^3/m^3).
H = Henry's Law coefficient (approximated as 0.03 for O_2 in air and water at 25°C).
D^* = bulk diffusion coefficient (m^2/s).
D_e = effective diffusion coefficient (m^2/s).
D_a = diffusion coefficient component through air phase (m^2/s).
D_w = diffusion coefficient component through water phase (m^2/s).
D^0_a = diffusion coefficient of gas through air (m^s/s).
D^0_w = diffusion coefficient of gas through water (m^2/s).
T_a = tortuosity coefficient for air phase.
T_w = tortuosity coefficient for water phase.
n = total porosity.
m = reaction order.
k_r^* = kinetic oxidation coefficient (1/time).
t = time (s).
k' = constant of reactivity (approximated as 15.8×10^{-3} m^3 O_2/m^2 pyrite/ year).
D_h = particle diameter (m).
C_p = pyrite concentration (kg/kg dry tailings).
D_{10} = grain diameter corresponding to 10% passing (m).
C_u = uniformity coefficient.
D_{60} = grain diameter corresponding to 60% passing (m).
Qm = mass flux of oxygen (kg/s).
Δt = timestep (s).
Δx = nodal spacing (cm).
k_{sat} = saturated hydraulic conductivity (m/s).
AEV = Air Entry Value (kPa).
m_v = coefficient of volume change.
G_s = specific gravity.

Chapter 1
INTRODUCTION

1.1 BACKGROUND

Acid Rock Drainage (ARD) from mining waste is one of the most important environmental issues facing the mining industry today (Aachib *et al.*, 1994, Wheeland & Feasby, 1991). Mining processes generate two types of solid waste: waste rock and tailings. Waste rock is produced during the removal of overburden. It consists of rock material sizes that vary from microscopic to meters in diameter and is typically disposed of in large piles. Tailings are the waste produced from the milling process and can vary from silt and clay-sized particles to sand-sized particles. Tailings consist of rock particles, water and the remainder of any of the reagents used in the flotation process. Tailings are typically discharged into impoundments. Effluent is produced from both waste rock and tailings due to precipitation that percolates through the materials. This effluent often has a low pH and is referred to as Acid Rock Drainage (ARD).

Acid rock drainage occurs when sulphide minerals oxidize in the presence of oxygen and water to produce sulphuric acid (Dubrovsky *et al.*, 1984, Blowes & Jambor, 1990). Sulphide minerals are common in mine wastes since they are abundant minerals in the earth's crust. The production of sulphuric acid resulting in low pH effluent is not the only concern with ARD. The low pH environment increases the solubility of many metals and therefore these effluents may develop high concentrations of dissolved heavy metals (Blowes & Jambor, 1990).

Reduction and prevention of ARD have been the subject of research over the past few decades. Prevention of ARD requires prevention of oxidation by limiting either oxygen or water availability. This can be accomplished with the use of covers. Water covers reduce the amount of oxygen that enters the surface of the tailings or waste rock. In some cases, soil covers use capillary barrier effects to create a saturated layer that reduces oxygen diffusion into the tailings or waste rock (Nicholson *et al.*, 1989, Barbour, 1990, Barbour *et al.* 1993, Yanful *et al.*, 1993a, Aachib *et al.*, 1994). There has also been investigations into the use of organic materials as a cover layer to consume oxygen (Tremblay, 1994, Elliott *et al.*, 1997, Tassé *et al.*, 1997). Disadvantages of using covers to reduce ARD are cost and availability. Water covers require a natural lake or water source. Organic covers require a source of viable organic material. Covers which use capillary barriers require soil with specific hydraulic properties. These soils are often brought onto site and placed at considerable cost to the mine operator.

The high cost of covers as a remediation technique has led to the investigation of non-reactive or low-reactive tailings as cover materials. A secondary flotation process can be used to decrease the sulphide content of reactive tailings to be used as a cover material. These tailings are often referred to as desulphurized or depyritized tailings. Laboratory testing of these types of covers has been completed but there has been limited research completed on field-scale desulphurized tailings covers.

A single layer desulphurized cover was installed at the Detour Lake Mine between 1998 and 1999. This desulphurized tailings cover was designed to maintain a degree of saturation of greater than 85% to reduce oxygen diffusion to low levels. The cover was also intended to scavenge any diffusing oxygen by sulphide oxidation of the remaining sulphide minerals. Since an installed cover of this nature has not been previously field

tested, a research study was initiated to determine how effective this desulphurized tailings cover would be at reducing oxygen diffusion into the sulphidic tailings.

1.2 RESEARCH OBJECTIVES

The objective of this research project was to determine the effectiveness of the desulphurized tailings cover at the Detour Lake Mine in reducing diffusion of oxygen into the underlying sulphidic tailings. The cover was examined to determine its effectiveness at two different processes: the reduction of oxygen diffusion by maintaining a high degree of saturation and the consumption of oxygen by kinetic oxidation of the remaining sulphide minerals in the desulphurized tailings.

The scope of this research included a field investigation, laboratory analysis and numerical modeling. The objective of the field and laboratory analyses was to characterize both the desulphurized and the sulphidic tailings for their geotechnical and geochemical characteristics. These characteristics were required to do the modeling analysis. The objective of the modeling analysis was to predict the oxygen concentration profile through the tailings and the resulting oxygen flux into the sulphidic tailings over the course of a typical season and for variable weather scenarios such as a 1 in 50 dry or wet year. Both the field/laboratory analysis and the modeling analysis were used to yield qualitative conclusions on the effectiveness of the desulphurized tailings cover at reducing oxygen diffusion into the underlying sulphidic tailings. The scope of this research did not include the measurement of *in situ* oxygen concentrations and fluxes. The scope of the modeling analysis was not to develop and verify an oxygen diffusion model for all cases but to create a model that could predict oxygen diffusion and consumption for the tailings facility at Detour Lake Mine.

1.3 ORGANIZATION OF THESIS

Chapter 2 provides a summary of previous research investigating the factors controlling sulphide mineral oxidation in tailings, oxygen movement in porous media and the effectiveness of cover systems using tailings. These three topics are relevant to the research since most tailings covers are designed to reduce oxygen movement and thereby reduce sulphide mineral oxidation.

A review of the relevant theory is presented in Chapter 3. Chapter 3 includes theory for both oxygen diffusion and kinetics. Empirical estimations of both the diffusion coefficient and first-order kinetic oxidation coefficient are introduced. Chapter 3 also includes the development of the partial differential equation describing transient oxygen diffusion and consumption. Lastly, the development and verification of a finite difference solution to this equation is described.

Chapter 4 is a summary of the field investigation carried out at the Detour Lake Mine site. Samples obtained during the field investigation were used for a laboratory analysis which is presented in Chapter 5.

The analysis and discussion of the results are presented in Chapter 6. Chapter 6 first includes an analysis of the field and laboratory results. The second part of the chapter is the results of the numerical modeling analysis.

Chapter 7 gives a summary of the major conclusions from the research and includes recommendations for future research.

Chapter 2
LITERATURE REVIEW

2.1 INTRODUCTION

Acid rock drainage (ARD) results from the oxidation of sulphide minerals present in waste rock and tailings. The purpose of this literature review is to first examine the factors affecting sulphide mineral oxidation in tailings. Next, a review of the literature on diffusion through porous media is included. Lastly, this review provides a summary of previous research on oxygen diffusion and pyrite oxidation kinetics in tailings. The literature covering the field and laboratory evaluation of covers is limited to that investigating covers using tailings as a cover material.

Cover design theory is a topic that is introduced in this research but will not be covered in this literature review. Theory on the design of covers using capillary breaks can be found in Nicholson *et al.* (1989), Barbour (1990), Yanful *et al.* (1993a) and Aachib *et al.* (1994). A comprehensive description of the theory for fluid and air flow through unsaturated soils can be found in Fredlund and Rahardjo (1993). The theory describing coupled soil and atmosphere fluxes modeled by SoilCover can be found in detail in Wilson (1990), Wilson *et al.* (1994), Wilson *et al.* (1997) as well as in the SoilCover manual (SoilCover, 1997).

2.2 SULPHIDE MINERAL OXIDATION IN TAILINGS

Sulphide mineral oxidation in tailings can result in the production of ARD. The most common sulphide mineral found in mine tailings is pyrite (FeS_2). Other sulphidic minerals such as pyrrhotite ($Fe_{1-x}S$) can also contribute to ARD but only pyrite will be examined in this literature review since it is the dominant sulphide mineral at Detour Lake Mine.

2.2.1 Factors Controlling the Rate of Sulphide Mineral Oxidation

To predict the oxidation of sulphide minerals, the factors that control the rate of sulphide mineral oxidation must be understood. There has been debate as to what is the dominant factor controlling pyrite oxidation in mine tailings. According to Nicholson *et al.* (1988), for near-neutral pH the major factors that affect the rate of pyrite oxidation are surface area of the mineral, oxygen concentration and temperature. The effects of bacterial mediated oxidation are insignificant at near-neutral pH.

Nicholson *et al.* (1988) investigated the relative effect of these different factors. The surface area of the pyrite particles was assumed to be spherical and a surface area index of $1/d$ was assumed where d represents the particle size. This assumption did not take into account a reactive surface area that differs from the measured surface area. The pyrite oxidation rate was found to be first order with respect to this surface area index.

The rate of oxidation with respect to oxygen concentration was found to be non-linear. The rate of pyrite oxidation with respect to oxygen was predicted as a reversible adsorption-desorption model combined with rate-limiting decomposition of reaction products. This differs from other predictions of the order of the reaction being either first-order or of fractional order. It was also found that for small concentrations of

oxygen, the reaction does follow a first-order relationship and for intermediate concentrations the order falls between zero and one.

The dependence of the reaction rate on temperature was also investigated. The rate of pyrite oxidation was found to vary with temperature according to the Arrhenius equation. The results of the investigation by Nicholson *et al.* (1988) found that if the adsorption/desorption and decomposition assumption is used, then it is not necessary to ascertain which of the three factors is dominant. Their predictive equation takes into account all three factors.

A later study by Nicholson *et al.* (1989) which focused specifically on pyrite oxidation in sulphidic tailings, presented research which concluded that the zone of oxidation was limited by the rate at which oxygen diffused into the tailings. The conclusion by the researchers was that for moist conditions, the concentration of oxygen was the dominant factor controlling pyrite oxidation.

In a study by Elberling *et al.* (1994a), the authors state that "it is generally agreed that the rate of acid production (in sulphidic tailings) is controlled by the availability of oxygen". A model was developed to predict diffusion of oxygen coupled with kinetic oxidation to determine whether or not a system was diffusion or kinetic controlled, especially for the first few decades of oxidation. The results of this study determined that, initially after deposition, high rates of oxidation were predominantly under kinetic control. After this period of high rates ends, the control over the oxidation rate shifts to diffusion controlled. The conclusion from this research was that a few years following deposition, the overall rate of oxidation in sulphidic tailings is diffusion controlled.

Scharer *et al.* (1995) performed an investigation comparing two different physical models defining kinetic oxidation. The two models most commonly used in oxidation of

metal sulphides are the shrinking core model and the shrinking radius model. Both of these models explain the factors controlling kinetic oxidation based on the physical process in which the mineral particles oxidize. The shrinking core model assumes that as the particle oxidizes, a layer of precipitate builds up on the surface. In order for the core of the particle to continue to oxidize, oxygen must diffuse through this layer to the reactive core. If this model is accepted, then diffusion through this precipitate layer controls oxidation. According to Scharer *et al.* (1995), the diffusion coefficient through this layer is similar to that of oxygen through water.

The shrinking radius model assumes that the particle shrinks in size as it oxidizes and therefore the rate of oxidation is under kinetic control. According to Scharer *et al* (1995), the shrinking radius model, where the reaction is under kinetic control, is applicable for fine particles oxidizing in an acidic environment. The shrinking core model has been found to correlate well to oxidation rates measured for large sulphide particles or sulphide inclusions. The final conclusion made from this research was that assuming diffusion (through the precipitate layer) control on oxidation in tailings is inappropriate. The shrinking radius model, which assumes kinetic control over oxidation, is applicable for grain sizes less than 1 mm. If kinetics are assumed to control the rate of oxidation at the particulate level, then the kinetic rate is still limited by the rate at which oxygen can travel to the particle.

2.3 OXYGEN MOVEMENT IN POROUS MEDIA

To predict the potential for acid rock drainage, a prediction of the rate of sulphide oxidation is required. As discussed in the previous section, a reasonable assumption of the factor controlling the rate of sulphide mineral oxidation is oxygen concentration. To

simplify predictions of the oxidation rate, it is useful to define the mechanisms that affect the oxygen concentration in porous materials such as tailings.

2.3.1 Processes Affecting Oxygen Movement in Porous Media

Oxygen movement in porous media can be advective due to barometric pumping, wind effects, thermal gradients or volume displacement during infiltration. Oxygen can also move by diffusion through both the air and water phases of porous media. A study by Kimball and Lemon (1971), investigated the significance of wind effects on soil gas exchange. The conclusion of the study was that for fine grained soils, diffusion is the dominant process of gas transport in soils. This research verifies the conclusions made by earlier authors who investigated soil respiration (Penman, 1940a).

Elberling *et al.* (1993) discuss the possible effects of barometric pumping and advection in the water phase on oxygen movement in mine tailings. The conclusion of the study was that for a water table 50 cm below the surface, barometric pumping would be insignificant but that for relatively deep water tables, barometric pumping may become significant. The conclusion regarding advection was that for the infiltration rates expected at the site (0.3 m/yr), oxygen movement by advection in the water phase would also be insignificant.

2.3.2 Oxygen Diffusion in Porous Media

Diffusion through porous media has been extensively studied primarily by soil physicists interested in the process of soil aeration. The major focus of these researchers was to define a method of predicting rates of diffusion through soils of varying grain-size, water content, aggregation and particle shape.

Penman (1940a & 1940b) investigated the relationship between diffusion rate and air-filled porosity. The research involved numerous laboratory experiments using soils of varying grain-size, particle shape and moisture content. It was determined that the normalized diffusion coefficient could be reasonably predicted as directly proportional to the air-filled porosity. Good results were found for all the soils using a proportionality constant of 0.66. The conclusion from the research was that the gaseous diffusion rate through porous materials was not a function of the grain-size, particle shape or aggregation but only dependent upon the air-filled porosity.

Following Penman's research, other researchers continued to investigate oxygen diffusion in porous media. The research involved experimental investigations on a variety of soils. Some investigators found data that confirmed Penman's relationship and others determined that Penman's relationship was not sufficient to take into account all the size, shape and aggregate variations. One of the assumptions of Penman's method was that the material was homogeneous and therefore any slice through the material would show the same proportion of void space. Soils such as micas which have a definite heterogeneity in different dimensions would not satisfy this criteria.

One investigator (Flegg, 1953), stated that Penman's experiments used soils of too limited a range of particle sizes. Flegg investigated the effect of aggregation on diffusion through porous media. The results of the study found that aggregate sizes over a range from smaller than 2 mm to 12.5 – 25 mm in diameter had no effect on the diffusion rate. The results confirmed Penman's relationship that showed that the diffusion rate was directly proportional to the air-filled porosity. Flegg found a proportionality constant of 0.6 which varied only slightly from Penman's value of 0.66.

Further research following Flegg and Penman investigated other relationships to define diffusion rate involving a shape factor unique for each material. Currie (1960a, 1960b & 1960c) provides a summary of this research. Currie investigated the diffusion coefficient as a function of both the internal geometry and the porosity of the soil. The research was based on the theory that a satisfactory relationship would include two shape factors. The experimental results, based on a wide variety of dry granular materials, confirmed this relationship. The effect of water content on the diffusion rate was also examined. The research determined that the relationship was considerably more complicated and would require up to five shape factors.

Continuing research moved away from purely empirical descriptions of diffusion rate towards defining a physical model of porous systems on which to base diffusion estimations. In 1971, Millington and Shearer published research that defined methods for calculating the diffusion coefficient for both aggregated and non-aggregated media. A definition of the effective pore area was developed which described the area available for gas to move "straight through" a medium. The effective pore area was described as a function of the total porosity of the medium. The relationship was developed based on solving for a minimum area of pore space and a maximum area of solid. This method was adapted to model both aggregated and non-aggregated media. The relationship for the non-aggregated media had two terms that were described as follows: the first term was defined as "the probability of continuity of air-filled pores within the pore continuum" and the second term, defined earlier as the effective pore area, was defined as "the probability of continuity of air in the whole bed".

Troeh *et al.* (1982), discussed the need for a better predictive relationship for diffusion through porous media. The physical models used to predict diffusion defined

an effective volume through the solid through which diffusion could occur. This effective path is tortuous in nature and these models used a tortuosity factor to normalize the flow paths. The model defined by Millington and Shearer (1971) was a model of this type. Troeh *et al.* determined that since it is difficult to estimate the actual tortuosity of a soil, the empirical estimations of diffusion were still required to predict diffusion through soils. It was suggested that the two empirical equations used in the literature, which included two shape factors, were insufficient for estimating diffusion coefficients. Troeh *et al.* suggested a relationship which combined these two empirical equations. They compared this relationship to published diffusion/porosity relationships and found that the modified equation fit the published data better than either of the previous empirical equations.

In 1985, Reardon and Moddle investigated gaseous diffusion through uranium tailings. The diffusion rate of carbon dioxide was measured through the tailings and it was found that the Troeh *et al.* equation fit the experimental data. It was assumed that the diffusion coefficient of carbon dioxide could be used as a reasonable estimate of the diffusion coefficient of oxygen. This assumed that the rate of oxygen consumption by sulphide oxidation was insignificant.

Collin and Rasmuson (1988) investigated predictive methods for diffusion through porous media. It was determined that the empirical equations published in the literature were insufficient for describing diffusion in materials at high water contents. The research involved investigating oxygen diffusion through covers over mine tailings that were designed to maintain high saturation. The results from their diffusion testing found that the Millington and Shearer (1971) method gave the most reasonable fit to their data. The Millington and Shearer model was adapted to include diffusion through the water

phase. This becomes important since diffusion through the water phase is the dominant method of oxygen transport in highly saturated media. Diffusion through the water phase was modeled as a parallel flow path where this flow path was made less available to the oxygen by the Henry's Law coefficient. This coefficient describes the partitioning of a gas between the gaseous and liquid phases for a given partial pressure.

The result of the Collin and Rasmuson (1988) research was an equation defining the diffusion coefficient of a gas in non-aggregated media as a function of the saturation, the total porosity, the diffusion coefficient of the gas through water, the diffusion coefficient of the gas through air, Henry's Law coefficient and two parameters unique to each material. The two parameters were defined as functions of saturation and total porosity. A similar equation was also defined for diffusion through aggregated media.

Collin and Rasumson (1988) compared the model for non-aggregated media to published data and found that it fit the data better than previous models. The model tended to overestimate the diffusion coefficient at low water contents and underestimate the diffusion coefficient at high water contents. The best agreement between estimated and experimental values occurred for sandy materials.

2.4 PREVIOUS RESEARCH INVESTIGATING THE EFFECTIVENESS OF TAILINGS COVER SYSTEMS

The use of covers as a method of remediation for reducing sulphide oxidation in mine wastes has been investigated for the last few decades. Engineered covers, which include capillary barrier effects, have become a popular design choice due to their ability, when constructed properly, to reduce the penetration of oxygen or water. The limitation of

these covers is their high cost. Research in the last decade has investigated the potential for single-layer covers or covers made with materials that cost less to obtain and construct. The difficulty faced by these researchers is how to evaluate the potential effectiveness of these covers. Laboratory experiments, pilot-scale field testing, full-scale field testing and modeling are tools used by researchers to determine cover effectiveness.

The following sections of this literature review summarize previous research evaluating covers using low-sulphur tailings as a constitutive material. The first section gives background to some of the evaluation methods used in the research. The last two sections divide the research into field and laboratory evaluations and modeling of oxygen diffusion and consumption.

2.4.1 Evaluation of Tailings Covers

A major limitation for determining a cover's effectiveness at reducing sulphide oxidation is a way of measuring oxidation rates in both field and laboratory scale experiments. An indirect method commonly used is to measure the sulphate in the leachate. Since factors such as carbonate buffering can affect the sulphate content, this method is not always satisfactory for measuring oxidation rates.

Elberling *et al.* (1994b), published research which evaluated three methods of evaluating oxidation rates in tailings: the sulphate-release method, the oxygen-gradient method, and the oxygen-consumption method. Since the sulphate-release method is inaccurate for field testing, only the last two methods were compared for field results. The oxygen-gradient method uses Fick's First Law to estimate the flux of oxygen across the surface and is related to sulphide oxidation by conservation of mass. The oxygen-

consumption method measures the decrease in oxygen concentration in the headspace of a chamber placed on the tailings surface. The results of the comparison of the methods found that the oxygen-consumption method was superior to the other two. The oxygen-consumption method could be used on tailings of any saturation, was non-destructive and could be easily used for repeated sampling over a tailings pond surface. This method has since been used by many researchers evaluating oxidation rates in tailings.

2.4.2 Field and Laboratory Investigations of Low-Sulphur Tailings Cover Systems

One of the earliest investigations of a cover system using low-sulphur tailings is described in the research published by Reardon and Moddle (1985). The purpose of this research was to design a cover system for sulphidic uranium tailings using layers of peat and desulphurized tailings. The goal for the cover system was to use peat as an oxygen consuming layer that would prevent oxygen from reaching the underlying tailings for 1000 years. The desulphurized tailings were designed to be a surface layer that would maintain a high level of saturation and allow only small amounts of oxygen to reach the peat layer below.

The methodology for the cover design was to determine the thickness of each layer required to meet the objective of preventing oxidation for 1000 years. From published data, the thickness of the peat layer that would contain sufficient carbon to consume a given oxygen flux was determined. The carbon consuming relationship, along with Fick's Law, was used to develop an equation defining the diffusion coefficient required in the desulphurized tailings to reduce the oxygen flux to an amount that could be consumed by the peat layer over 1000 years. Using this relationship, the diffusion

coefficients were determined that would correspond to different combinations of cover thicknesses.

Reardon and Moddle (1985) measured the diffusion coefficient of the desulphurized tailings at different water contents. The diffusion coefficient of the tailings was found to be too high and did not satisfy the criteria for 1000 years of prevention, regardless of the thickness of the layer. It was determined that the desulphurized tailings layer would require compaction during construction to sufficiently reduce the total porosity and therefore the diffusion coefficient. The conclusion of the study was that with sufficient compaction, the desulphurized tailings would reduce the diffusion of oxygen, even under relatively high suction conditions, enough to allow the peat to consume all the oxygen for 1000 years.

Aachib *et al.* (1994), published a study where low-sulphur tailings were investigated for use as a capillary barrier material in a multi-layer cover system. The study involved geochemical and geophysical characterization of the tailings as well as modeling of cover systems to determine the effectiveness of a tailings layer as a capillary barrier. Two cover scenarios were investigated: a single-layer cover of low-sulphur tailings and a multi-layer cover where low-sulphur tailings were sandwiched between layers of sand. The comparison of these two cover designs, using a simple analytical model of oxygen diffusion, found that the two cover scenarios both reduced oxygen flux rates. The conclusion from this study was that low-sulphur tailings held promise as a constitutive material in a cover system based on its relatively low hydraulic conductivity and high air-entry value.

To validate the conclusions from Aachib *et al.* (1994), the same group of researchers performed a comprehensive series of column experiments (Bussière *et al.*, 1997a,

Bussière *et al.*, 1997b and Benzaazoua and Bussière, 1998). The column experiments were designed to evaluate three different desulphurized tailings in a multi-layer capillary barrier system compared to a control column containing only sulphidic tailings. The three different types of desulphurized tailings each contained a different percentage of sulphide mineral. The purpose of the experiments was to evaluate the effectiveness of multi-layered covers made with desulphurized tailings and to determine the effect of different levels of desulphurization on that effectiveness.

The desulphurized and sulphidic tailings used in the experiments were processed in the laboratory using ore taken from a gold mine. The ore was crushed and ground to have a similar grain-size distribution as the tailings from the gold mine. To create the desulphurized tailings in the laboratory, the sulphide was removed using a standard flotation process. The desulphurization process created tailings with pyrite contents of 0.22%, 0.65% and 1.17%. The desulphurized tailings were finer than the sulphidic tailings with 80% by weight passing the 200 mesh for the desulphurized and 50% passing the 200 mesh for the sulphidic. The soil-water characteristic curves for the two types of tailings showed the desulphurized tailings to have an air-entry value of 27 kPa and 8 kPa for the sulphidic tailings.

Each of the four columns tested contained 0.3 m of sulphidic tailings. The water table was maintained 2.3 m below the surface of the sulphidic tailings by controlling the negative water pressure. The covers consisted of 0.6 m of desulphurized tailings sandwiched between a 0.3 m sand layer above and a 0.4 m sand layer below. The effectiveness of the covers was determined by measuring the oxygen flux rate through the surface of the tailings. The oxygen flux was measured using the sulphate-release method and the oxygen-consumption method. To isolate the amount of sulphide

oxidation contributing to the oxygen flux within the cover material, a theoretical oxygen flux rate through a non-reactive cover material was estimated. This estimation was based on SEEP/W modeling to determine the moisture profile. The diffusion coefficients were calculated for the profile based on an equation developed by Elberling *et al.* (1994b). Using this estimated flux rate, the amount of oxidation occurring in the cover material was estimated.

The results of the oxidation rate measurements found that the cover made with the tailings with the lowest percentage of pyrite reduced the oxidation by a factor of 20 compared to the control column. The covers made with desulphurized tailings with pyrite contents of 0.65% and 1.17% reduced the oxidation by factors of 5 and 4, respectively. The oxidation of the pyrite in the desulphurized tailings was found to be a significant factor affecting the performance of the covers.

A geochemical evaluation (Benzaazoua and Bussière, 1998) of the column tests found that the pH of the covered columns remained near-neutral whereas the uncovered column developed a pH of 3. The cumulative concentrations of zinc, iron and sulphates from the covered columns were lower than those in the uncovered column. The conclusion of the geochemical evaluation was that the metals and sulphate concentrations from the tailings were significantly reduced by the desulphurized tailings covers.

The overall conclusion of the column research was that to successfully use desulphurized tailings as a moisture retaining layer in a cover system there would need to be sufficient neutralization potential in the desulphurized tailings to neutralize the acid produced by the remaining sulphide minerals (Bussière, *et al.*, 1997a).

In 1997, Elliot *et al.* published the results of a research program where a pilot-scale laboratory test had been performed to evaluate the effectiveness of three organic materials and desulphurized tailings as potential cover materials. The pilot-scale model was designed to mimic a section taken out of a tailings pond. The model enabled weather control by controlling precipitation and setting temperature and evaporation rates to those measured in the field. Water drainage was controlled by allowing free drainage out the bottom and out one side of the model. This water was collected and measured to determine the water balance of the system. The pilot-scale model was instrumented in a vertical profile to measure water content, temperature, gas concentration, *Eh* and obtain pore fluid samples. The model constructed to evaluate desulphurized tailings consisted of 0.8 m of desulphurized tailings over 0.7 m of sulphidic tailings.

The results of one year of monitoring showed that the desulphurized tailings maintained a degree of saturation of approximately 90% throughout the year. The geochemical monitoring found that the pore water pH stayed the same as the control cell. Sulphate and iron concentrations from the desulphurized tailings model increased compared to the control column. The oxygen concentrations remained relatively high throughout the profile of the model and remained similar to those of the control column even though the saturation was 90%. Observations of the desulphurized tailings model found cracks forming on the surface. The conclusion from this research was that even though the system retained high saturation, the cracks were providing a direct pathway for oxygen. The study concluded that desulphurized tailings had potential as a cover material but a method for minimizing cracks was required.

A research project at the INCO Ltd. Copper Cliff Tailings Area (Hanton-Fong *et al.*, 1997) investigated the potential for desulphurizing all the tailings produced by the mine to separate the waste into two streams: low-sulphur tailings and a sulphide concentrate. The investigation involved the construction of three 10 m by 15 m lysimeters filled with desulphurized tailings (0.35% S), main tailings (0.98% S) and total tailings (2.3% S). Over three years, the lysimeters were measured for pore gas concentration, pore water composition and water content profiles. Cores taken from the lysimeters revealed segregation of the tailings due to the method of discharge. Acid-base accounting tests carried out for the three types of tailings gave a mean Net Neutralization Potential (NNP) for the desulphurized tailings as 3.6 (kg $CaCO_3$ eq/t), the main tailings as –17.8 and the total tailings as –46.8. These results indicated that only the desulphurized tailings contained sufficient carbonate minerals to buffer the acid that could be produced.

The results of the three year investigation found that the desulphurized tailings retained a pore water pH close to neutral whereas the other two types of tailings produced acidic pH. The concentration of dissolved constituents in the desulphurized tailings did not increase whereas the concentrations in the other two increased significantly. The conclusion of the study was that desulphurized tailings were relatively inert to oxidation and had potential as an alternative mining waste or for use in rock dams or tailings covers.

An Australian research project for a minesite in Tasmania (Ellerbroek *et al.*, 1997), investigated low-sulphur tailings as a potential cover material to create a saturated substrate on which to grow a wetland. The wetland was designed to act as a treatment facility for the discharge from a sulphide rich (10 – 30% S) tailings facility. This

research project evaluated the hydrology of the tailings dam system to determine whether or not the cover would remain sufficiently saturated to support a wetland ecosystem. The results of the geophysical testing of the tailings revealed that the desulphurized tailings were not significantly different from the sulphidic tailings and would not provide a capillary break. It was determined however, due to the humidity of the site and the soil-water characteristics of the tailings, the cover would likely remain saturated. The results of this preliminary investigation revealed that the desulphurized tailings would likely retain sufficient saturation to maintain a wetland.

An extensive laboratory and field investigation of a multi-layered cover using low-sulphur tailings was performed by Ricard *et al.* (1997) at Les Terrains Aurifères site in Quebec. The cover that was designed and installed at the site consisted of 0.8 m of low-sulphur tailings sandwiched between 0.3 m of sand and gravel above and 0.5 m of sand below. The cover was designed to create a capillary barrier such that the low-sulphur tailings remain saturated. This paper discusses the difficulties encountered during construction of the cover. The cover was instrumented to measure water content profiles and measure oxygen consumption at different depths.

The results of six months of measurements from the cover showed that the low-sulphur layer had an average saturation of 86%. The results of oxygen flux measurements at different locations over the tailings surface showed that the cover had reduced the oxygen flux by an average factor of 75 but up to a factor of 1000 through certain areas of the tailings.

2.4.3 Modeling of Oxygen Diffusion and Consumption through Tailings

There are few published attempts to model oxygen diffusion and consumption through tailings in the literature. The difficulties faced by modelers stem not only from the heterogeneity of tailings properties but from the effect of climate on the water content of tailings. Assuming that diffusion of oxygen is the process controlling the rate of sulphide mineral oxidation, it can be extrapolated that the factors controlling the diffusion of oxygen in turn control the rate of oxidation. One of the factors controlling the rate of diffusion is the water content of the material. Fluctuations in water content due to heavy precipitation events or long drying periods greatly affect the water content profile which affects diffusion and therefore controls the rate of oxidation. Most models assume a constant water content profile with time.

A model investigated by Blowes and Jambor (1990) used an approximate analytical solution to predict both diffusion of oxygen through a porous material as well as diffusion of oxygen through a precipitate layer (shrinking-core model) to determine the oxygen concentration profile through tailings. The assumptions made in the modeling were that the diffusion coefficient and porosity were constant with depth and with time. The results of the modeling compared to measured oxygen concentrations approximated the depth of penetration but was otherwise a fairly poor fit to the data likely due to the assumption of constant diffusion coefficients and porosity with depth.

In a research program comparing the efficiency of different cover scenarios, Aachib *et al.* (1994) used a simple analytical solution to solve transient oxygen diffusion in a non-reactive cover. The boundary conditions for this solution were constant oxygen concentrations at the top and bottom of the profile. The modified Millington and

Shearer method was used to calculate the diffusion coefficient. This solution assumed constant saturation, porosity and diffusion coefficient with depth and time. The results of the modeling were used to compare different cover scenarios and were not calibrated to measured data.

Elberling *et al.* (1994a) developed a model to predict oxygen diffusion and consumption in reactive tailings. The major assumption of this model was that at every time-step, the oxygen concentration profile had reached steady-state. The model used the shrinking-radius model which assumes that as the particle oxidizes, it shrinks and therefore the surface area available for oxidation decreases with time. At every time-step, a new particle size was calculated which resulted in a change of the oxidation rate over the following time-step. The model assumed a simple first-order reaction rate, that oxygen diffusion occurred only in the gaseous phase and a constant diffusion coefficient with depth and time. The driving force for oxygen diffusion in this model was not due to fluctuations in water contents but simply due to oxygen consumption by the sulphide minerals. An analytical solution for oxygen diffusion and consumption with fixed concentrations at the two boundaries was adopted.

2.5 SUMMARY

The purpose of the desulphurized tailings cover at Detour Lake Mine is to reduce acid rock drainage by reducing sulphide mineral oxidation. To evaluate the effectiveness of this cover, it is critical to understand the processes controlling sulphide mineral oxidation. A review of the literature concluded that a reasonable assumption of the factor controlling the rate of sulphide mineral oxidation is oxygen concentration. The

conclusion of many researchers is that oxygen diffusion, as opposed to advective processes, controls the concentration of oxygen in porous media.

Oxygen diffusion through porous media has been extensively researched throughout this last century. The objective of the research was to develop a method for predicting oxygen diffusion rates based on easily measured properties such as porosity and degree of saturation. Two types of relationships were examined, empirical relationships and those based on a physical model. Both types of relationships are still used in current research. There is yet to be a universally agreed upon method for calculating diffusion coefficients.

A review of previous research investigating low-sulphur or desulphurized tailings covers revealed that there has been limited field investigation on these types of cover systems. There have been a number of laboratory investigations involving column tests or pilot-scale models that have illustrated the potential of low-sulphur tailings as a cover material. Large lysimeters have been constructed to investigate different cover strategies but only one publication was found that described a field study on an installed low-sulphur cover system. Additional field investigations of low-sulphur covers are required to further the potential of this technology. The research presented in this thesis attempts to further the knowledge on using low-sulphur tailings in cover systems by performing a field and laboratory investigation on an installed desulphurized tailings system.

Modeling of oxygen diffusion and consumption through covers is a method used to evaluate the potential effectiveness of a cover through different weather scenarios or over the long term. A review of the literature determined that previous models did not account for variations in diffusion coefficients and reaction rates based on the

fluctuating water contents in a porous system due to weather fluctuations. Most models assumed constant tailings characteristics with time. An important tool in evaluating tailings covers would be to model oxygen diffusion and consumption coupled with atmospheric processes. The research presented in this thesis attempts to improve the information obtained from numerical modeling by evaluating oxygen diffusion and consumption as they are affected by atmospheric processes.

Chapter 3
THEORY

3.1 INTRODUCTION

The purpose of this chapter is to summarize the important theoretical relationships used to quantify oxygen diffusion through tailings and the subsequent oxygen consumption by sulphide mineral oxidation. Theory describing oxygen diffusion, the prediction of diffusion coefficients, the stoichiometry of sulphide mineral oxidation and the kinetics of sulphide mineral oxidation is developed in the following discussion. The last section describes the development and verification of a finite difference solution to solve transient oxygen diffusion and consumption.

3.2 OXYGEN DIFFUSION

Oxygen diffusion can be described by Fick's First Law. The following two sections define Fick's First Law and a method of predicting the diffusion coefficient in this Law.

3.2.1 Diffusion Theory

Fick's First Law defines the oxygen mass flux in a given direction as directly proportional to the negative of the concentration gradient in that direction (Crank, 1975). The constant of proportionality is defined as the diffusion coefficient. Fick's First Law is given in Equation 3.1:

$$q = -D\frac{\partial C}{\partial x} \tag{3.1}$$

where: q = mass flux of oxygen ($kg/m^2/s$),
D = diffusion coefficient (m^2/s),
C = oxygen concentration (kg/m^3), and
x = depth (m).

Equation 3.1 defines oxygen diffusion through a single phase. Fick's First Law can be modified to define oxygen diffusion through a porous media by making the assumption that only a portion of the material is available for diffusion. This portion of the material through which diffusion can occur is called an effective porosity. The air-filled portion of a porous material is an obvious candidate but only the interconnected pores would be available for diffusion. Pores completely isolated would not be available. Although oxygen does not diffuse as rapidly through water as it does through air, the water-filled pores should not be completely ignored as a potential pathway for oxygen diffusion. Since it is difficult to quantify the amount of isolated pores and diffusion through water is considered insignificant, most theoretical predictions of oxygen diffusion through porous media use the air-filled porosity as the effective porosity.

Aubertin *et al.* (2000) describes the use of an equivalent porosity to represent the effective porosity available for diffusion. This porosity represents the air-filled porosity plus a portion of the water-filled porosity. This relationship transforms the water-filled porosity into an equivalent air-filled porosity by portioning it with Henry's Law coefficient as shown in Equation 3.2:

$$n_{eq} = n_a + Hn_w \tag{3.2}$$

where: n_{eq} = equivalent porosity (m^3/m^3),
n_a = air-filled porosity (m^3/m^3),
n_w = water-filled porosity (m^3/m^3), and
H = Henry's Law coefficient (approximated as 0.03 for O_2 in air and water at 25 °C).

Fick's First Law defining oxygen diffusion through a porous media as a function of the equivalent porosity is defined in Equation 3.3:

$$q = -n_{eq} D^* \frac{\partial C}{\partial x} \tag{3.3}$$

where: q = mass flux of oxygen ($kg/m^2/s$),
n_{eq} = equivalent porosity (m^3/m^3),
D^* = bulk diffusion coefficient (m^2/s),
C = oxygen concentration in the gas phase (kg/m^3), and
x = depth (m).

The equivalent porosity and the bulk diffusion coefficient (D^*) are often combined into a variable D_e, the effective diffusion coefficient, as defined in Equation 3.4.

$$D_e = n_{eq} D^* \tag{3.4}$$

3.2.2 Diffusion Coefficient: Prediction

The diffusion coefficients for gases through homogeneous materials such as air and water are fairly well understood. As described in Chapter 2, the diffusion coefficient of a gas through a porous material is difficult to quantify. The relationship used in this research is that defined by Collin and Rasmuson (1988) as the modified Millington and Shearer method for prediction of the diffusion coefficient through non-aggregated porous media. The development of this relationship will follow that of Aubertin *et al.* (2000) and Mbonimpa *et al.* (2001).

The effective diffusion coefficient is defined in Equation 3.5 as a function of D_a and D_w which are the components of the diffusion coefficient in the air and water phase, respectively. These are defined by Equations 3.6 and 3.7.

$$D_e = D_a + HD_w \tag{3.5}$$

where: D_e = effective diffusion coefficient (m^2/s),
D_a = diffusion coefficient component through air phase (m^2/s), and

D_w= diffusion coefficient component through water phase (m^2/s).

$$D_a = n_a D_a^0 T_a \tag{3.6}$$

$$D_w = n_w D_w^0 T_w \tag{3.7}$$

where: D^0_a= diffusion coefficient of gas through air (m^s/s),
D^0_w= diffusion coefficient of gas through water (m^2/s),
T_a = tortuosity coefficient for air phase, and
T_w = tortuosity coefficient for water phase.

The tortuosity coefficients are related to the properties of the material through Equations 3.8 and 3.9. The variables *x* and *y* are obtained by solving Equations 3.10 and 3.11.

$$T_a = \frac{n_a^{2x+1}}{n^2} \tag{3.8}$$

$$T_w = \frac{n_w^{2y+1}}{n^2} \tag{3.9}$$

$$n_a^{2x} + (1 - n_a)^x = 1 \tag{3.10}$$

$$n_w^{2y} + (1 - n_w)^y = 1 \tag{3.11}$$

where: n = total porosity.

According to Aachib and Aubertin (2000 – unpublished report mentioned in Mbonimpa *et al.*, 2001), a reasonable estimation of the value of the variables *x* and *y* is 0.75. This was obtained from the analysis of tortuosity in fully dry and saturated media. The comparison between this estimation of the diffusion coefficient and that using Equations 3.10 and 3.11 is illustrated in Figure 3.1. Using this value for *x* and *y* and combining Equations 3.6 – 3.8, the diffusion coefficient equation can be simplified to Equation 3.12.

$$D_e = \frac{1}{n^2}\left[D_a^0 n_a^{3.5} + H D_w^0 n_w^{3.5}\right] \tag{3.12}$$

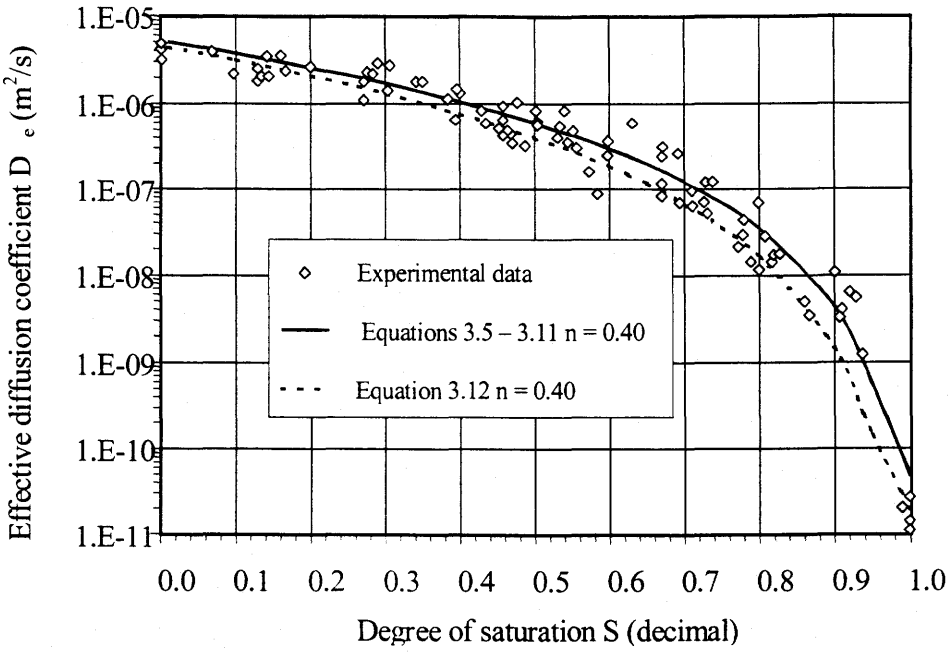

Figure 3.1 Comparison of diffusion coefficient estimations with measured data taken from Mbonimpa *et al.* (2001).

3.3 SULPHIDE MINERAL OXIDATION

Sulphide mineral oxidation is the critical process causing acid rock drainage. The following two sections describe the stoichiometric relationships of pyrite oxidation and a theoretical prediction of the kinetics of pyrite oxidation.

3.3.1 Stoichiometry of Pyrite Oxidation

Pyrite oxidation is initially a slow process that typically begins at near-neutral pH. This process is described in Equation 3.13, which shows pyrite being oxidized by oxygen and water and producing hydrogen ions which result in acidic pH (Moses and Herman, 1991).

$$FeS_2 + \tfrac{7}{2} O_{2(aq)} + H_2O \rightarrow Fe^{2+} + 2SO_4^{2-} + 2H^+ \qquad (3.13)$$

If the oxidation proceeds without buffering of the acid, the pH drops and the ferrous ion stays in solution. The ferrous ion is then oxidized to the ferric ion as illustrated in Equation 3.14 (Moses and Herman, 1991).

$$Fe^{2+} + \tfrac{1}{4} O_{2(aq)} + H^{+} \rightarrow Fe^{3+} + \tfrac{1}{2} H_2O \qquad (3.14)$$

If the acidity of the solution continues to increase such that the pH drops below 4, the environment becomes suitable for the growth of the *Thiobacillus* bacteria. This bacteria catalyzes pyrite oxidation and the rate of oxidation then increases by several orders of magnitude (Nicholson *et al.*, 1988).

For solutions with sufficient carbonate to buffer all of the acid and maintain near-neutral pH, the overall oxidation reaction can be defined by equation 3.15 (Nicholson *et al.*, 1988).

$$FeS_{2(s)} + \tfrac{15}{4} O_2 + \tfrac{7}{2} H_2O + 4CO_3^{2-} \rightarrow Fe(OH)_{3(s)} + 2SO_4^{2-} + 4HCO_3^{-} \qquad (3.15)$$

The tailings within the Detour Lake tailings facility have a relatively high buffering capacity and the pH remains near-neutral (The tailings properties are described in detail in Chapter 5). According to Nicholson *et al.* (1988), with a pH maintained near-neutral, the effects of ferric ion oxidation and bacterial oxidation are insignificant and the major factors that affect the rate of pyrite oxidation are surface area, oxygen concentration, temperature and degree of saturation.

3.3.2 Kinetics of Pyrite Oxidation

If oxygen concentration is assumed to be the dominant factor controlling the rate of pyrite oxidation, then a prediction of oxidation rate can be determined based on oxygen concentration. As discussed in Chapter 2, Nicholson *et al.* (1988) found that the oxidation rate based on oxygen concentration was best predicted by a coupled

adsorption/desorption and decomposition model. It was also found that for low and intermediate concentrations of oxygen the rate could be assumed to be of an order between zero and one. To simplify the prediction, many studies assume that the reaction rate has an order of one. According to Elberling and Nicholson (1996), assuming a first order reaction rate would result in a flux calculation uncertainty of approximately 25%.

Assuming that a first order reaction rate is sufficient for predicting pyrite oxidation, the following relationship can be used which describes the rate of change of concentration in the pore space with time:

$$\frac{\partial C}{\partial t} = -k_r^* C^m \tag{3.16}$$

where: C = oxygen concentration in the pore space,
m = reaction order assumed equal to 1,
k_r^* =kinetic oxidation coefficient (1/time), and
t = time.

Once the assumptions have been made that oxygen concentration controls the rate of pyrite oxidation and that this rate can be predicted as first order, the final requirement to predict pyrite oxidation is to determine a value for the first order kinetic oxidation coefficient (k_r^*).

Collin (1998) describes an estimation for the kinetic oxidation coefficient as a function of particle size and pyrite concentration:

$$k_r = k' \frac{6}{D_h}(1-n)C_p \tag{3.17}$$

where: k' = constant of reactivity (approximated as 15.8×10^{-3} m^3 O_2/m^2 pyrite/ year),
D_h= particle diameter (m),
n = total porosity, and
C_p= pyrite concentration (kg/kg dry tailings).

The particle diameter (D_h) can be estimated by the approximate relationship given by Aubertin *et al.* (1998):

$$D_h = \left[1 + 1.17 \log(C_u)\right] D_{10} \tag{3.18}$$

where: D_{10}= grain diameter corresponding to 10% passing (m),
C_u = uniformity coefficient,
= D_{60}/D_{10}, where
D_{60}= grain diameter corresponding to 60% passing (m).

Equation 3.17 defines a reaction rate constant k_r, which differs from the reaction rate constant (k_r^*) given in Equation 3.16. The two factors are related by the equivalent porosity as shown in Equation 3.19 (Mbonimpa *et al.*, 2001).

$$k_r = n_{eq} k_r^* \tag{3.19}$$

The kinetic oxidation coefficient can be measured in a variety of ways. Detailed methods involving rigorous chemical analysis can be found in Moses and Herman (1991), Nicholson *et al.* (1988) and Scharer *et al.* (1995). Methods that are more commonly used to determine the coefficients of tailings both in the laboratory and in the field are those methods that measure the oxygen diffusion coefficient and the kinetic oxidation coefficient simultaneously (Cabral *et al.*, 2000 and Mbonimpa *et al.*, 2001).

3.4 DEVELOPMENT OF THE PARTIAL DIFFERENTIAL EQUATION

The partial differential equation describing the change in oxygen concentration with depth and time as a function of oxygen diffusion and consumption is developed in the following discussion.

Beginning with a representative elementary volume (REV), conservation of mass states that the mass flux entering the volume (Qm_{in}) minus the mass flux exiting the volume (Qm_{out}) must equal the change in storage ($\partial M/\partial t$). This is illustrated in Figure 3.2 and defined in Equation 3.20. Although this partial differential equation will be used to examine vertical diffusion, this derivation will illustrate diffusion in the horizontal

direction. For clarity, the x-direction will always represent the direction of diffusion, considered here as unidirectional.

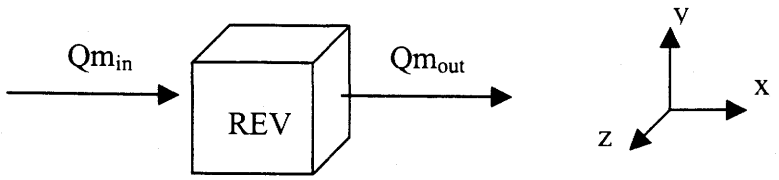

Figure 3.2 Representative elementary volume, REV, for derivation of partial differential equation.

$$Qm_{in} - Qm_{out} = \frac{\partial M}{\partial t} \tag{3.20}$$

Converting all mass fluxes into mass fluxes per unit area, denoted by q_{in} and q_{out}, Equation 3.20 becomes Equation 3.21. Equation 3.22 defines q_{out} as a function of q_{in}. Substituting Equation 3.22 into Equation 3.21 results in Equation 3.23. Simplifying Equation 3.23 results in Equation 3.24.

$$q_{in}dydz - q_{out}dydz = \frac{\partial M}{\partial t} \tag{3.21}$$

$$q_{out} = q_{in} + \frac{\partial q_{in}}{\partial x}dx \tag{3.22}$$

$$q_{in}dydz - \left(q_{in} + \frac{\partial q_{in}}{\partial x}dx\right)dydz = \frac{\partial M}{\partial t} \tag{3.23}$$

$$-\frac{\partial q_{in}}{\partial x}dxdydz = \frac{\partial M}{\partial t} \tag{3.24}$$

The mass flux entering the REV is that due to diffusion. This flux was defined in the previous section as Fick's First Law. The kinetic oxidation of the sulphide mineral is a mass sink and affects the change in storage. These two processes are defined in Equations 3.25 and 3.26.

$$q_{diff} = -D_e\frac{\partial C}{\partial x} \tag{3.25}$$

$$\frac{\partial M_{oxid}}{\partial t} = -k_r C dxdydz \tag{3.26}$$

The diffusive mass flux defines a mass of oxygen entering the REV. The oxidative mass flux defines a mass of oxygen leaving the REV. Substituting into Equation 3.24 both the mass source and sink gives Equation 3.27.

$$-\frac{\partial}{\partial x}\left(-D_e \frac{\partial C}{\partial x}\right)dxdydz = \frac{\partial}{\partial t}\left(n_{eq}C\right)dxdydz - \left(-k_r C dxdydz\right) \qquad (3.27)$$

Assuming that D_e is constant with depth and n_{eq} is constant with time, Equation 3.27 can be simplified and rearranged into Equation 3.28, the partial differential equation defining transient oxygen diffusion and consumption due to oxidation kinetics. This partial differential equation will be solved using a finite difference solution in following sections. The derivation of this Equation is also described in the CTRAN/W manual (1999).

$$D_e \frac{\partial^2 C}{\partial x^2} - k_r C = n_{eq} \frac{\partial C}{\partial t} \qquad (3.28)$$

3.5 *DEVELOPMENT AND VERIFICATION OF THE FINITE DIFFERENCE SOLUTION*

A finite difference solution to Equation 3.28 was developed using the program MATLAB. The development and verification of this model is described in the following sections.

3.5.1 Development of the Finite Difference Formulation

The partial differential equation describing oxygen diffusion and consumption through a porous media is highly non-linear. The finite difference numerical method of solution solves non-linear equations by solving the equation in a linear fashion over small time increments. The partial differential equation defining transient oxygen

diffusion and consumption assuming constant material properties with depth and time was developed in the previous section. The problem to be solved in this research involves material properties that vary with depth and with time. The partial differential equation defining varying properties with depth and time is given in Equation 3.29.

$$\frac{\partial}{\partial x}\left(D_e \frac{\partial C}{\partial x}\right) - k_r C = \frac{\partial}{\partial t}\left(n_{eq} C\right) \tag{3.29}$$

By using a finite difference method, Equation 3.29 does not need to be solved. Within each time-step and between each node, the partial differential equation for constant material properties is solved (Equation 3.28).

To develop the finite difference formulation defining the change in concentration at a given node, three nodes will be defined as illustrated in Figure 3.3. The nodes represent the center of the finite difference element.

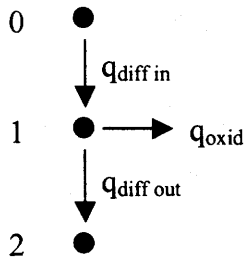

Figure 3.3 Three nodes and the mass fluxes entering and exiting node 1 for development of the finite difference formulation.

Conservation of mass states that the mass entering a volume minus the mass exiting a volume must equal the change in storage in the volume. This is defined in Equation 3.30. Equation 3.31 defines Equation 3.30 in terms of mass flux per unit area and mass in terms of concentration.

$$Qm_{in} - Qm_{out} = \frac{\partial M}{\partial t} \tag{3.30}$$

$$q_{diff_{in}}(dydz) - q_{diff_{out}}(dydz) - q_{oxid}(dydz) = \frac{\partial M}{\partial t} = \frac{n_{eq}\partial C}{\partial x} dxdydz \tag{3.31}$$

The definitions of the three mass fluxes shown in Figure 3.2 are given in Equations 3.32, 3.33 and 3.34. For the following equations, x is assumed to be positive in the downward direction.

$$q_{diff_{in}} = -D_e \frac{\partial C}{\partial x} = -D_{e_{0,1}} \frac{(C_1 - C_0)}{(x_1 - x_0)} \tag{3.32}$$

$$q_{diff_{out}} = -D_e \frac{\partial C}{\partial x} = -D_{e_{1,2}} \frac{(C_2 - C_1)}{(x_2 - x_1)} \tag{3.33}$$

$$q_{oxid} = k_r C dx = k_{r_1} C_1 \Delta x_{0,1,2} \tag{3.34}$$

Substituting these three equations into Equation 3.31 results in Equation 3.35.

$$-D_{e_{0,1}} \frac{(C_1 - C_0)}{|(x_1 - x_0)|} + D_{e_{1,2}} \frac{(C_2 - C_1)}{|(x_2 - x_1)|} - k_{r_1} C_1 |\Delta x_{0,1,2}| = \frac{n_{eq} \Delta C_1 |\Delta x_{0,1,2}|}{\Delta t} \tag{3.35}$$

Solving Equation 3.35 for the change in concentration (ΔC_1) gives Equation 3.36 which defines the change in concentration at node 1 over a given time-step (Δt).

$$\Delta C_1 = \frac{\Delta t}{|\Delta x_{0,1,2}| n_{eq_1}} \left[-D_{e_{0,1}} \frac{(C_1 - C_0)}{|(x_1 - x_o)|} + D_{e_{1,2}} \frac{(C_2 - C_1)}{|(x_2 - x_1)|} - k_{r_1} C_1 |\Delta x_{0,1,2}| \right] \tag{3.36}$$

The purpose for defining the x terms as absolute value is to avoid problems when using elevation versus depth values for x. Using this formulation, either depth or elevation can be used without changing Equation 3.36. The variable defined as $\Delta x_{0,1,2}$ in Equation 3.36 is the average of the two spaces on either side of node 1. This defines the thickness of the element associated with that node. For all the variables, the subset numbers separated by commas indicate the node(s) from which the variable must be calculated. For example, $D_{e\ 1,2}$ represents the harmonic mean of the D_e assigned to node 1 and the D_e assigned to node 2.

The boundary conditions for the finite difference solution are constant concentrations at the top and bottom nodes of the mesh. Atmospheric concentration is the constant value for the surface node and zero concentration is the constant value for the base node. By making the requirement that the base node must always be zero, the profile being modeled must agree with this assumption. In order that the base node be zero, the profile modeled must always include a portion below the water table. Since oxygen diffusion is greatly reduced in a saturated system, a profile that includes a meter below the water table will be in agreement with zero concentration at the base node.

3.5.1.1 MATLAB Program Summary

The finite difference solution described in the previous section required rigorous computing and was solved using the program MATLAB (MathWorks, 1997). MATLAB, which stands for matrix laboratory, is a programming language designed specifically for mathematical problems. The basic data element for this program is an array that does not need dimensioning. The formulations in the program can be written as vector and matrix manipulations that drastically reduce computing times compared to scalar languages. The following discussion describes the development of the MATLAB program used to solve the finite difference solution to the oxygen diffusion and consumption equation.

The objective of the oxygen diffusion/consumption model was to use the SoilCover saturation output as the input for the diffusion and consumption calculations. Therefore, it was most logical to tailor the MATLAB model as closely to SoilCover as possible. SoilCover generates a 1-dimensional mesh of nodes at fixed elevations. Each of these nodes is assigned a total porosity and for each of these nodes, the program outputs a

saturation value over a given time period. For the simulations conducted in this research, SoilCover was instructed to output saturation values for every node every 10 days. The most straightforward solution was to use the SoilCover mesh in the MATLAB program and assign each of the nodes the variables required for the finite difference solution.

The program structure is illustrated in the flowchart in Figure 3.4. The program structure consists of two nested loops: the innermost loop occurs for each time-step and is where the finite difference calculation occurs. The outer loop occurs for each SoilCover "day". For example, if SoilCover outputs saturation data at day 0, 1, 10 and 20, this would be four SoilCover "days". The terminology "day" will be used throughout the following discussion which elaborates on some other important details about the program.

The program starts by creating all the major matrices. A saturation data file is automatically loaded by the program into the saturation matrix. To create this data file, the saturation results from SoilCover must be saved as a text file.

A concentration matrix is created into which the program writes a concentration profile for every "day". The concentration profile for day 0 is defined by the boundary conditions of the model. These conditions define the surface node as atmospheric, the base node as zero and writes in zero concentration for the remaining nodes.

The saturation matrix from SoilCover only defines a new saturation profile for every "day". In most of the simulations for this research, a "day" was 10 days in length. Saturation values for every time-step increment between the 10 days were interpolated so that there was no sudden change in saturation values between the time-steps.

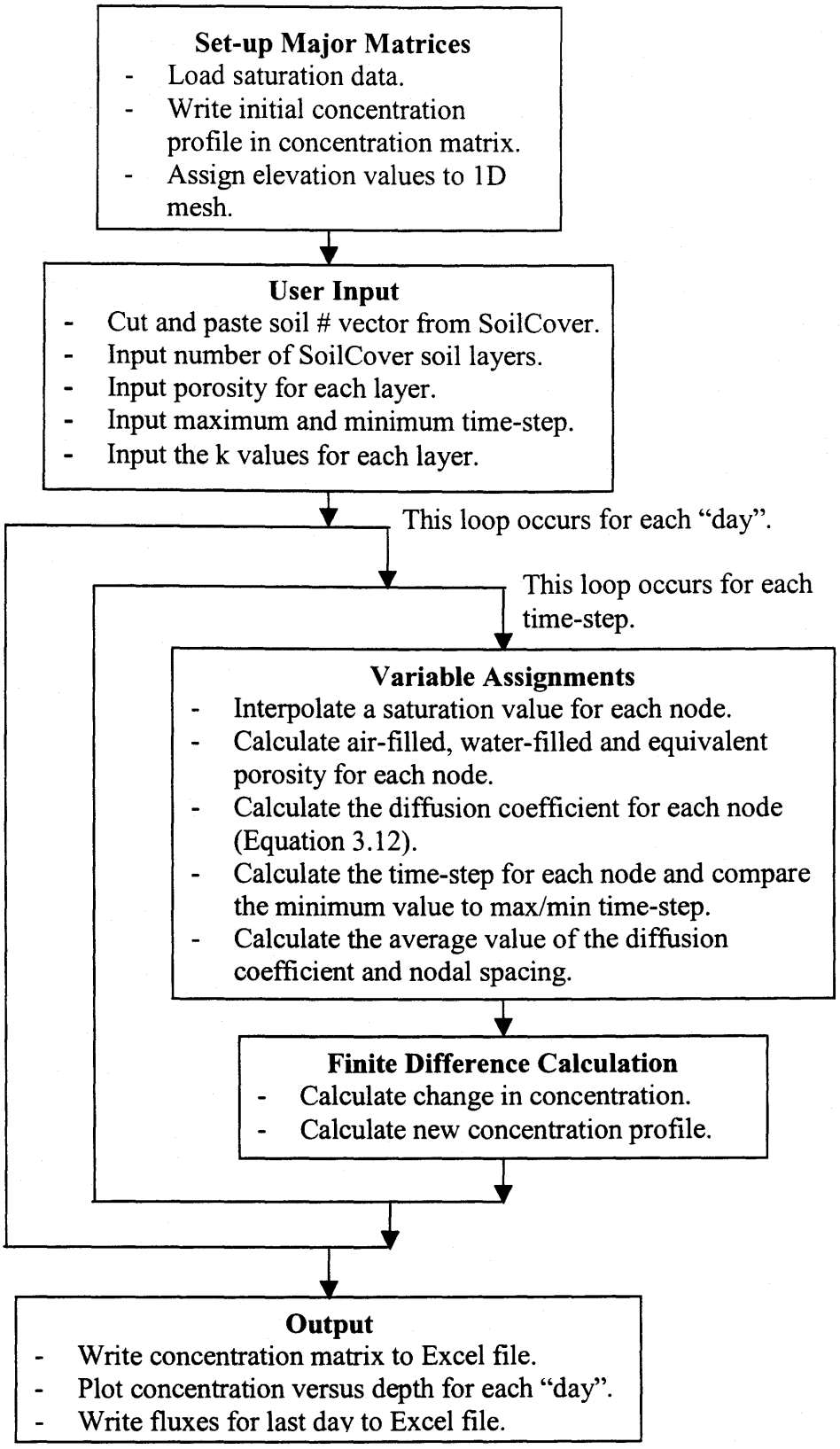

Figure 3.4 Flowchart for MATLAB program.

The input section of the model requires considerable user input. The first prompt asks the user to cut and paste the column from SoilCover that consists of a soil number for each node. The soil number designates which soil layer each node falls into. This column allows for new data to be assigned to each node based on the SoilCover layers. The user is then prompted to enter the porosity value for each layer. These layer numbers are used later in the program when kinetic constants are assigned to each layer.

The user is required to specify a minimum and maximum time-step value. These values limit how small or how large the time-step values get. The time-step is calculated as a function of the coefficients in the finite difference equation. The formula used to calculate the time-step is given in Equation 3.37 which defines the time-step required for mathematical stability (Zill & Cullen, 1992). The model calculates the time-step for each node then takes the minimum value and compares it to the maximum and minimum time-step specified by the user.

$$\lambda = \frac{D_e \Delta t}{\Delta x^2} = 0.5 \tag{3.37}$$

Large diffusion coefficients tend to drive the time-step to extremely small values that require very long computing times. Small nodal spacings (Δx) also drive the time-step to extremely small values. It was determined from trial simulations that for most modeling scenarios, the nodal spacing should be a minimum of 10 mm for reasonable computing times. This may require adjusting the SoilCover mesh to eliminate nodes that are too close together.

The last section of the input requirements is where the kinetic oxidation coefficients are entered. The user specifies whether or not the kinetic coefficients contain the equivalent porosity (i.e., k_r or k_r^*). The kinetic coefficients may be input in two ways:

according to the SoilCover layers or for layers in addition to the SoilCover layers. If the kinetic coefficients correlate to SoilCover layers, the user can input a kinetic coefficient for each layer number in the mesh. If the user wants layers that do not correlate to the SoilCover layers, the kinetic coefficients can be input according to the top and bottom elevation of the layers.

The final output of the model is a spreadsheet file containing the concentration profile for each "day" and a second spreadsheet file containing the diffusive and oxidative fluxes calculated at each node for the last "day". The model also plots the concentration profiles versus depth for each "day".

3.5.2 Model Verification

Three methods were used to verify the finite difference oxygen diffusion and consumption model. The first method was to compare the results of the model to a closed-form solution. This required simplifying the profile such that it had constant saturation and porosity with depth and with time. The second method allowed for a more detailed profile to be modeled. The program POLLUTE was used to predict transient oxygen diffusion through a profile with variable saturation. This program allowed a variable saturation profile with depth but not with time. Lastly, the model was compared to a published oxygen concentration profile for a material with known diffusion and kinetic properties.

3.5.2.1 Closed-Form Solution

The oxygen diffusion and consumption model was compared to closed-form solutions to the equations for transient diffusion without kinetic oxidation and transient diffusion

with kinetic oxidation. The following partial differential equations and their closed-form solutions have been taken from Crank (1975).

The partial differential equation for oxygen diffusion without kinetics is given in Equation 3.38. The closed-form solution to this equation is given in Equation 3.39 for the boundary condition in Equation 3.40 and the initial condition in Equation 3.41. These equations imply a semi-infinite medium where the boundary (surface) is a constant concentration (C_0) and the initial concentration throughout the medium is zero.

$$\frac{\partial C}{\partial t} = D^* \frac{\partial^2 C}{\partial x^2} \tag{3.38}$$

$$C = C_0 \operatorname{erfc} \frac{x}{2\sqrt{D^* t}} \tag{3.39}$$

$$C = C_0, \qquad x = 0, \qquad t > 0 \tag{3.40}$$

$$C = 0, \qquad x > 0, \qquad t = 0 \tag{3.41}$$

The partial differential equation for diffusion and oxidation was derived in Section 3.4 as Equation 3.28 and is restated here as Equation 3.42. Equation 3.42 is the same as Equation 3.28 except that the equivalent porosity (n_{eq}) has been divided out of all three terms. The closed-from solution to this equation is given in Equation 3.43 for a semi-infinite medium with a constant surface concentration.

$$\frac{\partial C}{\partial t} = D^* \frac{\partial^2 C}{\partial x^2} - k_r^* C \tag{3.42}$$

$$\frac{C}{C_0} = \tfrac{1}{2} \exp\left[-x\sqrt{k_r^*/D^*}\right] \operatorname{erfc}\left[\frac{x}{2\sqrt{D^* t}} - \sqrt{k_r^* t}\right] + \tfrac{1}{2} \exp\left[x\sqrt{k_r^*/D^*}\right] \operatorname{erfc}\left[\frac{x}{2\sqrt{D^* t}} + \sqrt{k_r^* t}\right] \tag{3.43}$$

To compare the results of the MATLAB finite difference model with the closed-form solution, a profile was required that would satisfy the boundary and initial conditions of

both the closed-form solution and the finite difference solution. Since a requirement for the finite difference solution was that the concentration at the base equal zero, it was necessary to create a profile deep enough such that oxygen would never diffuse below the base of the profile. The requirements of the closed-form solution was that the degree of saturation, diffusion coefficient and kinetic oxidation coefficient were constant with depth and with time.

The profile chosen was a 20 m deep profile with a constant degree of saturation of 40% and a porosity of 0.45. The diffusion coefficient used in the simulation was 0.1193 m^2/s (D^*) as calculated by the modified Millington and Shearer method. For the simulation including kinetic oxidation, a kinetic oxidation coefficient (k_r^*) of 54.03 1/yr was used. The comparison of the closed-form solution with the finite-difference model for the kinetic oxidation coefficient set to zero is illustrated in Figure 3.5. The comparison of the closed-form solution with the finite difference model including a kinetic oxidation coefficient of 54.03 1/yr is illustrated in Figure 3.6.

The solutions for the simulation without kinetics (Figure 3.5) show the finite difference solution virtually identical to the closed-form solution. The solution including kinetics (Figure 3.6) shows a slight variation between the two methods. Figure 3.6 only shows a small portion of the profiles since the penetration of the oxygen was greatly reduced due to the consumption by kinetic oxidation.

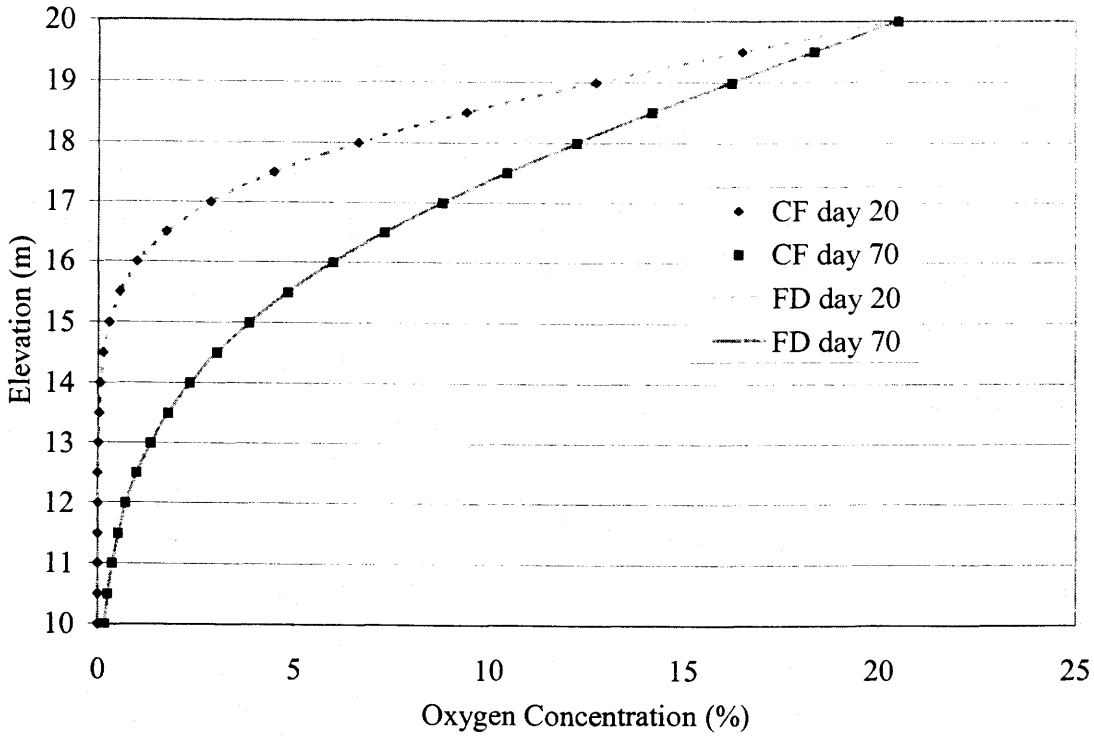

Figure 3.5 Comparison of closed-form (CF) and finite difference (FD) solutions for S = 40%, n = 0.45, $D^* = 0.1193\ m^2/s$ and $k_r^* = 0$.

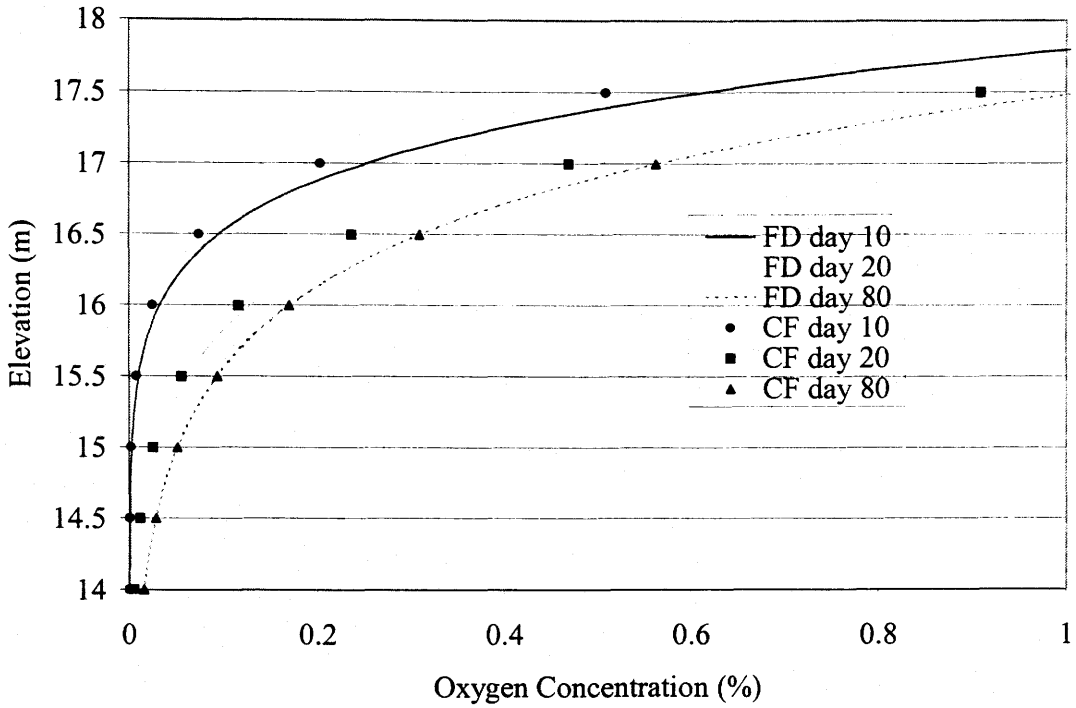

Figure 3.6 Comparison of closed-form (CF) and finite difference (FD) solutions for S = 40%, n = 0.45, $D^* = 0.1193\ m^2/s$ and $k_r^* = 54.03\ 1/yr$.

Although it is not illustrated in Figure 3.6, the closed-form solution did not calculate the profile surface as having atmospheric concentration even though this was one of the boundary conditions upon which the solution was based. A possible reason for this discrepancy is the complimentary error function (erfc) in the closed-form solution. The erfc function is an approximation of a standard integral and is therefore subject to error. The discrepancy in the two solutions is small but most pronounced for small depth (small x) and small time which would support the theory that there is error in the erfc function for small x and t. In general, the two solutions converge to the same steady-state value. It is important to note that the discrepancy is a fraction of a percent and is likely smaller than the accuracy of most measuring instruments.

The conclusion from the comparison of the closed-form solution with the MATLAB finite difference solution is that the MATLAB model predicts oxygen diffusion and consumption for constant conditions with depth and with time with a high degree of accuracy.

3.5.2.2 Comparison to POLLUTE Results

To evaluate the finite difference solution for variable saturation with depth, simulations were compared with those from the program POLLUTE. POLLUTE is a finite layer contaminant transport program that can be adapted to simulate oxygen diffusion and consumption (Rowe *et al.*, 1994). Research where this program has been used for oxygen diffusion and consumption modeling is described in Aubertin *et al.* (2000), Mbonimpa *et al.* (2001) and Yanful (1993b). The simulations were performed by M. Aubertin and the research group at École Polytechnique in Montréal, QC (Aubertin, 2001). A saturation profile showing desaturation was chosen from the

SoilCover modeling. This saturation profile is illustrated in Figure 3.7. The simulations for both methods assumed that this saturation profile was constant with time. Five meters of tailings were simulated with the water table at a depth of 4 m. The porosity for the profile was that for the coarse tailings material (n = 0.45). The diffusion coefficients for each node were calculated using Equation 3.12 (Modified Millington and Shearer). Simulations were performed with and without kinetic oxidation. For the simulations including kinetic oxidation, a kinetic oxidation coefficient (k_r) of 14.88 1/yr was used.

The comparison between the POLLUTE results and the finite difference solution for no kinetic oxidation is illustrated in Figure 3.8. The comparison between the POLLUTE results and the finite difference solution including kinetic oxidation is illustrated in Figure 3.9.

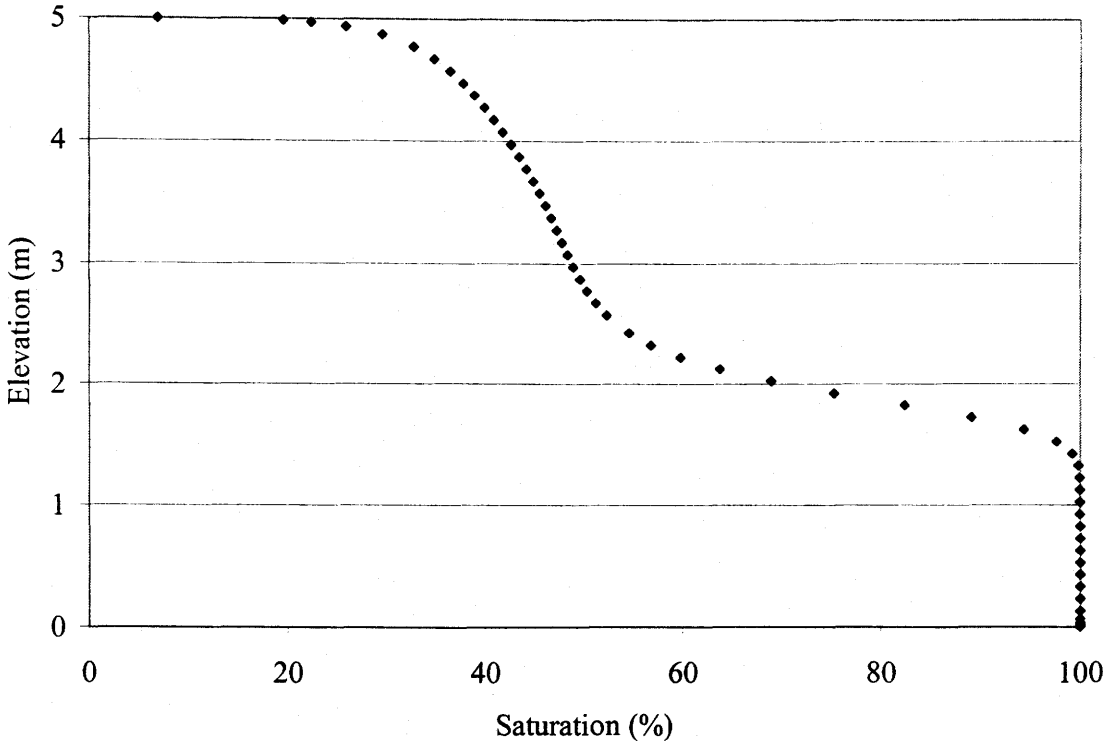

Figure 3.7 Saturation profile used for finite difference solution for comparison to POLLUTE solution.

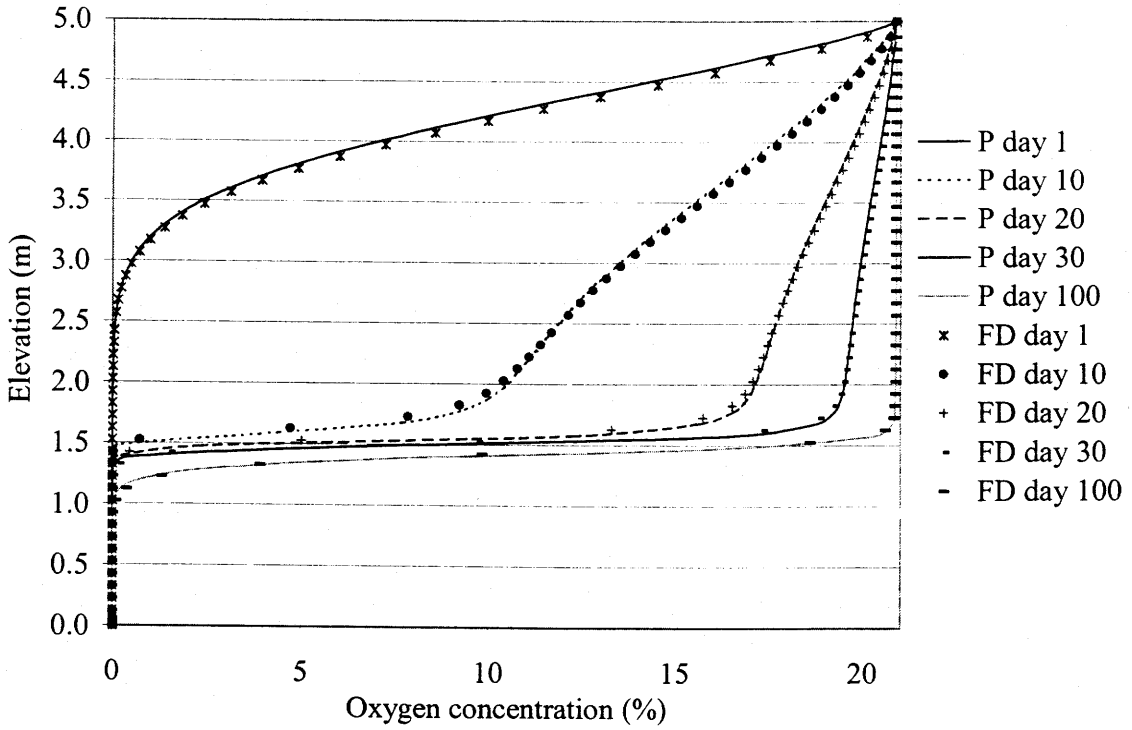

Figure 3.8 Comparison of the POLLUTE (P) and the finite difference (FD) solution results for a variable saturation profile and no kinetic oxidation.

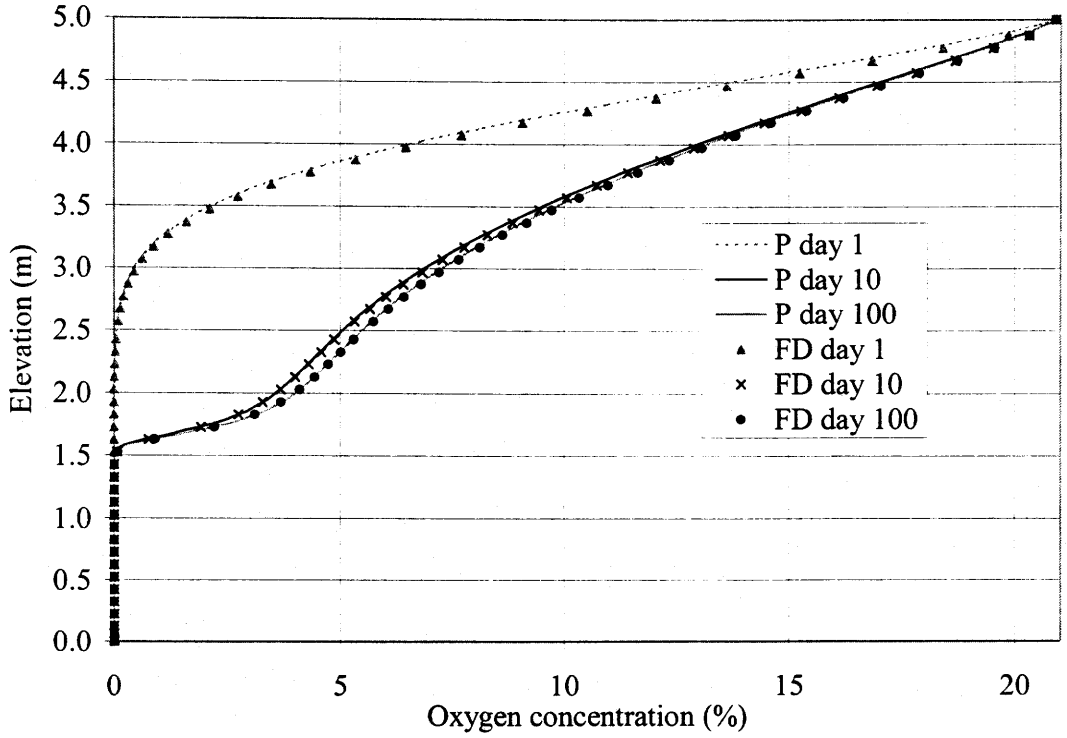

Figure 3.9 Comparison of the POLLUTE (P) and the finite difference (FD) solution results for a variable saturation profile including kinetic oxidation.

As illustrated in Figures 3.8 and 3.9, the finite difference solution and the POLLUTE solution show similar oxygen profiles for both transient and steady-state diffusion and oxidation. Both the solutions for the scenario without kinetic oxidation show oxygen penetrating to full depth just above the water table in the 100 day simulation period.

The two simulations including kinetic oxidation both illustrate the reduction in oxygen penetration when consumption by kinetic oxidation is included. Both simulations show the system reaching a steady-state oxygen profile after less than 20 days.

The comparison for the finite difference model and the POLLUTE solution shows that the finite difference model provides a reasonable estimation of transient diffusion and consumption for a variable saturation profile with depth.

3.5.2.3 Comparison to Published Results

The third method used to verify the finite difference model was to compare the model results to a measured oxygen concentration profile. Yanful (1993b) published the results of an extensive research program that had investigated a potential tailings cover system at the Heath Steele Mines site in Newcastle, New Brunswick. The research involved laboratory testing to obtain the diffusion and kinetic coefficients of the cover materials and the tailings, column experiments measuring the oxygen concentration profiles and lastly, field-scale test plots.

The oxygen profile through a column of homogenous reactive tailings was measured after a period of 65 days. The column was also measured for volumetric water content with depth. Diffusion and kinetic cell testing in the research determined the diffusion coefficient and kinetic oxidation coefficient for the tailings. Using the information from

the research, saturation and diffusion coefficient profiles were created as input parameters to the finite difference model.

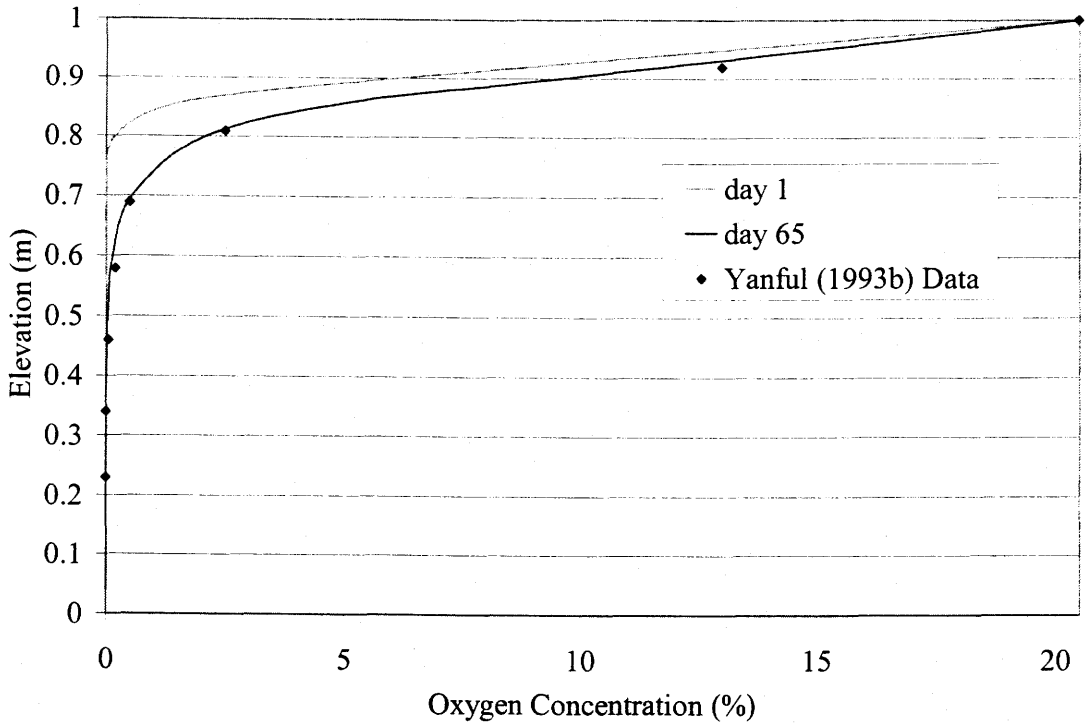

Figure 3.10 Comparison of the finite difference model results to a measured oxygen concentration profile from Yanful (1993b).

The result of the finite difference modeling compared to the measured oxygen concentration profile is illustrated in Figure 3.10. As shown in this figure, the prediction of the finite difference model closely approximates the measured oxygen concentration profile. It is interesting to note that the finite difference model assumed that the initial condition of the column was zero oxygen concentration. In the research described by Yanful (1993b), the columns were not purged to remove the oxygen before the column experiments began. Therefore, the column did not begin to diffuse from the initial condition of a zero oxygen concentration profile. As illustrated in the previous section, diffusion coupled with kinetic oxidation results in a rapid convergence for a steady-state

profile. The finite difference model accurately predicted the oxygen concentration after 65 days since the column had likely reached steady-state.

3.5.2.4 Summary of Verification Results

Three methods were used to verify the finite difference oxygen diffusion and consumption model. The finite difference model results were compared to a closed-form solution, a POLLUTE solution and a measured oxygen profile from a column experiment. The results of all three comparisons showed that the finite difference solution is a reasonable solution for the prediction of oxygen diffusion and consumption.

Chapter 4
FIELD INVESTIGATION

4.1 INTRODUCTION

This chapter presents the results of the field investigation conducted at the Detour Lake Mine site in July, 2000. A brief site description is followed by a description of the instrumentation and the results from one year of monitoring.

4.2 SITE DESCRIPTION

Detour Lake Mine is a gold mine operated by Placer Dome Inc. located 290 km northeast of Timmins, Ontario. Mining operations commenced in 1983 from an open pit and underground operations began in 1987. Production ceased in June, 1999. The mine tailings were deposited by end-pipe discharge into a dam impoundment. The tailings facility contains approximately 15 million tonnes of sulphidic tailings and covers an area of approximately 300 ha.

The Detour Lake Mine tailings have a sulphide sulphur content ranging from 1 to 2.5% and a net neutralization potential ranging from –5 to –75 (tons $CaCO_3$ equivalent per 1000 tons material). The tailings were deemed to have potential for producing acid rock drainage. The remediation strategy taken by Placer Dome was to cover the majority of the tailings with a water cover and to install a wet cover over the rest of the tailings.

The wet cover was designed using desulphurized tailings as the constitutive material. The desulphurized tailings used for the cover design were taken from the pilot plant which designed the flotation process later used to desulphurize the mill tailings. The cover was designed to create a capillary barrier effect when placed above the sulphidic tailings. The purpose of this capillary barrier was to create a layer which would remain saturated throughout the year and act as an oxygen barrier. Oxygen diffusion coefficients decrease significantly with degrees of saturation of greater than 85% (O'Kane *et al.*, 1995) (See Figure 3.1). The cover was also intended to act as an oxygen scavenger when the small quantity of remaining sulphide minerals oxidized.

The desulphurization process was designed to reduce the sulphide sulphur content to between 0.5 and 1%. The cover was designed to range in thickness from greater than 1 m at the dam to 0.5 m at the pond. The single layer desulphurized cover system was installed on the tailings facility beginning in 1998 and continuing until production ceased in the summer of 1999. The desulphurized tailings were deposited by end-pipe discharge onto the surface of the sulphidic tailings. The tailings facility at Detour Lake Mine is illustrated in Figure 4.1 showing the portion of the tailings covered with the desulphurized tailings cover.

The climate at the Detour Lake Mine site is defined as a moist continental mid-latitude climate with an annual precipitation of approximately 920 mm (Environment Canada). The total potential evaporation is approximately 800 mm (Barbour *et al.*, 1993). In general, one third of the total precipitation occurs as snowfall. The relative humidity between the months of May and October fluctuates daily between 50% and 90%. The temperature at the site fluctuates considerably with temperatures as high as

37 °C in the summer and as low as –47 °C in the winter (Climate data reproduced with permission of the Minister of Public Works and Government Services Canada, 2001).

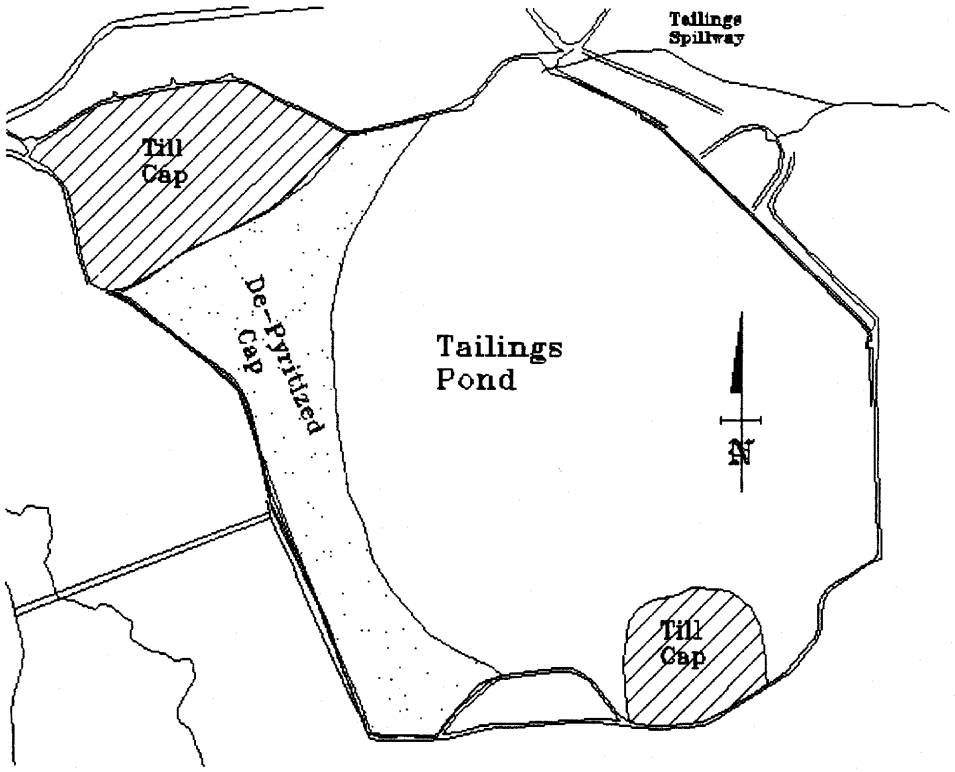

Figure 4.1 Schematic of Detour Lake Mine tailings facility illustrating the portion of tailings covered with the desulphurized (depyritized) tailings cover (not to scale). *Reproduced with permission from Placer Dome Inc.*

4.3 DESCRIPTION OF INSTRUMENTATION

Instrumentation was installed in the Detour Lake tailings facility in July, 2000. The purpose of the instrumentation program was to obtain detailed meteorological data, water content profiles and water levels at different locations in the tailings facility. Instrumentation was installed at nine locations throughout the desulphurized tailings cover. A site plan illustrating the locations of the instrumentation is shown in Figure 4.2. Three groups of instrumentation were installed to represent three profiles through

the cover. These profiles are shown as A, B and C in Figure 4.2. Location C202 was not used for the study since the instrumentation was too shallow. An additional location, C204, was installed as a replacement. A piezometer and a neutron probe access tube were installed at each of the nine locations. A typical profile through the tailings facility is shown in Figure 4.3.

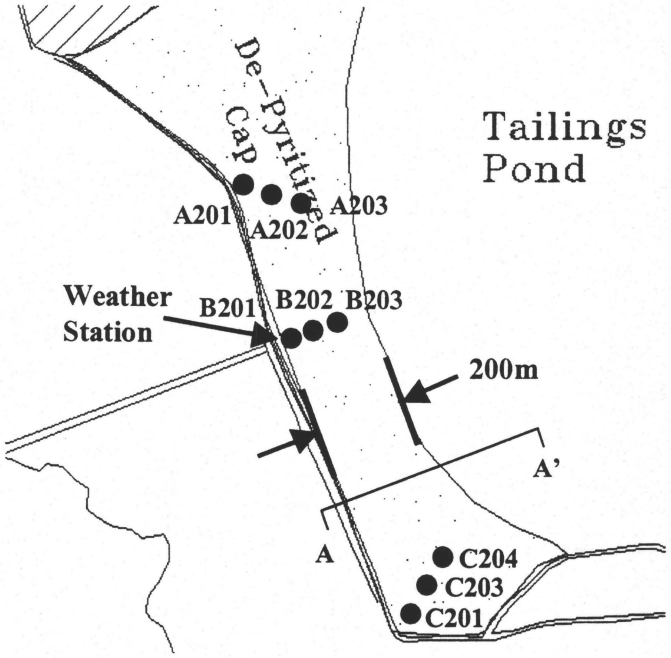

Figure 4.2 Site plan of tailings facility illustrating the location and designation of instrumentation.

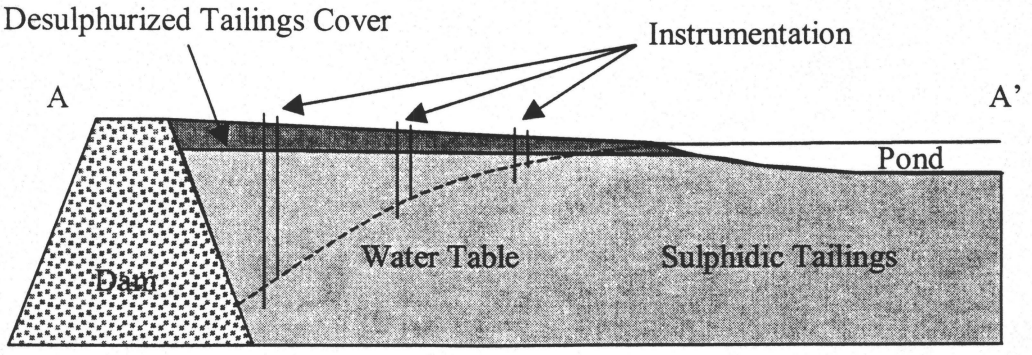

Figure 4.3 Schematic profile (A-A') through the Detour Lake tailings (not to scale).

The piezometers were constructed using 64 mm diameter PVC pipe with 850 mm of slotted (10 slot) PVC screen. A filter sock was placed over the screen to prevent fine tailings from passing through the slots. The neutron probe access tubes were constructed using 64 mm diameter aluminum tubing. Aluminum caps were welded on the ends to prevent water from entering the tubes. A schematic of the instrumentation installed at each location is shown in Figure 4.4. The piezometers were placed with the screened length below the water table whereas the neutron probe access tubes were placed just above the water table. The piezometers were used to measure the depth of the water table in the tailings using a water level indicator. The water content profiles were measured with a neutron probe inside the neutron probe access tubes.

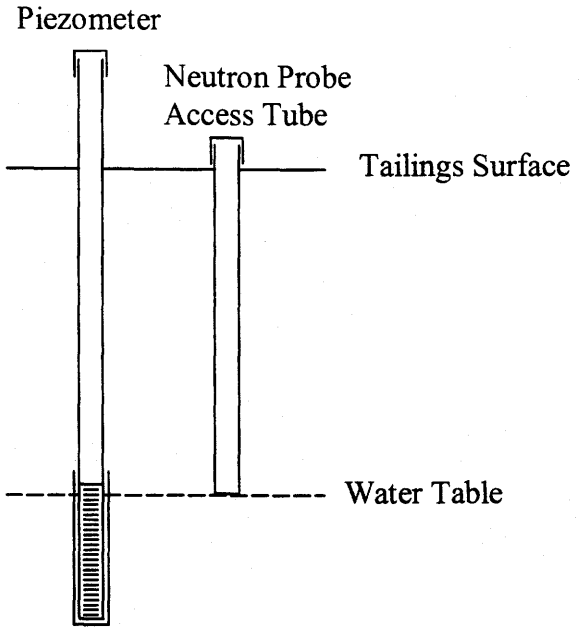

Figure 4.4 Schematic of instrumentation installed at each of the nine locations.

A weather station was installed at the tailings facility to measure detailed meteorological data. The weather station was located beside the B201 instrumentation as indicated in Figure 4.2. The weather station was a Campbell Scientific tripod weather

station equipped with sensors to measure wind speed, wind direction, relative humidity, temperature, net radiation and rainfall precipitation. The weather station was not equipped to measure precipitation due to snowfall or snowmelt. A CR10X datalogger was installed to record the weather station measurements. The datalogger downloaded measurements from every sensor on an hourly basis.

4.3.1 Neutron Probe Calibration

The neutron probe used to measure the water content profiles through the tailings was a Campbell Scientific 503 hydroprobe. A neutron probe uses the principle that neutron radiation reflects differently from air, water and soil particles. A probe containing a radiation source (americium 241/ beryllium) was inserted into an access tube. The radiation that was reflected back to the probe was measured and related to the amount of water in the surrounding soil/tailings. Since different soils reflect radiation differently, the neutron probe was calibrated specifically for the tailings at Detour Lake Mine.

The calibration curve used to interpret the neutron probe results for the Detour Lake tailings was obtained from two separate calibrations performed using the same neutron probe. In 1999, a calibration was performed at the Detour Lake Mine and at the nearby mine site of Dona Lake. The tailings at these two sites are very similar. The calibration of the neutron probe involved taking samples from various depths and measuring their water content. A neutron probe reading was then taken at each of the depths corresponding to the samples. These neutron probe readings were plotted against the water contents to calculate the calibration curve. The calibration data from both the Detour and Dona Lake sites were combined to create a single calibration curve illustrated in Figure 4.5.

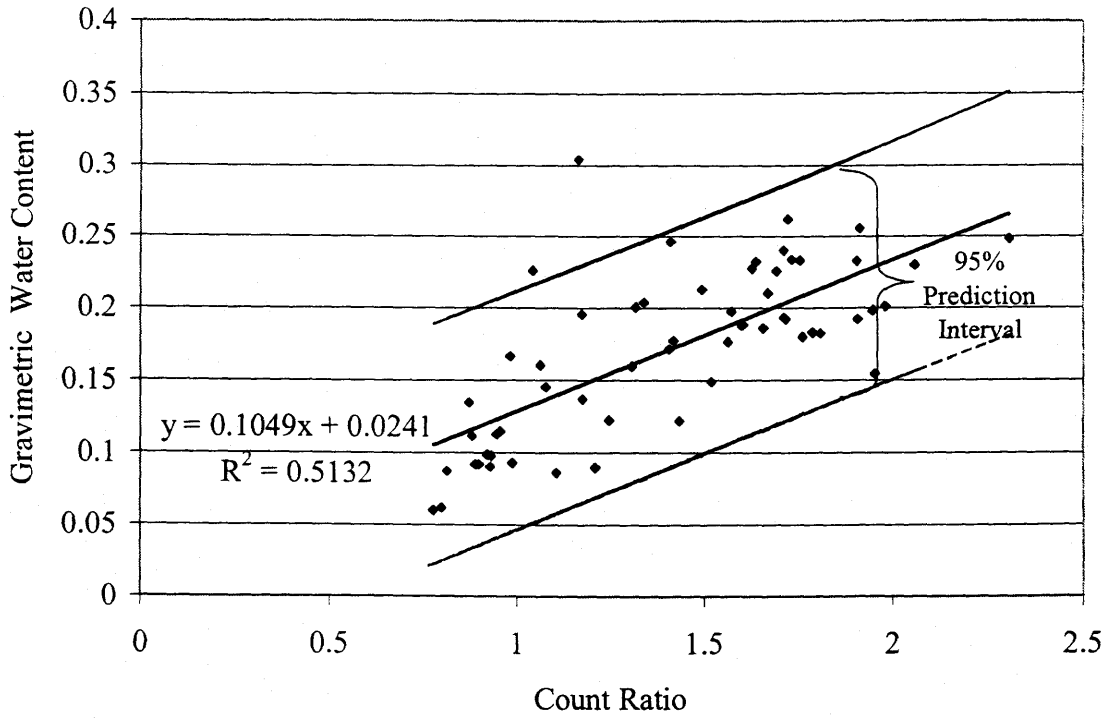

Figure 4.5 Neutron probe calibration curve relating neutron probe count ratio to gravimetric water content. The linear regression line and the 95% prediction interval are illustrated.

As shown in Figure 4.5, there was a wide spread in the calibration data. The 95% prediction interval represented a water content of approximately 0.08 on either side of the linear regression line. This indicated that there was error in the water content results due to the calibration. Error bars were included on one water content profile for bore-hole A201 to illustrate the uncertainty in the results. Due to the uncertainty, the water content profiles were used to make qualitative and relative comparison conclusions.

The variation in the calibration results could have been affected by the heterogeneity of the tailings facility. The neutron probe measures in a sphere around the neutron source. A thin layer of high or low water content tailings encountered in this sphere that was not accounted for during the sampling could affect the reading at a given depth.

4.4 SUMMARY OF RESULTS

The following sections summarize the water levels, water content profiles and weather data measured from July, 2000 to July, 2001. Also presented are the results of *in situ* testing performed in July, 2000 to determine water content and porosity.

4.4.1 Water Levels and Water Content Profiles

Water levels and water content profiles were measured monthly beginning in July, 2000. When the instrumentation was installed, the tailings impoundment was under construction to raise the level of the pond such that it covered a larger proportion of the tailings. According to the impoundment design, the pond level would rise by a few feet over the following one or two years. Since the instrumentation was installed in July, 2000, the water table in the area instrumented has continued to drop. As of July, 2001, the water table had dropped below the screen of five of the nine piezometers installed. The water level data for the nine piezometers is summarized in Table 4.1. As expected, the decline in the water table increases with increasing distance from the pond. The greatest depth to the water table was measured in piezometer B201 where it was found to fluctuate between 4 and 5 m below the surface of the tailings.

The water content profiles measured at the nine locations are presented in Figures 4.6 through 4.14. Error bars, due to the uncertainty in the calibration, are illustrated on one profile in Figure 4.6. The water tables indicated on the figures are those measured in July, 2001. The water tables in bore-holes A201, A203, B202, B203 and C204 have all dropped below the bottom of the piezometer. The depth of water table indicated on the water content profiles for these bore-holes is the depth to the bottom of the piezometer. The uncertain water table depths are indicated by a dashed line.

Table 4.1 Summary of water table depth data from July, 2000 to July, 2001.

Bore-hole	5-Jul-00	7-Oct-00	5-Nov-00	19-May-01	2-Jul-01
A201	2.91	> 3.03	> 3.03	> 3.03	> 3.03
A202	1.27	1.62	1.85	1.93	2.04
A203	1.31	1.63	1.81	2.00	> 2.33
B201	4.34	> 4.81	> 4.81	3.78	4.68
B202	2.53	3.00	3.10	> 3.16	> 3.16
B203	1.48	> 1.64	> 1.64	> 1.64	> 1.64
C201	2.70	3.07	3.07	2.85	2.99
C203	1.42	1.83	2.00	1.70	1.87
C204	1.17	1.44	1.60	> 1.65	> 1.65

The dominant characteristic of all the water content profiles was the fluctuation in water content with depth. The fluctuations represent heterogeneity of particle size within the tailings profile. This heterogeneity was also observed during installation of the instrumentation. The tailings were layered with the grain-size of the tailings layers varying from silt and clay-size particles to fine sand-sized particles. The layering is attributed to segregation of the tailings during deposition. The coarser tailings settled out closer to the discharge pipe whereas the finer tailings traveled further towards the pond. Variations in flow rates could account for the variation in grain-size at any given location. It was determined that the layering was due to a combination of factors.

It was observed from the water content profiles that there was a layer of tailings at high water content in the top 2 m of all the bore-holes. This occurred regardless of the water table depth. The surface tailings (~0.2 m) of all the bore-holes showed low water contents, indicating desaturation, throughout the year.

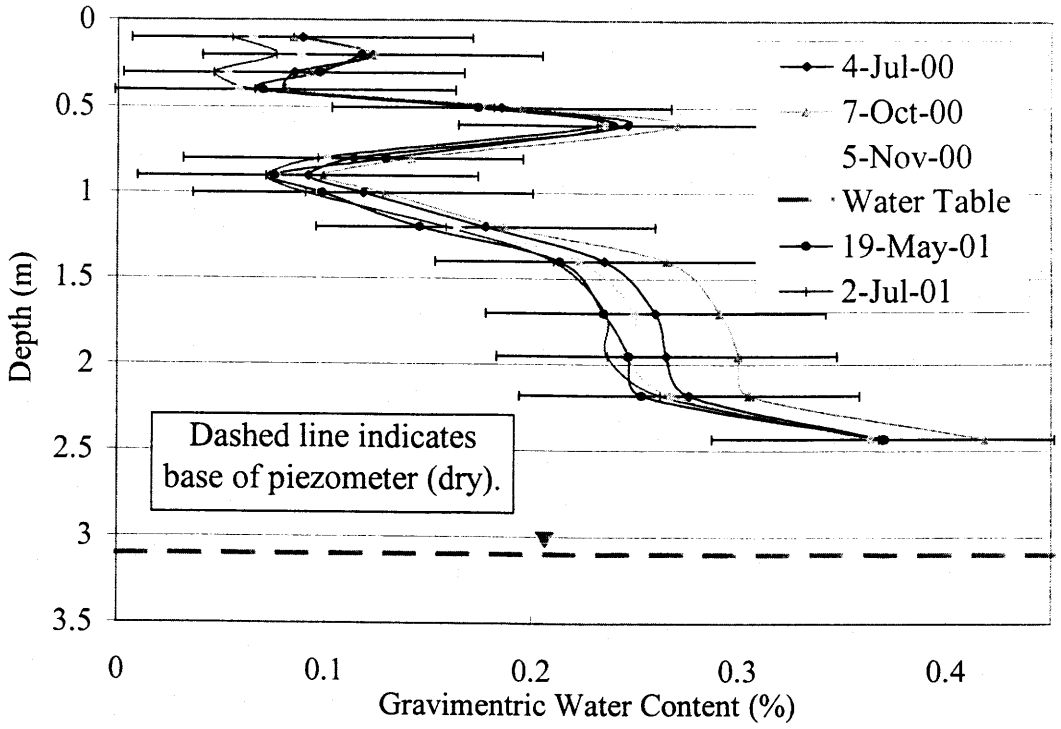

Figure 4.6 Water content profiles for bore-hole A201 from July, 2000 to July, 2001. Water table depth indicated is the approximate location as of July, 2001. Error bars shown for profile measured on July 4, 2000.

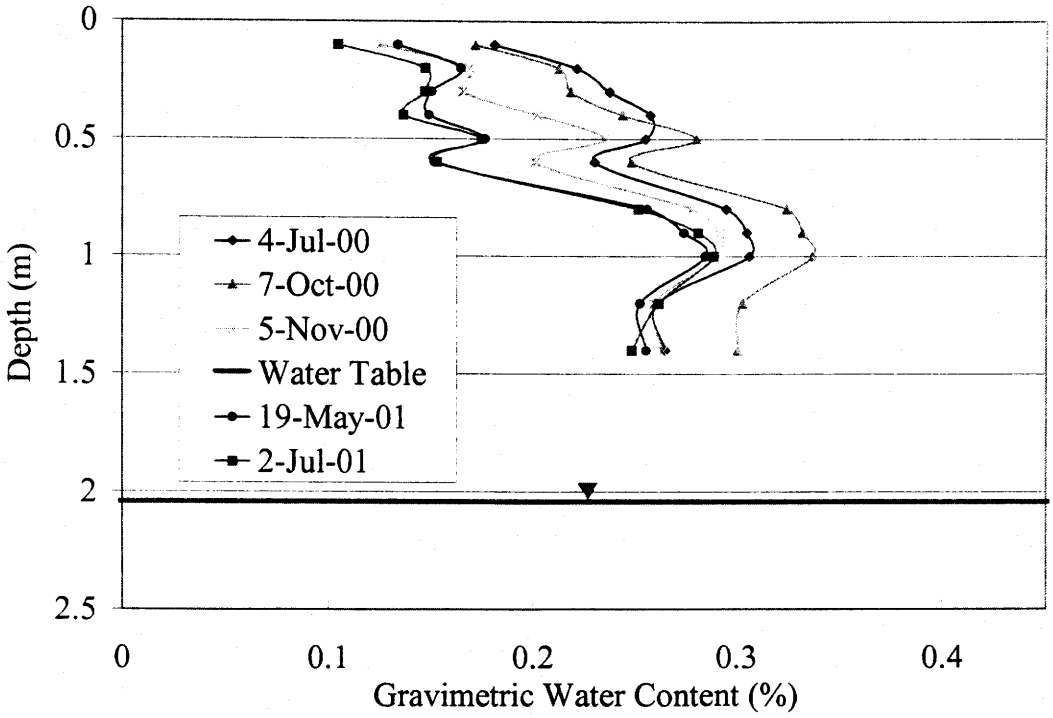

Figure 4.7 Water content profiles for bore-hole A202 from July, 2000 to July, 2001. Water table depth indicated is the approximate location as of July, 2001.

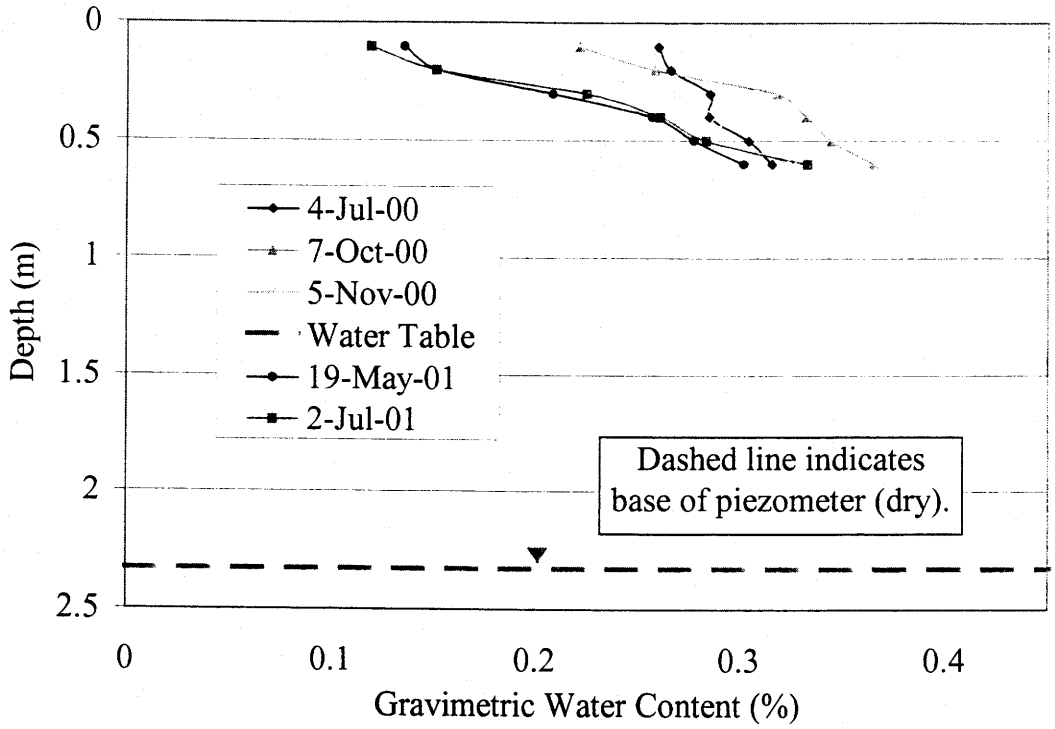

Figure 4.8 Water content profiles for bore-hole A203 from July, 2000 to July, 2001. Water table depth indicated is the approximate location as of July, 2001.

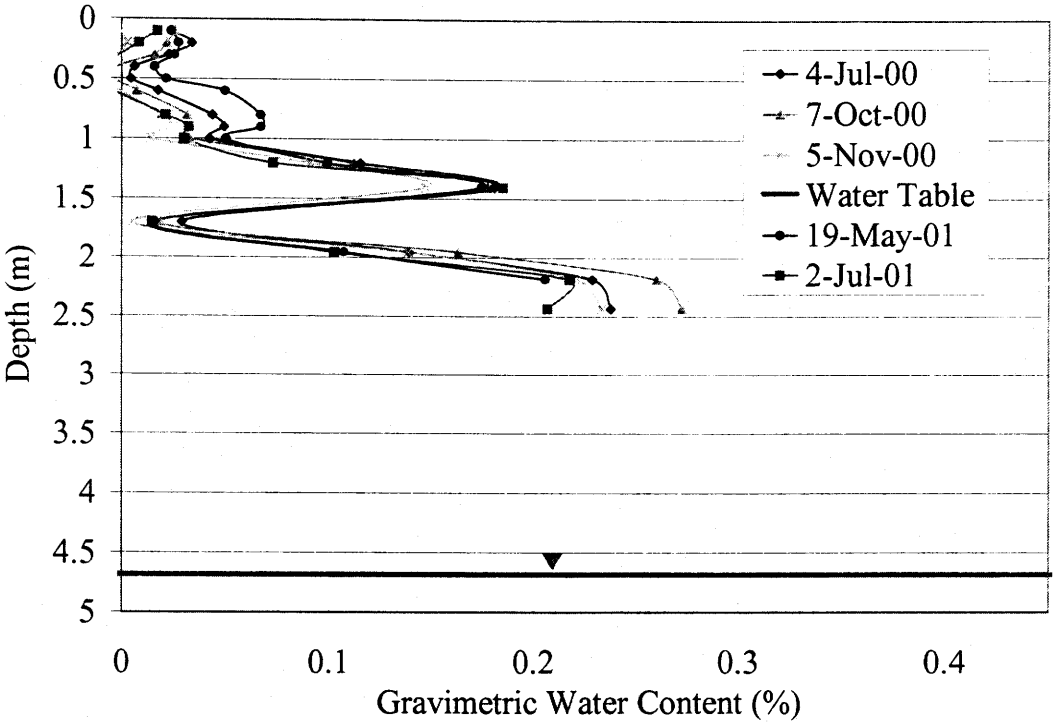

Figure 4.9 Water content profiles for bore-hole B201 from July, 2000 to July, 2001. Water table depth indicated is the approximate location as of July, 2001.

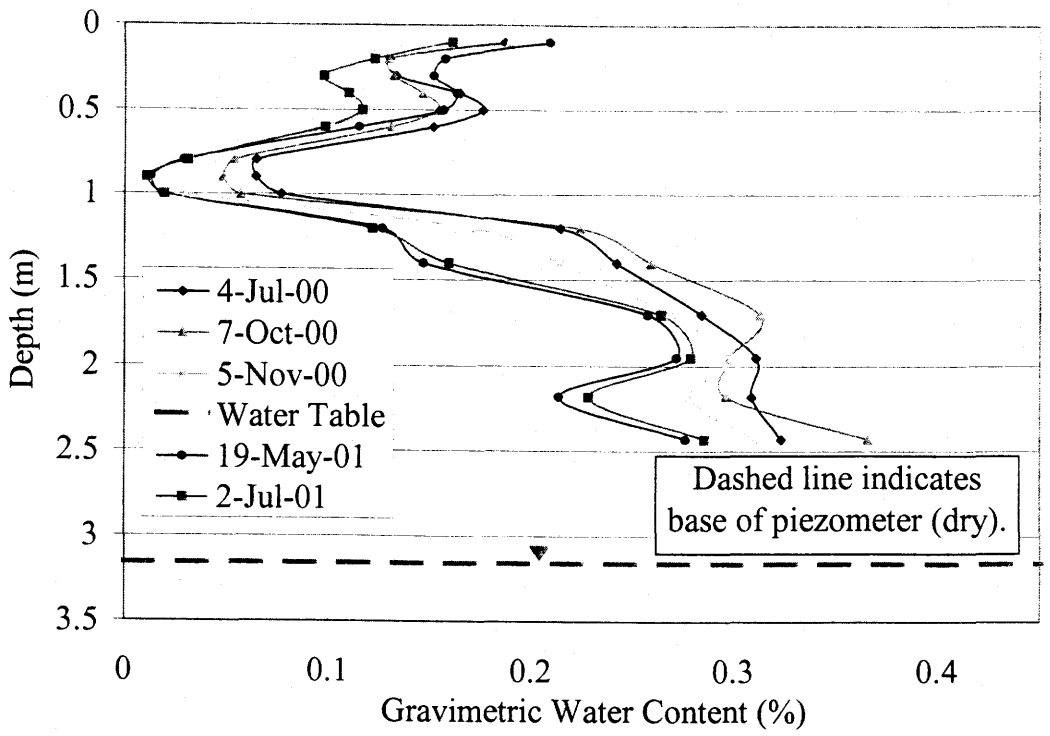

Figure 4.10 Water content profiles for bore-hole B202 from July, 2000 to July, 2001. Water table depth indicated is the approximate location as of July, 2001.

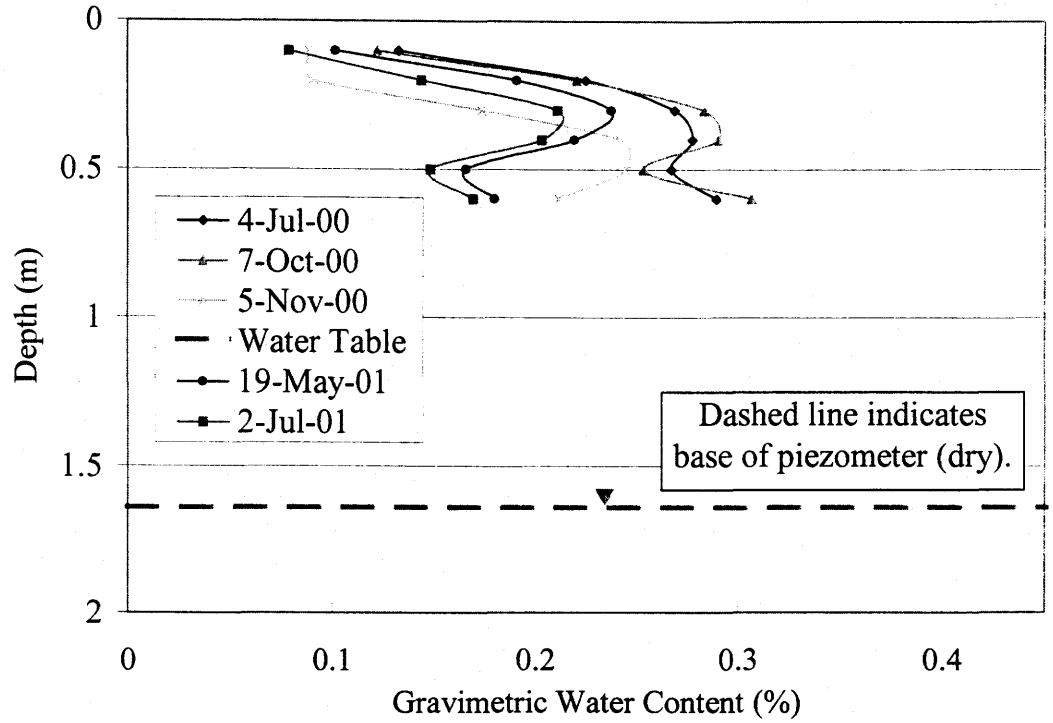

Figure 4.11 Water content profiles for bore-hole B203 from July, 2000 to July, 2001. Water table depth indicated is the approximate location as of July, 2001.

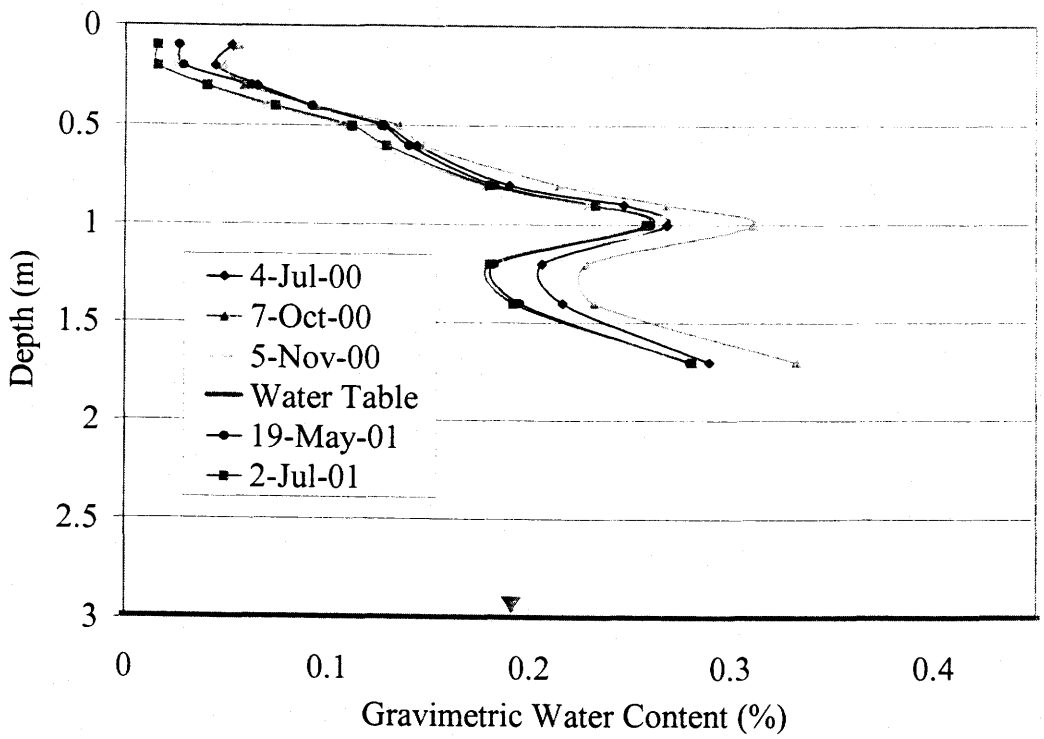

Figure 4.12 Water content profiles for bore-hole C201 from July, 2000 to July, 2001. Water table depth indicated is the approximate location as of July, 2001.

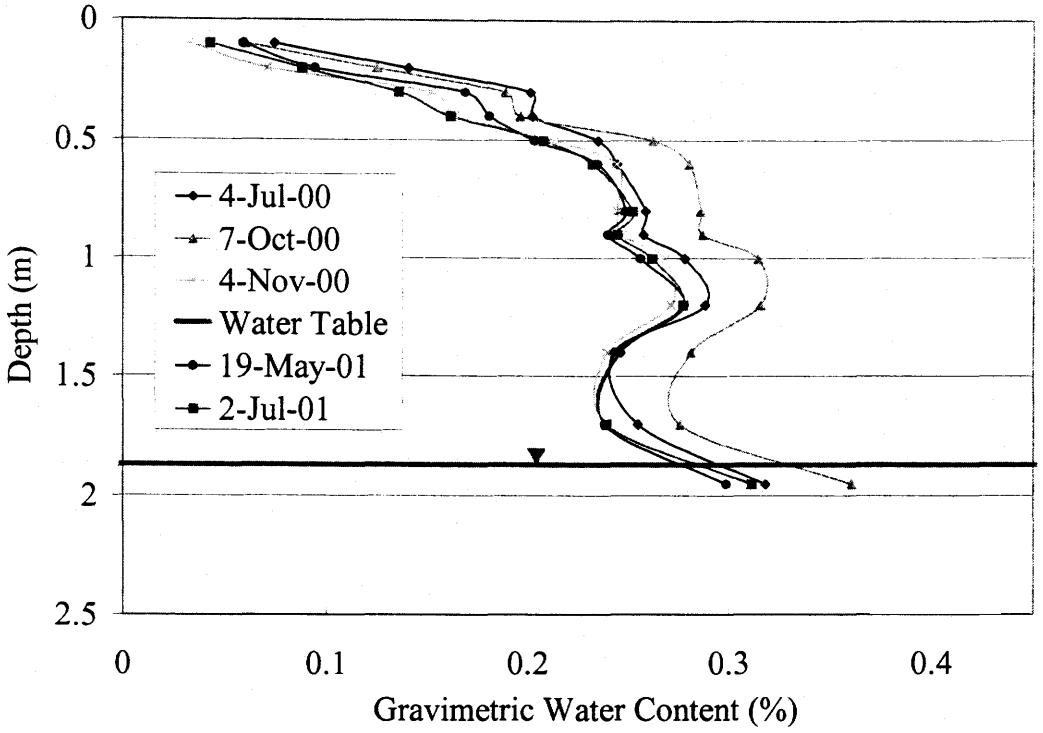

Figure 4.13 Water content profiles for bore-hole C203 from July, 2000 to July, 2001. Water table depth indicated is the approximate location as of July, 2001.

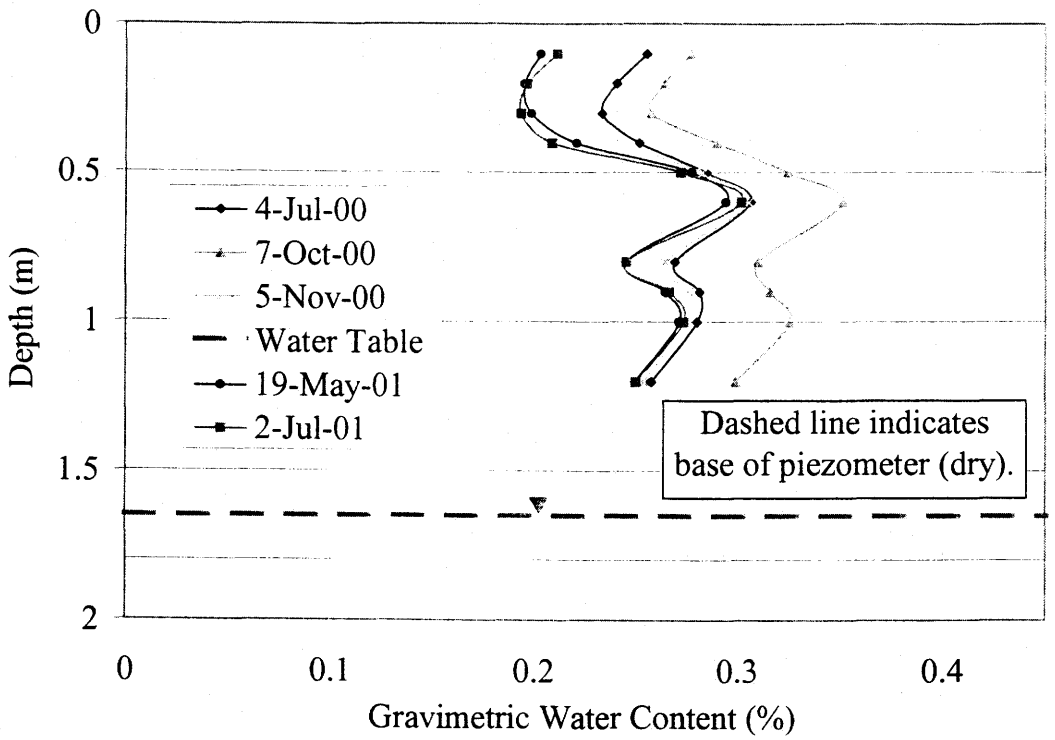

Figure 4.14 Water content profiles for bore-hole C204 from July, 2000 to July, 2001. Water table depth indicated is the approximate location as of July, 2001.

4.4.2 Weather Data

The weather station at Detour Lake Mine was programmed to measure hourly temperature, relative humidity, wind speed, wind direction, net radiation and rainfall precipitation. Every day at midnight, the program calculated the daily average, minimum and maximum temperature, minimum and maximum relative humidity, average net radiation, average windspeed and average wind direction. The weather data has been summarized in Table 4.2 which gives average, minimum and maximum values for each month and compares these results to climate normals for Timmins, Ontario. Timmins, Ontario was chosen for comparison to Detour Lake due to its proximity to the

Detour Lake site (290 km) and since Timmins has a weather station which records more detailed weather data than other stations closer to the site.

The average temperature values measured at Detour compare well with the climate normals for Timmins. The precipitation values are considerably different with the 2000/2001 year being drier than the normals values. Since precipitation due to snowfall and snowmelt was not measured, it is not known whether or not the snow precipitation was below or above average for the area. Based on the rainfall measurements, the 2000/2001 year was concluded to be a dry year.

The relative humidity values are difficult to compare since the normals values are those measured at two times throughout the day: 0600 hr and 1500 hr. The relative humidity values measured at Detour Lake are the maximum and minimum values of all the values measured throughout the day. The measured maximum relative humidity values compare fairly well to the normals but the measured minimum relative humidity values are lower than the normals values measured at 1500 hours. It is possible that being a drier than normal year, the relative humdity would be lower than average. It is also possible that 1500 hours is not when the minimum relative humidity occurs at Detour Lake.

Table 4.2 Summary of weather data from Detour Lake Mine: July, 2000 to June, 2001. Canadian climate normals for Timmins, Ontario. (Reproduced with permission of the Minister of Public Works and Government Services Canada, 2001).

	2000						2001					
	July	August	September	October	November	December	January	February	March	April	May	June
Average Temperature (°C)	16.1	15.3	9.3	4.9	-2.8	-18.2	-16.2	-18.1	-9.4	1.1	11.8	14.7
Climate Normal Temperature	16.7	15.2	10.1	4.2	-4.1	-14.6	-18.2	-16	-8.9	0.6	8.7	13.7
Maximum Temperature (°C)	22.9	21.9	20.0	14.2	9.5	-2.0	-6.0	-6.2	2.3	19.0	19.0	28.0
Climate Normal Temperature	24.3	22	16	9.3	0.3	-8.3	-10.9	-8.2	-1.1	7.5	16.1	21.4
Minimum Temperature (°C)	9.3	8.7	-1.0	-1.6	-17.3	-29.4	-27.3	-30.7	-24.0	-7.9	2.8	7.1
Climate Normal Temperature	10.3	8.9	4.4	-0.3	-8.0	-19.3	-23.7	-22	-14.9	-5.2	2.2	7.1
Precipitation (mm)	32.6	72.2	44.0	50.9	21.2	ND	ND	ND	ND	48.8	23.0	69.5
Climate Normal Precipitation	92.7	94.3	105.5	78.5	75.3	71.7	71.5	50.9	60.1	47.1	76.4	96.2
Maximum RH	0.97	0.97	0.97	0.97	1.0	0.95	0.92	0.94	0.96	0.97	0.97	0.97
Climate Normal RH - 0600	0.89	0.93	0.93	0.89	0.9	0.82	0.79	0.79	0.8	0.81	0.81	0.85
Minimum RH	0.22	0.17	0.25	0.13	0.2	0.57	0.32	0.41	0.16	0.17	0.11	0.17
Climate Normal RH - 1500	0.53	0.57	0.63	0.66	0.8	0.76	0.71	0.65	0.6	0.53	0.48	0.5
Average Net Radiation (MJ/m^2 day)	19.7	8.5	5.4	3.1	0.2	-0.9	-0.7	-0.9	0.3	8.7	11.0	10.5
Average Windspeed (km/hr)	12.1	10.9	13.0	11.2	9.9	11.9	11.2	11.2	10.5	13.1	14.0	13.5

ND = No Data

4.4.3 *In situ* Water Content and Porosity

During the installation of the instrumentation, three tailings cores were taken to determine *in situ* water content and porosity. Cores were obtained adjacent to bore-holes A202, B203 and C203. The location along each profile was chosen where the water table was approximately 1 m deep. This provided a range in water content with depth for each core. The cores were obtained using a 32 mm diameter steel corer. The cores ranged from 0.65 m to 1.2 m in length. The cores were extruded, cut into 0.15 m lengths and placed in sealed containers. The water content of each sample was measured within 24 hours. The water content measurement procedure followed the ASTM D 2216 – 92 standard for water content measurement of soils. The only variation to the method was that the samples were dried in a microwave oven since it was the only equipment available on site.

The variation of volumetric water content with depth in each of the three cores is plotted in Figure 4.15. The water content corresponding to each section of core is plotted with respect to an average depth corresponding to the mid-point of each core section. Bore-holes A202 and C203 both show a high water content layer above a low water content layer. This heterogeneity in water content supports the readings determined from the neutron probe. Variations in grain-size were noted during visual inspection of the cores. The porosity of each section of core was calculated based on the gravimetric water content and bulk density. The variation in computed porosity with depth is shown in Figure 4.16.

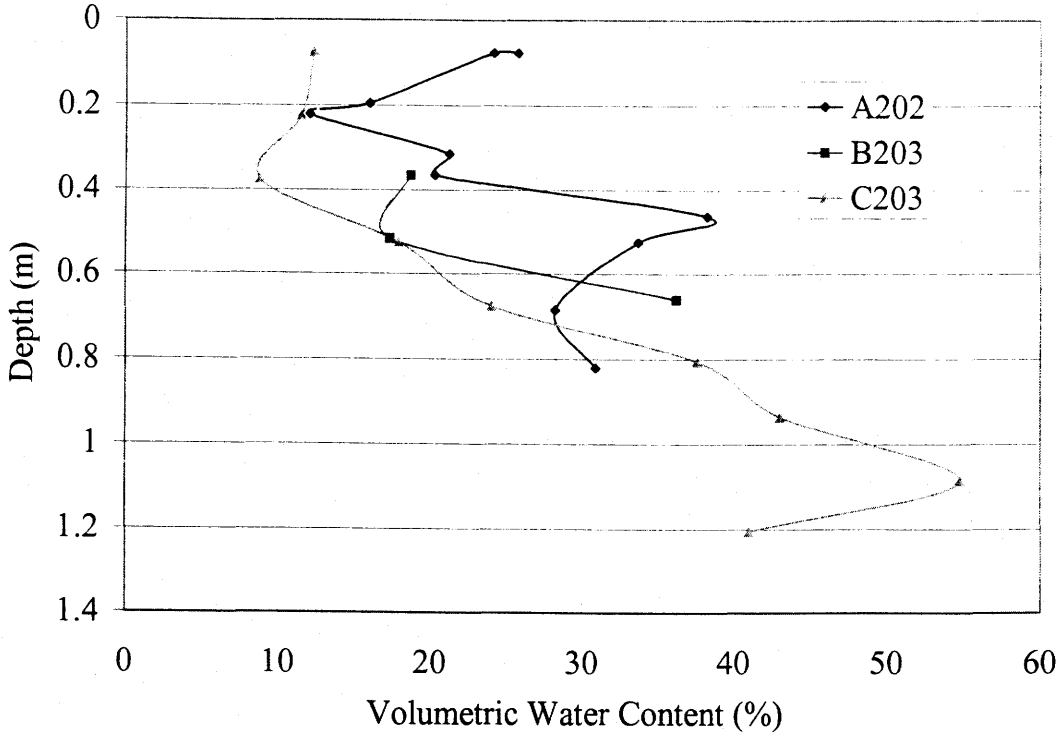

Figure 4.15 Volumetric water content with respect to depth for three core samples taken from Detour Lake Mine.

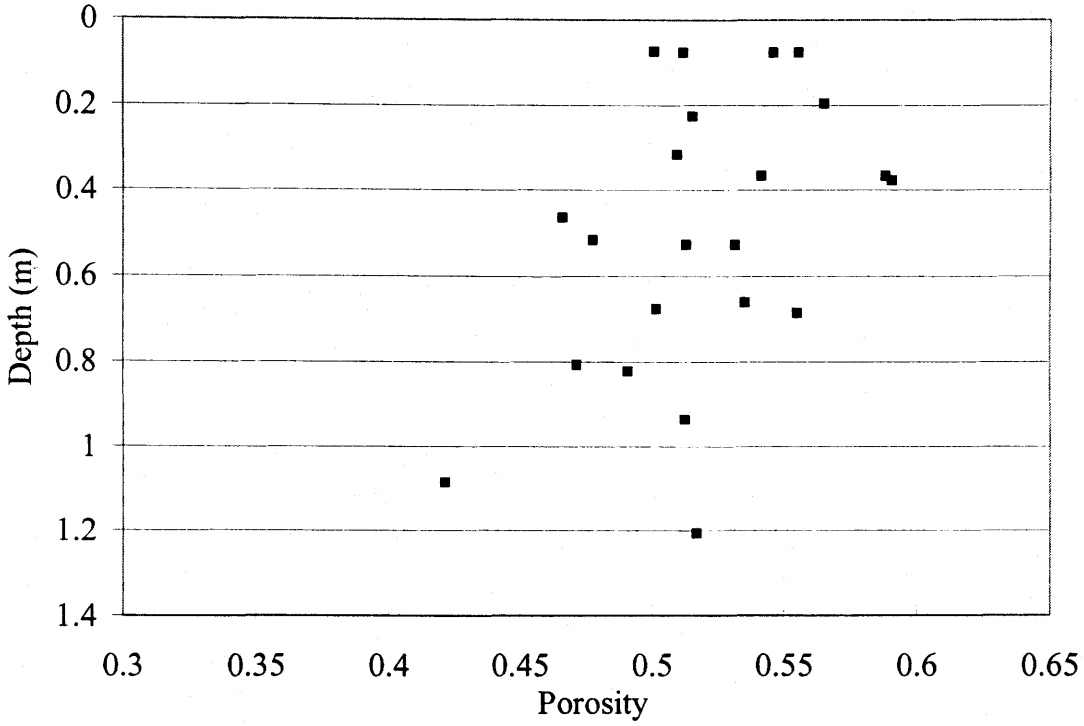

Figure 4.16 Porosity with respect to depth measured from three core samples taken from Detour Lake Mine.

4.5 SUMMARY

The field investigation for this research involved the installation of instrumentation in July, 2000 and monitoring the tailings facility over a one year period. The instrumentation consisted of nine piezometers, nine neutron probe access tubes and a weather station. The piezometers and the neutron probe access tubes were installed at nine locations representing three profiles through the tailings. During the installation, three cores were collected to determine *in situ* water content and porosity.

The monitoring program involved monthly measurements of water levels, water content profiles and weather data. Water levels and water content profiles were only measured for the frost-free months between May and October. The water levels, water content profiles and weather data obtained for Detour Lake Mine were for the period between July 5, 2000 and July 2, 2001.

Chapter 5
LABORATORY INVESTIGATION

5.1 INTRODUCTION

The following chapter describes the laboratory analyses conducted on the tailings samples from the Detour Lake tailings facility. The tailings samples used in the laboratory investigation were obtained during the installation of the field instrumentation in July, 2000.

5.2 SAMPLE DESCRIPTION

The bore-holes for the piezometers and the neutron probe access tubes described in the previous chapter were drilled using a hand auger. The auger bit used was hollow and filled with the drilled tailings. The bit held approximately 150 mm of a disturbed tailings sample. A disturbed sample was obtained at approximately every half meter of the piezometer bore-holes. A total of 41 samples were bagged, labeled and shipped back to the University of Saskatchewan, Saskatoon, for laboratory analysis.

The objective of the laboratory analyses was to obtain measurements of the geotechnical and geochemical characteristics for both the sulphidic and the desulphurized tailings in the Detour Lake tailings facility. Representative samples of both types of tailings were required for the laboratory analysis. There was no visual difference between the two types of tailings and there was no information as to how thick the desulphurized tailings cover was. Therefore, it was necessary to establish a

method of distinguishing between the two types of tailings before the representative samples could be chosen. Grain-size analyses of the tailings were conducted in an attempt to discriminate between the two types of tailings. Theoretically, the sulphide minerals occur in a specific grain-size fraction and when this fraction is removed, the grain-size distribution of the tailings changes.

5.3 GEOTECHNICAL CHARACTERIZATION

The geotechnical characterization of the Detour Lake tailings samples was completed at the University of Saskatchewan, Saskatoon. The testing program consisted of grain-size analyses, saturated hydraulic conductivity measurement, specific gravity measurement and measurement of the soil-water characteristic curve. A summary of the samples indicating which tests were performed is given in Table 5.1.

Table 5.1 Summary of samples used for geotechnical testing.

Sample Description	Grain-size Analysis	Saturated Hydraulic Conductivity	Soil-Water Characteristic Curve
A201 0.45-0.60	Y		
A201 1.30-1.45	Y	Y	Y
A201 2.7-2.85	Y		
A202 1.0-1.15	Y		
A202 1.7-1.88	Y		
A203 0.4-0.55	Y		
A203 1.45-1.6	Y		
B201 0.8-1.0	Y	Y	Y
B201 0-0.2	Y	Y	Y
B201 2-2.2	Y		
B201 3.1-3.3	Y		
B201 4.5-4.7	Y		
B202 0.85-1.0	Y		
B202 1.85-2.0	Y		
B202 2.7-2.9	Y		
B203 0-0.2	Y	Y	Y
C201 0.4-0.55	Y		
C201 1.65-1.80	Y	Y	Y
C203 0.85-1.0	Y		
C203 1.85-2.0	Y		
C204 0.35-0.50	Y		
C204 1.30-1.45	Y	Y	Y

5.3.1 Grain-size Analyses

Grain-size analyses were performed on 22 of the 41 samples obtained from the Detour Lake tailings facility. The samples represented approximately every metre of bore-hole depth. The samples were tested according to ASTM D 422 – 63: The Standard Test Method for Particle-Size Analysis of Soils. The results of the grain-size analyses indicated that the tailings become finer with depth. The grain-size distributions for all the samples tested are presented in Appendix D. Figure 5.1 illustrates six typical samples chosen for further testing. As illustrated in Figure 5.1, the grain-size distributions of the Detour Lake tailings show considerable variation. The measured grain-size distributions confirm the field observation of interbedded layers of silt/clay-sized materials with fine sand-sized particles.

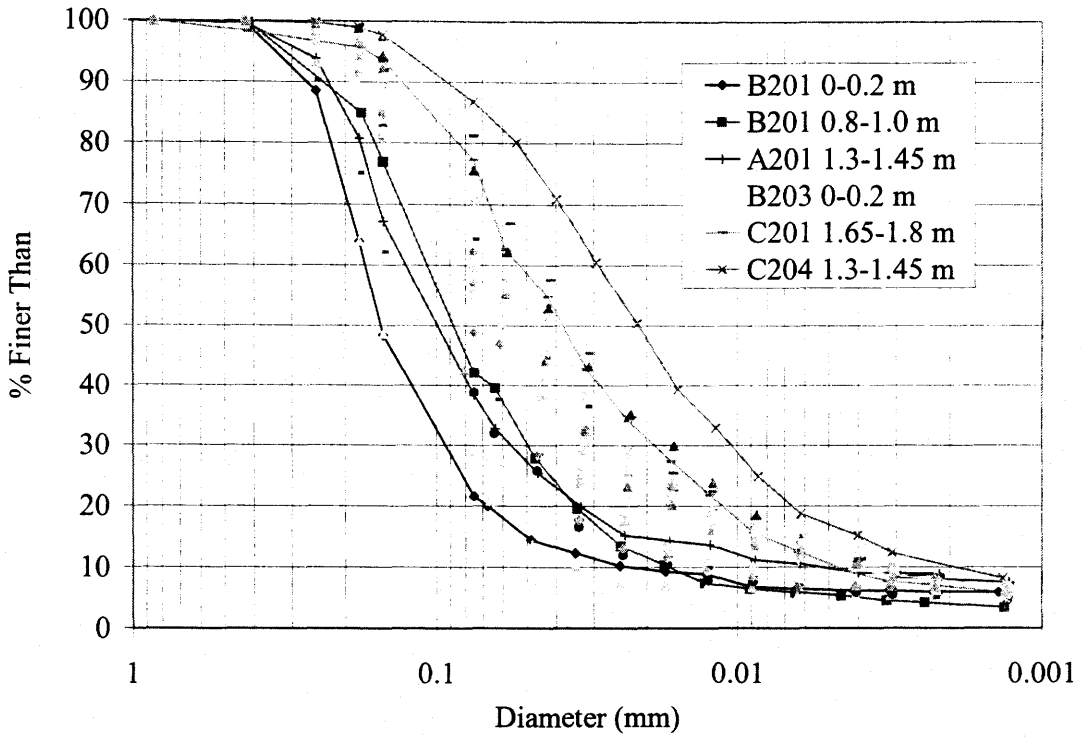

Figure 5.1 Grain-size distributions for Detour Lake tailings samples illustrating the six samples chosen for the remainder of the laboratory testing.

5.3.2 Representative Samples Chosen for Geotechnical Testing

A total of six representative samples were chosen on which to perform the remainder of the geotechnical testing. The samples represented the coarse, mid-range and fine grain-size distributions for each of the desulphurized and sulphidic tailings. The following discussion describes the methodology used to choose the six representative samples.

The main difficulty in choosing representative samples of desulphurized and sulphidic tailings was to determine a characteristic of the tailings which could discriminate between desulphurized and sulphidic tailings. The desulphurized tailings were known to be a surface layer. Since the tailings tended to be slightly finer with depth, it was assumed that the sulphidic tailings were finer than the desulphurized tailings. From the coarse half of the tailings samples, the samples B201 0 – 0.2 m, B201 0.8 – 1.0 m and A201 1.3 – 1.45 m were chosen to represent the coarse, mid-range and finest desulphurized tailings, respectively. From the fine half of the tailings samples, the samples B203 0 – 0.2 m, C201 1.65 – 1.8 m and C204 1.3 – 1.45 m were chosen to represent the coarse, mid-range and finest sulphidic tailings, respectively. The grain-size distributions of the six samples are illustrated in Figure 5.1. A subsequent geochemical analysis (See Section 5.4) confirmed that these were reasonable choices except for two samples: A201 1.3 – 1.45 m and B203 0 – 0.2 m. These samples had initially been designated as the incorrect type of tailings. By changing the desulphurized/sulphidic designation of the two samples, the six samples represented a reasonable choice for fine, mid-range and coarse for both the desulphurized and the

sulphidic tailings. The samples chosen for the remainder of the laboratory testing, with their final designations, are summarized in Table 5.2.

Table 5.2 Summary of six samples selected for geotechnical testing.

Particle Size	Sulphidic	Desulphurized
Coarse	A201 1.3 – 1.45 m	B201 0 – 0.2 m
Mid-range	C201 1.65 – 1.8 m	B201 0.8 – 1.0 m
Fine	C204 1.3 – 1.45 m	B203 0 – 0.2 m

5.3.3 Saturated Hydraulic Conductivity Measurement

The saturated hydraulic conductivity of the six tailings samples was measured using a modified consolidation/falling-head permeameter. Details regarding this apparatus and testing method can be found in Barbour (1986). The samples were slurried and placed in a ring. The ring was situated on the surface of a ceramic stone to maintain the saturation of the samples. A compressive load was applied to the sample and was incrementally increased up to 1000 kPa. At each consolidation increment, the saturated hydraulic conductivity was measured using the falling-head method. Deionized water was used for the falling-head test. The results of the saturated hydraulic conductivity tests for the desulphurized and the sulphidic tailings are presented in Figure 5.2 and Figure 5.3, respectively.

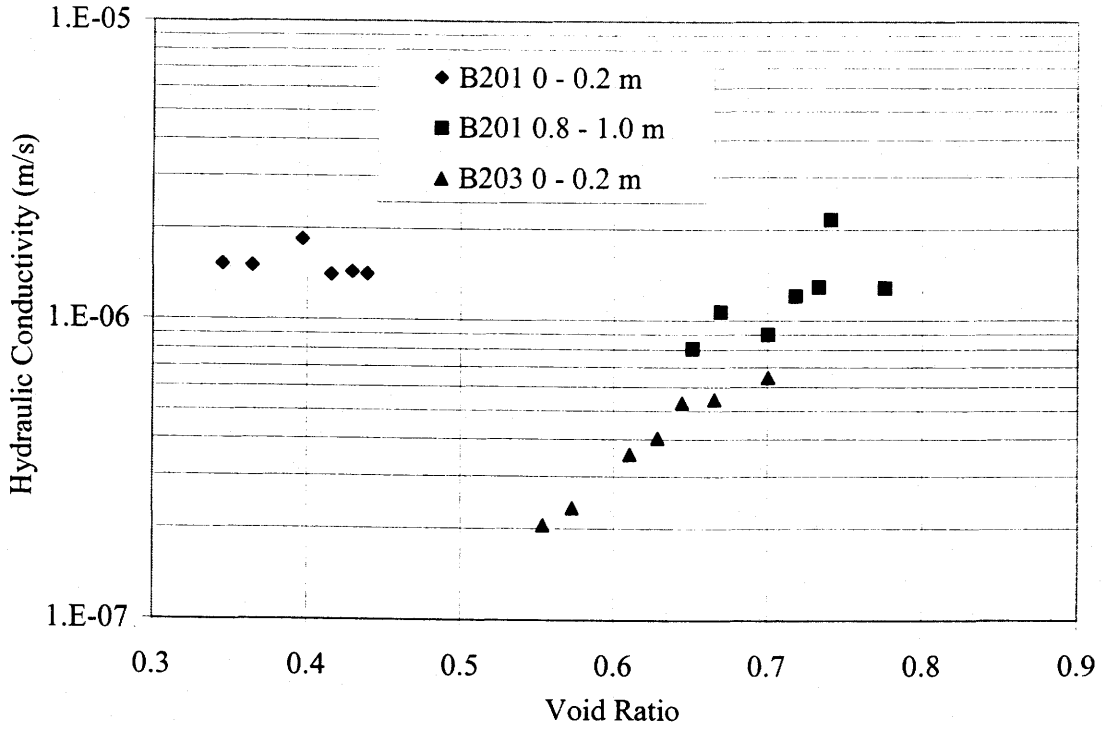

Figure 5.2 Saturated hydraulic conductivity of the desulphurized tailings samples.

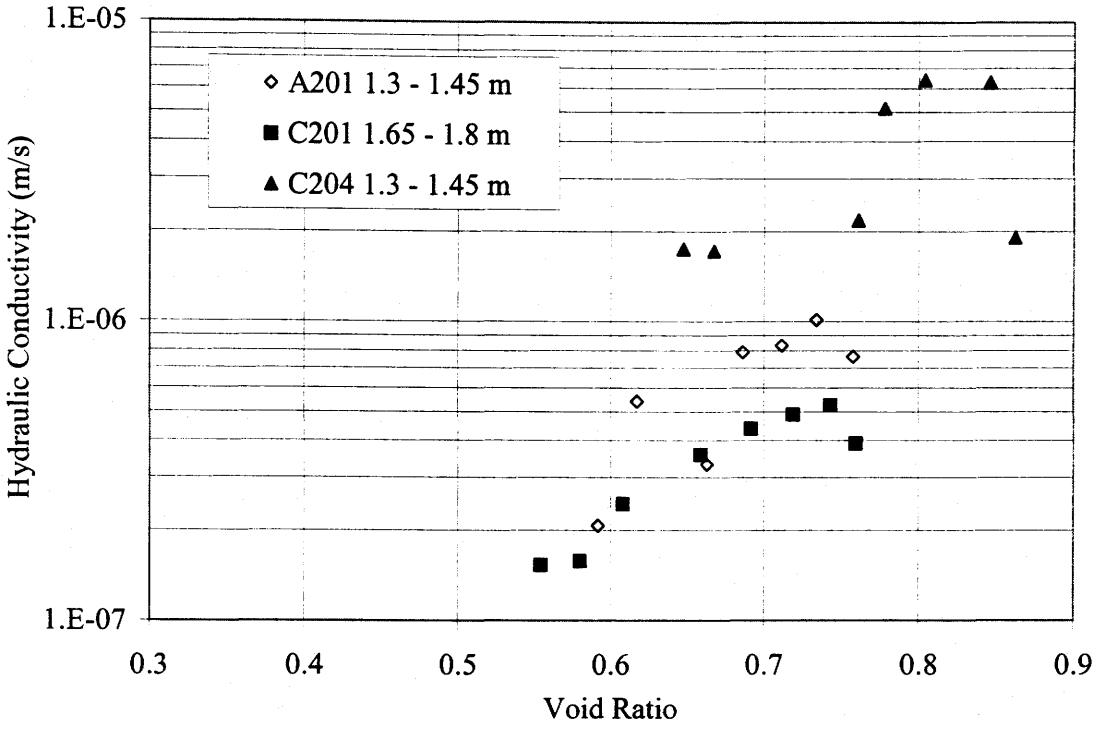

Figure 5.3 Saturated hydraulic conductivity of the sulphidic tailings samples.

The results of the saturated hydraulic conductivity show k_{sat} values falling in the range of 2 x 10^{-6} to 1 x 10^{-7} m/s for all the samples except for sample C204 1.3 – 1.45 m which varied between 1 x 10^{-5} and 1 x 10^{-6} m/s. Based on the grain-size distribution results, it can be seen that C204 1.3 – 1.45 m is the finest of the six samples. Therefore, it is considered unlikely that this sample would have the highest saturated hydraulic conductivity. Difficulties were encountered during testing and the data was considered not reliable. It is reasonable to conclude that the saturated hydraulic conductivity for all samples generally falls between 2 x 10^{-6} to 1 x 10^{-7} m/s.

5.3.4 Soil-Water Characteristic Curve Measurement

The soil-water characteristic curves for the six tailings samples were measured using a pressure plate apparatus (i.e. Tempe type cell). Details regarding this apparatus and testing method can be found in Fredlund and Rahardjo (1993). The samples were slurried and placed in a ring. The ring was placed inside a retaining cylinder on the surface of a high air-entry ceramic disk. The matric suction of the samples was incrementally increased first by controlling the negative water pressure on the sample and secondly, by generating positive air pressure inside the retaining cylinder. At each suction increment, the sample was weighed to determine the mass of water lost since the previous suction increment. This information was used at the end of the test to calculate the water content of the sample at each suction increment. The soil-water characteristic curves for the desulphurized and sulphidic tailings samples are presented in Figure 5.4 and Figure 5.5, respectively.

As illustrated in the two figures, the air-entry values for the desulphurized tailings vary between 6 and 20 kPa. The air entry values for the sulphidic tailings were found to

range between 8 and 50 kPa. Two of the three sulphidic tailings samples tested had an air entry value of 50 kPa. Given this, it can be postulated that the sulphidic tailings would more likely have an air entry value in the range of 50 kPa than 8 kPa. In summary, it can be generalized that the air entry value of the sulphidic tailings tends to be higher than that for the desulphurized tailings.

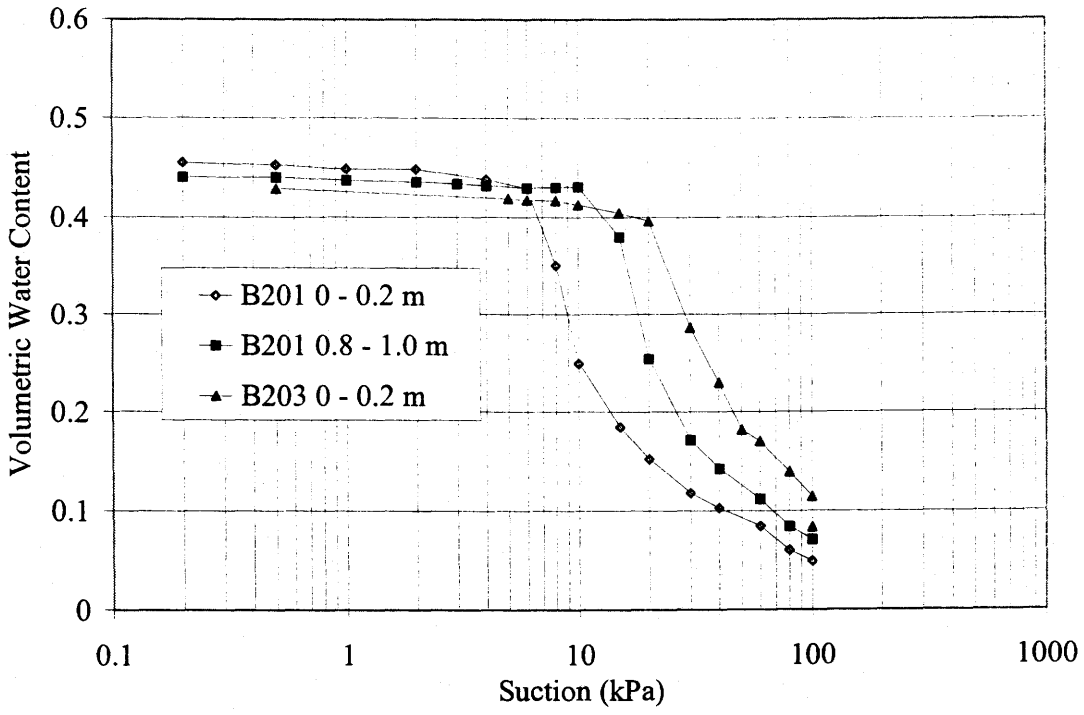

Figure 5.4 Soil-water characteristic curves for the desulphurized tailings samples.

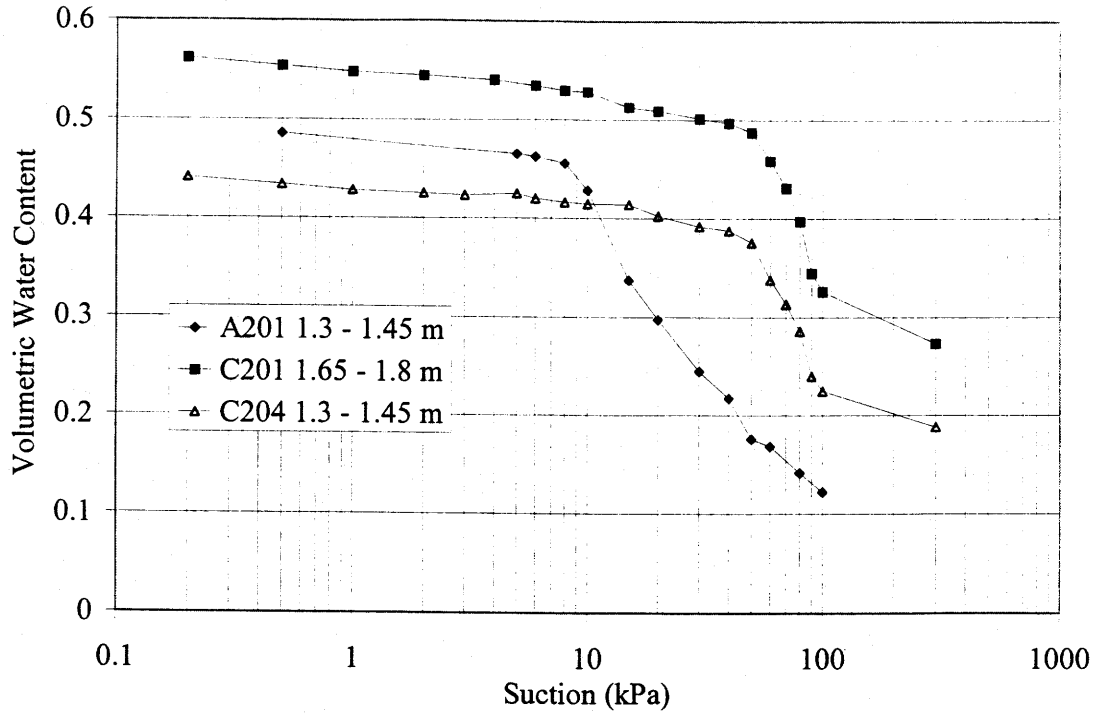

Figure 5.5 Soil-water characteristic curves for the sulphidic tailings samples.

5.3.5 Specific Gravity Measurement

Specific gravity analyses were performed on samples of both the desulphurized and the sulphidic tailings. The testing method followed ASTM D854 – 92: The standard test method for specific gravity of soils. Both the boiling procedure and the use of de-aired water was used as the air removal method. One sample of desulphurized tailings and two samples of sulphidic tailings were measured. The specific gravity was determined to be 2.87 for the desulphurized tailings and an average of 2.91 for the sulphidic tailings. The specific gravity values were used for calculation of the grain-size distribution, the soil-water characteristic curve, the saturated hydraulic conductivity measurement and the diffusion and kinetic cell testing.

5.4 GEOCHEMICAL AND MINERALOGICAL CHARACTERIZATION

The geochemical and mineralogical characterization of the Detour Lake tailings samples were conducted outside of the University of Saskatchewan, Saskatoon. The following sections describe the results of acid base accounting tests, mineralogy evaluations, and diffusion and kinetic cell testing.

5.4.1 Acid Base Accounting and Mineralogy

All of the tailing samples obtained during the field investigation were sent for geochemical analyses to the Placer Dome Inc. research laboratory in Vancouver, BC. Static acid base accounting tests were conducted on a total of 38 samples representing both desulphurized and sulphidic tailings. Details on the methods of these analyses can be found in Lawrence and Scheske (1997), Lawrence and Wang (1997) and Lapakko (1994). The results of these analyses are summarized in Table 5.3. The results for the sulphide sulphur analysis indicate definitively which tailings were desulphurized and which were sulphidic. The sulphide sulphur values in % tended to fall into two categories: less than 1% and greater than 1%. It was concluded that the desulphurized tailings had a sulphide sulphur content of less than 1% while the sulphidic tailings had a sulphide sulphur content of greater than 1%. Based on this criteria, it was determined that the desulphurized tailings cover at Detour Lake Mine ranges in thickness from 1 to 1.5 m.

Table 5.3 Summary of acid base accounting test results for tailings samples from all bore-holes.

Sample Description	% C (Leco)	S % (Leco)	*SO4 %	Sulphide S %	Tons $CaCO_3$ Equivalent/Thousand Tons Material		Paste pH	NAG pH
					Net Neutralization Potential	NNPs (based on S2 - S)		
A201 0.45-0.60	0.22	0.72	0.45	0.57	5	9	7.70	9.88
A201 0.86-1.00	0.23	0.41	0.38	0.28	13	17	7.40	10.70
A201 1.30-1.45	0.07	3.08	1.44	2.60	-88	-73	5.42	2.55
A201 1.95-2.12	0.27	1.90	0.42	1.76	-26	-22	7.67	2.95
A201 2.7-2.85	0.27	2.40	0.42	2.26	-44	-40	7.77	2.66
A202 0.50-0.65	0.18	0.51	0.41	0.37	7	11	7.88	10.20
A202 1.0-1.15	0.25	0.54	0.39	0.41	11	15	7.68	11.00
A202 1.3-1.45	0.29	1.15	0.66	0.93	-5	2	7.44	10.10
A202 1.7-1.88	0.21	2.42	0.90	2.12	-57	-47	7.14	2.60
A203 0.4-0.55	0.19	0.99	0.56	0.80	-6	0	7.82	3.20
A203 0.88-1.00	0.26	0.36	0.22	0.29	20	22	7.88	11.10
A203 1.45-1.6	0.31	1.42	0.59	1.22	-18	-12	7.42	9.56
B201 0.3-0.5	0.25	1.19	0.47	1.03	-7	-2	7.89	3.03
B201 0.8-1.0	0.22	0.72	0.38	0.59	5	8	7.71	9.87
B201 0-0.2	0.28	1.00	0.39	0.87	1	5	8.01	3.87
B201 2.6-2.8	0.18	1.45	0.29	1.35	-18	-15	7.57	10.40
B201 4.5-4.7	0.17	2.89	0.47	2.73	-65	-60	7.63	2.84
B202 0.3-0.5	0.27	0.62	0.58	0.43	3	9	7.76	10.90
B202 0.85-1.0	0.18	0.78	0.67	0.56	0	7	7.65	8.20
B202 1.35-1.50	0.28	0.89	0.42	0.75	-7	-2	7.83	9.20
B202 1.85-2.0	0.18	1.10	0.41	0.96	-10	-6	7.65	2.90
B202 2.45-2.55	0.14	1.71	1.19	1.31	-40	-28	6.90	2.70
B202 2.7-2.9	0.17	2.42	1.56	1.90	-51	-34	7.05	2.81
B203 0-0.2	0.29	0.94	0.42	0.80	-17	-13	7.34	9.76
B203 1.2-1.4	0.23	0.66	0.46	0.51	7	12	7.24	10.10
C201 0.4-0.55	0.26	0.65	0.45	0.50	-6	-2	7.74	10.80
C201 0.90-1.05	0.22	0.72	0.58	0.53	-10	-3	7.46	10.80
C201 1.65-1.80	0.15	2.00	1.22	1.59	-41	-28	7.24	3.06
C201 2.0-2.15	0.16	2.24	0.68	2.01	-61	-54	7.12	2.75
C203 0.35-0.50	0.23	0.82	0.37	0.70	2	6	8.26	8.23
C203 0.85-1.0	0.16	1.17	0.41	1.03	-16	-11	7.64	2.71
C203 1.2-1.35	0.27	1.14	0.32	1.03	-16	-12	7.65	10.50
C203 1.85-2.0	0.22	2.58	0.68	2.35	-55	-48	7.00	2.73
C204 0.35-0.50	0.29	0.53	0.41	0.39	4	9	8.10	10.90
C204 0.85-1.0	0.26	0.67	0.34	0.56	-3	1	7.90	10.30
C204 1.30-1.45	0.31	1.44	0.65	1.22	-12	-5	7.68	10.70
Depyr #1	0.29	0.11	0.19	0.05	9	11	8.27	11.40
Depyr #2	0.29	0.09	0.16	0.04	8	10	8.20	11.30

Samples of both the desulphurized and the sulphidic tailings were tested for their mineralogy using X-ray diffraction analysis and petrography (Bernier, 2001). Details on the mineralogical evaluation of mining waste can be found in Plumlee and Logsdon (1999) and Jambor and Blowes (1994). A summary of the mineralogical analysis is presented in Table 5.4. The results of the analysis show that the desulphurized and the sulphidic tailings have similar mineralogy. The primary minerals in both types of tailings are the same: quartz, albite, chlorite and micas. Of the secondary minerals, the sulphidic tailings have slightly more amphibole and pyrite and slightly less augite than the desulphurized tailings.

Table 5.4 Mineralogy for desulphurized and sulphidic tailings samples (Bernier, 2001).

Mineral	Sulphidic Sample	Desulphurized Sample
Quartz	VA	VA
Albite	LA	LA
Chlorite	LA	LA
Micas	M	M
Augite	nd	T
Amphibole	LA	T
Carbonates	na	na
Magnetite	T	T
Gypsum	T	T
Pyrite	M	T

VA very abundant >50%
A abundant 30 - 50%
LA less abundant 10 - 30%
M minor 2-10%
T <2%
nd not detected
na not available

5.4.2 Diffusion and Kinetic Cell Testing

Samples of both the desulphurized and the sulphidic tailings were analyzed by École Polytechnique in Montréal, QC. The samples were tested using a diffusion/kinetic cell to measure the diffusion and kinetic oxidation coefficients of the tailings. A detailed description of the apparatus and test method can be found in Aubertin *et al.* (2000). The test involves placing the tailings sample inside a cylinder on a perforated plate. The apparatus is first flushed with nitrogen to purge any oxygen in the sample pores. A finite oxygen concentration is created in an upper reservoir above the tailings. This oxygen is allowed to diffuse through the tailings. The decreasing concentration in the upper reservoir and the increasing concentration in the lower reservoir are measured with time. Using these two concentration curves, both the diffusion coefficient and the kinetic oxidation coefficient can be calculated.

Table 5.4 Sample conditions and results of the diffusion and kinetic oxidation coefficient testing for a desulphurized tailings sample.

Porosity (n)	0.443
Degree of Saturation (S)	82.4%
Equivalent Porosity (n_{eq})	0.089
Diffusion Coefficient (D^*)	2.14 x 10^{-7} m^2/s
Kinetic Oxidation Constant (k_r^*)	112 /yr
Effective Diffusion Coefficient (D_e)	1.9 x 10^{-8} m^2/s
k_r ($= n_{eq}k_r^*$)	10 /yr

Diffusion and kinetic oxidation testing was completed for a sample of desulphurized tailings obtained near bore-hole B201. A 30 kg sample was obtained by removing the surface 0.2 m of tailings and taking a sample of the underlying tailings using a shovel.

The results of the diffusion and kinetic oxidation cell testing along with the conditions used for the testing are summarized in Table 5.4.

5.5 SUMMARY

The purpose of the laboratory investigation was to determine the geotechnical and geochemical characteristics of the Detour Lake tailings. The geotechnical characterization involved grain-size analyses, saturated hydraulic conductivity measurement, specific gravity measurement and measurement of the soil-water characteristic curve. Based on the grain-size results and the geochemical testing results, six representative samples were chosen for the saturated hydraulic conductivity measurement and the soil-water characteristic curve measurement.

The geochemical characterization consisted of acid base accounting tests, a mineralogy evaluation and diffusion and kinetic cell testing. The geochemical tests were performed by Placer Dome Inc. and École Polytechnique.

Both the field and laboratory investigations yielded information on which to make conclusions regarding the effectiveness of the desulphurized tailings cover at Detour Lake Mine. The following chapter is an analysis of the information determined from the field and laboratory investigations.

Chapter 6
ANALYSIS AND DISCUSSION

6.1 INTRODUCTION

The purpose of the research program was to evaluate the effectiveness of a desulphurized tailings cover as a barrier to reduce oxygen diffusion into the sulphidic tailings at the Detour Lake Mine site. The desulphurized tailings cover was designed to function in two ways: first, by maintaining a high level of saturation to reduce the oxygen diffusion coefficient and secondly, by creating an oxygen sink where the small percentage of remaining sulphide minerals oxidized can consume any oxygen that may diffuse into the cover layer. To determine the effectiveness of this cover, a field analysis, laboratory analysis and modeling analysis were completed. The following chapter describes the analysis completed for the field and laboratory results that were presented in the previous two chapters together with the results of the numerical modeling.

The analysis of the field and laboratory results was intended to satisfy two goals. The first goal was to use the field and laboratory results to make qualitative conclusions regarding the effectiveness of the desulphurized tailings cover. The second goal was to establish representative profiles for performing numerical simulations to predict oxygen concentration profiles and mass flux. Since some tailings properties required by the numerical models were not measured in the field and laboratory analysis, a secondary

goal was to evaluate the accuracy of theoretical equations to predict the properties of the tailings such as diffusion coefficient and kinetic oxidation coefficient.

The purpose of the numerical modeling program was to predict the performance of the desulphurized tailings cover and to determine the relative effect of various weather scenarios, water table depths and vegetation scenarios. The relative effect of each of these factors could then be evaluated with respect to different theoretical tailings profiles. The primary parameters used to determine the effectiveness of the desulphurized cover were the oxygen concentration with respect to depth and the resulting oxygen flux into the sulphidic tailings. To evaluate the effect of weather, water table depth and vegetation on oxygen diffusion, it was necessary to first describe the effect of these factors on the degree of saturation in the tailings profile since it is the primary variable that controls the rate of oxygen diffusion.

The SoilCover model was selected to predict the saturation profiles in the tailings. SoilCover is a one-dimensional finite element model that predicts the exchange of water and energy between the atmosphere and the soil surface (SoilCover User's Manual, 1997). SoilCover uses daily weather data along with the growing season and quality of vegetation to predict the daily saturation profiles for a given material profile and water table. The model is useful in evaluating the relative effect of variations in material properties, daily weather data, different qualities of vegetation and different water table depths for a variety of different material profiles.

To calculate the oxygen concentration profiles and oxygen fluxes based on the SoilCover saturation profiles, a method of predicting transient oxygen diffusion and consumption through an unsaturated tailings profile was required. A finite difference solution was developed to predict coupled oxygen diffusion and consumption based on

Fick's Law and first order kinetic oxidation. This model was designed to use the same one-dimensional nodal mesh for the SoilCover simulations and to use the SoilCover saturation profiles as input.

Chapter 6 describes the development of the profiles used in the SoilCover modeling, the selection of weather and vegetation scenarios and summarizes the SoilCover modeling results. The chapter also describes the development of the profiles used in the oxygen diffusion and consumption modeling and a summary of the modeling results.

6.2 ANALYSIS OF FIELD AND LABORATORY RESULTS

The following two sections describe the analysis of the field and laboratory results. The first section is the analysis performed on the diffusion and kinetic cell testing results. The second section is an analysis of the tailings facility based on the results of the geochemical evaluation.

6.2.1 Analysis of Diffusion and Kinetic Cell Testing Results

Diffusion and kinetic cell testing was performed on one sample of the desulphurized tailings at Detour Lake Mine. Empirical equations describing the diffusion coefficient and kinetic oxidation coefficient were described in Chapter 3. These equation were used to predict the diffusion and kinetic coefficients for both types of tailings over a range of grain-size distributions. The measured results were compared with the calculated results to verify that the empirical relationships were suitable for the tailings material and conditions.

The comparison of the measured and calculated results is summarized in Table 6.1. The kinetic coefficient was calculated using the Collin (1998) method as described in

Equation 3.18. The values for D_{10} and D_{60} were taken from the grain-size distribution of sample B201 0 – 0.2 m since this sample represented the same location as the sample used for the diffusion and kinetic testing. The diffusion coefficient was calculated using the modified Millington and Shearer method as described in Equation 3.12.

Table 6.1 Comparison of measured diffusion and kinetic cell data with results from empirical calculations.

Coefficient	Measured	Calculated
k_r	10 /yr	7.1 /yr
D_e	1.9 x 10^{-8} m^2/s	1.2 x 10^{-8} m^2/s

The measured and calculated results were similar. It was concluded that the empirical estimations were sufficient for estimating the diffusion coefficient and kinetic oxidation coefficient for the Detour Lake Mine tailings.

6.2.2 Analysis of Geochemical Results

A geochemical analysis of the tailings consisting of static acid base accounting tests was performed on 38 of the tailings samples as summarized in Table 5.2. The primary purpose of the geochemical laboratory testing was to predict whether or not the tailings may produce acid rock drainage (ARD). The major indicators of acid generation are the net neutralization potential (NNP) and the net acid generation (NAG) pH values. The net neutralization potential defines the amount of neutralizing capacity of the system above what would be required to neutralize the acid producing constituents. In general, a positive NNP indicates that the system has adequate buffering capacity for the acid that would be produced if all the sulphidic minerals oxidized. This is not a definite

measure of whether or not ARD will occur. A comparison of the NNP with the NAG pH is a helpful indication for predicting ARD. A comparison for both the desulphurized and the sulphidic tailings is presented in Figure 6.1.

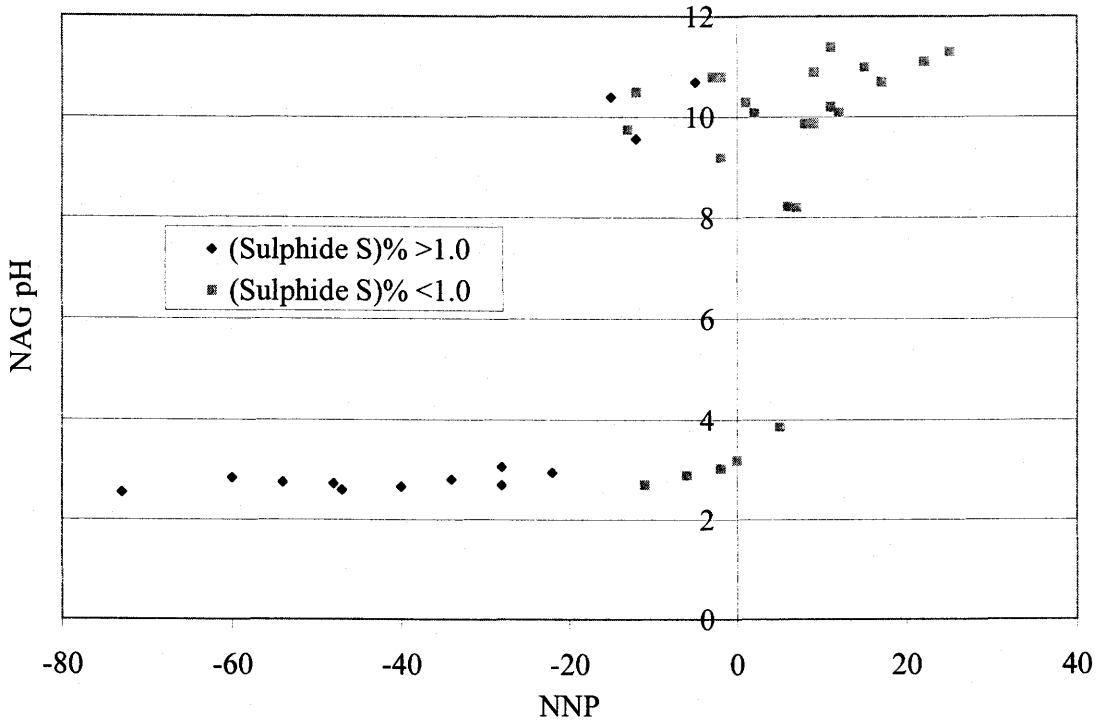

Figure 6.1 NAG pH versus NNP for the desulphurized tailings (Sulphide S % <1.0) and the sulphidic tailings (Sulphide S % >1.0).

It can be seen in Figure 6.1 that some samples have a NNP greater than zero but still generate an acidic pH. Conversely, some samples have values for NNP less than zero but generate an alkaline pH. Based on Figure 6.1, the tailings can be divided into three groups: tailings that will potentially generate acid, tailings that will not generate acid and tailings for which there is uncertainty with respect to acid generation. As illustrated in Figure 6.1, tailings with a NNP between approximately –15 and 5 (tons $CaCO_3$ equivalent per thousand tons material) may or may not produce acidic pH. Tailings with a NNP greater than 5 do not produce acidic pH and tailings with a NNP less than –15

produce acidic pH. Figure 6.2 visually summarizes the NNP, NAG pH and sulphide sulphur content results as they vary with depth in each bore-hole. The sulphide sulphur (%) increases with depth as expected as the tailings change from desulphurized to sulphidic. In each bore-hole, there is a noticeable change in the sign of the NNP values from positive near the surface to negative. Based on the criteria determined in Figure 6.1, each bore-hole was classified into three layers: 1) non-acid generating, ii) uncertain, and iii) acid generating. The approximate thickness of each layer as well as the location where the tailings become greater than 85% saturated is presented in Figure 6.3. Since the layer thicknesses and saturation boundaries are approximate, Figure 6.3 can only be used to make qualitative conclusions.

As indicated by Figure 6.3, bore-holes A201, B201, C201 and C203 are less than 85% saturated as deep as the acid producing tailings layer. This indicates that oxygen may diffuse in relatively large quantities to the acid generating tailings and produce acidity. Bore-holes A202, B202, B203 and C204 are greater than 85% saturated in the acid producing tailings layer but some of the uncertain layer tailings are unsaturated. This indicates that oxygen may reach the uncertain layer but it is not known whether this layer will generate acidity. A201 is the only bore-hole where the entire depth of the uncertain layer is saturated and therefore unlikely to produce acidity.

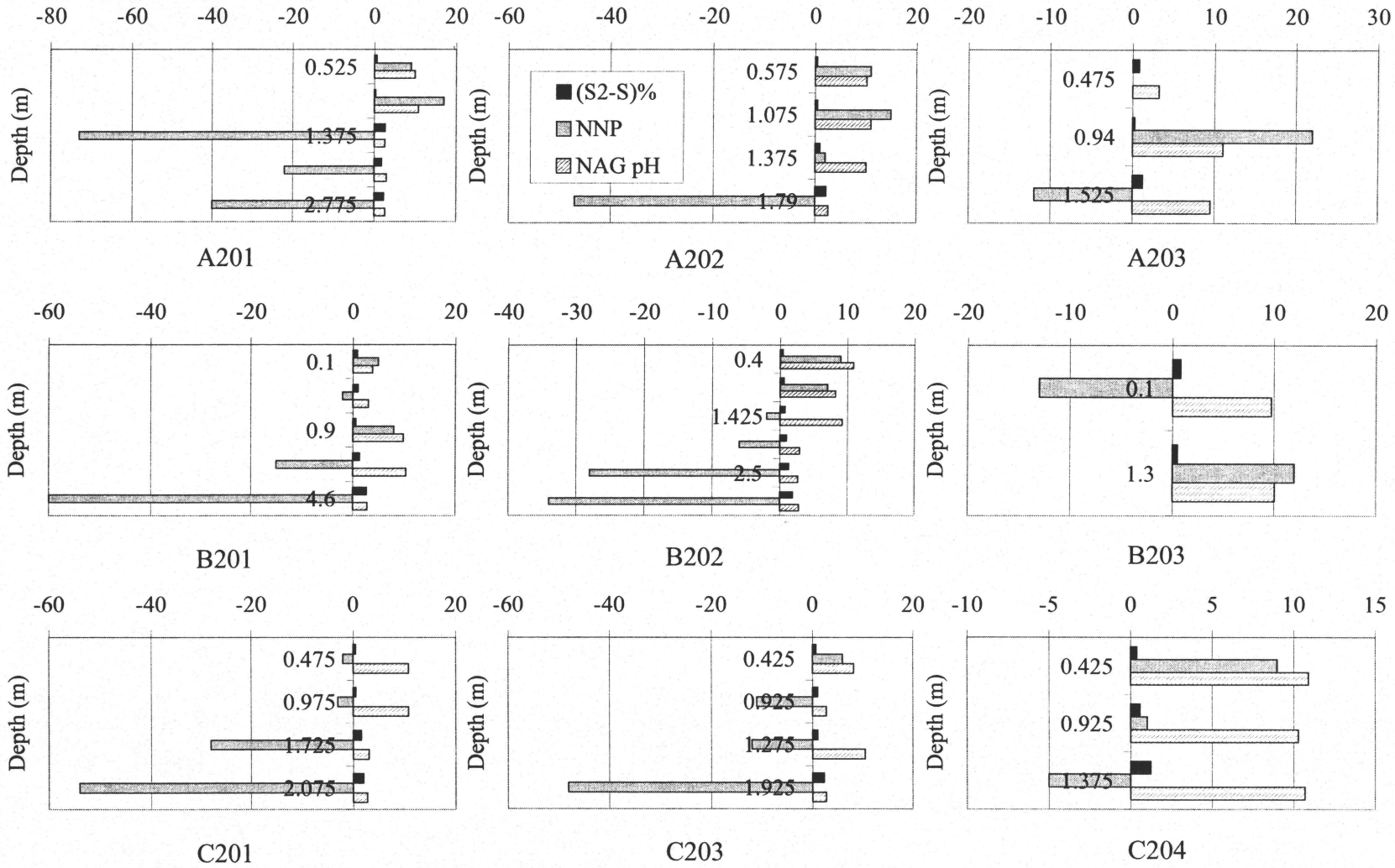

Figure 6.2 Summary of geochemical data with depth for all bore-holes

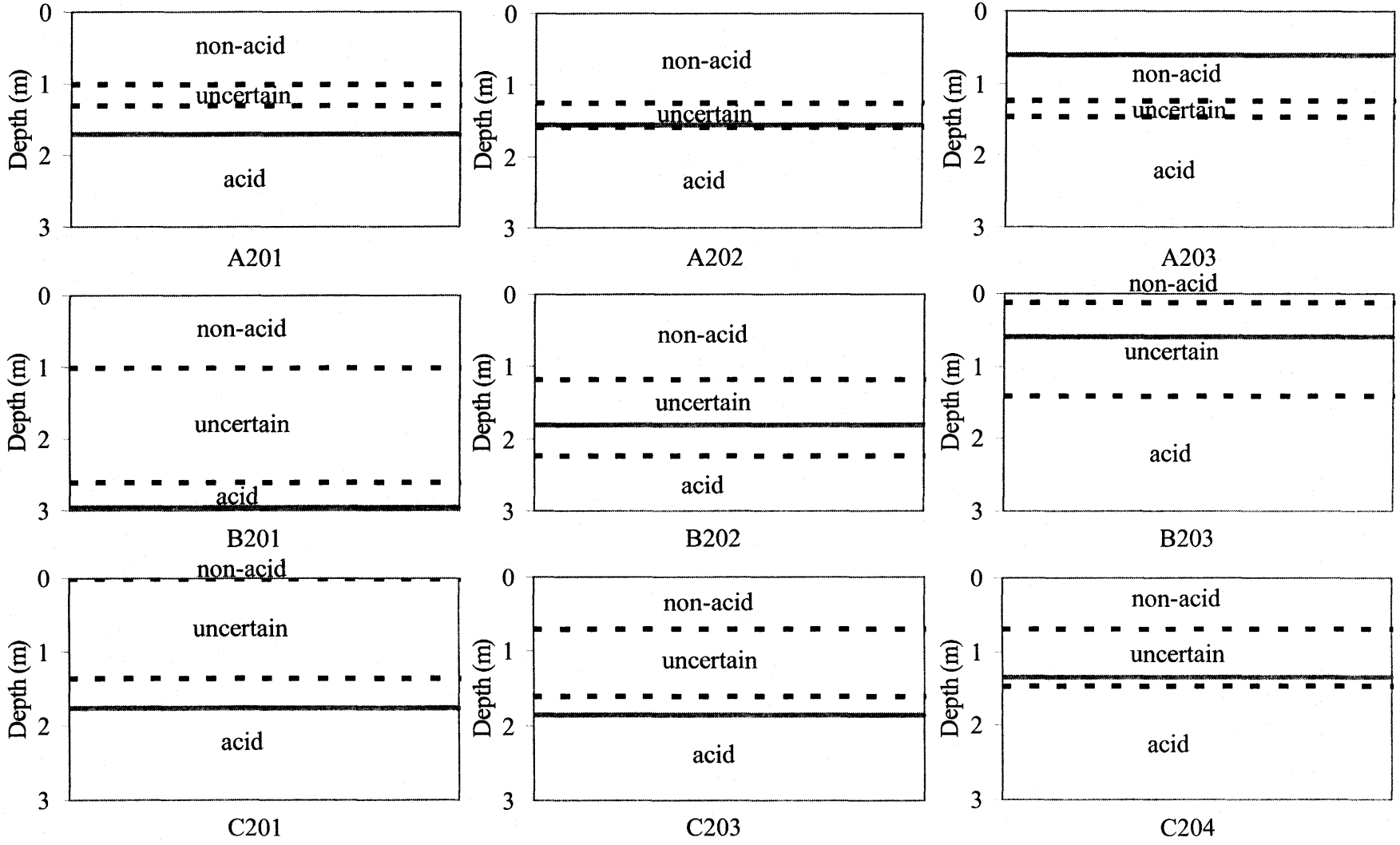

Figure 6.3 Illustration for the three layers of tailings. The solid gray line indicates the approximate location where the tailings become > 85% saturated. The saturation values are based on the water table depths measured in July, 2000.

6.3 SOILCOVER MODELING

The objective of the numerical modeling program was to create a simplified representation of the tailings facility at the Detour Lake Mine and determine the relative effects of weather, vegetation and water table depth on the gaseous oxygen penetration. Knowing the oxygen concentration and flux, it would then be possible to estimate the amount of sulphide mineral oxidation. The first stage in the modeling analysis was to choose a representative profile that was sufficiently simplified for modeling but sufficiently detailed to provide useful results. The Detour Lake Mine tailings facility proved very difficult to simplify. The following discussion describes the development of the four profiles selected for the SoilCover modeling.

6.3.1 Profile Development

The first option explored for choosing representative profiles was to determine geotechnical variation between the desulphurized tailings and the sulphidic tailings and to create a layered profile from these two types. As discussed in Chapter 5, the desulphurized and the sulphidic tailings showed very little variation with respect to physical characteristics. Both types of tailings had highly variable grain-size distributions but both varied within similar envelopes. The results for the saturated hydraulic conductivity and the soil-water characteristic curve were similar for both types of tailings. It was determined that the geotechnical variation between the two types of tailings was insufficient for determining representative profiles.

The second option explored was to use the three layers defined by the geochemical analysis for the representative profiles. The three layers were the non-acid generating,

uncertain and acid generating tailings layers. Most of the bore-holes could be represented by one of two layering scenarios. These two geochemical layering scenarios are illustrated in Figure 6.4.

To use the profiles shown in Figure 6.4 for the SoilCover modeling, definition of the geotechnical characteristics such as the saturated hydraulic conductivity and soil-water characteristic curve were required for each layer. Since the three layers were defined based on the Net Neutralization Potential (NNP) for each sample, an attempt was made to correlate the NNP with the geotechnical characteristics. The comparison of NNP with grain-size distribution, saturated hydraulic conductivity and the soil-water characteristic curve showed that no correlation existed between the geochemical characteristics and the geotechnical characteristics. Therefore, it was not reasonable to use the profiles in Figure 6.4 since there was no logical way to assign each layer a set of geotechnical characteristics.

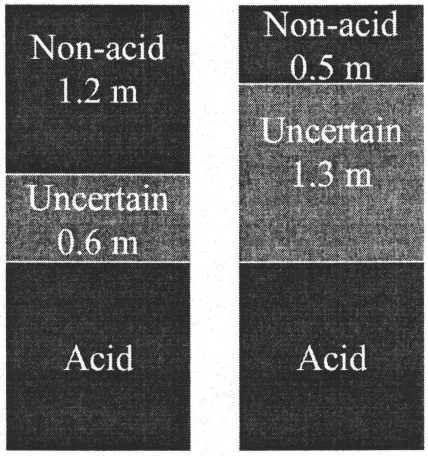

Figure 6.4 Two potential tailings profiles using the three tailings layers developed from the geochemistry analysis.

An alternative option to develop representative profiles was to move away from a detailed categorization of the tailings profile. The geotechnical analysis revealed a

considerable variation of characteristics throughout the tailings facility. The final conclusion was to create profiles based on the extreme limits of the tailings characteristics such that the results would determine worst and best case scenarios. The two types of tailings selected to model were the coarsest and the finest tailings. Since the tailings had been observed to be heterogeneous, a layered profile was necessary to provide a variation in tailings properties. A layer thickness of 1.8 m was chosen based on the geochemical profiles illustrated in Figure 6.4. Both the non-acid generating and the uncertain layers, regardless of their individual thicknesses, gave a total depth of 1.8 m in both profiles. As illustrated in Figure 6.1, all of the low-sulphur tailings had NNP values greater than –15 which placed them into either the uncertain or the non-acid generating layers. In summary, it was considered reasonable to combine the non-acid generating and the uncertain layers to represent the desulphurized tailings layer. The resulting four representative profiles chosen for the SoilCover modeling are illustrated in Figure 6.5.

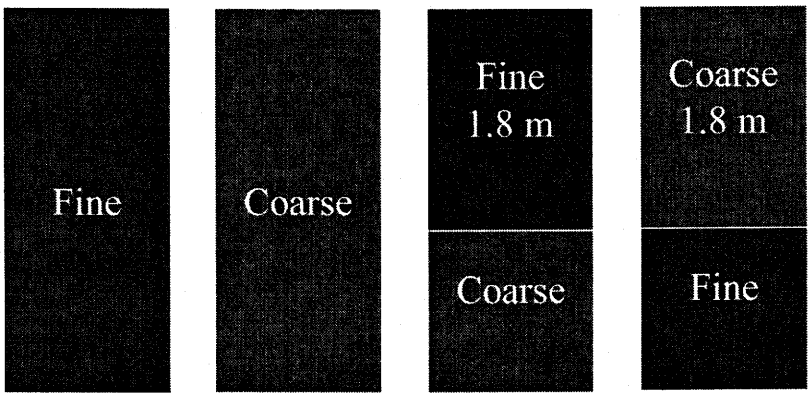

Figure 6.5 Four representative profiles chosen for SoilCover modeling analysis.

The samples chosen to represent the finest and coarsest tailings were C204 1.3 – 1.45 m and B201 0 – 0.2 m, respectively. The parameters chosen for each material are

summarized in Table 6.2. The parameters were not necessarily those measured during the laboratory testing. The hydraulic conductivity values for the tailings were chosen to represent the extremes of the range over which all the samples varied. The porosity values chosen correspond to those measured during the measurement of the soil-water characteristic curve. The porosity values chosen were lower than those measured in the field (Figure 4.16). The decreased porosity observed in the laboratory could be due to slurrying the sample. Slurrying versus field deposition could account for the variation in porosity values.

Table 6.2 Summary of material parameters for the coarse and fine materials chosen for the SoilCover modeling.

	Finest Tailings C204 1.3 – 1.45 m	Coarsest Tailings B201 0 – 0.2 m
n	0.44	0.45
k_{sat}	1×10^{-7} m/s	1×10^{-6} m/s
AEV	50 kPa	8 kPa
m_v	6.5×10^{-5}	6.5×10^{-5}
G_s	2.89	2.89

6.3.2 Weather Data Development

One of the goals of the modeling analysis was to determine the relative effect of variations in climate conditions. The weather scenarios chosen for this evaluation were a mean year, a 1 in 50 dry year and a 1 in 50 wet year. The following discussion describes the rationale for the data chosen to represent each of these weather scenarios.

SoilCover requires either a set of detailed daily weather data or a more simplified set of data. The detailed weather data specifies daily maximum and minimum temperature and relative humidity, windspeed, average net radiation and precipitation. The simplified set of data requires only daily maximum and minimum temperature and

relative humidity, potential evaporation and precipitation. The weather data measured at Detour Lake Mine between July, 2000 and July, 2001 were insufficient for preparing the three weather scenarios. Daily precipitation data since 1955 for Timmins, ON, was obtained from Environment Canada. From these data, it was determined that the precipitation at Detour Lake from July, 2000 to July, 2001 was comparable to a 1 in 50 dry year. Therefore, the detailed weather data measured at the site was used as the 1 in 50 dry year.

Two years of daily precipitation data were chosen to represent the mean and 1 in 50 wet years: 1972 was chosen as the mean year and 1961 as the wet year. Using the daily precipitation results from Environment Canada, a simplified set of weather data was created for each of the mean and wet years. The Detour Lake measured maximum and minimum temperature and relative humidity were chosen for these weather years since they were the only detailed data available. Daily potential evaporation rates were obtained from published data for Amos, QC (Barbour *et al.*, 1993) which is located approximately 300 km east of Detour Lake Mine at approximately the same latitude. These data were the mean monthly pan evaporation rates measured between 1968 and 1991.

The period chosen to conduct the SoilCover modeling was the period from April 8 to November 1, 2000. The weather data for each of the mean, wet and dry years were assembled for this period. This period represents the season during which liquid water transport could occur within the tailings facility. Since weather data for the Detour Lake site was measured from July, 2000 to July, 2001, the data for April, May and June, 2000 were missing. The data measured at the site for April, May and June, 2001 were substituted for the missing data.

6.3.3 Summary of Modeling Scenarios

The modeling scenarios chosen for the SoilCover modeling of the Detour Lake Mine tailings facility were the four profiles as illustrated in Figure 6.5 each for variations in weather data, vegetation and water table. Each profile was evaluated for every combination of the following:

1) Weather Data: Dry, mean and wet years.
2) Vegetation: No, poor and good vegetation.
3) Water Table: 1 m and 4 m depth to the water table.

The vegetation descriptions (no, poor and good) are based on the SoilCover vegetation options. SoilCover generates a leaf area index function ranging from 1.0 for poor and 3.0 for excellent vegetation. Excellent vegetation was not chosen for the modeling since the vegetation that will be planted on the tailings will not likely be sufficiently lush to warrant using a high leaf area index. Information regarding the SoilCover vegetation modeling and leaf area indices is available in Tratch (1994). The water table depths of 1 m and 4 m were chosen based on the measured water table depths in the tailings which were generally between 1 m and 4 m. Not all combinations were necessarily modeled since it was determined that some combinations were redundant.

6.3.4 Modeling Results

Not all of the SoilCover modeling results are presented in this section. Three profiles were chosen from the results representing a worst-case scenario, best-case scenario and the most realistic scenario. The profile representing the worst-case scenario was the homogeneous coarse tailings. The profile representing the best-case scenario was the

fine tailings layer over the coarse tailings, which illustrates how a capillary break is effective in maintaining high degrees of saturation. The most realistic scenario was the coarse tailings over the fine tailings since this profile most accurately represents the profile of the tailings at the Detour Lake tailings facility. Most of the results are for the 1 in 50 dry year to illustrate the most desaturated conditions likely to occur.

The results of the SoilCover modeling are summarized in Figures 6.6 – 6.13. Figure 6.6 and Figure 6.7 illustrate the homogeneous coarse tailings profile for 1 m and 4 m water tables, respectively. In both figures, the surface desaturates over the model year. Figure 6.6 shows that almost 0.5 m of the surface tailings are less than 85% saturated for the entire model year. Figure 6.7 shows that most of the tailings above the water table are less than 85% saturated for the entire model year. Only approximately 0.75 m of tailings above the water table stay above 85% saturated.

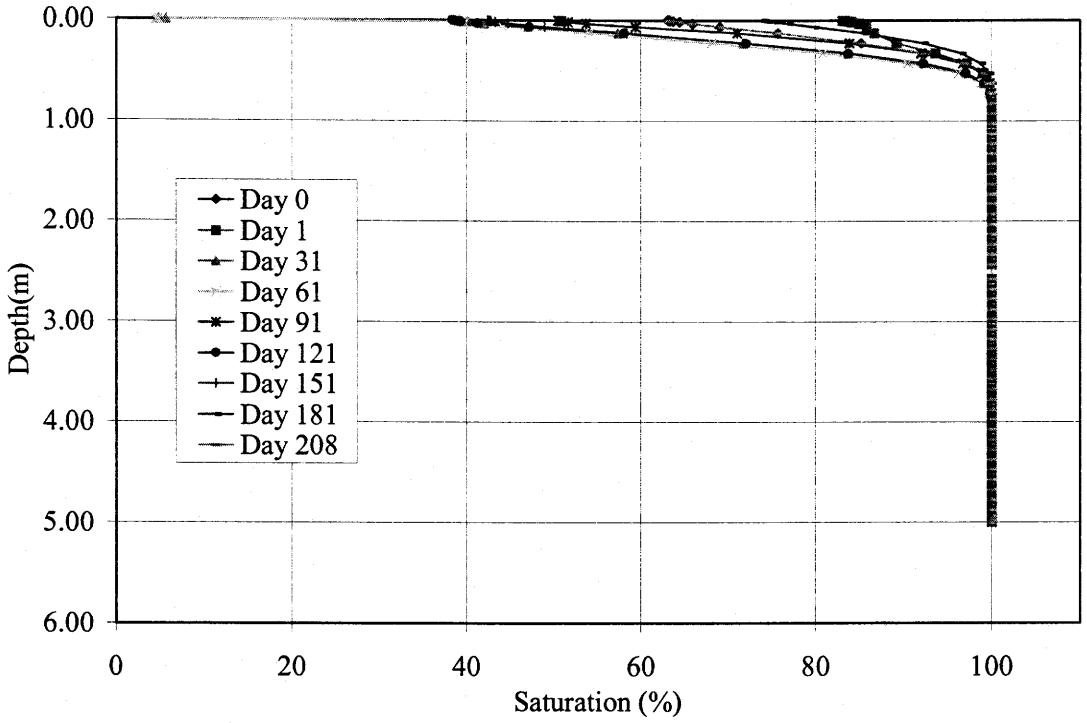

Figure 6.6 Saturation profiles from SoilCover modeling. Scenario: Dry year, coarse tailings, 1 m depth to water table and good vegetation.

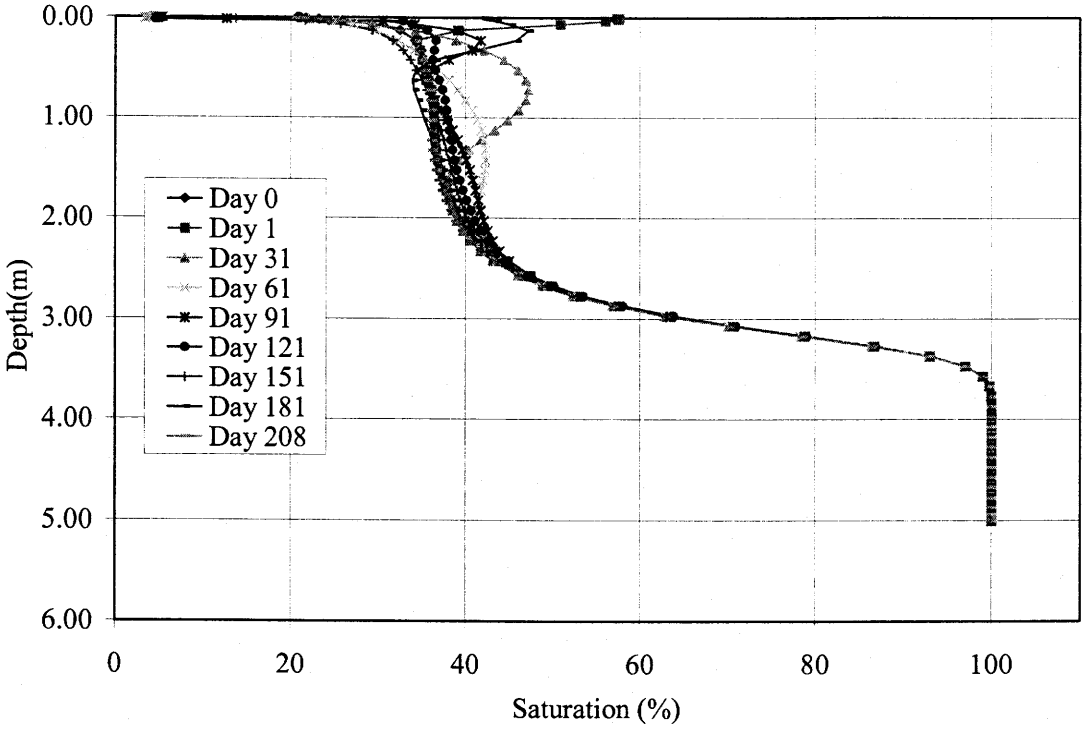

Figure 6.7 Saturation profiles from SoilCover modeling. Scenario: Dry year, coarse tailings, 4 m depth to water table and good vegetation.

Figure 6.8 and Figure 6.9 show the results of the SoilCover modeling for a fine tailings layer over coarse tailings. Both figures illustrate a capillary break system. The 1 m water table scenario in Figure 6.8 shows that all the tailings remain greater than 85% saturated throughout the entire model year. Since this is the driest year, it can be concluded that this profile would always remain fully saturated. For the 4 m water table in Figure 6.9, approximately 1 m of the fine surface tailings are less than 85% saturated for most of the year. The remaining 0.8 m of fine tailings stay saturated throughout the year and would therefore provide an adequate oxygen barrier to reduce oxygen diffusion into the unsaturated coarse tailings below.

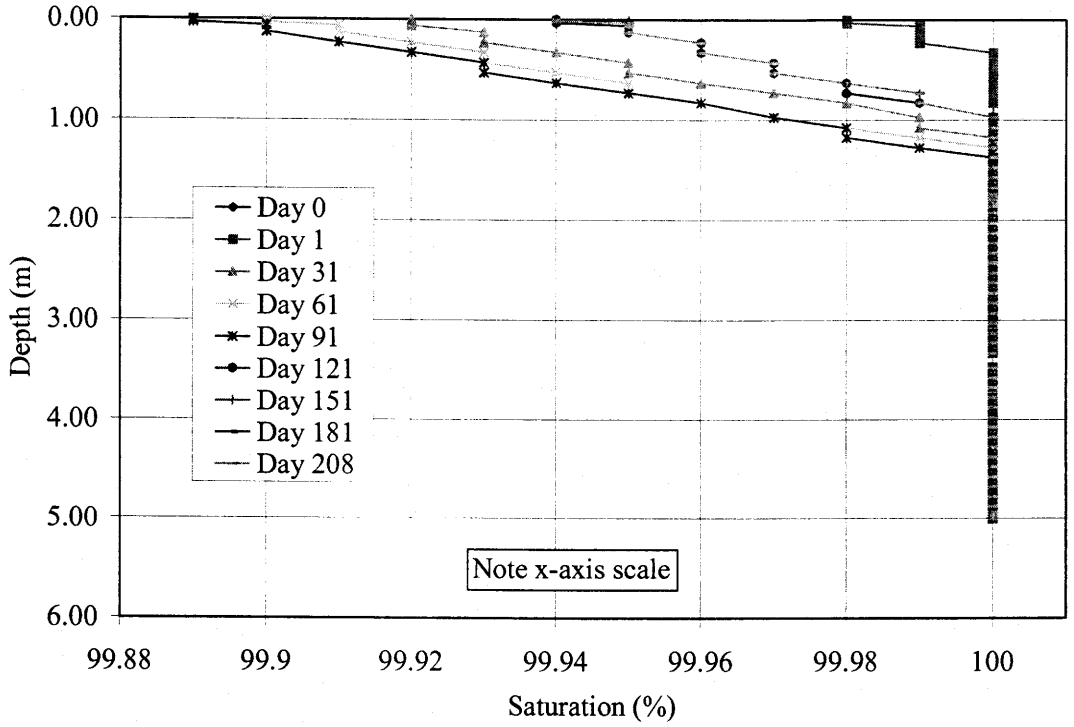

Figure 6.8 Saturation profiles from SoilCover modeling. Scenario: Dry year, 1.8 m fine tailings layer over coarse tailings, 1 m depth to water table and good vegetation.

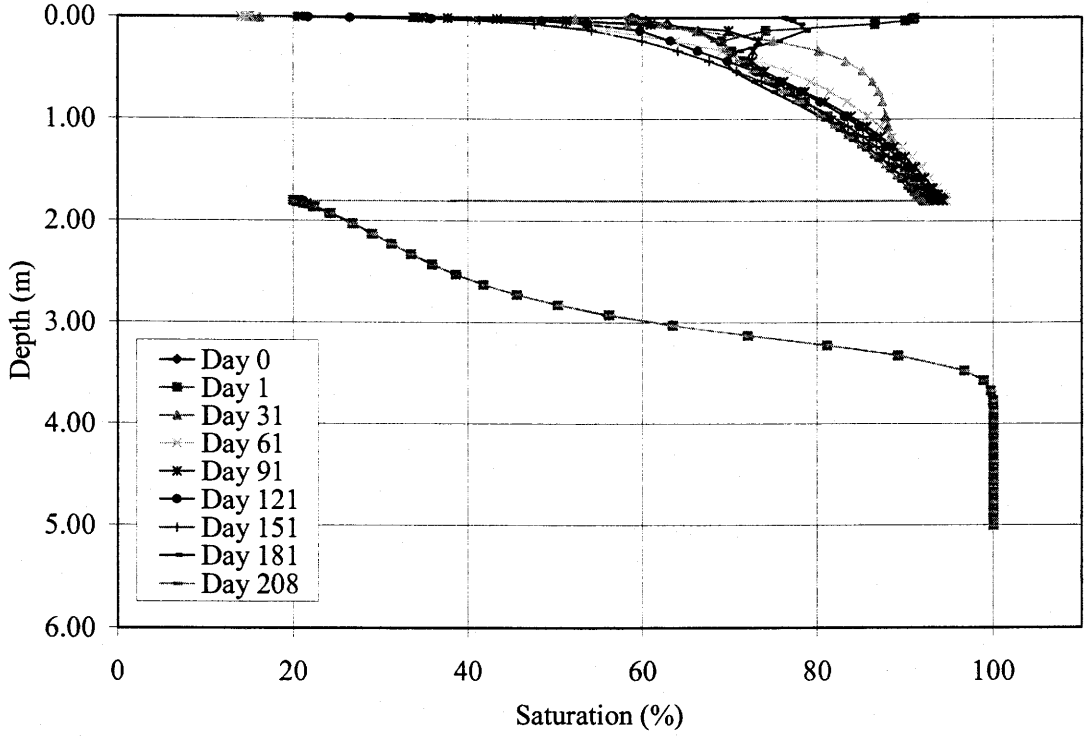

Figure 6.9 Saturation profiles from SoilCover modeling. Scenario: Dry year, 1.8 m fine tailings layer over coarse tailings, 4 m depth to water table and good vegetation.

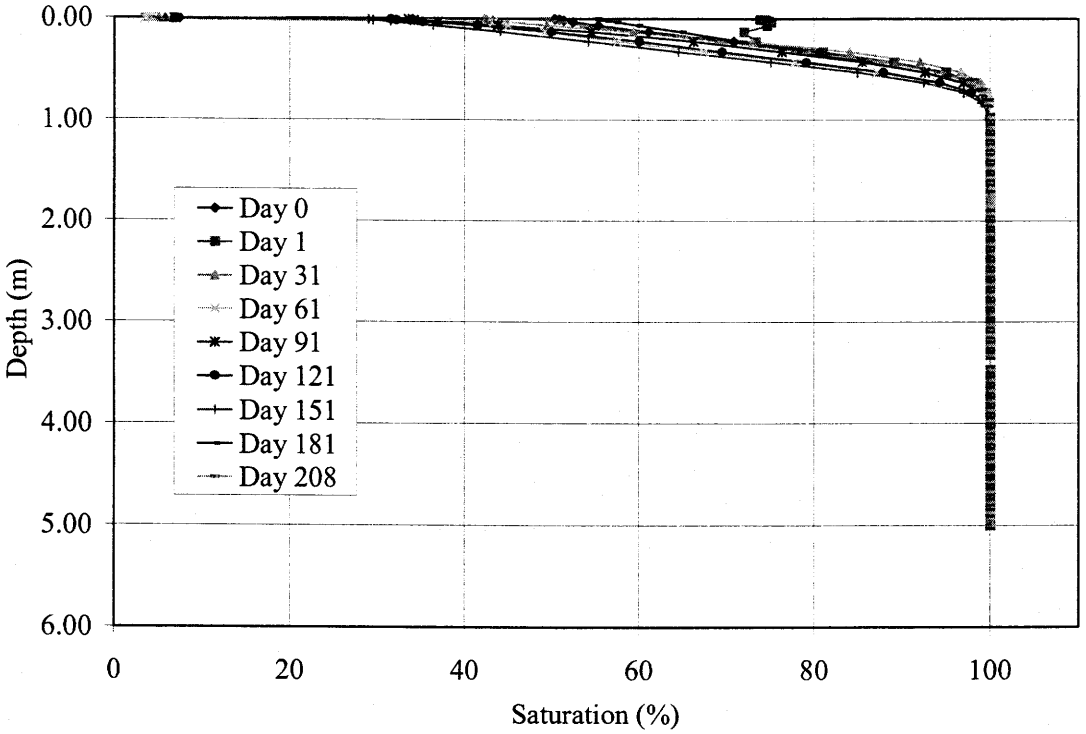

Figure 6.10 Saturation profiles from SoilCover modeling. Scenario: Dry year, 1.8 m coarse tailings layer over fine tailings, 1 m depth to water table and good vegetation.

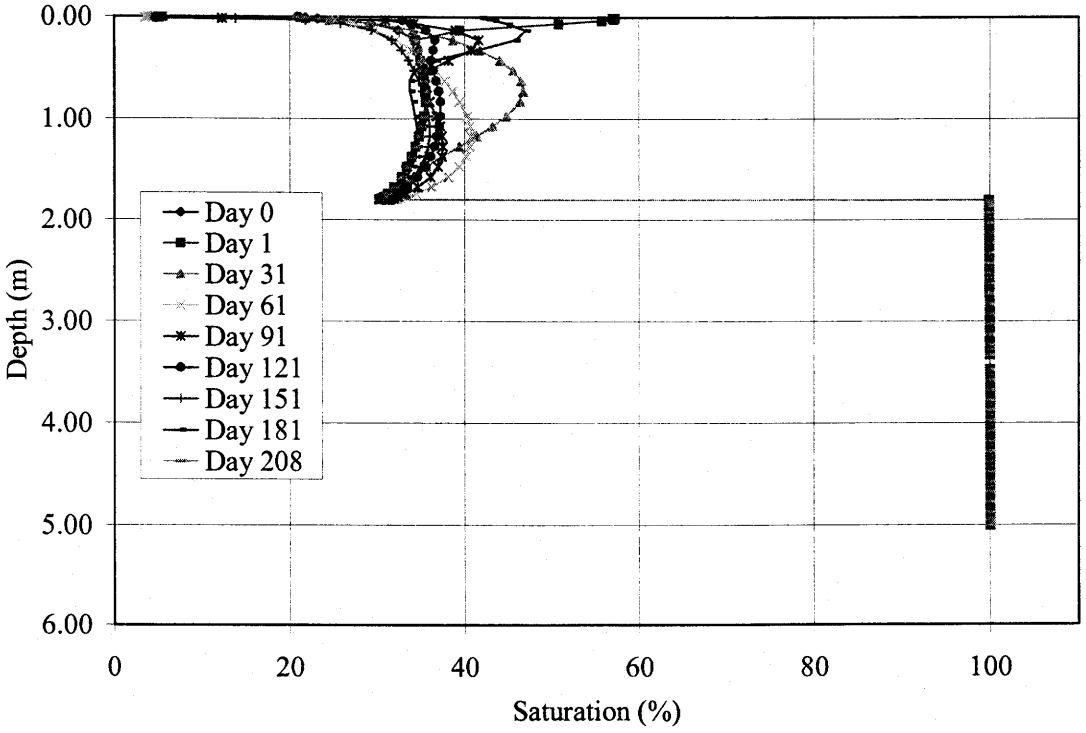

Figure 6.11 Saturation profiles from SoilCover modeling. Scenario: Dry year, 1.8 m coarse tailings layer over fine tailings, 4 m depth to water table and good vegetation.

Figure 6.10 and Figure 6.11 illustrate the most realistic representation of the tailings facility at the Detour Lake mine: a coarse tailings layer over fine tailings. Both scenarios show considerable desaturation at the surface. The 1 m water table scenario shows 0.5 m of the surface tailings remain less than 85% saturated for most of the year. The 4 m water table scenario illustrated in Figure 6.11 shows the entire 1.8 m layer of coarse tailings desaturates to approximately 35% for most of the model year. According to this representation of the tailings facility, a large portion of the tailings have the potential to desaturate well below the surface.

Figure 6.12 and Figure 6.13 illustrate the relative effect of weather and vegetation on the saturation profiles. Figure 6.12 a) and b) show the coarse over fine tailings profile for the mean weather data and for the 1 in 50 years wet weather data. These scenarios can be compared to Figure 6.11 to evaluate the relative effect of weather. For the dry year, the surface desaturated to approximately 5% and the entire coarse layer remained at approximately 35% saturation for most of the year. For the mean year (Figure 6.12 a)), the surface desaturated to 5% and the entire coarse layer remained approximately 40% saturated for most of the year. The wet year (Figure 6.12 b)) showed the surface tailings desaturating to 5% and the entire coarse layer remaining at approximately 50% saturation for most of the model year.

By comparing the three scenarios with different weather conditions, the relative effect of weather is apparent. The surface saturation varied little between the wettest and the driest years although the average saturation of the entire coarse tailings layer varied by approximately 15% between the wettest and the driest years. This illustrates that the weather at the Detour Lake mine site can affect the entire saturation profile of the tailings.

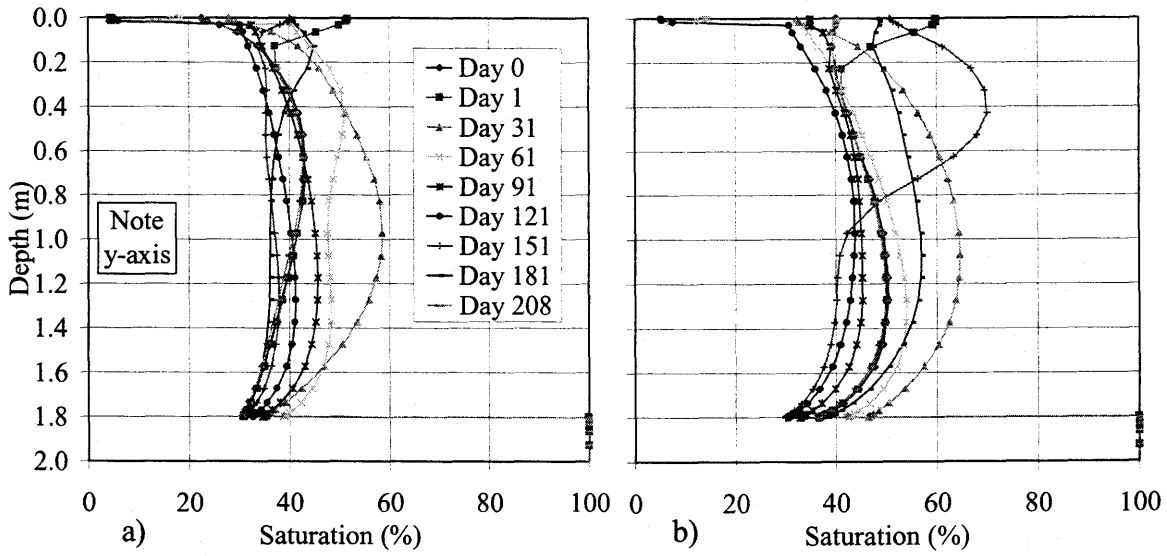

Figure 6.12 Saturation profiles from SoilCover modeling. Scenario: 1.8 m coarse tailings layer over fine tailings, 4 m depth to water table and good vegetation. a) Mean weather data. b) Wet weather data.

Figure 6.13 a) and b) illustrate the relative effect of different vegetation scenarios on the saturation profile of the tailings. As in Figure 6.12, these scenarios are variations on the scenario illustrated in Figure 6.11: a coarse tailings layer over fine tailings with a 4 m water table. Figure 6.13 a) shows the scenario with a poor vegetative cover and Figure 6.13 b) shows the scenario with no vegetation. The saturation profiles for all three vegetation scenarios are virtually identical. By examining the flux rates for each scenario (Appendix B), it can be seen that the evapotranspiration rates are constant regardless of vegetation quality. The quality of the vegetation defines the potential rate of transpiration. The actual transpiration rate is a portion of the potential rate dependant upon the moisture available to the plants. There is a finite rate at which moisture can be removed from the system which is a function of the hydraulic conductivity of the tailings. If the plants remove a portion of this moisture, then that available for

evaporation decreases. In summary, the tailings profile is unaffected by the mechanism with which moisture is removed: transpiration versus evaporation.

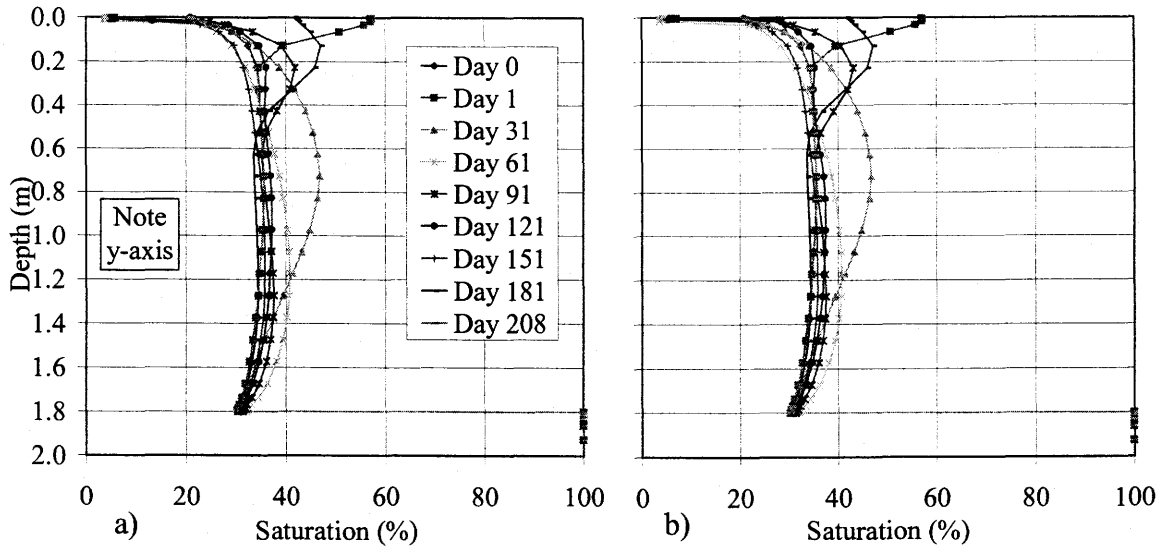

Figure 6.13 Saturation profiles from SoilCover modeling. Scenario: Dry year, 1.8 m coarse tailings layer over fine tailings and 4 m depth to water table. a) Poor vegetation. b) No vegetation.

The reason that the saturation profile in the Detour Lake tailings is unaffected by the mechanism of moisture removal is due to the large potential for evaporation and the low hydraulic conductivity of the material. Accounting for transpiration rates simply reduce evaporation rates.

6.4 OXYGEN DIFFUSION AND CONSUMPTION MODELING

The objective of the numerical modeling analysis was to determine the relative oxygen concentration profile and oxygen flux in the Detour Lake tailings for different weather scenarios, vegetation and water table depths. The SoilCover modeling produced degree of saturation profiles through the different tailings profiles for combinations of weather, vegetation and water table depths. To predict the oxygen concentration, it was necessary to develop a model to predict the diffusion and consumption of oxygen

through an unsaturated profile as the saturation profile varied from day to day. Since SoilCover used a one-dimensional mesh of nodes, it was logical to use the same mesh to calculate the diffusion and consumption of oxygen. A finite difference method was selected for its simplicity. The development of the finite difference formulation and the resulting program written to perform the calculations were described in detail in Chapter 3.

6.4.1 Modeling Results

To proceed with the oxygen diffusion and consumption modeling of the representative profiles outlined in section 6.3.1, it was necessary to add geochemical characteristics to the profiles. The following section describes the selection of kinetic oxidation constants for each of the tailings layers. The second section summarizes the results of the oxygen diffusion and consumption modeling.

6.4.1.1 Profile Development

As previously discussed, the geochemical laboratory evaluation of the tailings revealed three layers: non-acid generating, uncertain and acid-generating. Based on these criteria, it was possible to determine the k_r value for each of these layers for both a coarse and fine grain-size distribution. The pyrite concentrations for each of the three layers were obtained by averaging the sulphide sulphur content of all the samples in each layer. These values were 0.46%, 0.88% and 2% for the non-acid, uncertain and acid layers, respectively. The k_r values and the data used for the calculations are summarized in Table 6.3.

Table 6.3 Kinetic oxidation coefficients (k_r) calculated for the three geochemical layers each for a fine and coarse grain-size distribution.

Layer (S_2-S)%	**Coarse** D_{10} = 0.038 mm D_{60} = 0.2 mm	**Fine** D_{10} = 0.0022 mm D_{60} = 0.044 mm
Non-acid 0.46%	3.42 / yr	44 / yr
Uncertain 0.88%	5.36 / yr	84 / yr
Acid 2%	14.88 / yr	191/ yr

As illustrated in Table 6.3, the kinetic oxidation coefficient is sensitive to the grain-size distribution of the tailings. For the same pyrite content, the finer tailings have a considerably higher kinetic oxidation coefficient than the coarse tailings due to the increase in particle surface area exposed to oxygen and water. Since the coarse and fine particle size distributions represent the high and low values measured for the Detour Lake Mine tailings, it can be concluded that the kinetic coefficients given in Table 6.3 represent high and low values that could be expected in this tailings facility.

The SoilCover runs considered most significant were summarized in Section 6.3.4. These runs were chosen for the oxygen diffusion and consumption modeling. The homogeneous coarse tailings profile was chosen to represent a worst-case profile. The best-case profile was considered to be a capillary break system consisting of fine tailings over coarse tailings. The profile most comparable to the real tailings profile was concluded to be the coarse over fine tailings profile.

The kinetic coefficient chosen for the coarse tailings was 10 / yr, which was the value measured for a sample of coarse desulphurized tailings by the diffusion/kinetic cell as discussed in Chapter 5. 10 / yr is greater than the value corresponding to that of the non-

acid generating coarse tailings (Table 6.3) and is similar to that for the acid generating coarse tailings (14.88 / yr). Since the desulphurized tailings would generally be finer than the coarsest tailings sample, it was considered reasonable to assume that the kinetic coefficient for most of the desulphurized tailings would be higher than that calculated for the coarsest tailings sample with a low pyrite content. Therefore, 10 / yr was concluded to be a reasonable value for the kinetic coefficient of the coarse tailings.

The kinetic coefficient chosen for the fine tailings was 44 / yr, which corresponds to the non-acid generating fine tailings in Table 6.3. Being the finest grain-size distribution, the fine tailings are not representative of all the sulphidic tailings. Most of the sulphidic tailings would be coarser than the finest sample. It was concluded that a reasonable kinetic coefficient to represent the fine-grained sulphidic tailings would be a value lower than that listed in Table 6.3 for acid-generating tailings. For this reason, the kinetic coefficient for non-acid generating fine tailings in Table 6.3 was chosen to represent the k_r value for the fine-grained sulphidic tailings.

The scenarios chosen for the oxygen diffusion and consumption modeling are summarized in Table 6.4. Low k and high k refer to the values 10 / yr and 44 / yr, respectively.

Table 6.4 Summary of scenarios for the oxygen diffusion and consumption modeling.

Index	Profile	Weather	Vegetation	Water Table	Kinetic Coefficient
1	Coarse	Dry	Good	1 m	k = 0
2	Coarse	Dry	Good	4 m	k = 0
3	Coarse	Dry	Good	1 m	Low k
4	Coarse	Dry	Good	4 m	Low k
5	Fine over Coarse	Dry	Good	1m	k = 0
6	Fine over Coarse	Dry	Good	4 m	k = 0
7	Fine over Coarse	Dry	Good	1 m	High k over low k
8	Fine over Coarse	Dry	Good	4 m	High k over low k
9	Coarse over Fine	Dry	Good	1 m	Low k over high k
10	Coarse over Fine	Dry	Good	4 m	Low k over high k
11	Coarse over Fine	Dry	Good	1m	k = 0
12	Coarse over Fine	Dry	Good	4 m	k = 0
13	Coarse over Fine	Mean	Good	4 m	Low k over high k
14	Coarse over Fine	Wet	Good	4 m	Low k over high k
15	Coarse over Fine	Dry	No	4 m	Low k over high k
16	Coarse over Fine	Dry	Poor	4 m	Low k over high k

The SoilCover saturation profiles for the scenarios with layers of contrasting materials and a 4 m water table produced sudden saturation changes at the interface between the two types of tailings. Figure 6.9 and Figure 6.11 illustrated the sudden change in saturation at the interface both for fine over coarse and coarse over fine tailings. For example, in Figure 6.9, the saturation changed from 95% just above the interface to 20% just below the interface. During the oxygen diffusion modeling, it was found that a large change in saturation between two nodes resulted in the calculation of unreasonable results. To produce reasonable results from these scenarios, it was necessary to adjust the saturation profiles to reduce the saturation change between any two nodes. The SoilCover mesh had already been reduced so that the minimum nodal spacing between any given node was approximately 30 mm. This was done to reduce computing times. The mesh was adjusted such that the saturation change occurred over

four nodes as opposed to the previous two. The resulting transition in saturation then occurred over a distance of approximately 200 mm compared to 30 mm. The nodes that were adjusted were always those in the more saturated material. The result of this adjustment meant that for the coarse over fine scenarios, the oxygen was predicted to penetrate slightly deeper than it would without the adjustment. The adjusted saturation profiles are presented in Appendix C.

6.4.1.2 Summary of Modeling Results

The oxygen concentration profiles for the homogeneous coarse tailings profile with a 4 m water table are illustrated in Figure 6.14 and Figure 6.15. Figure 6.14 shows the depth of oxygen penetration without accounting for oxygen consumption by kinetic oxidation. Figure 6.15 shows the effect of the kinetic oxidation on the depth of penetration. As illustrated by the two figures, the effect of kinetic oxidation on the depth of oxygen penetration is significant. Without accounting for kinetic oxidation (Figure 6.14), the atmospheric concentration of oxygen penetrates to the top of the capillary fringe at day 208 of the simulation period. Accounting for kinetic oxidation (Figure 6.15), the oxygen concentration profile reaches a steady-state value after approximately 90 days of simulation. The steady-state profile shows the oxygen concentration reduced to 14% at a depth of 1 m. Small fluctuations in the steady-state concentration profile are due to variations in the saturation profiles with time.

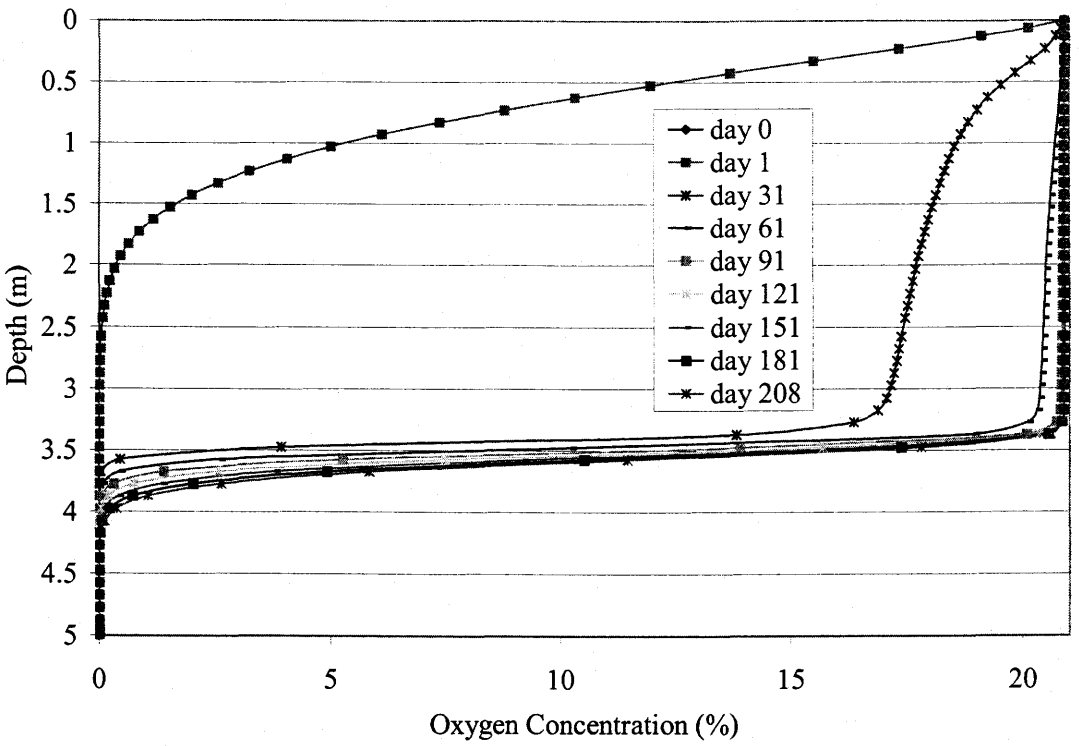

Figure 6.14 Oxygen profiles for homogeneous coarse tailings, 4 m depth to water table, dry year, good vegetation and $k_r = 0$.

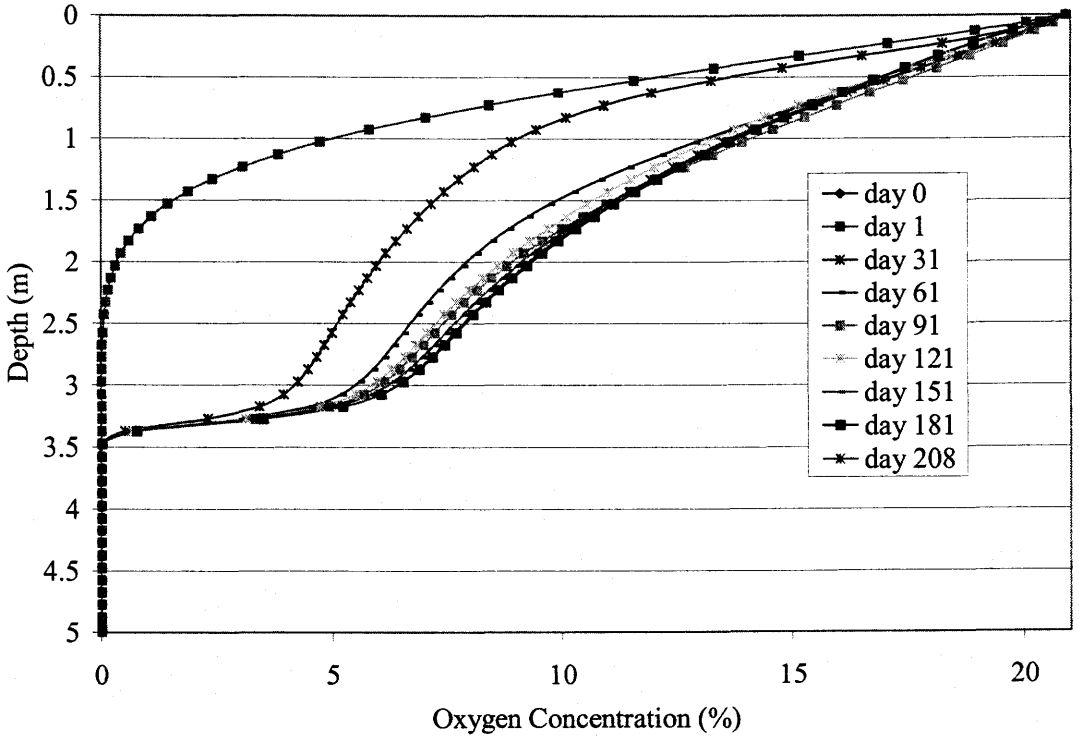

Figure 6.15 Oxygen profile for homogeneous coarse tailings, 4 m depth to water table, dry year, good vegetation and $k_r = 10$ / yr.

Figure 6.16 and Figure 6.17 illustrate the effect of a capillary break on the oxygen penetration into a tailings profile. The scenario used for these Figures was a 1.8 m thick layer of fine tailings over coarse tailings with a 4 m water table. Figure 6.16 shows the oxygen concentration profiles with the kinetic oxidation coefficient equal to zero. In this simulation, oxygen penetrated through the fine tailings since most of the layer was less than 85% saturated. Once the oxygen front reached the coarse tailings, there was little resistance to diffusion and the concentration at the interface penetrated to the top of the capillary fringe. By day 208, an oxygen concentration of 2% had penetrated the entire unsaturated portion of the coarse tailings.

Figure 6.17 illustrates the effect of kinetic oxidation on the fine over coarse tailings profile. In this simulation, kinetic oxidation consumes sufficient oxygen to prevent oxygen from reaching the interface between the coarse and fine tailings. Therefore, no oxygen penetrates into the coarse tailings. It is important to note that even though this scenario prevents oxygen from reaching the coarse tailings, it does so because of the relatively high reactivity of the fine (cover) tailings. To prevent acid generation, this layer would require considerable buffering capacity.

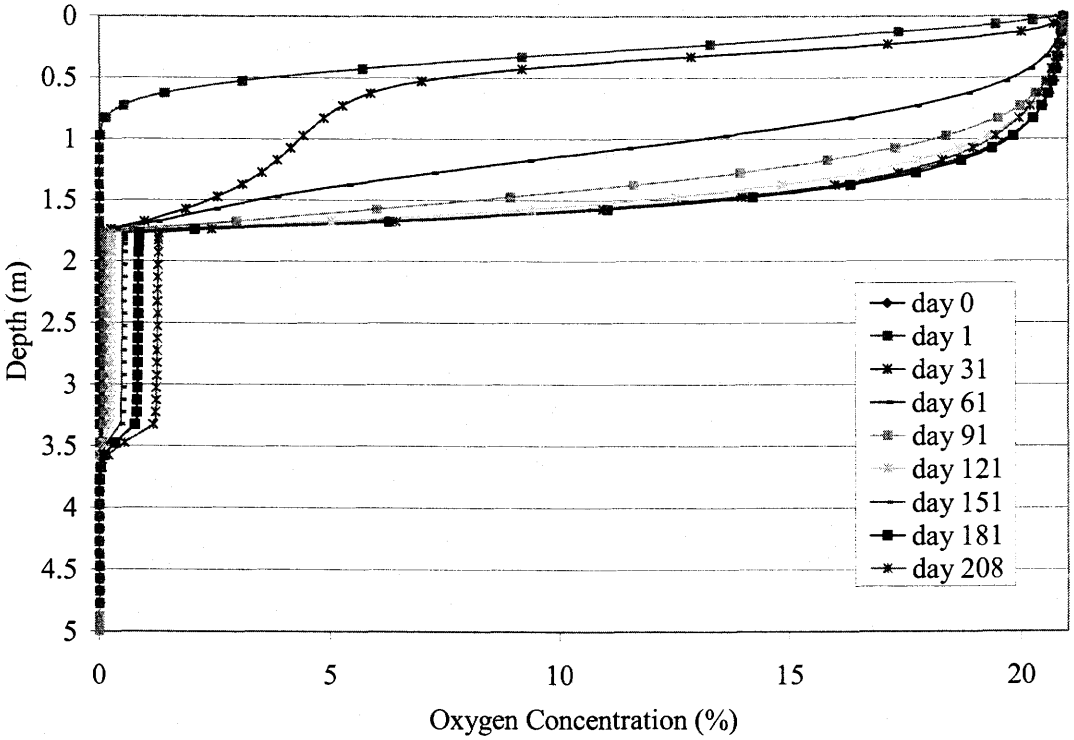

Figure 6.16 Oxygen profile for fine tailings layer over coarse tailings, 4 m depth to water table, dry year, good vegetation and $k_r = 0$.

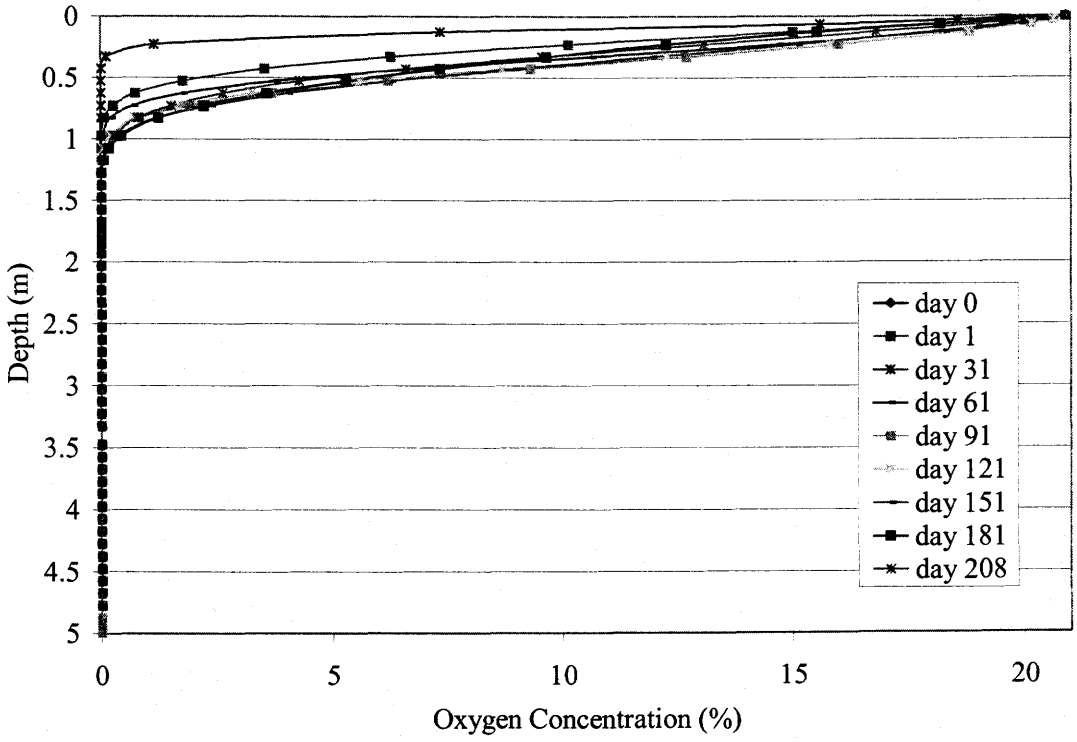

Figure 6.17 Oxygen profile for fine tailings layer over coarse tailings, 4 m depth to water table, dry year and good vegetation Fine tailings: $k_r = 44$ / yr, coarse tailings: $k_r = 10$ / yr.

The most realistic representation of the tailings facility at Detour Lake Mine was concluded to be a layer of coarse tailings over fine tailings. The following oxygen concentration profiles illustrate the effect of varying water table depth, weather conditions and vegetation for a profile consisting of a 1.8 m thick layer of coarse tailings over fine tailings.

Figure 6.18 and Figure 6.19 illustrate the oxygen penetration into the coarse over fine tailings profile for a 1 m water table and a 4 m water table, respectively. For the 1 m water table, the oxygen concentration reduces through the profile to a residual value at the top of the capillary fringe. For the scenario with a 4 m water table, an oxygen concentration of 13% penetrates to the surface of the fine tailings which remain fully saturated above the water table.

Figure 6.20 a) and b) show the effect of the mean and wet weather scenarios on the coarse over fine tailings profile. Comparing these two Figures with Figure 6.19 illustrates the variation in oxygen penetration over the weather variations. For the dry year, an oxygen concentration of 13% penetrated to the top of the fine tailings layer. For the mean and wet years, the oxygen concentrations penetrating to the top of the fine tailings layer were approximately 12.5% and 11.5%, respectively

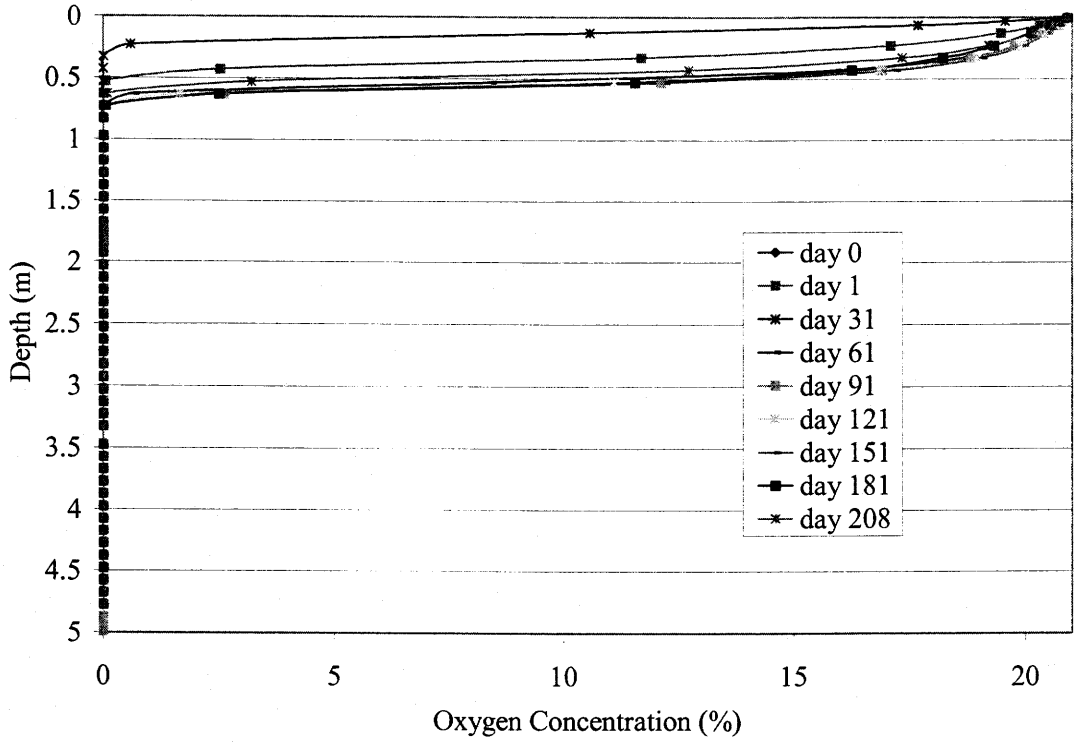

Figure 6.18 Oxygen profile for coarse tailings layer over fine tailings, 1 m depth to water table, dry year, good vegetation. Coarse tailings k_r = 10 / yr, fine tailings k_r = 44 / yr.

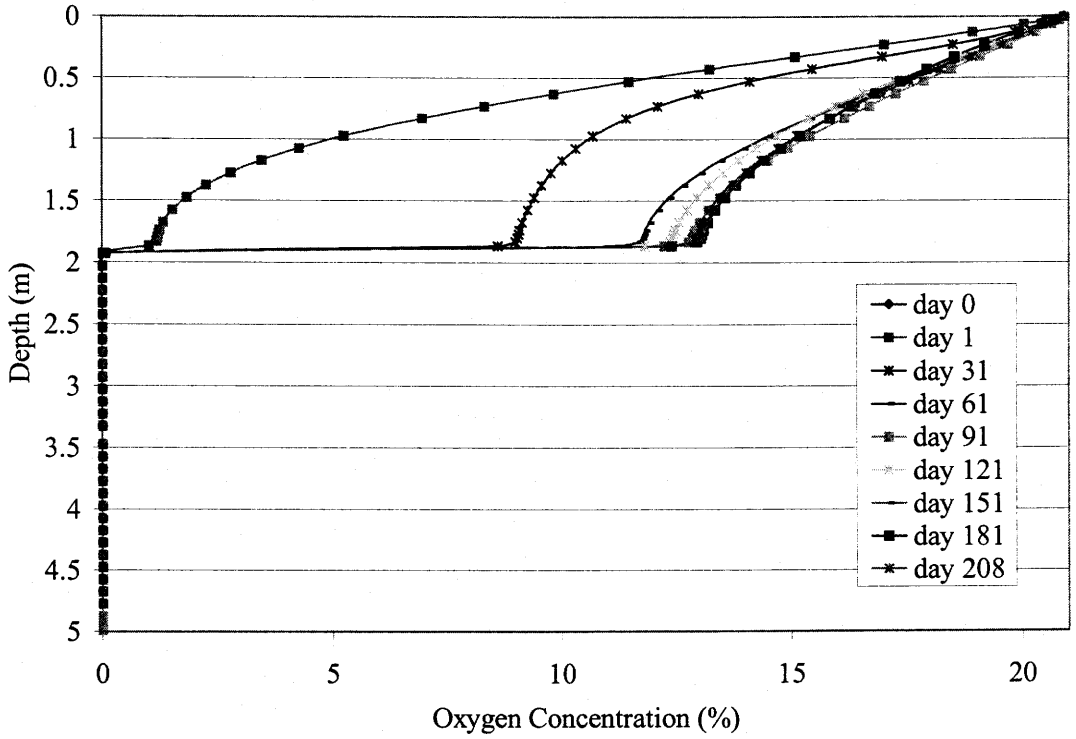

Figure 6.19 Oxygen profile for coarse tailings layer over fine tailings, 4 m depth to water table, dry year, good vegetation. Coarse tailings k_r = 10 / yr, fine tailings k_r = 44 / yr.

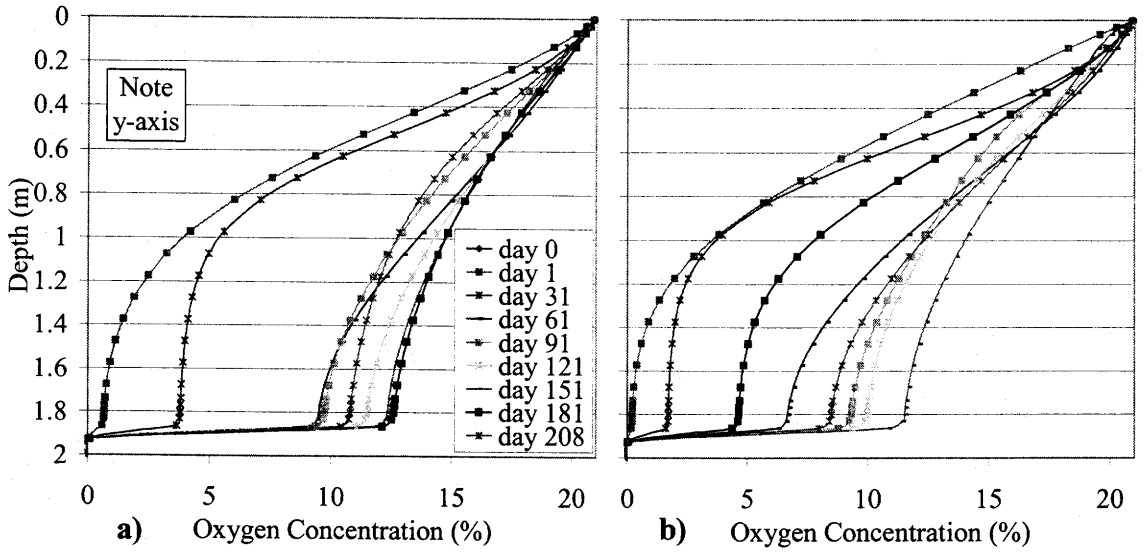

Figure 6.20 Oxygen profiles for weather comparisons to Figure 6.19. a) Mean weather data. b) Wet weather data.

Figure 6.21 a) and b) illustrate the effect of poor and no vegetation on the coarse over fine tailings profile. Comparing Figure 6.21 to Figure 6.19 illustrates the negligible effect of vegetation on the oxygen penetration. For all the simulations, vegetation was found to have little effect on the saturation profiles and therefore on the oxygen profiles.

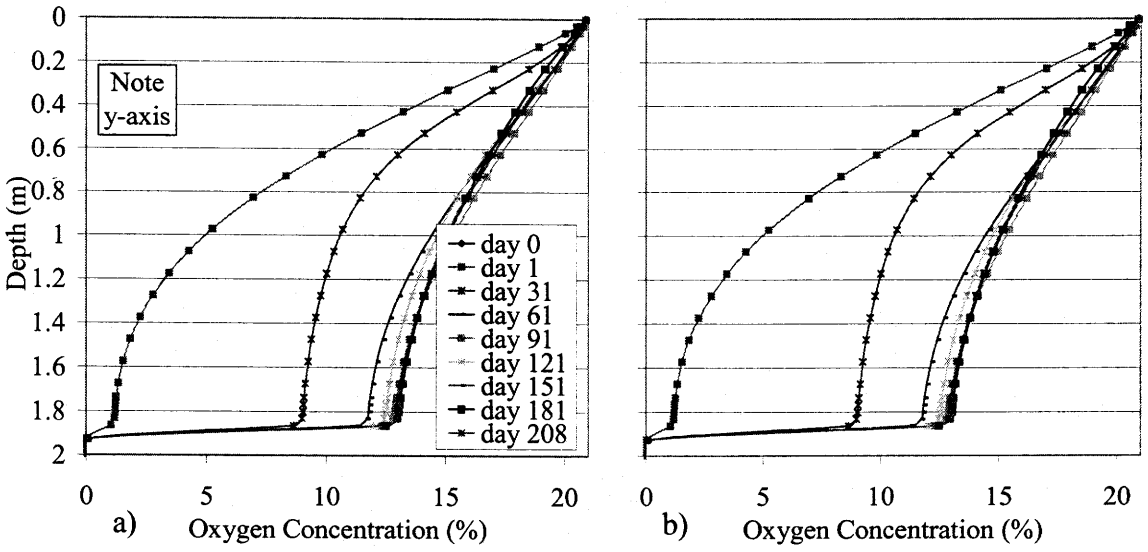

Figure 6.21 Oxygen profiles for vegetation comparisons to Figure 6.19. a) Poor vegetation. b) No vegetation.

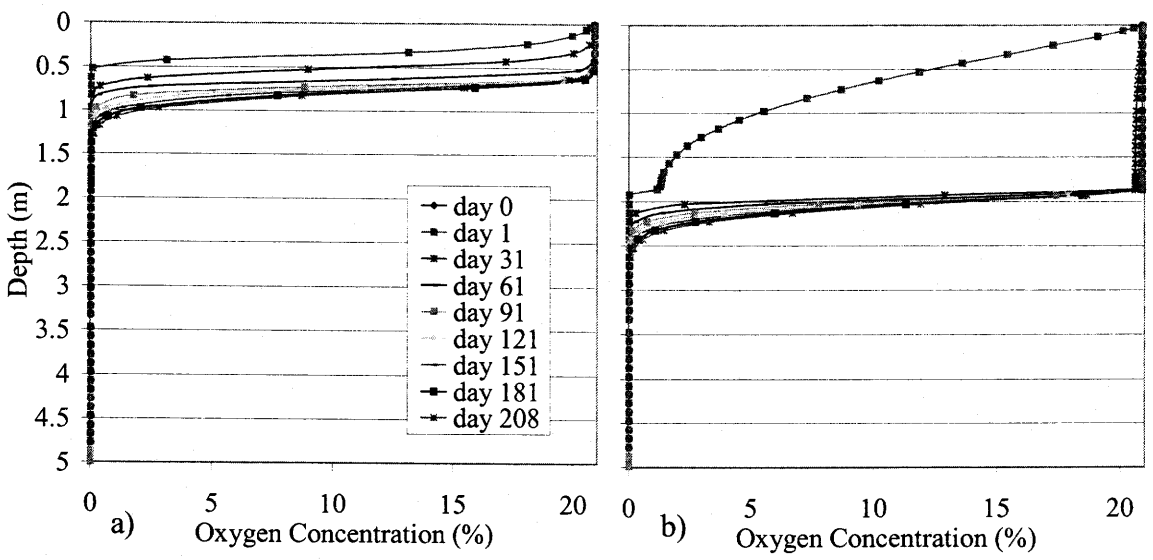

Figure 6.22 Oxygen profiles for kinetic oxidation comparisons. a) Same scenario as Figure 6.18 with $k_r = 0$. b) Same scenario as Figure 6.19 with $k_r = 0$.

Figure 6.22 illustrates the oxygen concentration profile for the coarse over fine tailings profile with the kinetic oxidation coefficient equal to zero. Figure 6.22 a) illustrates that oxygen penetrates fully to the top of the capillary fringe for a 1 m water table. Figure 6.22 b) illustrates that oxygen penetrates fully to the top of the saturated fine tailings layer. Figure 6.22 b) also shows oxygen penetrating somewhat into the highly saturated fine tailings.

6.4.1.3 Comparison of Oxygen Fluxes

To predict the extent of sulphide mineral oxidation from the numerical modeling results, it was necessary to predict the oxygen flux at different locations throughout the tailings profile. According to Elberling and Nicholson (1996), the oxidation rates in mine tailings can be estimated by evaluating the Fickian flux of oxygen through the surface of the tailings and assuming that this is the rate at which oxygen is consumed by sulphide mineral oxidation throughout the entire profile.

To evaluate the flux of oxygen through the surface, Elberling and Nicholson used the mean oxygen concentration gradient over the top 0.2 m of tailings. The harmonic mean of the diffusion coefficients measured for the 0.2 m profile was used in Fick's first law to calculate the flux of oxygen. The tangent of the concentration gradient along with the diffusion coefficient at depth z were used to determine the flux at a given depth z for non-linear concentration gradients.

For the scenarios modeled in this numerical modeling analysis, it was determined that the important locations to compute the oxygen flux were at the surface and the interface between the two layers of tailings. The MATLAB model was programmed to calculate the diffusive fluxes and the oxidative fluxes into and out of every node for the last run "day" (day 208). The last day was assumed to be at approximately steady-state. The diffusive flux between the top two nodes was assumed to approximate the surface flux.

The determination of the flux at the interface was complicated due to the sudden change in material properties and the alteration in the saturation profile due to numerical instability in the oxygen concentration calculations. For these reasons, the location chosen to calculate the flux at the interface was the top node of the material directly below the interface. To reduce the effect of the altered saturation profile on the flux results, the node chosen was always the one below the two altered nodes. The interface fluxes presented are the diffusive fluxes entering and exiting this node. The location of the interface node used for the flux calculation is illustrated in Figure 6.23. The difference between the fluxes entering and exiting the node is largely due to oxidative consumption at the node. It was also determined that the assumption of steady-state conditions on day 208 was not always valid. Small differences in the diffusive fluxes

into and out of the interface node for scenarios without any oxidative consumption (k_r = 0) illustrate small changes in storage due to non-steady-state conditions.

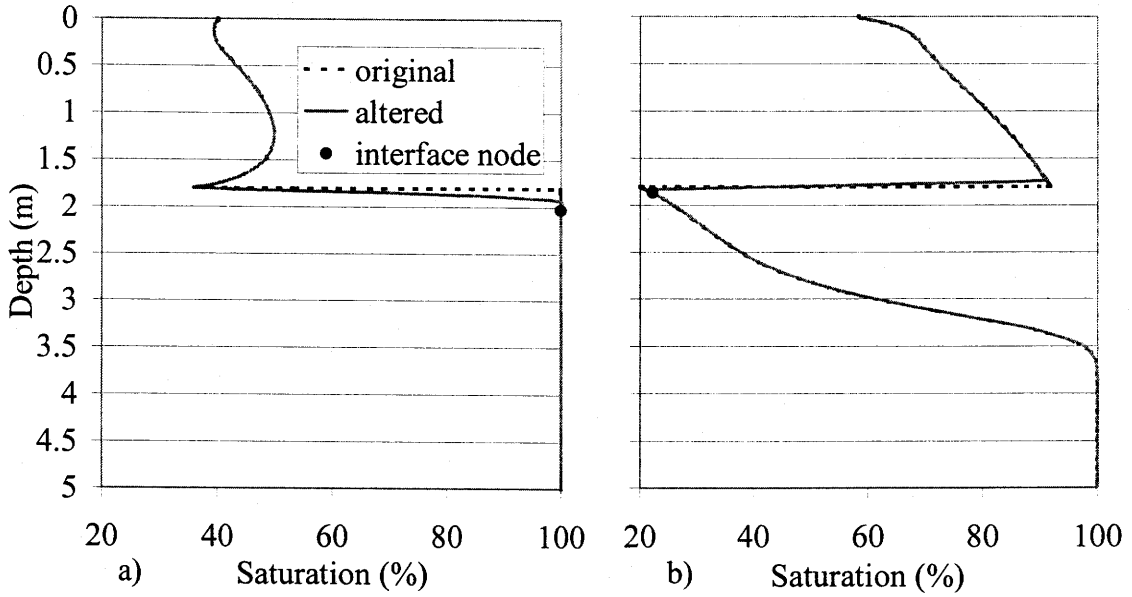

Figure 6.23 Examples of original and altered saturation profiles illustrating the location of the node where the interface fluxes were calculated. a) Example of a coarse over fine tailings profile. b) Example of a fine over coarse tailings profile.

The oxygen fluxes for each of the oxygen concentration profiles are summarized in Table 6.5. The first six columns describe the index number and the parameters used for each scenario. The profile column indicates the tailings type: C = coarse and F = fine. The layered profiles are indicated by: top layer/ bottom layer (i.e. F/C = fine over coarse tailings). The kinetic oxidation coefficients are indicated by Y or N indicating whether or not kinetic oxidation was included in the simulation.

The oxygen flux results show interesting trends. Scenario 1 shows that for a homogeneous coarse profile with a 1 m water table, there is a small diffusive flux at the surface and at the interface to the sulphidic tailings. Scenario 3 illustrates how accounting for kinetic oxidation increases the flux through the surface (due to demand from the oxidizing sulphide minerals) but decreases the flux entering the sulphidic

tailings. This illustrates that kinetic oxidation of the sulphide minerals in the cover material consumes sufficient oxygen to reduce the flux into the interface to low levels.

Table 6.4 Oxygen flux rates for each of the oxygen concentration profiles

#	Profile	Weather	Water Table (m)	Veg.	k_r	Surface Flux ($kg/m^2/yr$)	Interface Flux In ($kg/m^2/yr$)	Interface Flux Out ($kg/m^2/yr$)
1	C	Dry	1	Good	N	4.96E-4	7.84E-9	1.50E-9
2	C	Dry	4	Good	N	1.25E-3	1.25E-3	1.21E-3
3	C	Dry	1	Good	Y	0.736	~0	~0
4	C	Dry	4	Good	Y	5.53	1.91	1.75
5	F/C	Dry	1	Good	N	6.88E-4	4.23E-13	1.45E-13
6	F/C	Dry	4	Good	N	0.0329	0.0332	0.0316
7	F/C	Dry	1	Good	Y	3.32E-3	~0	~0
8	F/C	Dry	4	Good	Y	4.38	2.88E-8	2.75E-8
9	C/F	Dry	1	Good	Y	1.24	~0	~0
10	C/F	Dry	4	Good	Y	4.86	7.30E-6	1.14E-8
11	C/F	Dry	1	Good	N	3.40E-4	3.16E-10	5.25E-11
12	C/F	Dry	4	Good	N	7.26E-4	6.72E-4	5.22E-4
13	C/F	Mean	4	Good	Y	4.29	6.14E-6	9.56E-9
14	C/F	Wet	4	Good	Y	4.09	4.71E-6	7.35E-9
15	C/F	Dry	4	No	Y	4.86	7.33E-6	1.14E-8
16	C/F	Dry	4	Poor	Y	4.86	7.35E-6	1.15E-8

This trend is not illustrated in scenarios 2 and 4 where accounting for kinetic oxidation increases the diffusive flux through both the surface and the interface. In these scenarios, the water table is at a depth of 4 m and the tailings above the water table are relatively unsaturated. The consumption of oxygen by kinetic oxidation throughout the entire tailings profile becomes the driving force for a considerably greater oxygen flux than that without oxidation.

Scenarios 5 and 7 illustrate the fine over coarse tailings scenarios with a 1 m water table. These scenarios stayed fully saturated to the surface and this is reflected by the small oxygen fluxes at the surface and very small fluxes at the interface. Scenarios 6 and 8 show the fine over coarse profiles with a 4 m water table. Without kinetic oxidation, the flux entering the interface is similar to that entering the surface. With

kinetic oxidation, the flux entering the surface increases but the flux entering the interface decreases. As with scenarios 1 and 3, this illustrates how the oxidation in the cover consumes most of the oxygen and reduces the flux into the sulphidic tailings.

Scenarios 9 – 16 illustrate the fluxes for the coarse over fine tailings profiles. As with the previous profiles, for the shallow water table, the surface flux increases and the flux at the interface decreases when kinetic oxidation is accounted for. For the deep water table, the addition of kinetic oxidation increases the oxygen flux at the surface and decreases the flux at the interface. This shows a positive effect of kinetic oxidation on the effectiveness of the coarse tailings cover.

Scenarios 13 and 14 illustrate the reduction in oxygen flux at the surface and at the interface for mean and wet weather scenarios as compared to the dry weather scenario (10). Scenarios 15 and 16 illustrate the insignificant effect of no and poor vegetation compared to the good vegetation scenario (10). As discussed previously, vegetation showed little effect on the saturation and oxygen concentration profiles for the coarse over fine profiles. Therefore, little variation in the oxygen fluxes was expected.

6.5 SUMMARY

Based on the analysis of the field, laboratory and numerical modeling results, conclusions were made on the effectiveness of the desulphurized tailings cover at Detour Lake mine for reducing acid rock drainage. The following sections divide the conclusions into those made based on the field and laboratory analysis and those based on the numerical modeling analysis.

6.5.1 Qualitative Observations based on the Field and Laboratory Analysis

After completion of the field and laboratory investigations of the Detour Lake tailings facility, it was possible to make qualitative conclusions regarding the potential for acid rock drainage at the site.

A water table decline was observed over the period from July, 2000 to July, 2001. The water table in most bore-holes dropped from 0.5 to 1.0 m. This was unexpected since the pond level had recently been raised. One factor that would have contributed to the water table drop was the dry at Detour Lake year (2000/2001) as measured by the weather station. Low water content values in the surface tailings (~0.2 m) were observed in all the bore-holes, most extensively during the summer months. Since high water content values are required to reduce oxygen diffusion, this indicated that there is the potential for oxygen to enter the tailings surface.

Considerable layering of fine and coarse tailings was observed from fluctuations in water content profiles with depth, core samples and the grain-size results. As illustrated in the water content profiles, most bore-holes had a layer of tailings at a high water content at a maximum 2 m depth. This seemed to occur regardless of the water table depth. It is possible that layering could create a capillary barrier effect within the tailings profile that was not accounted for by generalized models. A thin layer of fine-grained tailings could reduce oxygen diffusion through the profile.

The laboratory investigation of the tailings from Detour Lake determined that the desulphurized tailings did not show considerable variation in geotechnical characteristics from the sulphidic tailings. A geochemical analysis was required to discriminate between the two types of tailings. The results of the geochemical analysis indicated that

the desulphurized tailings cover ranges in thickness from 1 to 1.5 m. It may be concluded from the laboratory analysis that there is likely not a capillary barrier effect present in the desulphurized cover. However, since the grain-size of both types of tailings varied appreciably, it is possible for there to be a capillary barrier created at various local areas of the tailings. In general, the sulphidic tailings tended to be slightly finer with a higher air-entry value than the desulphurized tailings.

The geochemical analysis for the tailings also allowed for a qualitative conclusion regarding the potential for acid generation. Three hypothetical layers were developed based on the geochemistry of the tailings in each bore-hole: non-acid generating, uncertain and acid generating. By comparing the depth of each layer to the depth to 85% saturation, it was concluded that there is a potential for acid generation to occur at some of the locations.

6.5.2 Observations based on the Numerical Modeling Results

Based on the numerical modeling results, it was possible to make conclusions regarding the effectiveness of the cover at the Detour Lake mine site. The numerical modeling yielded three types of information: saturation profiles from SoilCover, oxygen concentration profiles from the oxygen modeling and oxygen fluxes from the oxygen concentration profile on the last simulation day.

The saturation profiles from SoilCover were sufficient to make predictions with respect to the potential for oxygen diffusion into the tailings. The homogeneous coarse tailings profile and the coarse over fine tailings profile both produced considerable desaturation in the coarse tailings regardless of the water table depth. Both of these profiles show potential for oxygen penetration. The fine over coarse tailings and the

homogeneous fine tailings demonstrated the ability of the fine tailings to maintain high saturation well above the water table. The fine over coarse tailings profile with a 4 m water table showed some desaturation at the surface that would indicate there is potential in this scenario for oxygen penetration through the cover layer.

The oxygen diffusion and consumption modeling supported the predictions based on the saturation profiles and gave additional information with respect to the effect of kinetic oxidation. It was observed that two factors affect whether or not accounting for kinetic oxidation reduces the oxygen flux at a given interface: the degree of saturation of the material and the reactivity of the material. For the less reactive material (coarse tailings), a desaturated profile led to an increased oxygen flux at an interface within the desaturated zone when oxidation was included. For a more reactive material (fine tailings), a desaturated profile produced a decreased oxygen flux at the interface within the desaturated zone when oxidation was included. This was illustrated by the fine over coarse tailings profile with a 4 m water table that resulted in the consumption of all the oxygen penetrating into the fine tailings thus preventing any from reaching the sulphidic tailings.

The evaluation of the coarse over fine tailings profile illustrated that accounting for kinetic oxidation does reduce the oxygen flux into the sulphidic tailings compared to that predicted without kinetic oxidation. As was expected from the saturation profiles, the oxygen flux into the tailings during a mean or wet year was reduced from that compared to the dry year. Also as expected from the saturation profiles, the effect of vegetation on the oxygen concentration profiles was insignificant for the dry years. In general, for the coarse over fine tailings scenarios, only the scenarios with a shallow water table show small oxygen fluxes reaching the sulphidic tailings. Regardless of vegetation or

amount of precipitation, oxygen penetrated into the sulphidic tailings for all the scenarios modeled with a 4 m depth to water table.

Chapter 7
SUMMARY AND CONCLUSIONS

7.1 SUMMARY

The use of oxygen-consuming materials as cover materials on mine tailings has been investigated over the last decade to determine the potential of these materials to reduce acid rock drainage. Of the oxygen-consuming materials investigated, low-sulphur tailings are intriguing due to their potential abundance at a mine site. The research that has previously investigated low-sulphur tailings as a cover material has primarily focused on laboratory experiments. Field-scale experiments have predominantly consisted of instrumented test covers.

A desulphurized tailings cover was installed at Detour Lake Mine in 1998/99 covering a portion of the tailings impoundment not under a water cover. The cover was intended to reduce oxygen diffusion into the underlying sulphidic tailings in two ways: 1) by maintaining a high degree of saturation to reduce the diffusive flux of oxygen through the cover, and 2) by consuming any of the oxygen that did penetrate the cover by oxidation of the remaining sulphide minerals in the desulphurized tailings. Once the cover was installed, a research program was initiated to determine the effectiveness of the cover at reducing oxygen diffusion into the underlying sulphidic tailings.

The scope of the research involved a field investigation, laboratory analyses and numerical modeling. The field investigation involved instrumenting the tailings facility to measure water table depth, water content profiles and detailed meteorological data.

Nine bore-hole locations, each consisting of a piezometer and a neutron probe access tube, were installed representing three profiles through the cover. During the installation of the instrumentation, samples of the tailings were removed for the laboratory analysis.

The laboratory analysis consisted of grain-size analyses, saturated hydraulic conductivity analyses, specific gravity determination and measurement of the soil-water characteristic curve. Analyses performed outside of the University of Saskatchewan were acid-base accounting tests, mineralogy, and measurement of the diffusion and kinetic oxidation coefficients. The goal of the laboratory analysis was to satisfy two objectives: 1) to make qualitative conclusions on the effectiveness of the cover, and 2) to characterize the tailings facility on which to base the numerical modeling.

The purpose of the numerical modeling was to evaluate the oxygen concentration profile through different potential tailings profiles to determine the relative effect of weather, vegetation and water table depth. The program SoilCover was used to determine the saturation profiles as they changed over a simulation year for different scenarios. To predict oxygen concentration profiles, a finite difference model was developed using the program MATLAB to evaluate oxygen diffusion and consumption based on the saturation profiles calculated from SoilCover. Using the oxygen concentration profile on the last day of the simulation, oxygen fluxes were estimated at the surface and at the interface between the desulphurized and sulphidic tailings.

7.2 CONCLUSIONS

The field investigation, laboratory analysis and numerical modeling performed on the desulphurized tailings cover at Detour Lake allowed for qualitative conclusions to be made on the effectiveness of the cover at reducing oxygen penetration into the sulphidic

tailings. The results of the field investigation indicated that, during the dry year of 2000/2001, there was desaturation of the tailings above the water table. Low water contents were measured in the surface tailings (~0.2 m) at most bore-hole locations. This indicates there is the potential for oxygen to enter the tailings surface.

The tailings were observed to be highly stratified with interbedded layers of fine and coarse tailings. The water content profiles were in agreement with this observation since they showed notable variation with depth. Most of the bore-holes contained a layer of tailings with a high water content at a maximum depth of 2 m, regardless of the water table depth. It is possible that interbedded layers of fine and coarse tailings could create a capillary barrier effect within the tailings profile that was not accounted for by generalized models.

The laboratory investigation determined that the desulphurized tailings did not show considerable variation in geotechnical characteristics from the sulphidic tailings. Based on the geochemical analysis, the cover was found to range in thickness from 1 to 1.5 m. The desulphurized tailings were determined to be slightly coarser than the sulphidic tailings. The saturated hydraulic conductivity of all the tailings ranged between 2×10^{-6} to 1×10^{-7} m/s. The air-entry values of the tailings ranged from 6 to 20 kPa and 8 to 50 kPa for the desulphurized and sulphidic tailings, respectively.

The geochemical analysis of the tailings resulted in the development of three hypothetical layers: non-acid generating, uncertain and acid generating. The thickness of each of these layers in each of the bore-holes was compared to the depth to 85% saturation. Based on this analysis, it was concluded that there was potential for acid generation at most of the locations.

To perform the numerical modeling, it was necessary to simplify the Detour Lake tailings facility into representative profiles based on the geotechnical and geochemical data obtained during the laboratory analysis. This was difficult since both the desulphurized and the sulphidic tailings had similar geotechnical characteristics. The tailings chosen for the modeling were the coarsest and finest samples determined from the grain-size analyses. The tailings profiles chosen were homogeneous fine, homogeneous coarse, 1.8 m fine over coarse and 1.8 m coarse over fine tailings. For the SoilCover modeling, each of these profiles were evaluated for combinations of dry, mean or wet weather, non-vegetated, good or poor vegetation and a 1 or 4 m depth to the water table. For the oxygen diffusion and consumption modeling, a portion of the SoilCover results were chosen as the most representative and these scenarios were evaluated with and without kinetic oxidation. Kinetic oxidation coefficients were chosen to represent each of the coarse and fine tailings layers. The value of 10 / yr was chosen for the coarse tailings coefficient and the value of 44 / yr was chosen for the fine tailings coefficient.

The results of the SoilCover modeling illustrated the saturation profiles changing with time for the different tailings profiles for different weather, vegetation and water table depths. The homogeneous coarse tailings, regardless of water table depth, showed desaturation above the water table. The surface of the coarse tailings profile desaturated to 5% for a period of the model year for both the 1 m and 4 m depths to the water table.

The fine over coarse profile, illustrating the effect of a capillary break, remained fully saturated to the surface for the shallow water table. The 4 m water table scenario showed the fine tailings layer reaching 85% saturation approximately 1 m from the surface for most of the model year.

The coarse over fine tailings profile was concluded to be the profile most representative of the tailings facility at Detour Lake Mine. The saturation profiles for this profile illustrated considerable desaturation of the coarse tailings layer above the water table. The average saturation of the coarse tailings layer was observed to be sensitive to the weather year. The mean saturation of the 4 m water table scenario for the dry year was approximately 35% compared to 40% and 50% for the mean and wet weather scenarios, respectively. Vegetation was determined to have an insignificant effect on the coarse over fine tailings profile, regardless of water table depth or weather. The moisture flux rates from the different vegetation scenarios revealed that regardless of the vegetation quality, the evapotranspiration rate was constant. It was concluded that the effect of vegetation was to reduce the evaporation rate. In summary, it was determined that the tailings profile was unaffected by the mechanism with which moisture was removed: transpiration versus evaporation.

Based on the SoilCover modeling results, it was concluded that there is potential for oxygen diffusion into the tailings surface for all the scenarios except the homogeneous fine tailings and the fine over coarse tailings with a shallow water table.

The oxygen diffusion and consumption modeling predicted the oxygen concentration profiles through the tailings with time using the saturation profiles calculated using SoilCover. Using the oxygen concentration profiles, the flux of oxygen into the surface and the flux entering the sulphidic tailings were estimated. Only the homogeneous coarse, fine over coarse and coarse over fine tailings scenarios were chosen for the oxygen diffusion and consumption modeling. These were chosen to represent the worst-case, best-case and realistic-case scenarios.

The oxygen diffusion and consumption modeling illustrated the effect of accounting for kinetic oxidation of the sulphide minerals on the oxygen concentration profile and the resulting oxygen flux through the tailings. Accounting for kinetic oxidation was found to reduce the oxygen flux entering the sulphidic tailings in some cases, and increase the flux in other cases. Two factors were found to affect whether the flux increased or decreased: the saturation of the material around the interface and the reactivity of the material.

It was concluded that whether or not the flux into the sulphidic tailings was reduced when kinetic oxidation was included depended on the balance between the saturation and reactivity of the tailings. On one hand, if diffusion was slow and reactivity fast, the consumption by kinetic oxidation could keep up with the diffusion rate and consume all the oxygen. On the other hand, if diffusion was fast and reactivity slow, the consumption could not keep up with the diffusion rate and would allow oxygen to penetrate deep into the tailings. For the homogeneous coarse tailings, which experienced considerable desaturation, accounting for kinetic oxidation increased the oxygen flux both at the surface and into the sulphidic tailings. For the fine over coarse tailings profile, the fine layer remained somewhat saturated and, due to its higher reactivity, was able to consume virtually all the oxygen that penetrated through the surface.

The coarse over fine tailings profile showed an increase in oxygen flux into the surface and a reduction in the oxygen flux into the sulphidic tailings when kinetic oxidation was included. As was expected, the oxygen flux both into the surface and into the sulphidic tailings decreased for the mean and wet years from that during the dry year. Also as expected, vegetation did not affect the oxygen concentration or flux.

Regardless of the weather or vegetation scenarios, oxygen penetrated to the interface between the tailings layers for the coarse over fine tailings scenario with a 4 m water table. It was concluded that, for the coarse over fine tailings profile with a 4 m water table, there is the potential for considerable oxygen penetration into the sulphidic tailings. The coarse over fine tailings scenario with a 1 m water table was observed to reduce the oxygen penetration into the sulphidic tailings to low levels for all weather and vegetation scenarios.

The general conclusion from this research is that the desulphurized tailings cover at Detour Lake Mine is likely not reducing oxygen penetration into the sulphidic tailings to low levels over the entire tailings surface. The desulphurized tailings were not found to have sufficient variation in hydraulic properties from the sulphidic tailings to maintain a high degree of saturation above the water table. The factors acting to reduce oxygen penetration into the sulphidic tailings were determined to be the ability of the sulphidic tailings to remain saturated above the water table, the consumption of oxygen penetrating into the coarse tailings, and, based on field observations, the interbedded nature of the tailings allowing for fine tailings layers to act as potential oxygen barriers.

7.3 APPLICATION OF RESEARCH

The use of oxygen-consuming materials as cover materials has potential for the remediation of wastes where the purpose of the cover is to reduce oxygen penetration. Often these materials are wastes themselves that would otherwise require their own remediation. Desulphurized or low-sulphur tailings are an attractive cover material since they provide a lower cost alternative to layered soil covers where the materials

need to be brought to site. Development of this technology may be an important step in reducing global pollution from acid rock drainage.

The design of low-sulphur covers involves many factors. A balance between the hydraulic properties of the tailings and the reactivity of the tailings must be attained for the cover to consume more oxygen than it allows to diffuse through. Depending on the reactivity, the tailings must have sufficient buffering capacity to prevent the cover itself from producing acid rock drainage. The most important application of this research is to use what has been discovered regarding the balance between hydraulic properties and reactivity to improve the design of low-sulphur tailings covers in the future.

Segregation of the tailings during deposition was determined to be a factor affecting cover performance. For future low-sulphur tailings cover designs, the method of deposition of the tailings should be considered during the cover design. This research illustrated how layering and segregation of the tailings can affect cover performance.

7.4 FURTHER RESEARCH

This research project predicted the oxygen concentration profiles through the Detour Lake tailings using numerical modeling based on simplified representations of the tailings facility. The modeling allowed for a qualitative estimation of the effectiveness of the cover and illustrated the relative effect of weather, vegetation and water table depth on oxygen penetration. The research did not allow for quantitative conclusions based on measured oxygen concentrations or fluxes. To quantify the oxygen fluxes reaching the sulphidic tailings, a detailed field program measuring the oxygen concentration with depth and the oxygen flux through the surface at various locations throughout the tailings profile would be required. Once the actual oxygen flux was

measured, the sulphide oxidation rate in the sulphidic tailings could be quantified. This would allow a more definitive conclusion to be made with respect to the potential for acid rock drainage from the Detour Lake Mine tailings.

Using measured oxygen concentration profiles, the oxygen diffusion and consumption model developed for this research could be verified. If data was available giving the kinetic coefficient of the tailings with depth, the model could predict oxygen concentrations and fluxes at various locations throughout the cover using measured saturation profiles through the cover with time.

REFERENCES

Aachib, M., Aubertin, M. and Chapuis, R.P. 1994. Column tests investigation of milling wastes properties used to build cover systems. *3rd International Conference on the Abatement of Acidic Drainage.* **2**: 128 – 137.

Aubertin, M. 2001. Personal Communication.

Aubertin, M., Aachib, M, and Authier, K. 2000. Evaluation of diffusive flux through covers with a GCL. *Geotextiles and Geomembranes.* **18:** 215 – 233.

Aubertin, M., Ricard, J.F. and Chapuis, R.P. 1998. A predictive model for water retention curve: application to tailings from hard-rock mines. *Canadian Geotechnical Journal.* **35:** 55-69.

Barbour, S.L. 1986. Osmotic flow and volume change in clay soils. Ph. D. Thesis, Univerisity of Saskatchewan, Saskatoon, SK, Canada.

Barbour, S.L. 1990. Reduction of acid generation in mine tailings through the use of moisture-retaining cover layers as oxygen barriers: Discussion. *Canadian Geotechnical Journal.* **27**: 398-401.

Barbour, S.L., Wilson, G.W. and St. Arnaud, L.C. 1993. Evaluation of the saturated – unsaturated groundwater conditions of a thickened tailings deposit. *Canadian Geotechnical Journal.* **30:** 935 – 946.

Benzaazoua, M. and Bussière, B. 1998. Geochemical behaviour of a multi-layered cover composed of desulfurized mine tailings. *Tailings and Mine Waste '98: Proceedings of the 5th International Conference.* 389 – 398.

Bernier, L. 2001. Mineralogical and chemical analysis of pyritized and de-pyritized tailings samples. Géoberex Recherche technical report prepared for the University of Saskatchewan.

Blowes, D.W. and Jambor, J.L. 1990. The pore-water geochemistry and the mineralogy of the vadose zone of sulfide tailings, Waite Amulet, Quebec, Canada. *Applied Geochemistry.* **5:** 327 – 346.

Bussière, B., Nicholson, R.V., Aubertin, M. and Benzaazoua, M. 1997a. Evaluation of the effectiveness of covers built with desulfurized tailings for preventing acid mine drainage. *50th Canadian Geotechnical Conference.* **1**: 17 – 25.

Bussière, B., Nicholson, R.V., Aubertin, M. and Servant, S. 1997b. Effectiveness of covers built with desulphurized tailings: column test investigation. *Fourth International Conference on Acid Rock Drainage.* **2:** 763 – 778.

Cabral, A., Racine, I., Burnotte, F. and Lefebvre, G. 2000. Diffusion of oxygen through a pulp and paper residue barrier. *Canadian Geotechnical Journal.* **37:** 201 – 217.

Collin, M. 1998. The Bersbo Pilot Project. Numerical simulation of water and oxygen transport in the soil covers at mine waste deposits. Swedish Environmental Protection Agency. Report 4763, 46 pages, plus appendix.

Collin, M. and Rasmuson, A. 1988. A comparison of gas diffusivity models for unsaturated porous media. *Soil Science Society of America Journal.* **52:** 1559 – 1565.

Crank, J. 1975. The mathematics of diffusion. 2nd Ed. Clarendon Press, Oxford, UK.

CTRAN/W User's Manual. 1999. Geo-Slope International Ltd. Calgary, AB, Canada.

Currie, J.A. 1960a. Gaseous diffusion in porous media. Part 1.- A non-steady state method. *British Journal of Applied Physics.* **11:** 314 – 317.

Currie, J.A. 1960b. Gaseous diffusion in porous media. Part 2.- Dry granular materials. *British Journal of Applied Physics.* **11:** 318 – 324.

Currie, J.A. 1960c. Gaseous diffusion in porous media. Part 3.- Wet granular materials. *British Journal of Applied Physics.* **12:** 275 – 281.

Dubrovsky, N.M., Morin, K.A., Cherry, J.A. and Smyth, D.J.A. 1984. Uranium tailings acidification and subsurface contaminant migration in a sand aquifer. *Water Pollution Research Journal of Canada.* **19**(2): 55 – 89.

Elberling, B., and Nicholson, R.V. 1996. Field determination of sulphide oxidation rates in mine tailings. *Water Resources Research.* **32:** 1773-1784.

Elberling, B., Nicholson, R.V. and David, D.J. 1993. Field evaluation of sulphide oxidation rates. *Nordic Hydrology.* **24:** 323-338.

Elberling, B., Nicholson, R.V. and Scharer, J.M. 1994a. A combined kinetic and diffusion model for pyrite oxidation in tailings: a change in controls with time. *Journal of Hydrology.* **157:** 47-60.

Elberling, B., Nicholson, R.V., Reardon, E.J. and Tibble, P. 1994b. Evaluation of sulphide oxidation rates: a laboratory study comparing oxygen fluxes and rates of oxidation product release. *Canadian Geotechnical Journal.* **31:** 375 – 383.

Ellerbroek, D.A. and Jones, D.R. 1997. Hydrochemical characterization to support decommissioning of sulfidic tailings. *Tailings and Mine Water '97: Proceedings of the 4th International Conference.* 443 – 452.

Elliot, L.C.M., Liu, L. and Stogran, S.W. 1997. Evaluation of single layer organic and inorganic cover materials for oxidized tailings. *Tailings and Mine Waste '97: Proceedings of the 4th International Conference.* 247 – 256.

Flegg, P.B. 1953. The effect of aggregation on diffusion of gases and vapour through soils. *Journal of the Science of Food and Agriculture.* **4:** 104 – 108.

Fredlund D.G. and Rahardjo H.R. 1993. Soil Mechanics for Unsaturated Soils. John Wiley & Sons Inc. New York, N.Y.

Hanton-Fong, C.J., Blowes, D.W. and Stuparyk, R.A.. 1997. Evaluation of low sulphur tailings in the prevention of acid mine drainage. *Proceedings of the 4th International Conference on Acid Rock Drainage.* **2:** 835 – 851.

Jambor, J.L. and Blowes, D.W. 1994. The environmental geochemistry of sulfide mine-wastes. *Mineralogical Association of Canada, Short Course Series.* **22.**

Kimball, B.A. and Lemon, E.R. 1971. Air turbulence effects upon soil gas exchange. *Soil Science Society of America Proceedings.* **35:** 16-21.

Lawrence, R.W. and Scheske, M. 1997. A Method to calculate the neutralization potential of Mining Wastes. *Environmental Geology.* **32**(2): 100 – 106.

Lawrence, R.W. and Wang, Y. 1997. Determination of Neutralization Potential in the Prediction of Acid Rock Drainage. *Fourth International Conference on Acid Rock Drainage, Vancouver B.C.*, **2:** 449 – 464.

Lapakko, K.A. 1994. Evaluation of neutralization potential determination for metal waste and a proposed alternative. *Proceedings of the International Land Reclamation and Mine Drainage Conference and 3rd International Conference on the Abatement of Acidic Drainage, Pittsburgh.* **1** : 129 – 137.

MathWorks Inc. 1997. The Student Edition of MATLAB® (Version 5 User's Guide) Prentice-Hall Canada Inc., Toronto, ON.

Mbonimpa, M., Aubertin, M., Aachib, M. and Bussière, B. 2001. Oxygen diffusion and consumption in unsaturated cover materials. Submitted to *Canadian Geotechnical Journal* – November, 2001.

Millington, R.J. and Shearer, R.C. 1971. Diffusion in aggregated porous media. *Soil Science.* **111:** 372 – 378.

Minister of Public Works and Government Services Canada. 2001. Environment Canada: Canadian Climate Normals Website: http://www.msc-smc.ec.gc.ca/climate/climate_normals/index_e.cfm

Moses, C.O. and Herman, J.S. 1991. Pyrite oxidation at circumneutral pH. *Geochimica et Cosmochimica Acta.* **55:** 471-482.

Nicholson, R.V., Gillham, R.W., Cherry, J.A. and Reardon, E.J. 1989. Reduction of acid generation in mine tailings through the use of moisture-retaining cover layers as oxygen barriers. *Canadian Geotechnical Journal.* **26:** 1-8.

Nicholson, R.V., Gillham, RW., and Reardon, E.J. 1988. Pyrite oxidation in carbonate-buffered solution: 1. Experimental kinetics. *Geochimica et Cosmochimica Acta.* **52:** 1077-1085.

O'Kane, M., Wilson, G.W., Barbour, S.L. and Swanson, D.A. 1995. Aspects on the performance of the till cover system at Equity Silver Mines Ltd. *Sudbury '95, Conference on Mining and the Environment.*

Penman, H.L. 1940a. Gas and Vapour Movements in the Soil: I. The diffusion of vapours through porous solids. *Journal of Agricultural Science.* **30:** 437-462.

Penman, H.L. 1940b. Gas and Vapour Movements in the Soil: II. The diffusion of carbon dioxide through porous solids. *Journal of Agricultural Science.* **30:** 570 – 581.

Plumlee, G.S. and Logsdon M.J. 1999. The environmental geochemistry of mineral deposits. Part A : Processes, Techniques, and Health Issues. Part B : Cases Studies and Research Topics. *Society of Economic Geology, Reviews in Economic Geology.* **6A** and **6B**: 371p.

Reardon, E.J. and Moddle, P.M. 1985. Gas diffusion coefficient measurements on uranium mill tailings: implications to cover layer design. *Uranium.* **2:** 111 – 131.

Ricard, J.F., Aubertin, M., Firlotte, F.W., Knapp, R., McMullen, J. and Julien, M. 1997. Design and construction of a dry cover made of tailings for the closure of Les Terrains Aurifères site, Malartic, Québec, Canada. *Proceedings of the 4th International Conference on Acid Rock Drainage.* **4:** 1516 – 1530.

Rowe, R.K., Booker, J.R. and Fraser, M.J. 1994. POLLUTE v6. GAEA Environmental Engineering Ltd., London, ON.

Scharer, J.M., Kwong, E.C.M., Nicholson, R.V., Pettit, C.M. and Chambers, D.W. 1995. Factors affecting ARD production: kinetics of sulphide oxidation. In: *Sudbury '95 Mining and the Environment.* **2:** 451-459.

SoilCover User's Manual. 1997. Unsaturated Soils Group, University of Saskatchewan, Saskatoon, SK, Canada.

Tassé, N., Germain, D., Dufour,C. and Tremblay, R. 1997. Organic-waste cover over the East Sullivan mine tailings: Beyond the oxygen barrier. *Proceedings of the 4th International Conference on Acid Rock Drainage, Vancouver, BC,* **4:** 1627 – 1642.

Tratch, D. 1994. Moisture uptake within the root zone. M. Sc. Thesis, Department of Civil Engineering, University of Saskatchewan, Saskatoon, SK, Canada.

Tremblay, R.L., 1994. Controlling acid mine drainage using an organic cover: The case of the East Sullivan Mine, Abitibi, QC. *Proceedings of the 3rd International Conference on the Abatement of Acidic Drainage, Pittsburgh, PA.* **2:** 122 – 127.

Troeh, F. R., Jabro, J.D. and Kirkham, D. 1982. Gaseous diffusion equations for porous materials. *Geoderma.* **27:** 239 – 253.

Wheeland, K.G., and Feasby, G. 1991. Innovative decommission technologies via Canada's MEND program. *Proceedings of the 12th National Conference on Hazardous Material Control/ Superfund '91.* Hazardous Material Control Research Institute. pp. 23 – 28.

Wilson, G.W. 1990. Soil Evaporative Fluxes for Geotechnical Engineering Problems. Ph. D. Thesis. Department of Civil Engineering, University of Saskatchewan, Saskatoon, SK, Canada.

Wilson, G.W., Fredlund, D.G. and Barbour, S.L. 1994. Coupled soil-atmosphere modeling of soil evaporation. *Canadian Geotechnical Journal.* **31:** 151 – 161.

Wilson, G.W., Fredlund, D.G. and Barbour, S.L. 1997. The effect of soil suction on evaporative fluxes from soil surfaces. *Canadian Geotechnical Journal.* **34:** 145 – 155.

Yanful, E.K., Bell, A.V., and Woyshner, M.R.. 1993a. Design of a composite soil cover for an experimental waste rock pile near Newcastle, New Brunswick, Canada. *Canadian Geotechnical Journal.* **30:** 578-587.

Yanful, E.K. 1993b. Oxygen diffusion through soil covers on sulphidic mine tailings. *Journal of Geotechnical Engineering.* **119:** 1207 – 1228.

Zill, D. G. and Cullen, M. R. 1992. Advanced Engineering Mathematics. PWS Publishing Company, Boston, MA.

Appendix A: Weather Data for SoilCover Modeling

Day	PE mm/day	Max Temp C	Min Temp C	Max RH dec	Min RH dec	Mean Year 1972 Precip mm/day	Wet Year 1961 Precip mm/day
8-Apr-00	-2	5.627	-0.246	0.953	0.852	11.95	13.221
9-Apr-00	-2	-0.162	-6.751	0.944	0.844	11.95	13.221
10-Apr-00	-2	4.759	-7.21	0.918	0.43	11.95	13.221
11-Apr-00	-2	11.04	-4.256	0.845	0.29	13.45	13.221
12-Apr-00	-2	7.61	3.034	0.968	0.397	11.95	13.221
13-Apr-00	-2	6.911	-8.02	0.95	0.571	11.95	17.321
14-Apr-00	-2	2.593	-13.82	0.909	0.291	11.95	13.221
15-Apr-00	-2	2.347	-8.07	0.85	0.259	11.95	13.221
16-Apr-00	-2	0.679	-11.22	0.888	0.277	12.45	15.721
17-Apr-00	-2	-3.487	-12.37	0.81	0.495	12.25	15.021
18-Apr-00	-2	1.108	-11.35	0.869	0.366	12.75	13.221
19-Apr-00	-2	11.4	-11.78	0.847	0.261	11.95	13.221
20-Apr-00	-2	16.7	-1.32	0.6382	0.264	11.95	13.221
21-Apr-00	-2	12.68	2.813	0.966	0.446	11.95	18.021
22-Apr-00	-2	6.302	-7.87	0.966	0.417	0	0
23-Apr-00	-2	11.25	-3.409	0.968	0.665	0.3	0
24-Apr-00	-2	4.311	-4.834	0.95	0.555	0	0
25-Apr-00	-2	11.97	-8.37	0.914	0.245	0	0
26-Apr-00	-2	14.2	-1.134	0.917	0.496	0	0
27-Apr-00	-2	3.417	-4.758	0.737	0.312	0	0
28-Apr-00	-2	9.14	-8.99	0.821	0.233	0	0
29-Apr-00	-2	19.35	-3.695	0.76	0.17	0	0
30-Apr-00	-2	27.75	10.23	0.5682	0.235	0	3
1-May-00	-4.774	23.17	12.54	0.748	0.361	0	12.7
2-May-00	-4.774	22.4	9.92	0.958	0.295	0	11.4
3-May-00	-4.774	17.14	6.072	0.749	0.354	12.4	0.5
4-May-00	-4.774	7.57	-1.85	0.915	0.522	0	0
5-May-00	-4.774	13.97	-4.724	0.944	0.143	0	0
6-May-00	-4.774	20.32	-0.924	0.745	0.153	10.7	6.6
7-May-00	-4.774	25.38	3.614	0.5901	0.179	0	0.5
8-May-00	-4.774	21.08	13.8	0.801	0.197	0	1.5
9-May-00	-4.774	18.19	5.976	0.67	0.264	0	1.3
10-May-00	-4.774	22.12	0.285	0.937	0.231	0	0
11-May-00	-4.774	12.93	-0.989	0.942	0.608	0	0
12-May-00	-4.774	9.1	-2.268	0.901	0.299	0	0
13-May-00	-4.774	12.69	-2.196	0.904	0.197	0	16.5
14-May-00	-4.774	14.89	-3.895	0.93	0.156	0.5	8.9
15-May-00	-4.774	19.12	1.888	0.629	0.111	0	39.9
16-May-00	-4.774	21.75	5.599	0.89	0.272	0	0
17-May-00	-4.774	20.45	10.54	0.913	0.468	0	0
18-May-00	-4.774	17.21	10.6	0.951	0.562	0	0
19-May-00	-4.774	21.35	10.04	0.964	0.368	0	0
20-May-00	-4.774	26.78	7.57	0.943	0.222	0	1

21-May-00	-4.774	26.67	10.82	0.779	0.24	0	0
22-May-00	-4.774	21.83	14.51	0.6657	0.412	0	0
23-May-00	-4.774	17.79	10.47	0.964	0.653	0	0
24-May-00	-4.774	22.37	7.84	0.972	0.486	0	0.3
25-May-00	-4.774	25.3	11.85	0.933	0.304	0	0
26-May-00	-4.774	21.18	13.39	0.89	0.376	0	0
27-May-00	-4.774	20.27	11.03	0.926	0.503	0	1.8
28-May-00	-4.774	12.86	0.632	0.972	0.823	8.6	0
29-May-00	-4.774	6.179	-0.542	0.933	0.608	53.8	0
30-May-00	-4.774	9.1	-2.005	0.92	0.471	11.4	0
31-May-00	-4.774	20.32	-1.663	0.924	0.206	0	0.5
1-Jun-00	-5.267	21.45	4.976	0.748	0.252	0	11.2
2-Jun-00	-5.267	14.6	5.669	0.96	0.489	0	11.9
3-Jun-00	-5.267	9.51	4.911	0.972	0.926	25.4	3.8
4-Jun-00	-5.267	10.82	3.442	0.965	0.782	0	3.3
5-Jun-00	-5.267	16.35	5.044	0.923	0.262	0	0
6-Jun-00	-5.267	19.13	1.333	0.5386	0.173	1.3	0
7-Jun-00	-5.267	15.96	-0.551	0.836	0.235	4.8	2.5
8-Jun-00	-5.267	22.13	-0.058	0.857	0.253	7.1	0
9-Jun-00	-5.267	27.27	6.408	0.836	0.24	0	0
10-Jun-00	-5.267	27.34	3.437	0.9	0.197	0	0
11-Jun-00	-5.267	27.3	11.89	0.783	0.298	0	0
12-Jun-00	-5.267	20.98	5.411	0.937	0.57	0	0
13-Jun-00	-5.267	16.9	2.541	0.886	0.405	0	0
14-Jun-00	-5.267	34.33	10.56	0.937	0.245	13.5	0
15-Jun-00	-5.267	33.55	17.03	0.949	0.349	0.8	0
16-Jun-00	-5.267	26.04	14.09	0.948	0.19	0.3	0
17-Jun-00	-5.267	17.64	9.03	0.855	0.324	0	0.5
18-Jun-00	-5.267	22.13	1.568	0.935	0.222	0	4.8
19-Jun-00	-5.267	24.11	11.71	0.956	0.409	0	0
20-Jun-00	-5.267	19.31	7.95	0.88	0.307	34.3	0
21-Jun-00	-5.267	20.54	7.46	0.905	0.348	0	0
22-Jun-00	-5.267	14.48	9.35	0.879	0.522	0	8.4
23-Jun-00	-5.267	25.96	8.64	0.93	0.258	6.1	45.2
24-Jun-00	-5.267	23.23	7.35	0.933	0.409	0.5	4.1
25-Jun-00	-5.267	28.59	5.083	0.933	0.424	3.6	0
26-Jun-00	-5.267	35.1	20.91	0.6621	0.322	11.4	0
27-Jun-00	-5.267	27.27	9.15	0.823	0.386	0	4.8
28-Jun-00	-5.267	21.45	7.45	0.879	0.291	0	0
29-Jun-00	-5.267	26.6	10.94	0.955	0.633	0	0
30-Jun-00	-5.267	14.46	7.54	0.942	0.665	1.5	0
1-Jul-00	-5.581	10.7	2.75	0.946	0.522	0	5.3
2-Jul-00	-5.581	10.7	2.75	0.946	0.522	0.5	0
3-Jul-00	-5.581	10.7	2.75	0.946	0.522	0	10.4
4-Jul-00	-5.581	10.7	2.75	0.946	0.522	0	0
5-Jul-00	-5.581	16.11	4.93	0.938	0.422	0	0
6-Jul-00	-5.581	17.13	4.797	0.908	0.395	0	16.8
7-Jul-00	-5.581	19.94	5.785	0.928	0.32	0	4.6
8-Jul-00	-5.581	23.09	6.438	0.913	0.295	0	0
9-Jul-00	-5.581	18.7	13.14	0.965	0.84	20.1	0
10-Jul-00	-5.581	20.85	8.2	0.959	0.363	0	0

11-Jul-00	-5.581	20.76	5.749	0.904	0.311	0	0
12-Jul-00	-5.581	26.86	2.457	0.968	0.234	11.2	3.8
13-Jul-00	-5.581	23.39	11.42	0.827	0.362	0	0
14-Jul-00	-5.581	22.09	14.83	0.939	0.569	6.6	15.5
15-Jul-00	-5.581	25.55	12.82	0.927	0.436	0	3.3
16-Jul-00	-5.581	26.95	13.11	0.966	0.386	0	25.7
17-Jul-00	-5.581	26.25	10.57	0.909	0.416	3.3	33
18-Jul-00	-5.581	12.3	6.32	0.943	0.579	2.5	0
19-Jul-00	-5.581	18.67	3.352	0.89	0.333	0	0
20-Jul-00	-5.581	18.89	6.61	0.93	0.418	0	3
21-Jul-00	-5.581	13.77	9.01	0.908	0.681	0	0
22-Jul-00	-5.581	17.02	8.12	0.962	0.63	0.8	0
23-Jul-00	-5.581	23.39	10.34	0.807	0.324	7.4	0
24-Jul-00	-5.581	25.88	10.42	0.876	0.318	4.8	8.9
25-Jul-00	-5.581	26.8	16.7	0.809	0.363	13.5	0
26-Jul-00	-5.581	28.18	14.97	0.79	0.327	1	3.6
27-Jul-00	-5.581	28.32	13.63	0.931	0.387	0.3	8.4
28-Jul-00	-5.581	20.63	9.48	0.965	0.479	0	0
29-Jul-00	-5.581	27.06	8.35	0.97	0.332	0	0.3
30-Jul-00	-5.581	30.95	11.04	0.944	0.216	0	5.1
31-Jul-00	-5.581	30.23	15.49	0.854	0.378	6.1	0
1-Aug-00	-4.355	27.2	15.78	0.973	0.519	0	0
2-Aug-00	-4.355	15.82	9.18	0.974	0.886	3.3	7.1
3-Aug-00	-4.355	10.96	7.53	0.957	0.871	1.3	0
4-Aug-00	-4.355	20.77	8.84	0.93	0.303	0	1.8
5-Aug-00	-4.355	26.23	4.915	0.942	0.297	1.3	1.5
6-Aug-00	-4.355	22.75	14.38	0.907	0.477	0	0
7-Aug-00	-4.355	17.68	15.47	0.935	0.861	0	0
8-Aug-00	-4.355	24.72	14.35	0.966	0.445	0	0
9-Aug-00	-4.355	25.12	10.82	0.799	0.307	0.5	0
10-Aug-00	-4.355	24.42	8.16	0.822	0.295	2	16
11-Aug-00	-4.355	24.75	9.7	0.927	0.348	0.8	3
12-Aug-00	-4.355	27.89	8.41	0.963	0.294	0	0.8
13-Aug-00	-4.355	21.45	12.91	0.864	0.571	6.1	1
14-Aug-00	-4.355	24.96	5.662	0.967	0.3	0	0
15-Aug-00	-4.355	23.84	12.24	0.942	0.601	0	2.5
16-Aug-00	-4.355	12.27	6.843	0.943	0.753	2	0
17-Aug-00	-4.355	18.77	4.356	0.906	0.317	5.8	0
18-Aug-00	-4.355	15.24	7.86	0.95	0.574	0	2.5
19-Aug-00	-4.355	11.86	5.634	0.95	0.71	0	11.9
20-Aug-00	-4.355	17.04	3.382	0.958	0.359	0	0
21-Aug-00	-4.355	19.22	1.076	0.959	0.422	4.8	0
22-Aug-00	-4.355	22.54	12.82	0.938	0.555	3.8	0
23-Aug-00	-4.355	20.74	11.39	0.97	0.496	0	0
24-Aug-00	-4.355	23.64	12.18	0.961	0.389	22.4	2.8
25-Aug-00	-4.355	28.96	14.82	0.938	0.301	0.8	0
26-Aug-00	-4.355	18.62	9.23	0.945	0.408	0	14.5
27-Aug-00	-4.355	23	6.005	0.942	0.17	0	13.5
28-Aug-00	-4.355	25.08	7.21	0.83	0.194	0	0
29-Aug-00	-4.355	19.32	10.87	0.958	0.528	0	0
30-Aug-00	-4.355	22.45	9.68	0.888	0.339	14.7	0

31-Aug-00	-4.355	23.64	6.578	0.944	0.644	5.6	77.2
1-Sep-00	-2.567	10.17	3.826	0.931	0.556	4.6	43.9
2-Sep-00	-2.567	14.77	1.316	0.935	0.387	0	2.3
3-Sep-00	-2.567	14.68	1.667	0.96	0.349	0	0
4-Sep-00	-2.567	10.25	0.319	0.955	0.52	0	0
5-Sep-00	-2.567	15.43	-1.099	0.963	0.353	6.9	0
6-Sep-00	-2.567	19.1	3.576	0.898	0.253	0	0.8
7-Sep-00	-2.567	22.6	12.6	0.833	0.408	0	0
8-Sep-00	-2.567	16.74	6.537	0.949	0.498	0	0
9-Sep-00	-2.567	22.97	4.686	0.969	0.42	0	32.3
10-Sep-00	-2.567	24.99	15.1	0.857	0.684	0.3	10.7
11-Sep-00	-2.567	24.37	9.73	0.857	0.566	2.3	6.4
12-Sep-00	-2.567	19.81	8.15	0.946	0.452	0	0
13-Sep-00	-2.567	18	7.78	0.957	0.503	4.3	10.7
14-Sep-00	-2.567	15	3.715	0.966	0.423	0	20.1
15-Sep-00	-2.567	10.5	5.181	0.938	0.629	9.7	1.8
16-Sep-00	-2.567	12.6	3.826	0.946	0.477	16.5	0
17-Sep-00	-2.567	12.64	5.921	0.937	0.475	1.8	0
18-Sep-00	-2.567	11.87	6.155	0.888	0.649	2.5	0
19-Sep-00	-2.567	24.4	9.61	0.953	0.507	0	0
20-Sep-00	-2.567	19.03	11.93	0.945	0.56	0	0
21-Sep-00	-2.567	12.38	2.539	0.952	0.804	0.8	0
22-Sep-00	-2.567	9.95	0.446	0.894	0.445	0	12.7
23-Sep-00	-2.567	7.22	0.522	0.958	0.75	0	0
24-Sep-00	-2.567	4.525	-1.541	0.948	0.611	0	0.5
25-Sep-00	-2.567	9.01	2.211	0.938	0.483	0	0
26-Sep-00	-2.567	6.102	0.159	0.936	0.618	16.3	0
27-Sep-00	-2.567	2.512	-4.577	0.931	0.381	0	2.5
28-Sep-00	-2.567	6.037	-5.465	0.792	0.334	5.6	7.4
29-Sep-00	-2.567	16.78	2.704	0.845	0.604	4.1	0
30-Sep-00	-2.567	15.83	8.86	0.968	0.586	0	16.8
1-Oct-00	-1.581	21.9	6.409	0.971	0.477	1.3	1
2-Oct-00	-1.581	19.2	5.777	0.942	0.63	0	0
3-Oct-00	-1.581	13.9	3.108	0.954	0.49	15.2	0
4-Oct-00	-1.581	5.885	-0.285	0.874	0.454	0	1
5-Oct-00	-1.581	6.988	-1.168	0.849	0.347	0	4.1
6-Oct-00	-1.581	6.756	0.87	0.805	0.502	8.9	0
7-Oct-00	-1.581	3.358	-2.216	0.917	0.431	4.3	0
8-Oct-00	-1.581	1.429	-1.749	0.943	0.637	4.8	0
9-Oct-00	-1.581	11.01	-2.031	0.91	0.377	0.8	0.8
10-Oct-00	-1.581	13.96	-3.278	0.943	0.241	0	0
11-Oct-00	-1.581	6.726	-2.792	0.946	0.606	11.2	0
12-Oct-00	-1.581	17.82	-2.056	0.945	0.368	0	0.5
13-Oct-00	-1.581	6.635	0.992	0.958	0.621	3.8	20.3
14-Oct-00	-1.581	5.626	-1.831	0.917	0.642	0.8	1.3
15-Oct-00	-1.581	4.254	-4.965	0.905	0.343	1.8	0
16-Oct-00	-1.581	8.04	-6.671	0.889	0.312	8.9	0
17-Oct-00	-1.581	10.86	-5.773	0.942	0.337	1.3	0
18-Oct-00	-1.581	8.67	1.559	0.943	0.747	0.5	0
19-Oct-00	-1.581	10.96	1.396	0.954	0.428	0	0
20-Oct-00	-1.581	17.76	6.195	0.928	0.551	0	0

21-Oct-00	-1.581	7.63	-0.462	0.896	0.593	5.6	0
22-Oct-00	-1.581	7.96	-3.178	0.848	0.325	0	0
23-Oct-00	-1.581	11.03	4.227	0.888	0.497	0	0
24-Oct-00	-1.581	13.84	2.047	0.877	0.436	0	0
25-Oct-00	-1.581	17.06	-0.116	0.935	0.247	0	3.3
26-Oct-00	-1.581	15.16	10.07	0.968	0.842	2.3	1.3
27-Oct-00	-1.581	15.26	-1.774	0.939	0.748	0	0
28-Oct-00	-1.581	1.343	-4.545	0.893	0.581	0	7.1
29-Oct-00	-1.581	8.92	-9.15	0.931	0.249	0	0.5
30-Oct-00	-1.581	10.62	-7.58	0.896	0.134	0	2
31-Oct-00	-1.581	12.23	-1.964	0.6951	0.259	0	2.5
1-Nov-00	-1.581	14.21	2.787	0.82	0.381	0	2.3

Dry Year Detour Lake 2000/2001

Date	Max Temp °C	Min Temp °C	Net Rad MJ/m2 day	Max RH dec	Min RH dec	Wind Speed km/hr	dry snow daily precip mm/day
08-Apr-01	5.63	0.00	2.52	0.95	0.85	18.00	14.88
09-Apr-01	-0.16	0.00	2.70	0.94	0.84	21.55	5.78
10-Apr-01	4.76	0.00	6.20	0.92	0.43	7.60	6.38
11-Apr-01	11.04	0.00	8.84	0.85	0.29	11.94	6.18
12-Apr-01	7.61	3.03	2.79	0.97	0.40	19.39	15.28
13-Apr-01	6.91	0.00	3.94	0.95	0.57	18.77	6.68
14-Apr-01	2.59	0.00	9.94	0.91	0.29	7.34	6.28
15-Apr-01	2.35	0.00	14.29	0.85	0.26	13.83	5.68
16-Apr-01	0.68	0.00	14.29	0.89	0.28	15.96	5.78
17-Apr-01	-3.49	0.00	10.31	0.81	0.49	18.07	5.68
18-Apr-01	1.11	0.00	14.83	0.87	0.37	8.78	5.68
19-Apr-01	11.40	0.00	13.40	0.85	0.26	7.33	5.68
20-Apr-01	16.70	0.00	12.93	0.64	0.26	9.18	5.68
21-Apr-01	12.68	2.81	6.16	0.97	0.45	13.20	13.58
22-Apr-01	6.30	0.00	16.37	0.97	0.42	18.97	2.50
23-Apr-01	11.25	0.00	1.45	0.97	0.67	12.21	7.90
24-Apr-01	4.31	0.00	11.70	0.95	0.55	17.00	4.20
25-Apr-01	11.97	0.00	13.57	0.91	0.25	10.18	1.00
26-Apr-01	14.20	0.00	4.34	0.92	0.50	18.58	3.40
27-Apr-01	3.42	0.00	16.30	0.74	0.31	16.28	0.00
28-Apr-01	9.14	0.00	15.99	0.82	0.23	6.95	0.00
29-Apr-01	19.35	0.00	13.75	0.76	0.17	15.82	0.00
30-Apr-01	27.75	10.23	14.10	0.57	0.23	17.93	0.00
01-May-01	23.17	12.54	10.78	0.75	0.36	12.45	0.00
02-May-01	22.40	9.92	8.37	0.96	0.30	14.47	0.10
03-May-01	17.14	6.07	15.20	0.75	0.35	16.79	0.00
04-May-01	7.57	0.00	9.82	0.92	0.52	14.19	0.00
05-May-01	13.97	0.00	16.71	0.94	0.14	7.77	0.70
06-May-01	20.32	0.00	14.97	0.75	0.15	10.64	0.00
07-May-01	25.38	3.61	14.00	0.59	0.18	14.86	0.00
08-May-01	21.08	13.80	9.34	0.80	0.20	18.36	0.00
09-May-01	18.19	5.98	13.79	0.67	0.26	14.58	0.00
10-May-01	22.12	0.29	8.04	0.94	0.23	12.59	1.80

11-May-01	12.93	0.00	9.69	0.94	0.61	17.21	0.00
12-May-01	9.10	0.00	13.89	0.90	0.30	14.04	0.00
13-May-01	12.69	0.00	13.53	0.90	0.20	10.82	1.30
14-May-01	14.89	0.00	15.27	0.93	0.16	6.81	0.00
15-May-01	19.12	1.89	14.33	0.63	0.11	13.74	0.00
16-May-01	21.75	5.60	11.19	0.89	0.27	19.35	0.50
17-May-01	20.45	10.54	8.94	0.91	0.47	16.15	0.00
18-May-01	17.21	10.60	7.95	0.95	0.56	10.83	3.40
19-May-01	21.35	10.04	11.04	0.96	0.37	5.56	0.00
20-May-01	26.78	7.57	12.75	0.94	0.22	6.77	0.00
21-May-01	26.67	10.82	13.12	0.78	0.24	18.04	0.00
22-May-01	21.83	14.51	4.65	0.67	0.41	25.51	0.00
23-May-01	17.79	10.47	2.70	0.96	0.65	17.17	12.00
24-May-01	22.37	7.84	10.70	0.97	0.49	7.56	1.10
25-May-01	25.30	11.85	14.66	0.93	0.30	13.53	0.00
26-May-01	21.18	13.39	7.97	0.89	0.38	10.43	0.40
27-May-01	20.27	11.03	9.50	0.93	0.50	11.68	0.00
28-May-01	12.86	0.63	2.93	0.97	0.82	18.62	1.10
29-May-01	6.18	-0.54	12.23	0.93	0.61	26.22	0.50
30-May-01	9.10	-2.01	10.87	0.92	0.47	21.55	0.10
31-May-01	20.32	-1.66	13.43	0.92	0.21	6.78	0.00
01-Jun-01	21.45	4.98	7.65	0.75	0.25	8.67	0.00
02-Jun-01	14.60	5.67	2.51	0.96	0.49	14.48	3.60
03-Jun-01	9.51	4.91	5.07	0.97	0.93	15.82	1.10
04-Jun-01	10.82	3.44	4.98	0.97	0.78	16.34	0.70
05-Jun-01	16.35	5.04	15.05	0.92	0.26	19.44	0.20
06-Jun-01	19.13	1.33	15.24	0.54	0.17	16.79	0.00
07-Jun-01	15.96	-0.55	14.55	0.84	0.24	12.51	0.00
08-Jun-01	22.13	-0.06	13.66	0.86	0.25	7.65	0.00
09-Jun-01	27.27	6.41	10.90	0.84	0.24	11.37	0.00
10-Jun-01	27.34	3.44	9.68	0.90	0.20	6.91	0.00
11-Jun-01	27.30	11.89	9.81	0.78	0.30	9.05	0.00
12-Jun-01	20.98	5.41	6.27	0.94	0.57	15.01	7.90
13-Jun-01	16.90	2.54	11.22	0.89	0.40	8.28	0.00
14-Jun-01	34.33	10.56	13.69	0.94	0.24	13.90	19.20
15-Jun-01	33.55	17.03	12.06	0.95	0.35	13.33	0.00
16-Jun-01	26.04	14.09	15.65	0.95	0.19	18.17	7.10
17-Jun-01	17.64	9.03	13.56	0.86	0.32	11.99	0.00
18-Jun-01	22.13	1.57	13.90	0.94	0.22	10.42	0.00
19-Jun-01	24.11	11.71	8.54	0.96	0.41	27.62	6.60
20-Jun-01	19.31	7.95	11.41	0.88	0.31	11.60	0.00
21-Jun-01	20.54	7.46	13.48	0.91	0.35	11.05	0.20
22-Jun-01	14.48	9.35	3.86	0.88	0.52	13.36	0.70
23-Jun-01	25.96	8.64	15.37	0.93	0.26	9.95	0.00
24-Jun-01	23.23	7.35	8.50	0.93	0.41	12.54	0.50
25-Jun-01	28.59	5.08	7.57	0.93	0.42	10.09	0.00
26-Jun-01	35.10	20.91	13.88	0.66	0.32	22.79	0.00
27-Jun-01	27.27	9.15	11.40	0.82	0.39	17.83	0.00
28-Jun-01	21.45	7.45	10.87	0.88	0.29	6.39	0.50
29-Jun-01	26.60	10.94	7.86	0.96	0.63	17.73	20.40
30-Jun-01	14.46	7.54	6.96	0.94	0.66	13.71	0.80

01-Jul-01	10.70	2.75	3.11	0.95	0.52	23.72	8.30
02-Jul-01	10.70	2.75	3.11	0.95	0.52	23.72	8.30
03-Jul-01	10.70	2.75	3.11	0.95	0.52	23.72	8.30
04-Jul-01	10.70	2.75	3.11	0.95	0.52	23.72	8.30
05-Jul-01	16.11	4.93	15.41	0.94	0.42	17.14	0.00
06-Jul-01	17.13	4.80	11.70	0.91	0.39	18.91	0.00
07-Jul-01	19.94	5.79	14.00	0.93	0.32	13.00	0.00
08-Jul-01	23.09	6.44	7.39	0.91	0.30	6.97	0.10
09-Jul-01	18.70	13.14	3.31	0.97	0.84	10.34	22.40
10-Jul-01	20.85	8.20	19.73	0.96	0.36	17.78	0.00
11-Jul-01	20.76	5.75	17.75	0.90	0.31	13.63	0.00
12-Jul-01	26.86	2.46	16.46	0.97	0.23	5.87	0.00
13-Jul-01	23.39	11.42	6.34	0.83	0.36	8.91	0.00
14-Jul-01	22.09	14.83	7.53	0.94	0.57	12.21	3.00
15-Jul-01	25.55	12.82	10.50	0.93	0.44	7.88	0.00
16-Jul-01	26.95	13.11	14.94	0.97	0.39	10.76	0.00
17-Jul-01	26.25	10.57	8.93	0.91	0.42	14.56	5.10
18-Jul-01	12.30	6.32	5.75	0.94	0.58	13.66	0.10
19-Jul-01	18.67	3.35	11.26	0.89	0.33	12.66	0.00
20-Jul-01	18.89	6.61	5.80	0.93	0.42	7.35	1.70
21-Jul-01	13.77	9.01	6.46	0.91	0.68	14.36	0.20
22-Jul-01	17.02	8.12	5.58	0.96	0.63	7.10	0.00
23-Jul-01	23.39	10.34	11.13	0.81	0.32	7.65	0.00
24-Jul-01	25.88	10.42	13.22	0.88	0.32	11.34	0.00
25-Jul-01	26.80	16.70	10.18	0.81	0.36	16.37	0.00
26-Jul-01	28.18	14.97	10.85	0.79	0.33	13.20	0.00
27-Jul-01	28.32	13.63	9.51	0.93	0.39	10.38	0.00
28-Jul-01	20.63	9.48	13.18	0.97	0.48	15.40	0.00
29-Jul-01	27.06	8.35	13.39	0.97	0.33	7.91	0.00
30-Jul-01	30.95	11.04	12.65	0.94	0.22	8.22	0.00
31-Jul-01	30.23	15.49	10.37	0.85	0.38	11.35	0.00
01-Aug-01	27.20	15.78	6.03	0.97	0.52	7.80	8.00
02-Aug-01	15.82	9.18	4.13	0.97	0.89	9.23	9.60
03-Aug-01	10.96	7.53	4.66	0.96	0.87	13.25	3.60
04-Aug-01	20.77	8.84	12.29	0.93	0.30	14.82	1.50
05-Aug-01	26.23	4.92	12.86	0.94	0.30	7.78	0.00
06-Aug-01	22.75	14.38	5.00	0.91	0.48	6.16	0.10
07-Aug-01	17.68	15.47	2.89	0.94	0.86	9.31	3.40
08-Aug-01	24.72	14.35	9.56	0.97	0.44	8.85	0.00
09-Aug-01	25.12	10.82	14.37	0.80	0.31	14.84	0.00
10-Aug-01	24.42	8.16	12.87	0.82	0.30	13.21	0.00
11-Aug-01	24.75	9.70	11.57	0.93	0.35	12.38	0.00
12-Aug-01	27.89	8.41	10.61	0.96	0.29	11.34	0.00
13-Aug-01	21.45	12.91	3.74	0.86	0.57	13.69	1.80
14-Aug-01	24.96	5.66	12.43	0.97	0.30	5.35	0.00
15-Aug-01	23.84	12.24	3.77	0.94	0.60	11.86	6.90
16-Aug-01	12.27	6.84	5.20	0.94	0.75	17.36	4.20
17-Aug-01	18.77	4.36	12.91	0.91	0.32	8.72	0.00
18-Aug-01	15.24	7.86	4.19	0.95	0.57	8.32	8.00
19-Aug-01	11.86	5.63	8.22	0.95	0.71	13.44	3.30
20-Aug-01	17.04	3.38	13.01	0.96	0.36	8.74	0.00

21-Aug-01	19.22	1.08	8.35	0.96	0.42	8.42	0.00
22-Aug-01	22.54	12.82	10.49	0.94	0.56	11.96	1.50
23-Aug-01	20.74	11.39	8.61	0.97	0.50	8.66	0.70
24-Aug-01	23.64	12.18	8.18	0.96	0.39	9.39	2.80
25-Aug-01	28.96	14.82	11.50	0.94	0.30	15.05	0.10
26-Aug-01	18.62	9.23	11.67	0.95	0.41	12.72	2.10
27-Aug-01	23.00	6.01	9.42	0.94	0.17	6.03	0.00
28-Aug-01	25.08	7.21	7.84	0.83	0.19	11.05	0.00
29-Aug-01	19.32	10.87	2.80	0.96	0.53	13.29	8.80
30-Aug-01	22.45	9.68	11.96	0.89	0.34	7.59	0.00
31-Aug-01	23.64	6.58	3.82	0.94	0.64	17.11	5.80
01-Sep-01	10.17	3.83	9.87	0.93	0.56	18.21	0.20
02-Sep-01	14.77	1.32	9.62	0.94	0.39	11.31	0.00
03-Sep-01	14.68	1.67	7.10	0.96	0.35	8.95	0.00
04-Sep-01	10.25	0.32	6.68	0.96	0.52	12.40	0.30
05-Sep-01	15.43	-1.10	8.10	0.96	0.35	6.13	0.00
06-Sep-01	19.10	3.58	5.34	0.90	0.25	13.00	0.00
07-Sep-01	22.60	12.60	5.86	0.83	0.41	17.69	0.50
08-Sep-01	16.74	6.54	2.75	0.95	0.50	15.21	1.60
09-Sep-01	22.97	4.69	7.76	0.97	0.42	8.22	0.10
10-Sep-01	24.99	15.10	5.24	0.86	0.68	19.37	0.00
11-Sep-01	24.37	9.73	1.90	0.86	0.57	13.04	0.40
12-Sep-01	19.81	8.15	4.14	0.95	0.45	13.47	9.80
13-Sep-01	18.00	7.78	5.98	0.96	0.50	12.61	7.10
14-Sep-01	15.00	3.72	7.52	0.97	0.42	9.10	0.20
15-Sep-01	10.50	5.18	6.96	0.94	0.63	20.34	0.70
16-Sep-01	12.60	3.83	8.33	0.95	0.48	17.06	1.60
17-Sep-01	12.64	5.92	6.47	0.94	0.47	13.94	2.80
18-Sep-01	11.87	6.16	2.82	0.89	0.65	9.10	0.00
19-Sep-01	24.40	9.61	5.45	0.95	0.51	14.27	0.40
20-Sep-01	19.03	11.93	4.86	0.95	0.56	13.61	1.50
21-Sep-01	12.38	2.54	2.40	0.95	0.80	15.04	3.30
22-Sep-01	9.95	0.45	6.07	0.89	0.45	11.43	0.00
23-Sep-01	7.22	0.52	1.62	0.96	0.75	8.67	7.30
24-Sep-01	4.53	-1.54	4.30	0.95	0.61	13.54	1.00
25-Sep-01	9.01	2.21	7.03	0.94	0.48	13.56	1.00
26-Sep-01	6.10	0.16	2.53	0.94	0.62	12.32	3.60
27-Sep-01	2.51	-4.58	3.54	0.93	0.38	11.26	0.00
28-Sep-01	6.04	-5.47	4.96	0.79	0.33	10.49	0.00
29-Sep-01	16.78	2.70	4.09	0.85	0.60	12.56	0.10
30-Sep-01	15.83	8.86	2.80	0.97	0.59	12.72	0.50
01-Oct-01	21.90	6.41	4.55	0.97	0.48	14.28	1.30
02-Oct-01	19.20	5.78	2.39	0.94	0.63	17.14	27.80
03-Oct-01	13.90	3.11	6.91	0.95	0.49	11.22	3.60
04-Oct-01	5.89	-0.29	1.90	0.87	0.45	9.77	0.00
05-Oct-01	6.99	-1.17	3.25	0.85	0.35	8.35	0.00
06-Oct-01	6.76	0.87	4.23	0.81	0.50	13.67	0.00
07-Oct-01	3.36	-2.22	3.48	0.92	0.43	16.49	0.00
08-Oct-01	1.43	-1.75	3.14	0.94	0.64	11.36	1.00
09-Oct-01	11.01	-2.03	4.85	0.91	0.38	6.18	0.00
10-Oct-01	13.96	-3.28	5.68	0.94	0.24	6.72	0.00

11-Oct-01	6.73	-2.79	2.34	0.95	0.61	10.94	0.00
12-Oct-01	17.82	-2.06	5.11	0.95	0.37	15.65	0.10
13-Oct-01	6.64	0.99	4.24	0.96	0.62	8.36	0.10
14-Oct-01	5.63	-1.83	2.53	0.92	0.64	13.22	0.10
15-Oct-01	4.25	-4.97	4.13	0.91	0.34	5.85	0.00
16-Oct-01	8.04	-6.67	2.55	0.89	0.31	5.62	0.00
17-Oct-01	10.86	-5.77	4.59	0.94	0.34	6.73	0.00
18-Oct-01	8.67	1.56	0.68	0.94	0.75	9.13	1.10
19-Oct-01	10.96	1.40	3.62	0.95	0.43	8.10	0.00
20-Oct-01	17.76	6.20	2.03	0.93	0.55	13.93	1.60
21-Oct-01	7.63	-0.46	1.65	0.90	0.59	18.58	0.70
22-Oct-01	7.96	-3.18	2.35	0.85	0.33	11.76	0.00
23-Oct-01	11.03	4.23	1.03	0.89	0.50	12.36	1.20
24-Oct-01	13.84	2.05	2.33	0.88	0.44	12.39	0.10
25-Oct-01	17.06	-0.12	2.84	0.94	0.25	9.95	0.80
26-Oct-01	15.16	10.07	0.84	0.97	0.84	13.54	9.90
27-Oct-01	15.26	-1.77	2.22	0.94	0.75	24.54	1.50
28-Oct-01	1.34	-4.55	2.07	0.89	0.58	17.40	0.00
29-Oct-01	8.92	-9.15	3.42	0.93	0.25	3.69	0.00
30-Oct-01	10.62	-7.58	1.89	0.90	0.13	3.34	0.00
31-Oct-01	12.23	-1.96	2.15	0.70	0.26	7.53	0.00
01-Nov-01	14.21	2.79	2.22	0.82	0.38	4.95	0.00

Appendix B: SoilCover Modeling Results

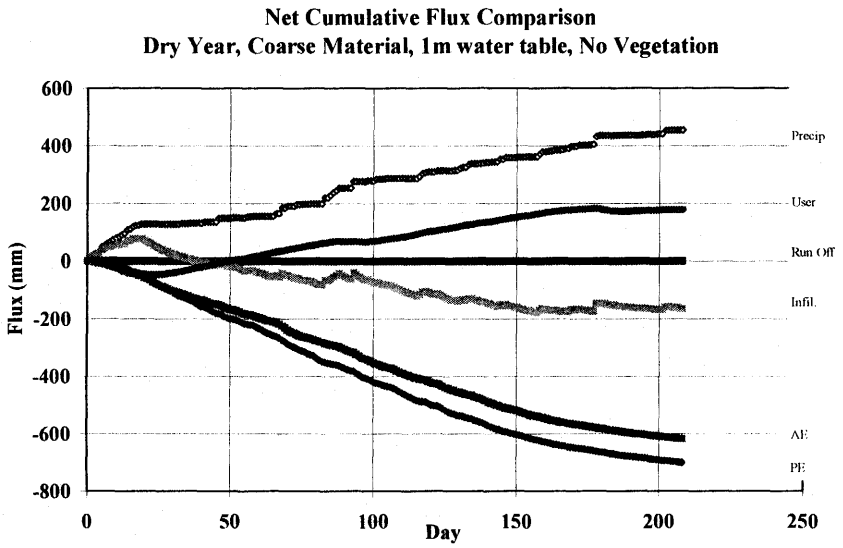
Net Cumulative Flux Comparison
Dry Year, Coarse Material, 1m water table, No Vegetation
Flux (mm)
Day
Precip
User
Run Off
Infil.
AE
PE

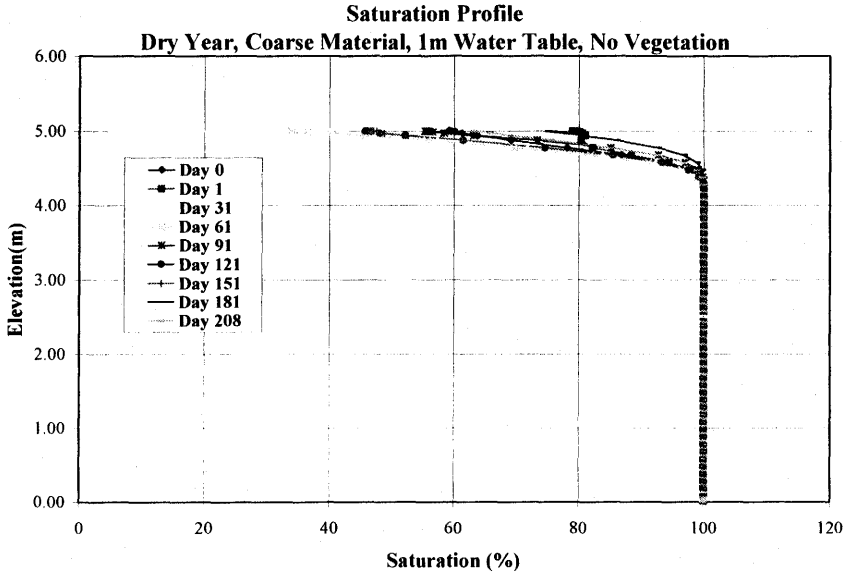
Saturation Profile
Dry Year, Coarse Material, 1m Water Table, No Vegetation
Elevation(m)
Saturation (%)
Day 0
Day 1
Day 31
Day 61
Day 91
Day 121
Day 151
Day 181
Day 208

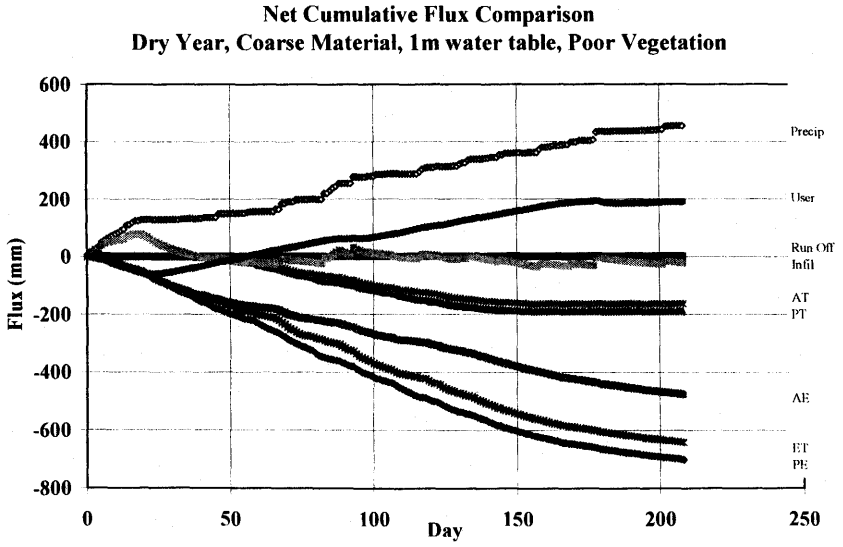
Net Cumulative Flux Comparison
Dry Year, Coarse Material, 1m water table, Poor Vegetation
Flux (mm)
Day
Precip
User
Run Off
Infil
AT
PT
AE
ET
PE

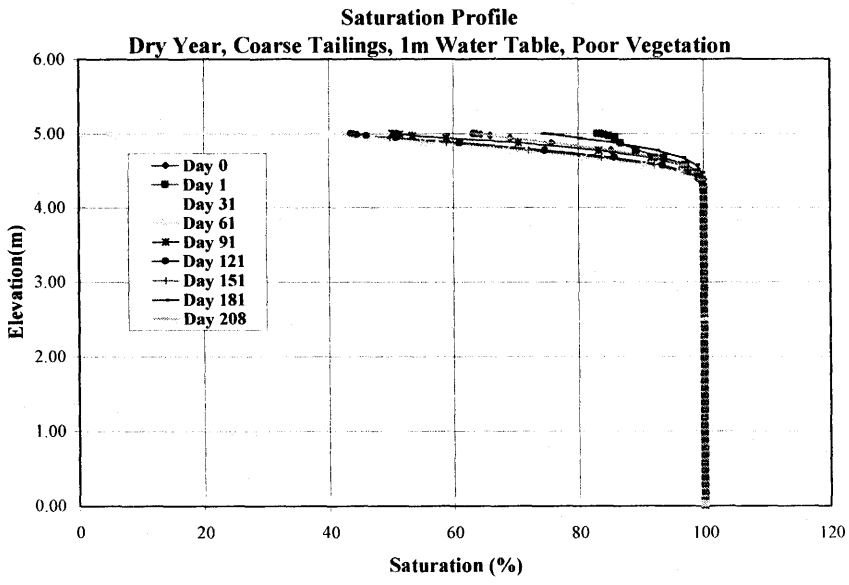
Saturation Profile
Dry Year, Coarse Tailings, 1m Water Table, Poor Vegetation
Elevation(m)
Saturation (%)
Day 0
Day 1
Day 31
Day 61
Day 91
Day 121
Day 151
Day 181
Day 208

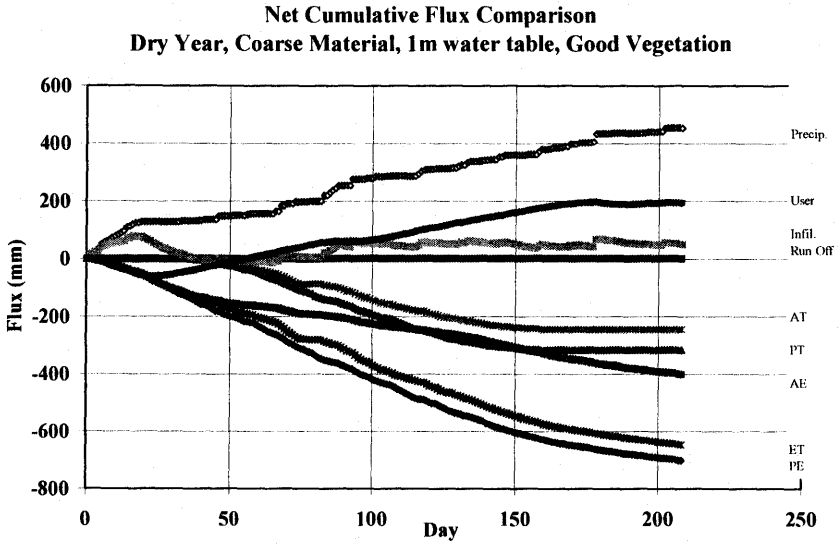
Net Cumulative Flux Comparison
Dry Year, Coarse Material, 1m water table, Good Vegetation
Flux (mm)
Day
Precip.
User
Infil.
Run Off
AT
PT
AE
ET
PE

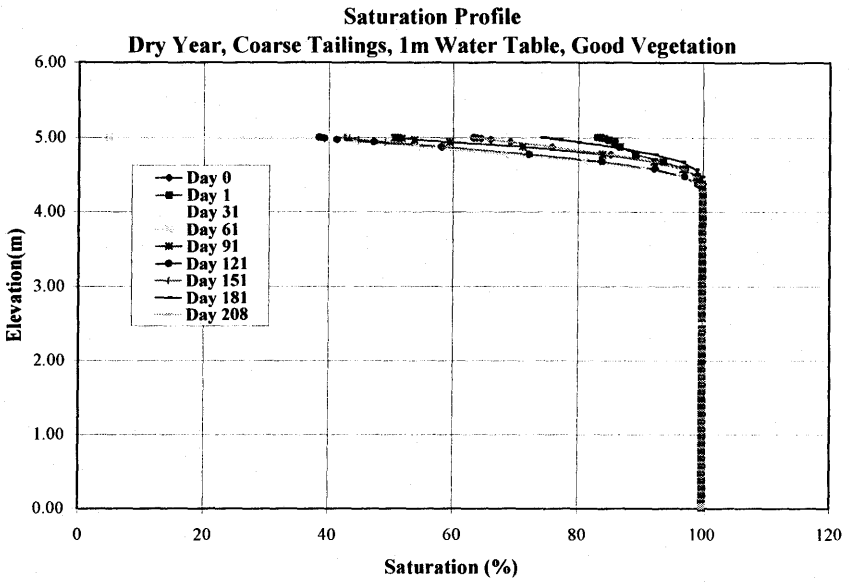
Saturation Profile
Dry Year, Coarse Tailings, 1m Water Table, Good Vegetation
Elevation(m)
Saturation (%)
Day 0
Day 1
Day 31
Day 61
Day 91
Day 121
Day 151
Day 181
Day 208

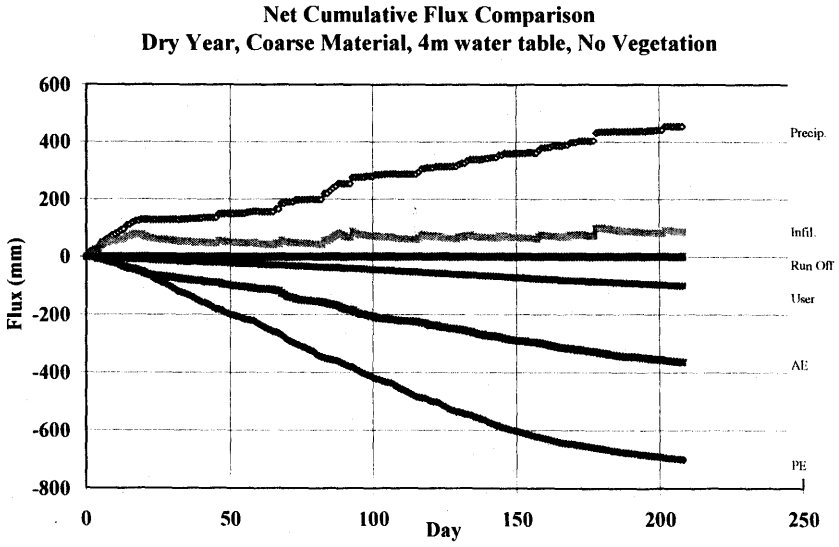
Net Cumulative Flux Comparison
Dry Year, Coarse Material, 4m water table, No Vegetation
Flux (mm)
Day
Precip.
Infil.
Run Off
User
AE
PE

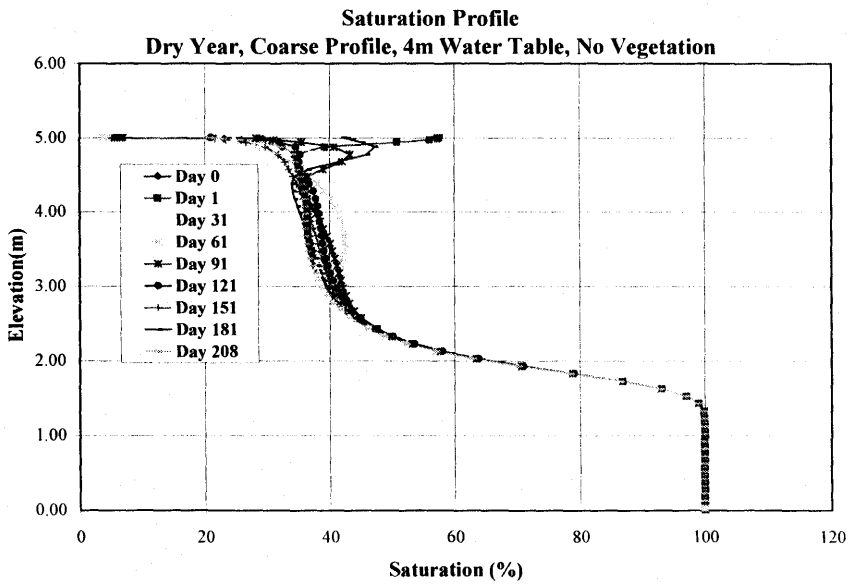
Saturation Profile
Dry Year, Coarse Profile, 4m Water Table, No Vegetation
Elevation(m)
Saturation (%)
Day 0
Day 1
Day 31
Day 61
Day 91
Day 121
Day 151
Day 181
Day 208

Net Cumulative Flux Comparison
Dry Year, Coarse Material, 4m water table, Poor Vegetation

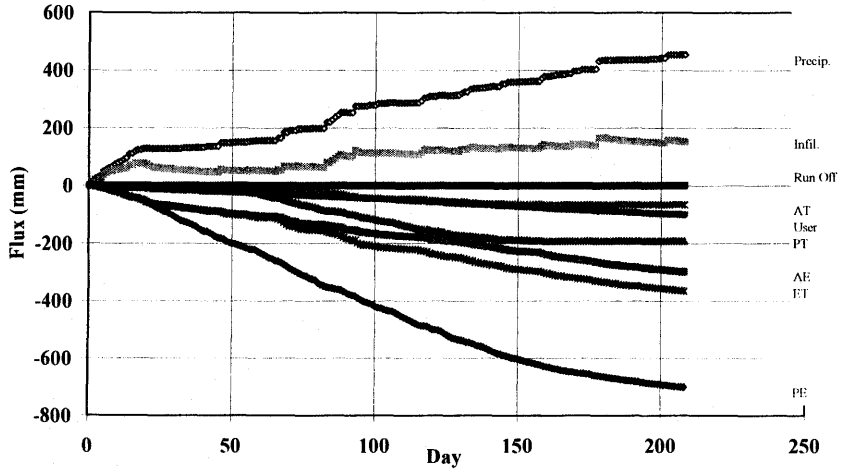

Saturation Profile
Dry Year, Coarse Tailings, 4m Water Table, Poor Vegetation

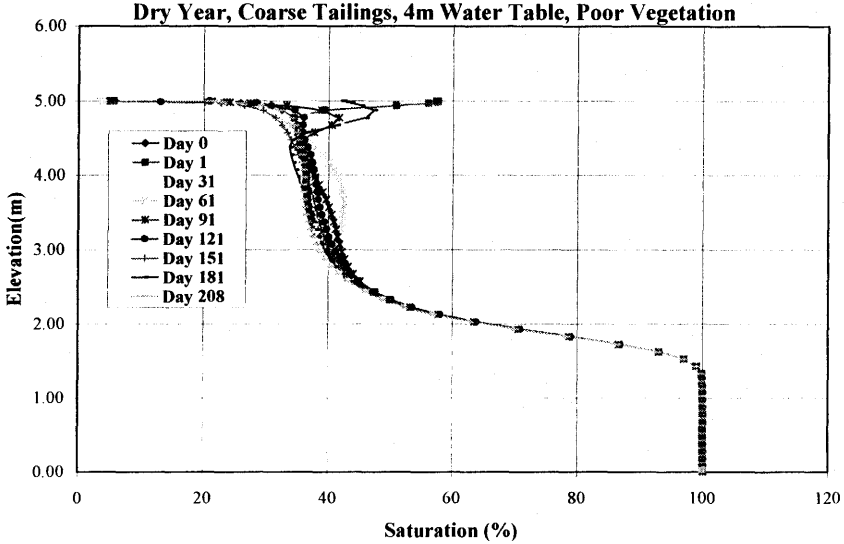

Net Cumulative Flux Comparison
Dry Year, Coarse Material, 4m water table, Good Vegetation

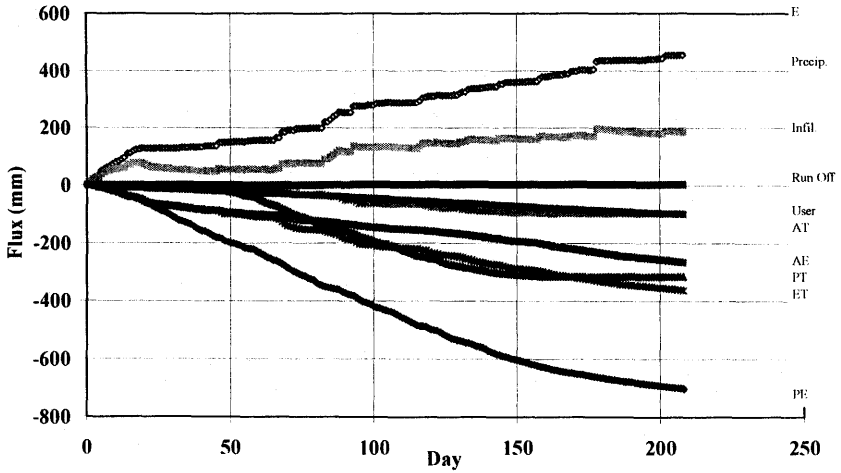

Saturation Profile
Dry Year, Coarse Tailings, 4m Water Table, Good Vegetation

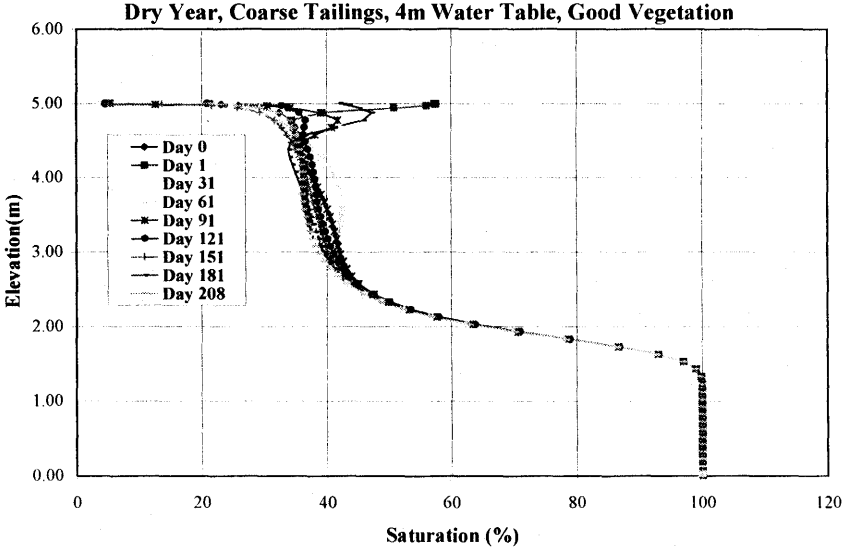

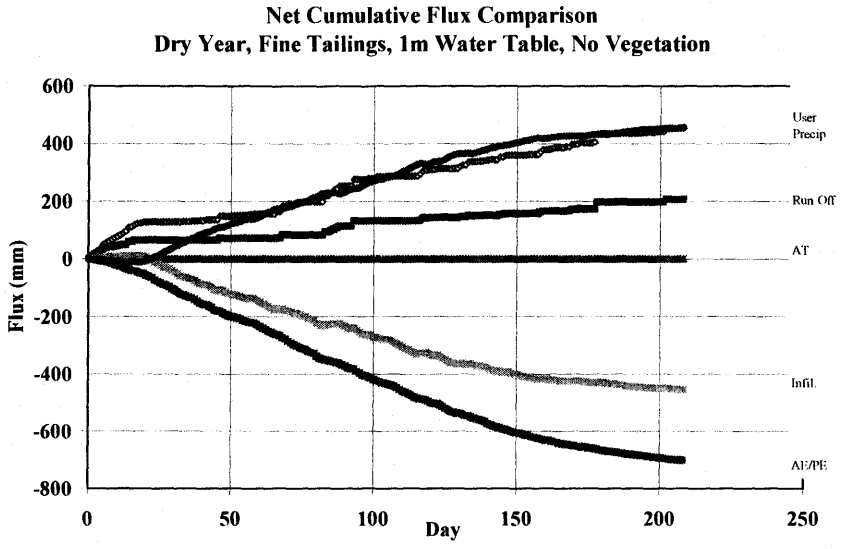
Net Cumulative Flux Comparison
Dry Year, Fine Tailings, 1m Water Table, No Vegetation
Flux (mm)
Day
User Precip
Run Off
AT
Infil.
AE/PE

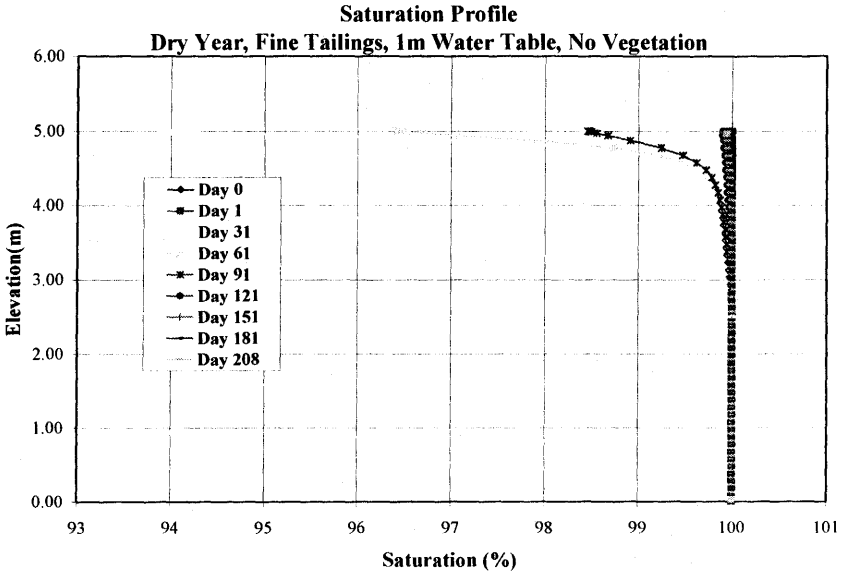
Saturation Profile
Dry Year, Fine Tailings, 1m Water Table, No Vegetation
Elevation(m)
Saturation (%)
Day 0
Day 1
Day 31
Day 61
Day 91
Day 121
Day 151
Day 181
Day 208

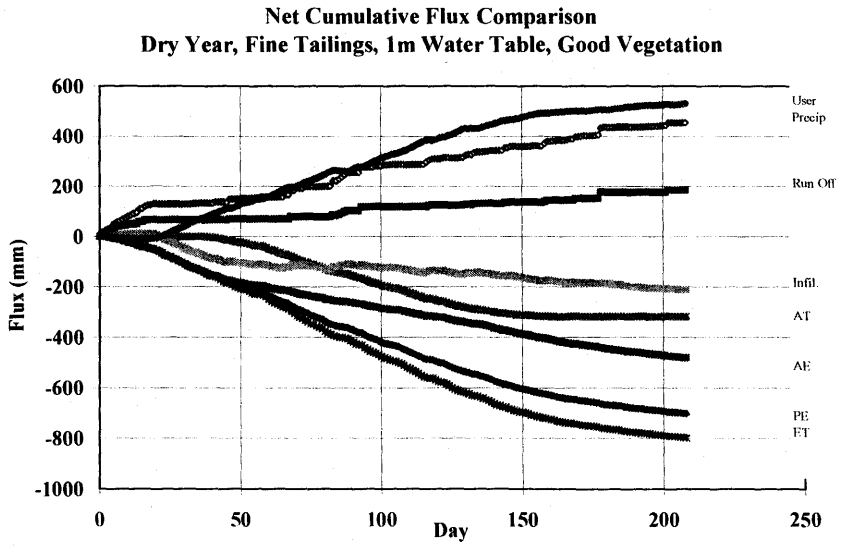
Net Cumulative Flux Comparison
Dry Year, Fine Tailings, 1m Water Table, Good Vegetation
Flux (mm)
Day
User Precip
Run Off
Infil.
AT
AE
PE
ET

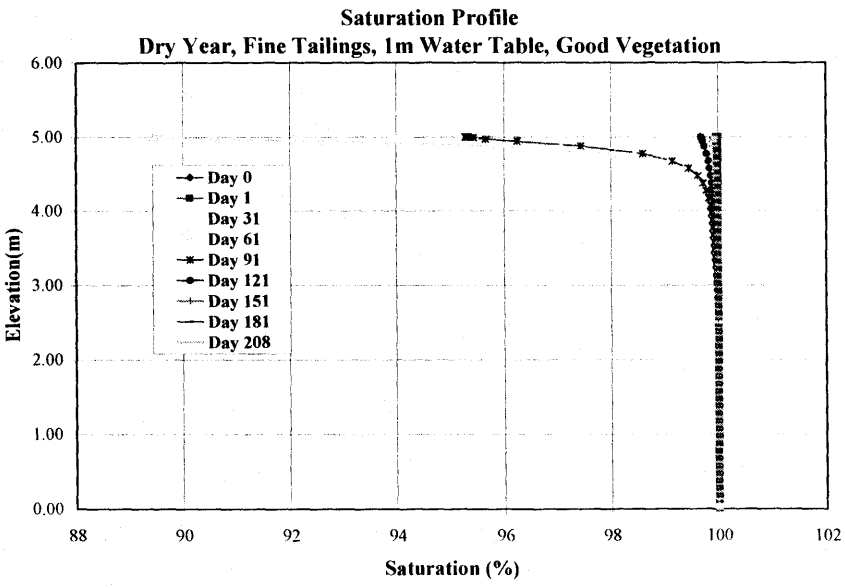
Saturation Profile
Dry Year, Fine Tailings, 1m Water Table, Good Vegetation
Elevation(m)
Saturation (%)
Day 0
Day 1
Day 31
Day 61
Day 91
Day 121
Day 151
Day 181
Day 208

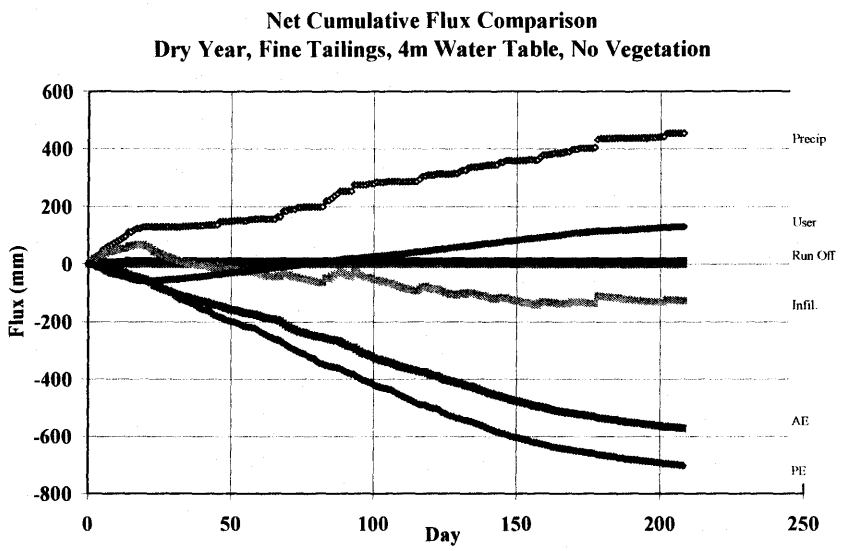
Net Cumulative Flux Comparison
Dry Year, Fine Tailings, 4m Water Table, No Vegetation
Flux (mm)
600
400
200
0
-200
-400
-600
-800
0
50
100
150
200
250
Day
Precip
User
Run Off
Infil.
AE
PE

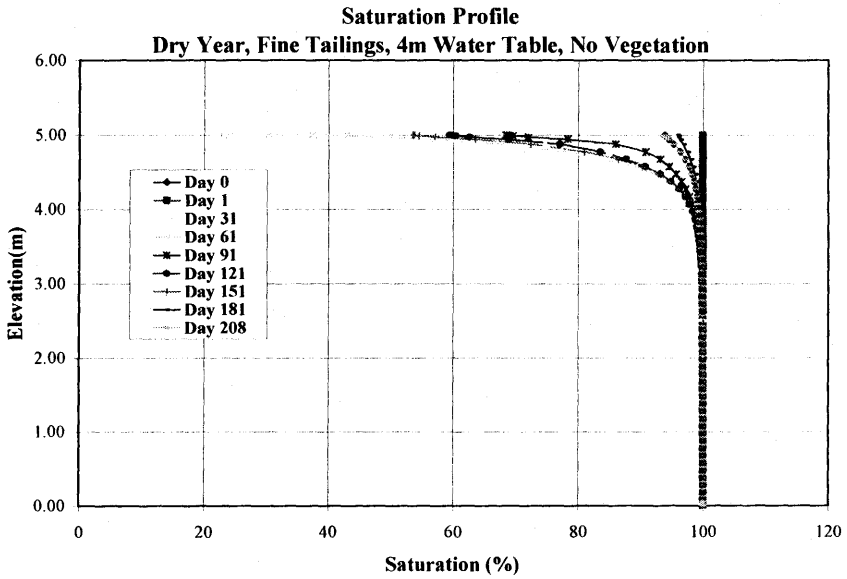
Saturation Profile
Dry Year, Fine Tailings, 4m Water Table, No Vegetation
Elevation(m)
6.00
5.00
4.00
3.00
2.00
1.00
0.00
0
20
40
60
80
100
120
Saturation (%)
Day 0
Day 1
Day 31
Day 61
Day 91
Day 121
Day 151
Day 181
Day 208

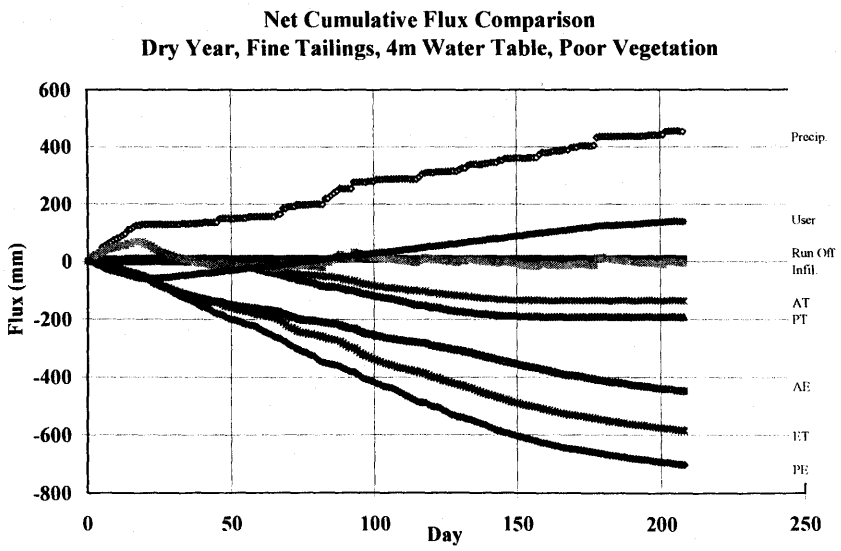
Net Cumulative Flux Comparison
Dry Year, Fine Tailings, 4m Water Table, Poor Vegetation
Flux (mm)
600
400
200
0
-200
-400
-600
-800
0
50
100
150
200
250
Day
Precip.
User
Run Off
Infil.
AT
PT
AE
ET
PE

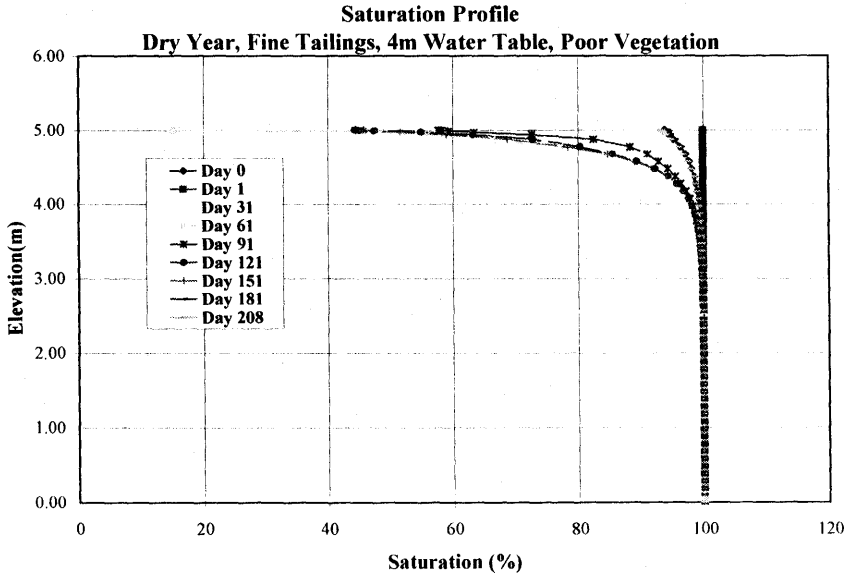
Saturation Profile
Dry Year, Fine Tailings, 4m Water Table, Poor Vegetation
Elevation(m)
6.00
5.00
4.00
3.00
2.00
1.00
0.00
0
20
40
60
80
100
120
Saturation (%)
Day 0
Day 1
Day 31
Day 61
Day 91
Day 121
Day 151
Day 181
Day 208

Net Cumulative Flux Comparison
Dry Year, Fine Tailings, 4m Water Table, Good Vegetation

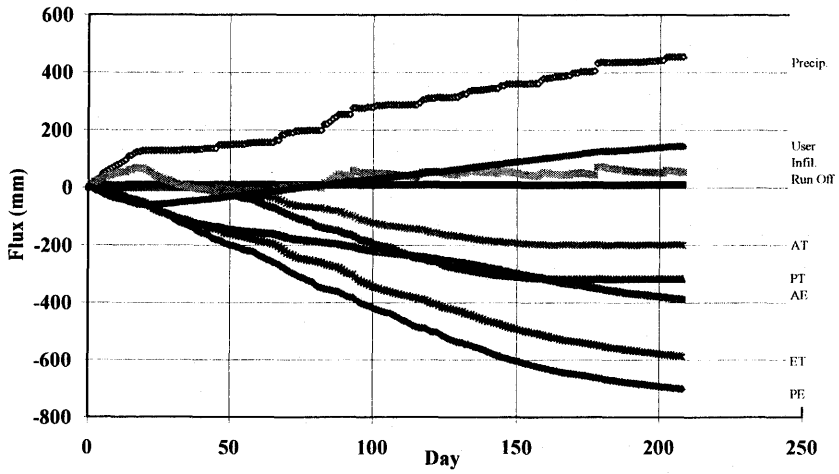

Saturation Profile
Dry Year, Fine Tailings, 4m Water Table, Good Vegetation

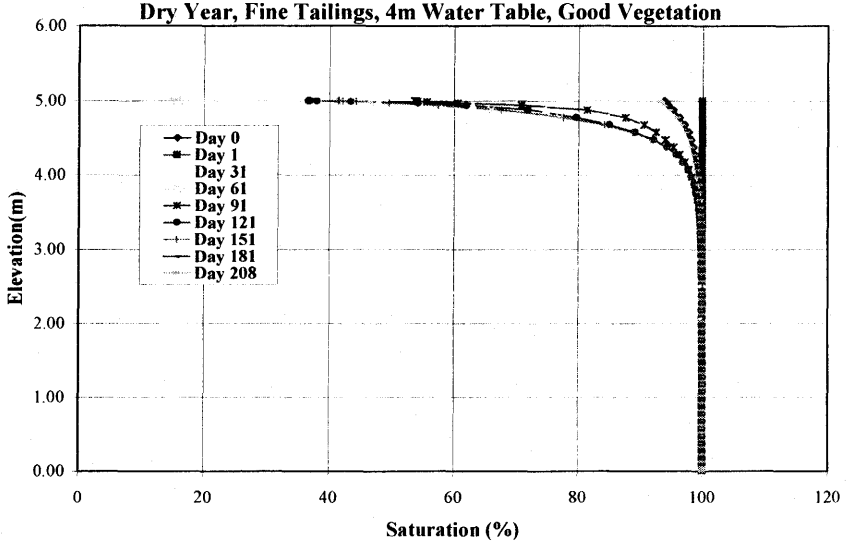

Net Cumulative Flux Comparison
Dry Year, Fine Tailings over Coarse, 1m Water Table, No Vegetation

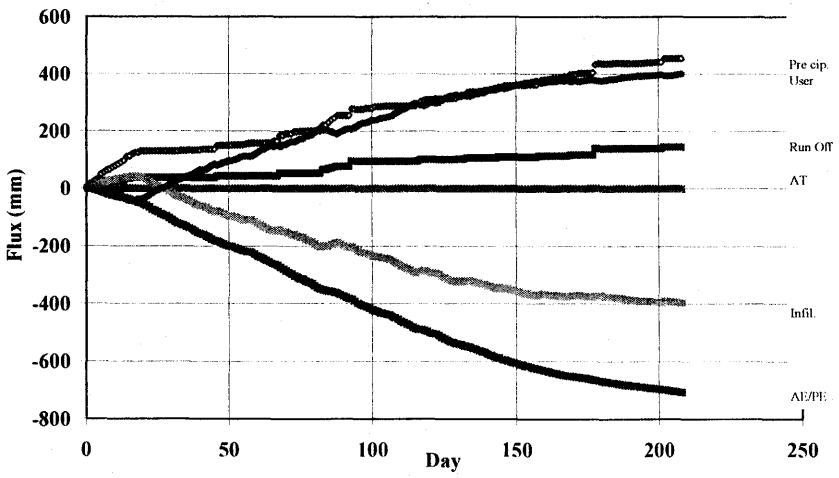

Saturation Profile
Dry Year, Fine Tailings over Coarse, 1m Water Table, No Vegetation

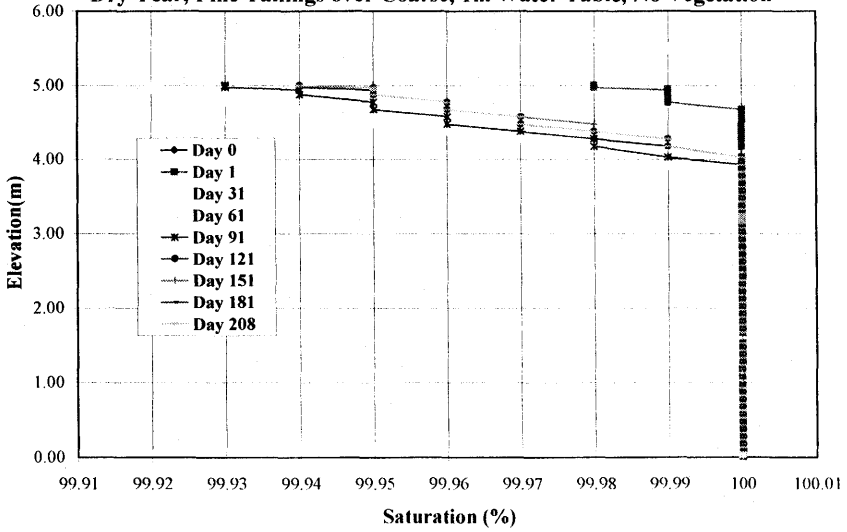

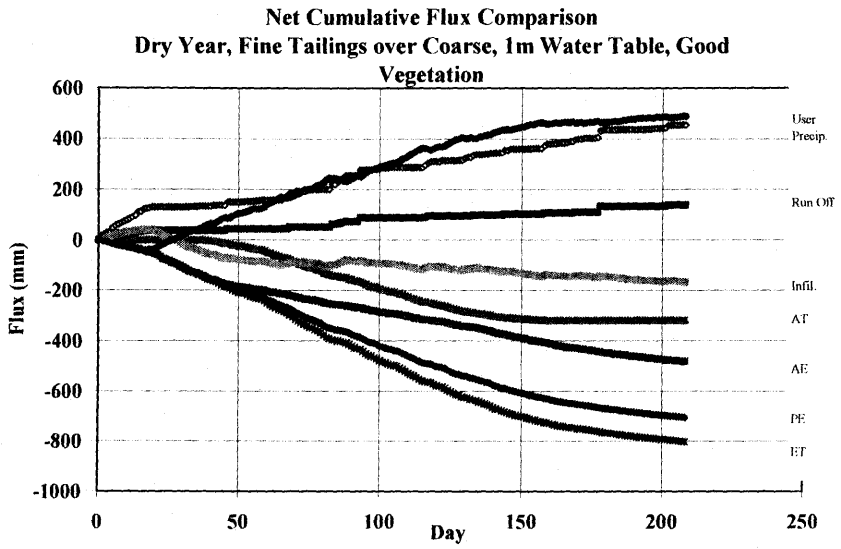
Net Cumulative Flux Comparison
Dry Year, Fine Tailings over Coarse, 1m Water Table, Good Vegetation
Flux (mm)
Day
User Precip.
Run Off
Infil.
AT
AE
PE
PT

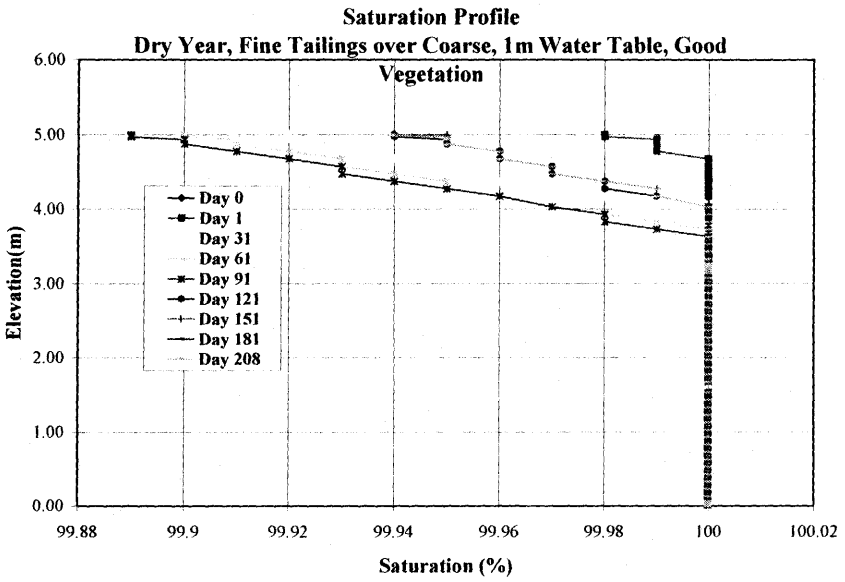
Saturation Profile
Dry Year, Fine Tailings over Coarse, 1m Water Table, Good Vegetation
Elevation(m)
Saturation (%)
Day 0
Day 1
Day 31
Day 61
Day 91
Day 121
Day 151
Day 181
Day 208

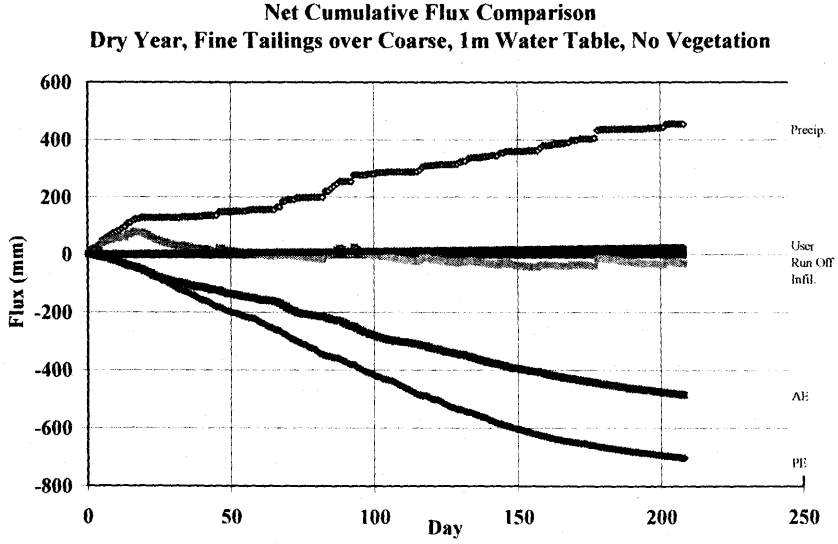
Net Cumulative Flux Comparison
Dry Year, Fine Tailings over Coarse, 1m Water Table, No Vegetation
Flux (mm)
Day
Precip.
User Run Off Infil.
AE
PE

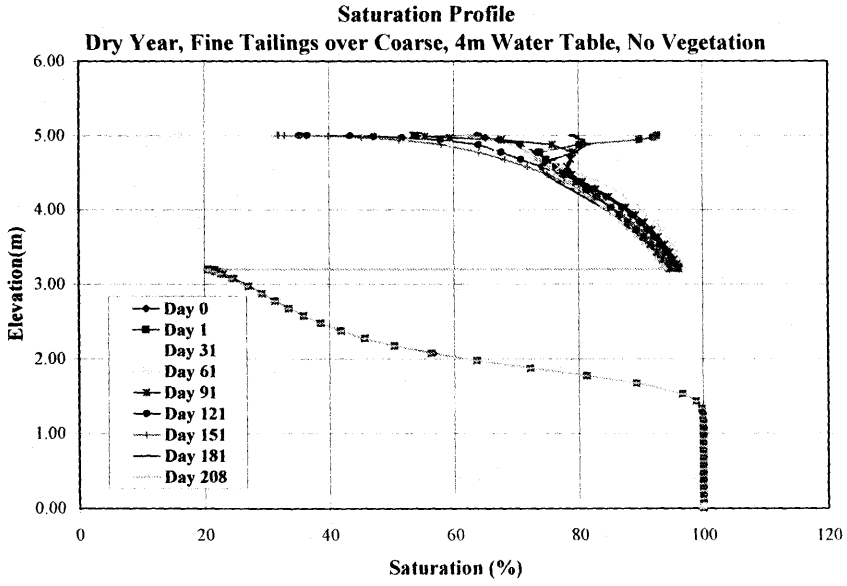
Saturation Profile
Dry Year, Fine Tailings over Coarse, 4m Water Table, No Vegetation
Elevation(m)
Saturation (%)
Day 0
Day 1
Day 31
Day 61
Day 91
Day 121
Day 151
Day 181
Day 208

Net Cumulative Flux Comparison
Dry Year, Fine Tailings over Coarse, 1m Water Table, Good Vegetation

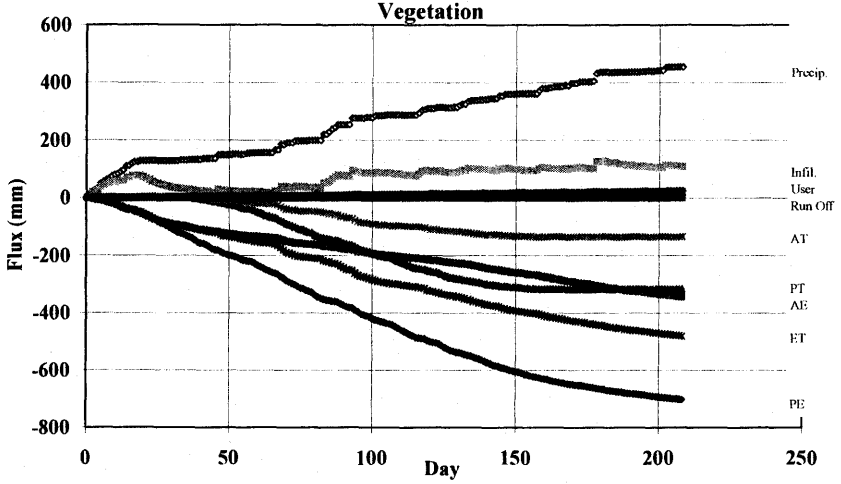

Saturation Profile
Dry Year, Fine Tailings over Coarse, 4m Water Table, Good Vegetation

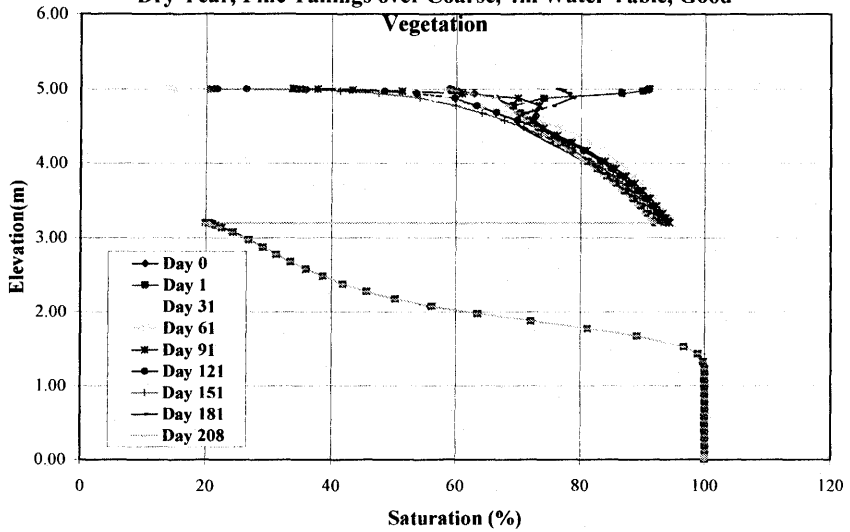

Net Cumulative Flux Comparison
Dry Year, Coarse Tailings over Fine, 1m Water Table, No Vegetation

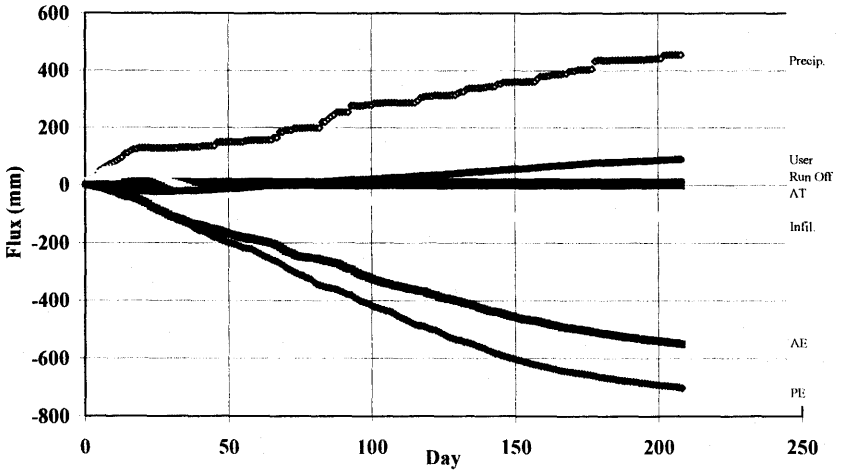

Saturation Profile
Dry Year, Coarse over Fine Tailings, 1m Water Table, No Vegetation

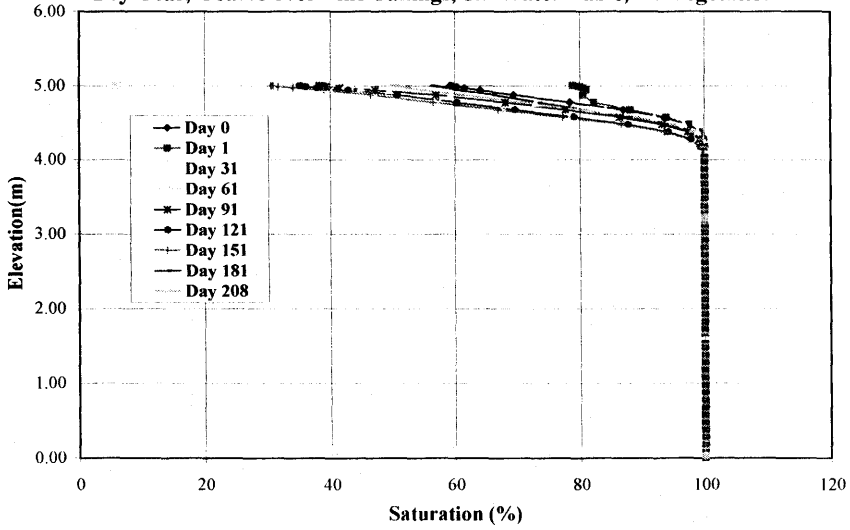

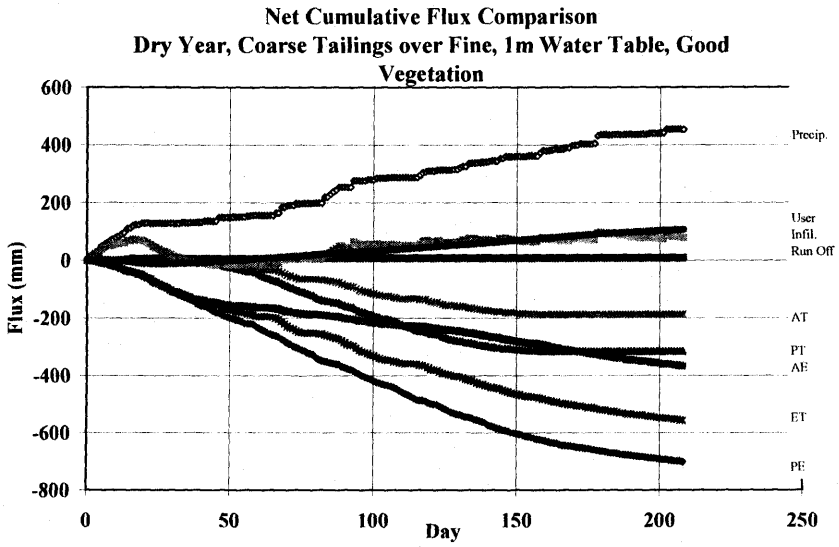
Net Cumulative Flux Comparison
Dry Year, Coarse Tailings over Fine, 1m Water Table, Good Vegetation
Flux (mm)
Day
Precip.
User
Infil.
Run Off
AT
PT
AE
ET
PE

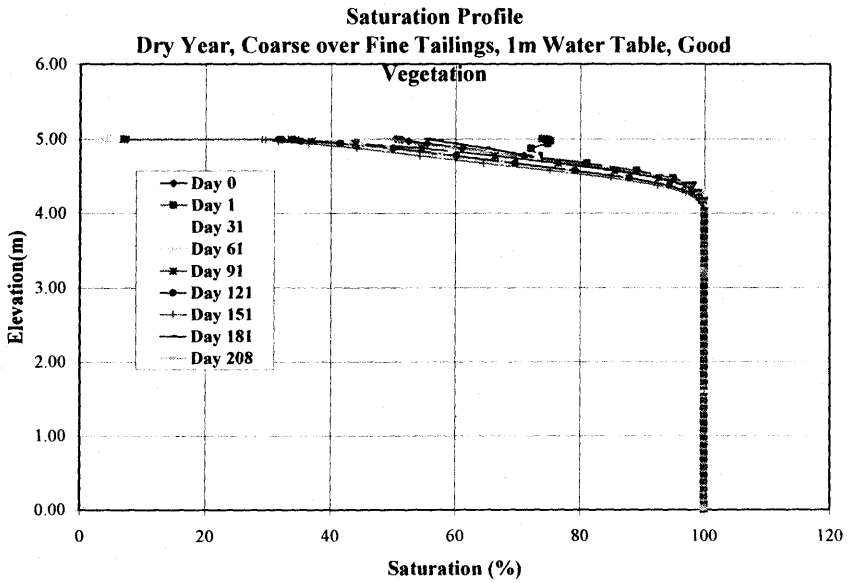
Saturation Profile
Dry Year, Coarse over Fine Tailings, 1m Water Table, Good Vegetation
Elevation(m)
Saturation (%)
Day 0
Day 1
Day 31
Day 61
Day 91
Day 121
Day 151
Day 181
Day 208

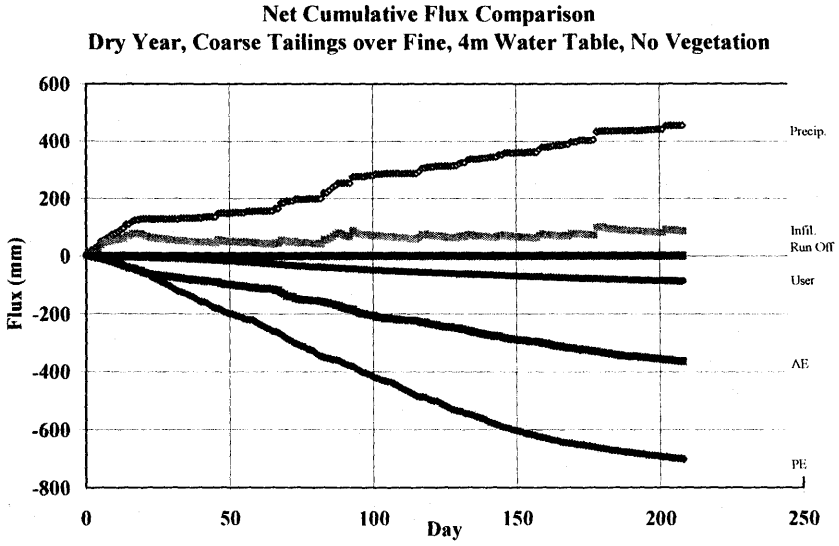
Net Cumulative Flux Comparison
Dry Year, Coarse Tailings over Fine, 4m Water Table, No Vegetation
Flux (mm)
Day
Precip.
Infil.
Run Off
User
AE
PE

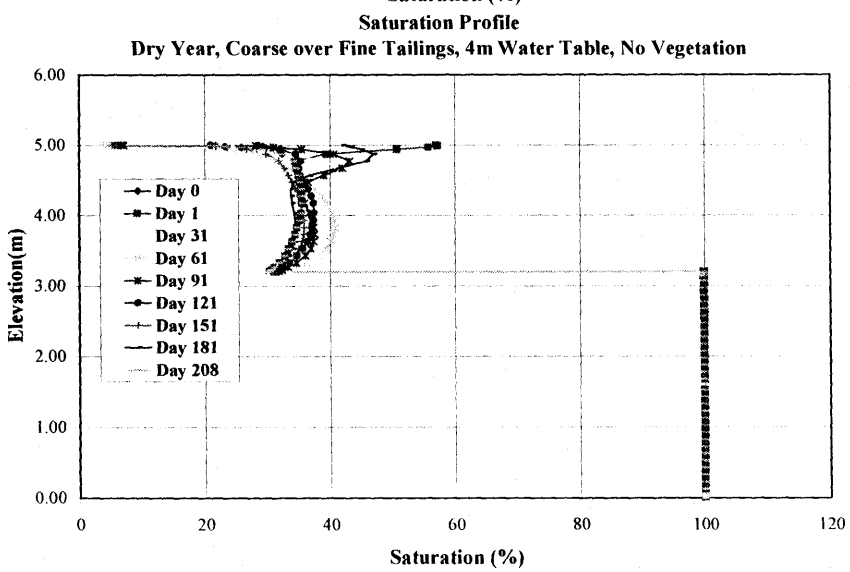
Saturation Profile
Dry Year, Coarse over Fine Tailings, 4m Water Table, No Vegetation
Elevation(m)
Saturation (%)
Day 0
Day 1
Day 31
Day 61
Day 91
Day 121
Day 151
Day 181
Day 208

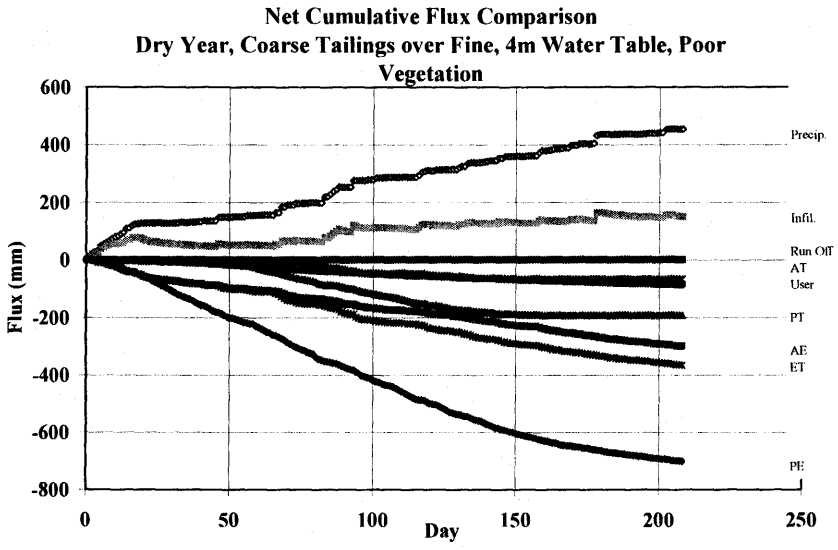
Net Cumulative Flux Comparison
Dry Year, Coarse Tailings over Fine, 4m Water Table, Poor Vegetation
Flux (mm)
Day
Precip.
Infil.
Run Off
AT
User
PT
AE
ET
PE

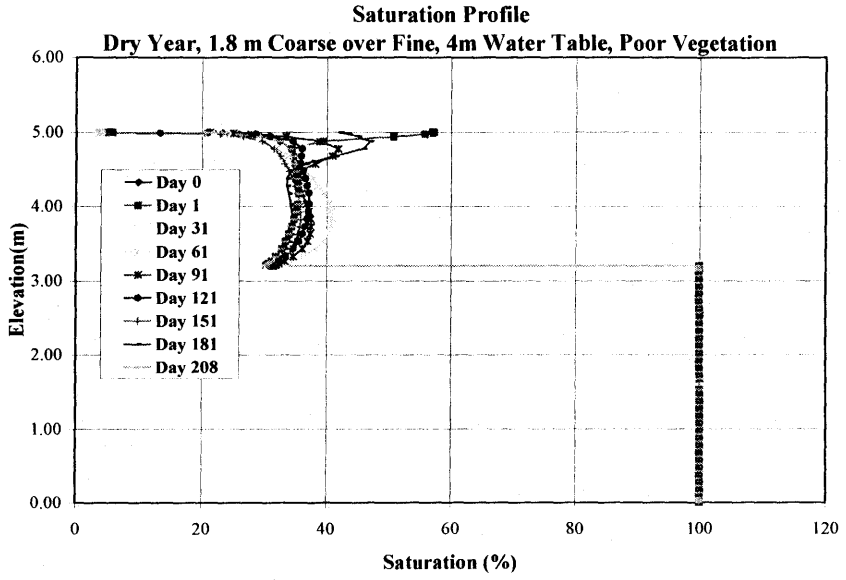
Saturation Profile
Dry Year, 1.8 m Coarse over Fine, 4m Water Table, Poor Vegetation
Elevation(m)
Saturation (%)
Day 0
Day 1
Day 31
Day 61
Day 91
Day 121
Day 151
Day 181
Day 208

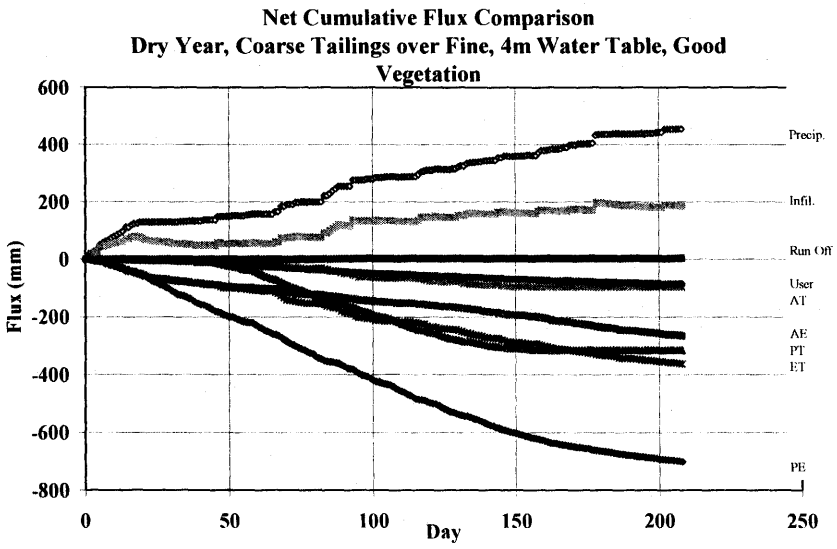
Net Cumulative Flux Comparison
Dry Year, Coarse Tailings over Fine, 4m Water Table, Good Vegetation
Flux (mm)
Day
Precip.
Infil.
Run Off
User
AT
AE
PT
ET
PE

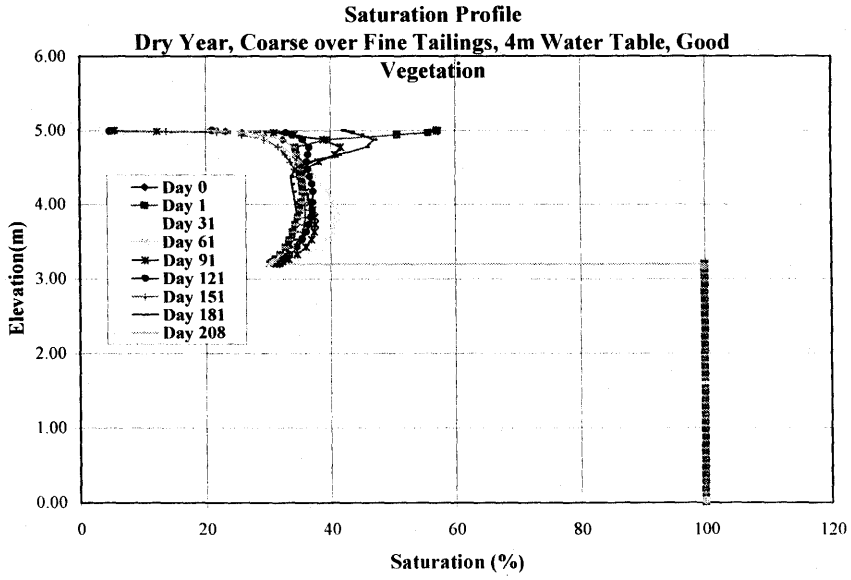
Saturation Profile
Dry Year, Coarse over Fine Tailings, 4m Water Table, Good Vegetation
Elevation(m)
Saturation (%)
Day 0
Day 1
Day 31
Day 61
Day 91
Day 121
Day 151
Day 181
Day 208

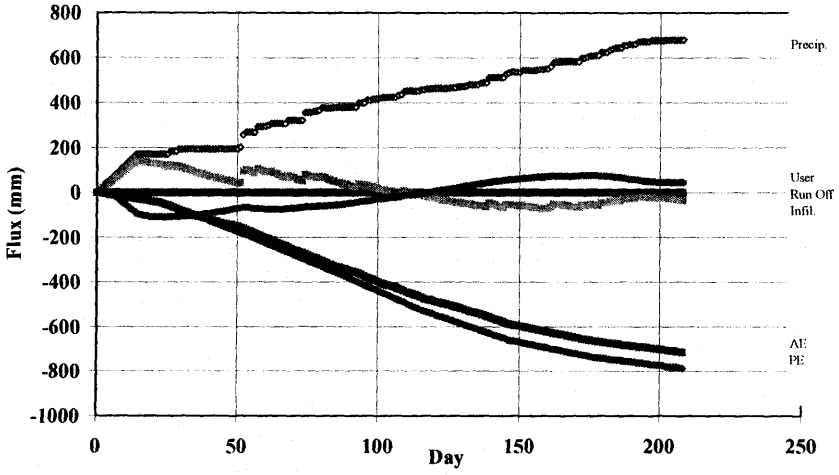
Net Cumulative Flux Comparison
Mean Year, Coarse Material, 1m water table, No Vegetation
Flux (mm)
Day
Precip.
User
Run Off
Infil.
AE
PE

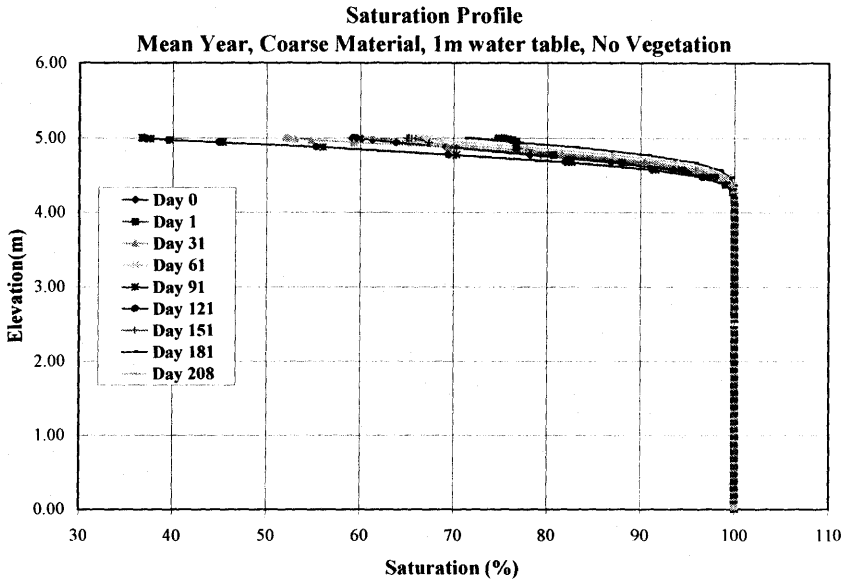
Saturation Profile
Mean Year, Coarse Material, 1m water table, No Vegetation
Elevation(m)
Saturation (%)
Day 0
Day 1
Day 31
Day 61
Day 91
Day 121
Day 151
Day 181
Day 208

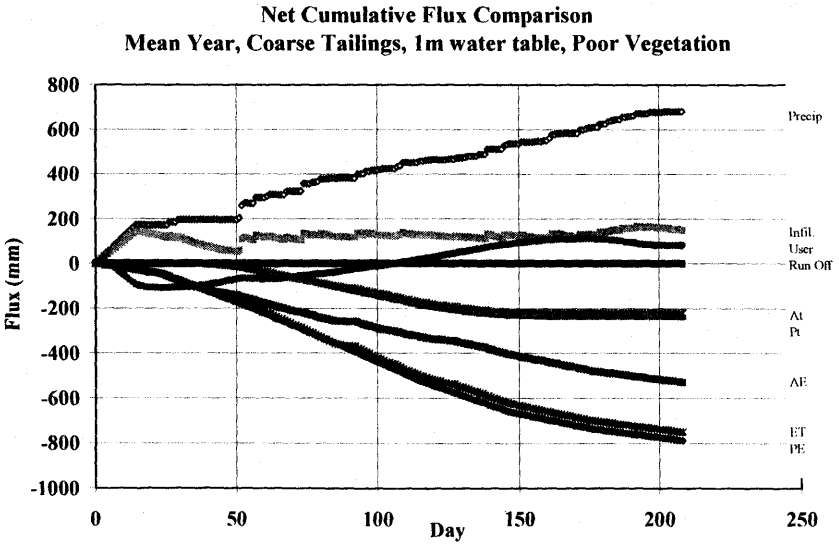
Net Cumulative Flux Comparison
Mean Year, Coarse Tailings, 1m water table, Poor Vegetation
Flux (mm)
Day
Precip
Infil.
User
Run Off
At
Pt
AE
ET
PE

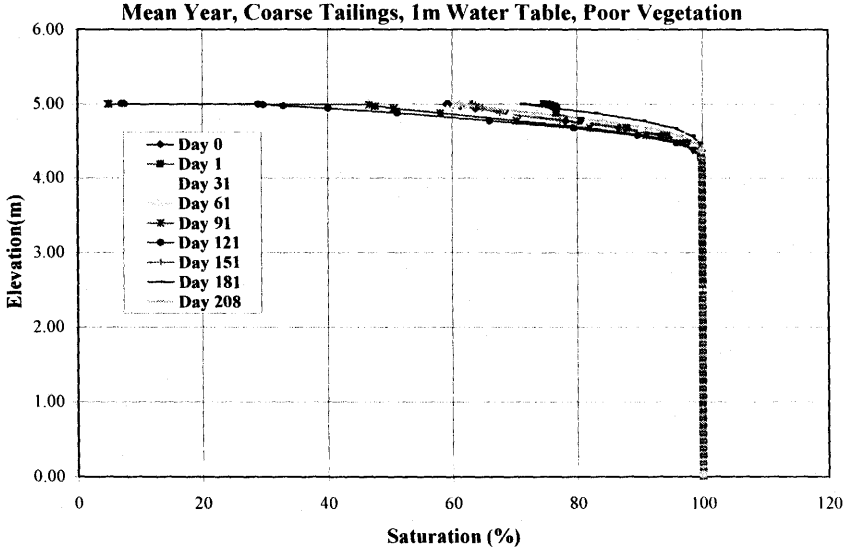
Saturation Profile
Mean Year, Coarse Tailings, 1m Water Table, Poor Vegetation
Elevation(m)
Saturation (%)
Day 0
Day 1
Day 31
Day 61
Day 91
Day 121
Day 151
Day 181
Day 208

Net Cumulative Flux Comparison
Mean Year, Coarse Tailings, 1m water table, Good Vegetation

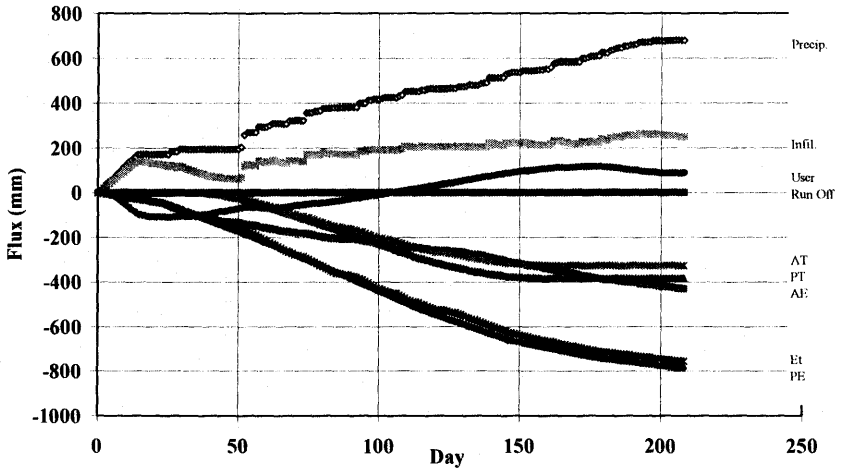

Saturation Profile
Mean Year, Coarse Tailings, 1m Water Table, Good Vegetation

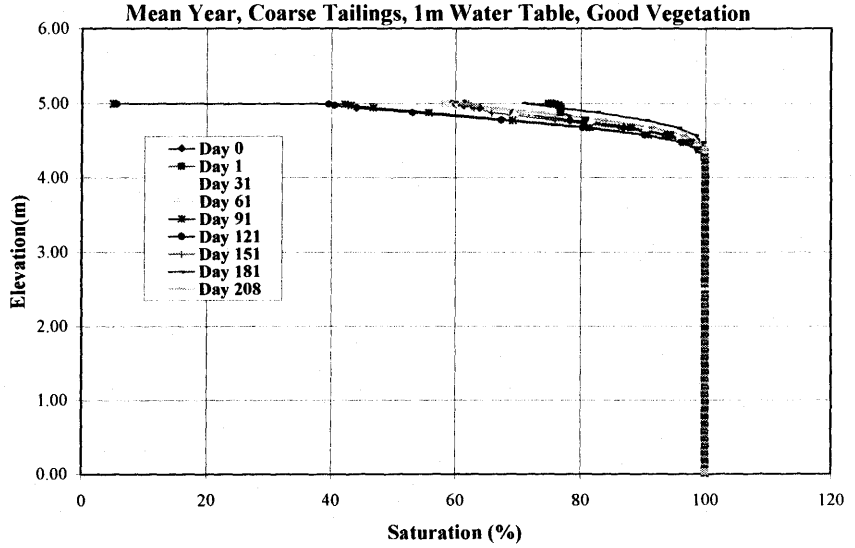

Net Cumulative Flux Comparison
Mean Year, Coarse Material, 4m water table, No Vegetation

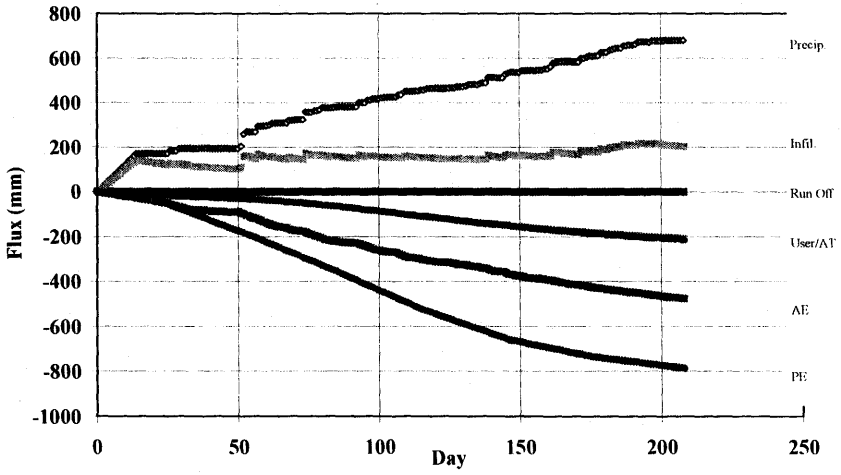

Saturation Profile
Mean Year, Coarse Material, 4m water table, No Vegetation

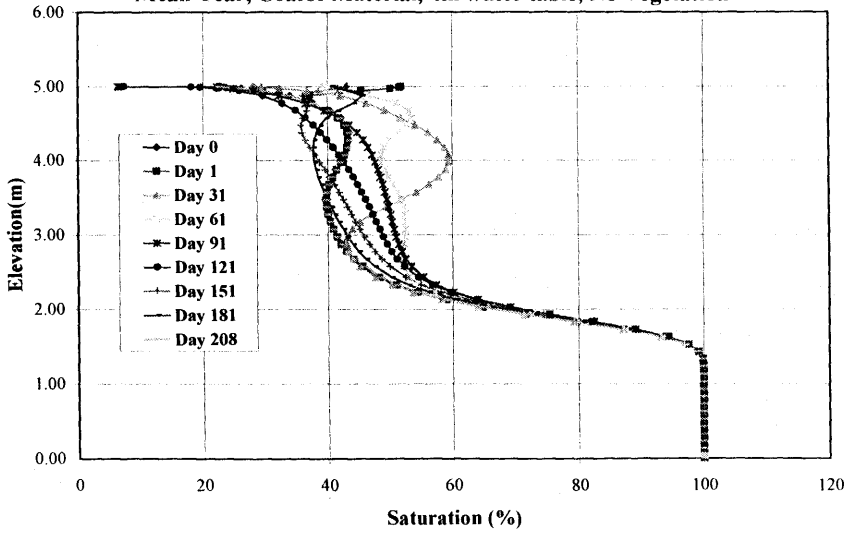

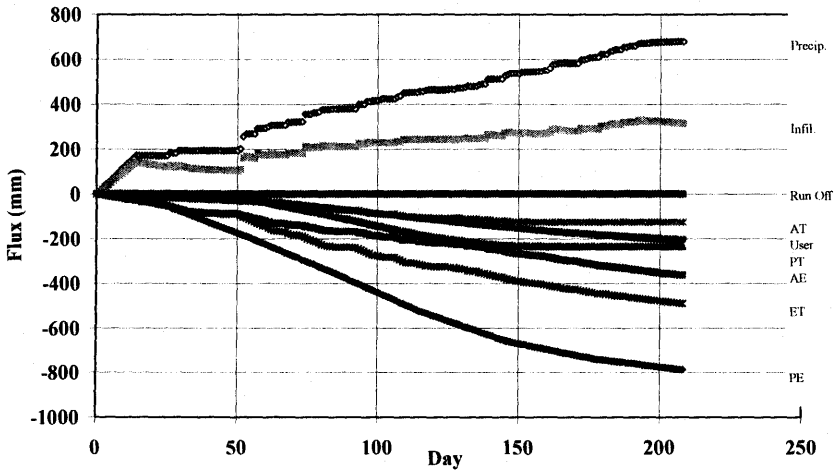
Net Cumulative Flux Comparison
Mean Year, Coarse Tailings, 4m water table, Poor Vegetation
Flux (mm)
Day
Precip.
Infil.
Run Off
AT
User
PT
AE
ET
PE

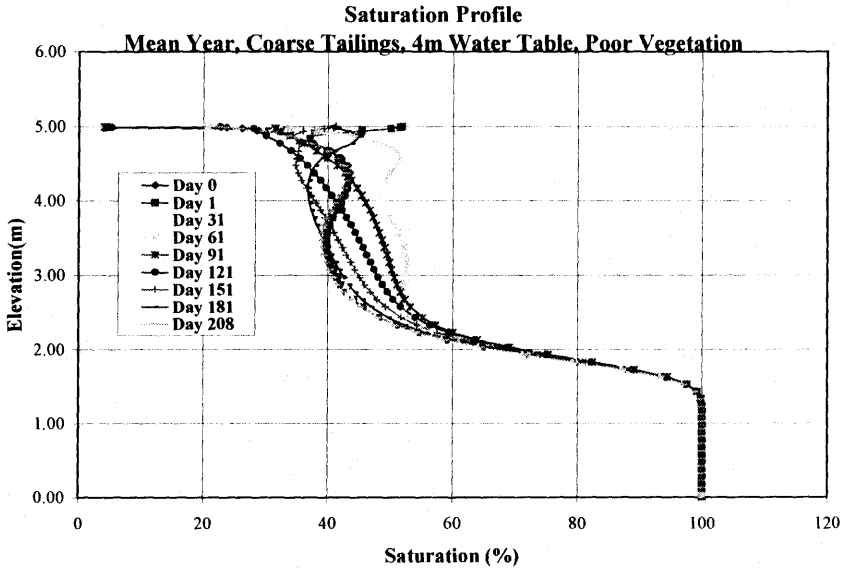
Saturation Profile
Mean Year, Coarse Tailings, 4m Water Table, Poor Vegetation
Elevation(m)
Saturation (%)
Day 0
Day 1
Day 31
Day 61
Day 91
Day 121
Day 151
Day 181
Day 208

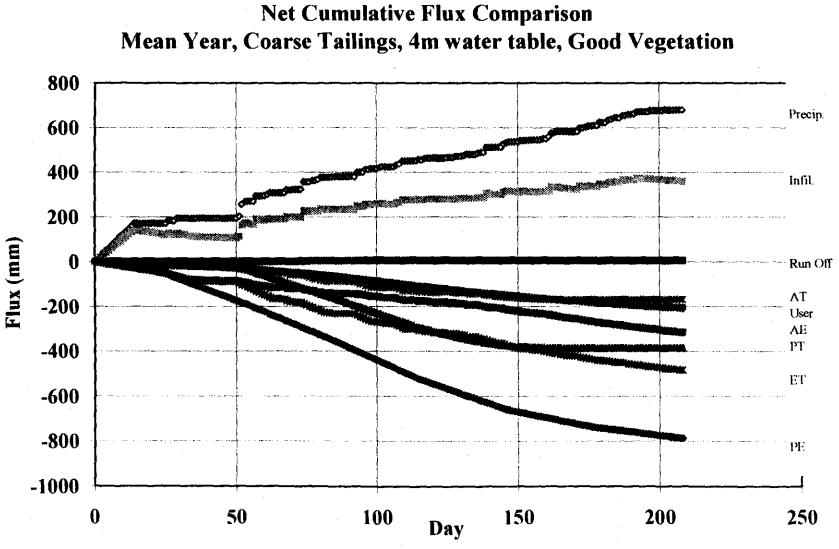
Net Cumulative Flux Comparison
Mean Year, Coarse Tailings, 4m water table, Good Vegetation
Flux (mm)
Day
Precip.
Infil.
Run Off
AT
User
AE
PT
ET
PE

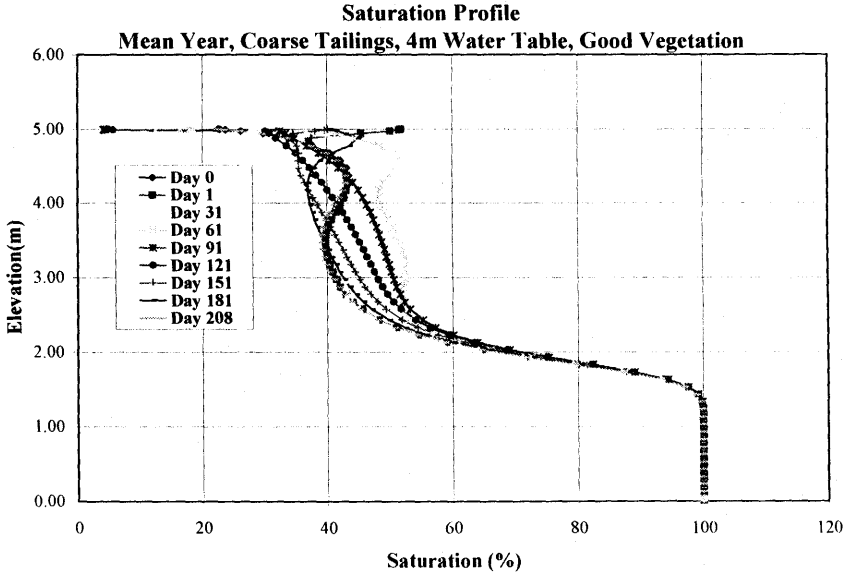
Saturation Profile
Mean Year, Coarse Tailings, 4m Water Table, Good Vegetation
Elevation(m)
Saturation (%)
Day 0
Day 1
Day 31
Day 61
Day 91
Day 121
Day 151
Day 181
Day 208

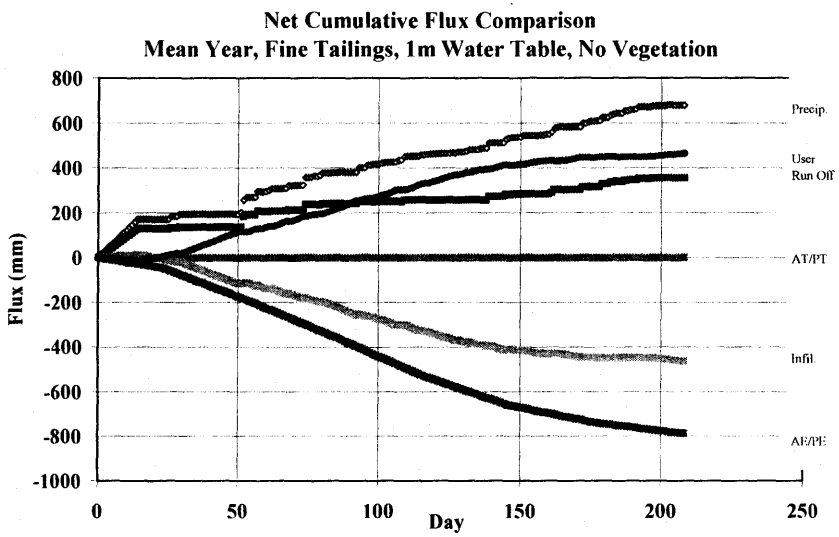
Net Cumulative Flux Comparison
Mean Year, Fine Tailings, 1m Water Table, No Vegetation
Flux (mm)
Day
Precip.
User
Run Off
AT/PT
Infil.
AE/PE

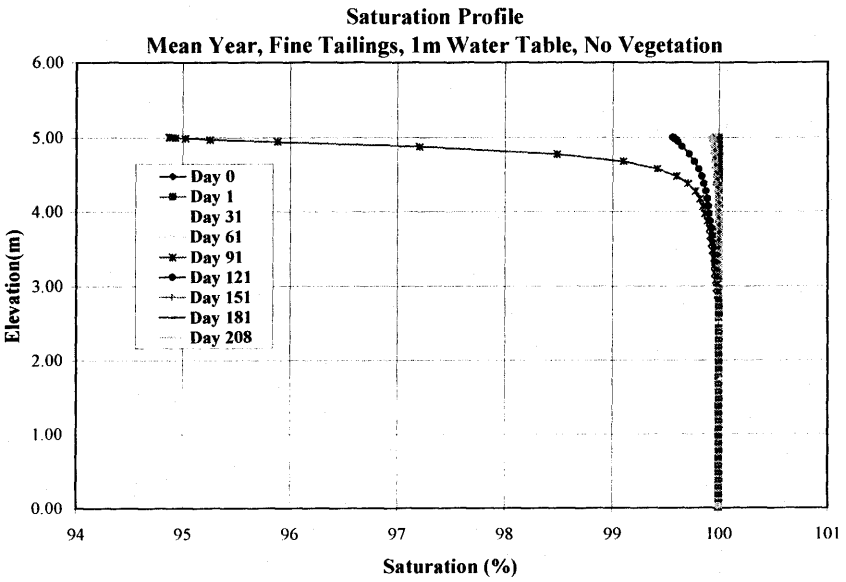
Saturation Profile
Mean Year, Fine Tailings, 1m Water Table, No Vegetation
Elevation(m)
Saturation (%)
Day 0
Day 1
Day 31
Day 61
Day 91
Day 121
Day 151
Day 181
Day 208

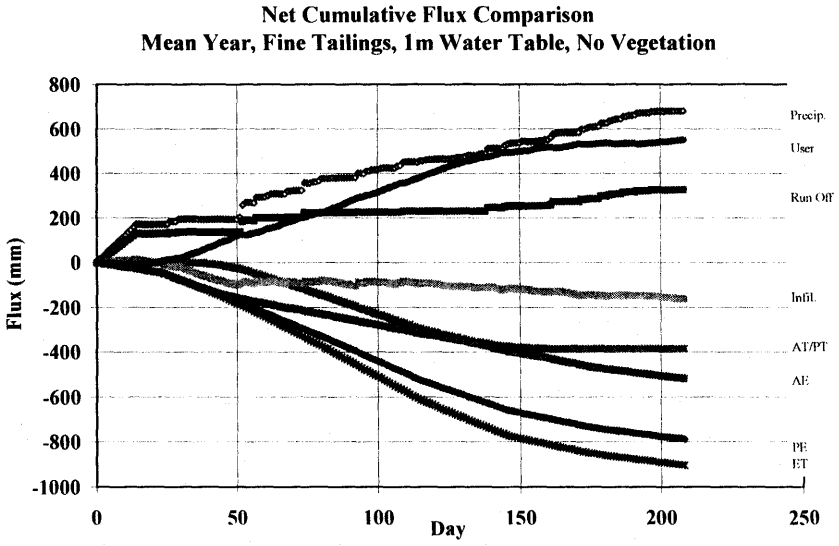
Net Cumulative Flux Comparison
Mean Year, Fine Tailings, 1m Water Table, No Vegetation
Flux (mm)
Day
Precip.
User
Run Off
Infil.
AT/PT
AE
PE
ET

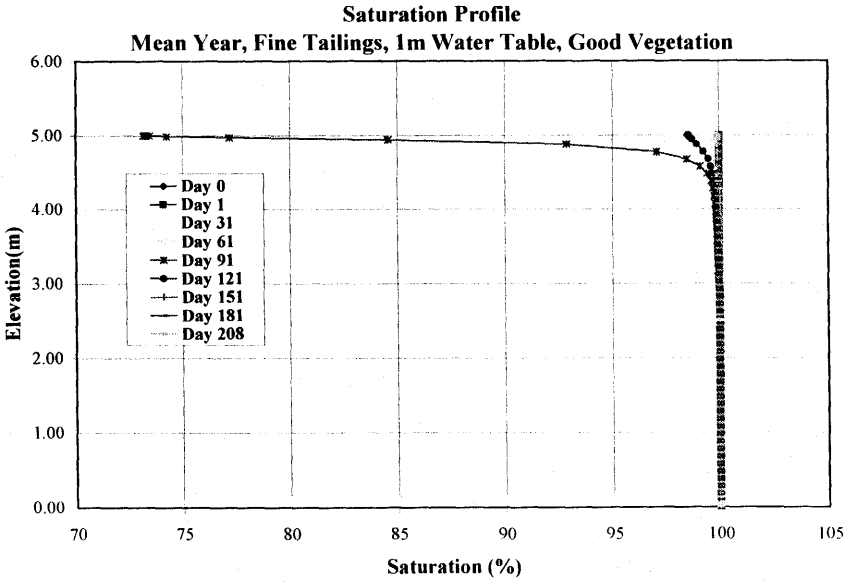
Saturation Profile
Mean Year, Fine Tailings, 1m Water Table, Good Vegetation
Elevation(m)
Saturation (%)
Day 0
Day 1
Day 31
Day 61
Day 91
Day 121
Day 151
Day 181
Day 208

Net Cumulative Flux Comparison
Mean Year, Fine Material, 4m water table, No Vegetation

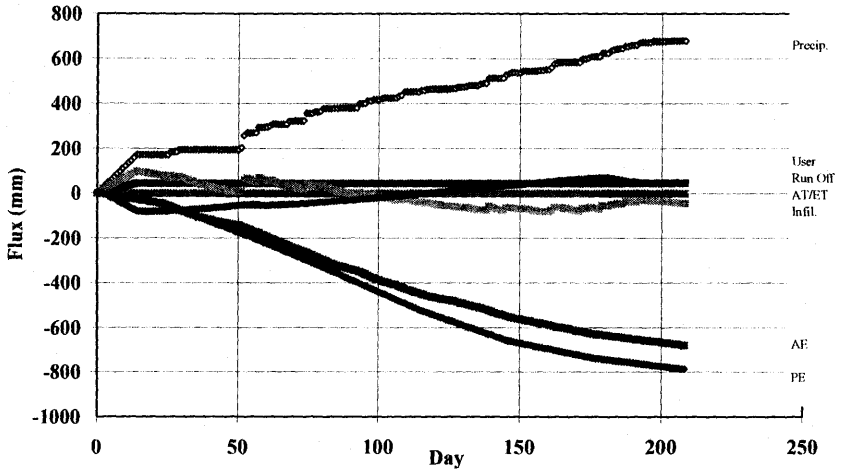

Saturation Profile
Mean Year, Fine Material, 4m water table, No Vegetation

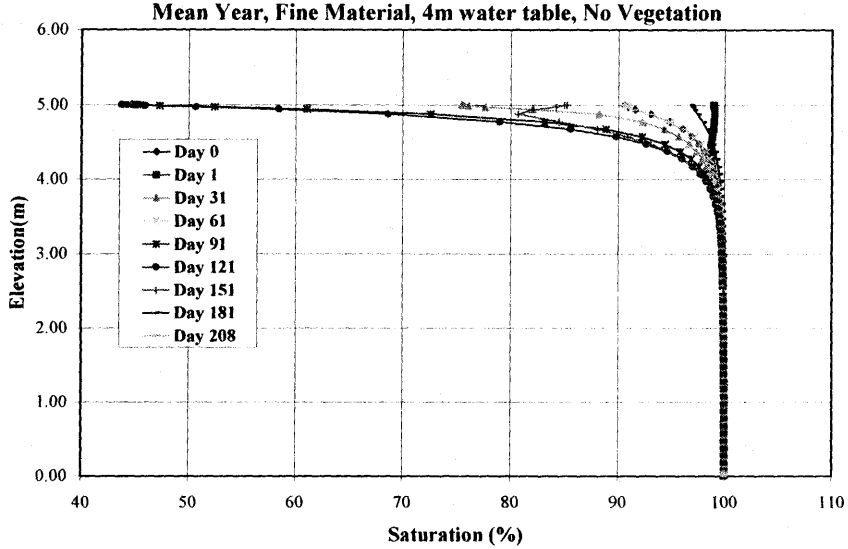

Net Cumulative Flux Comparison
Mean Year, Fine Tailings, 4m Water Table, Poor Vegetation

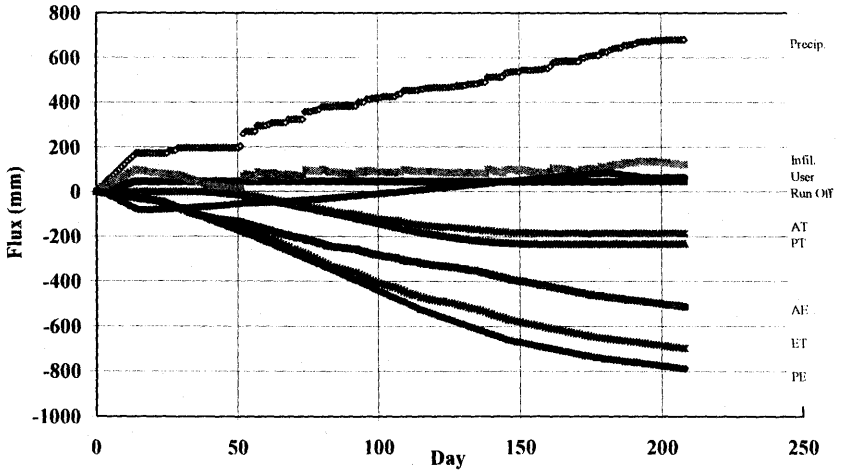

Saturation Profile
Mean Year, Fine Tailings, 4m Water Table, Poor Vegetation

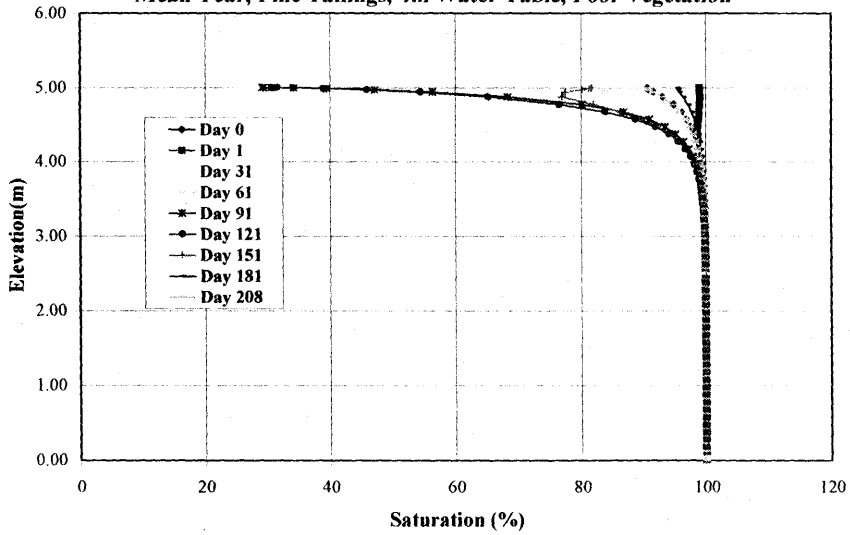

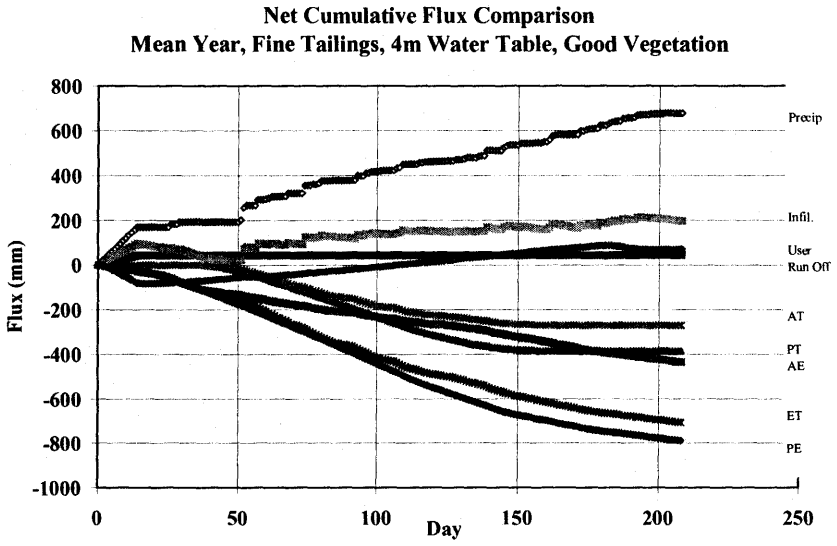
Net Cumulative Flux Comparison
Mean Year, Fine Tailings, 4m Water Table, Good Vegetation
Flux (mm)
Day
Precip
Infil.
User Run Off
AT
PT
AE
ET
PE

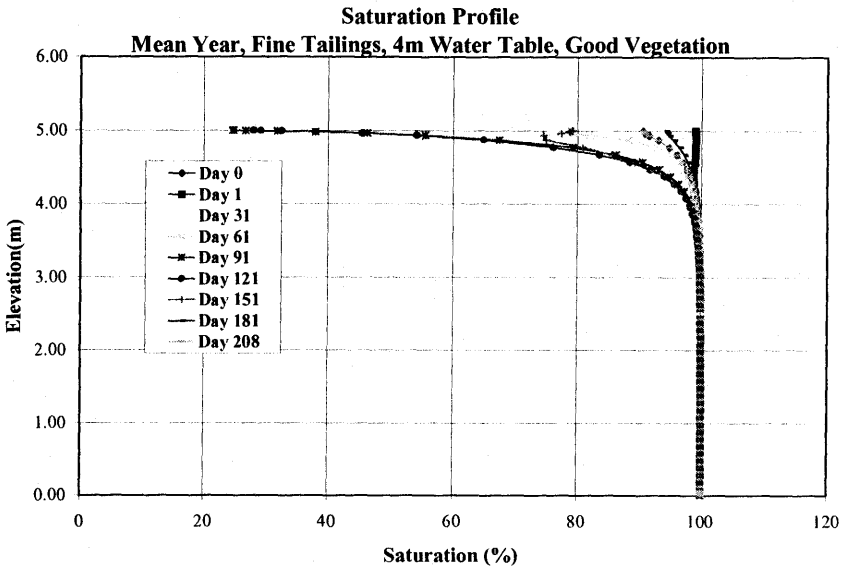
Saturation Profile
Mean Year, Fine Tailings, 4m Water Table, Good Vegetation
Elevation(m)
Saturation (%)
Day 0
Day 1
Day 31
Day 61
Day 91
Day 121
Day 151
Day 181
Day 208

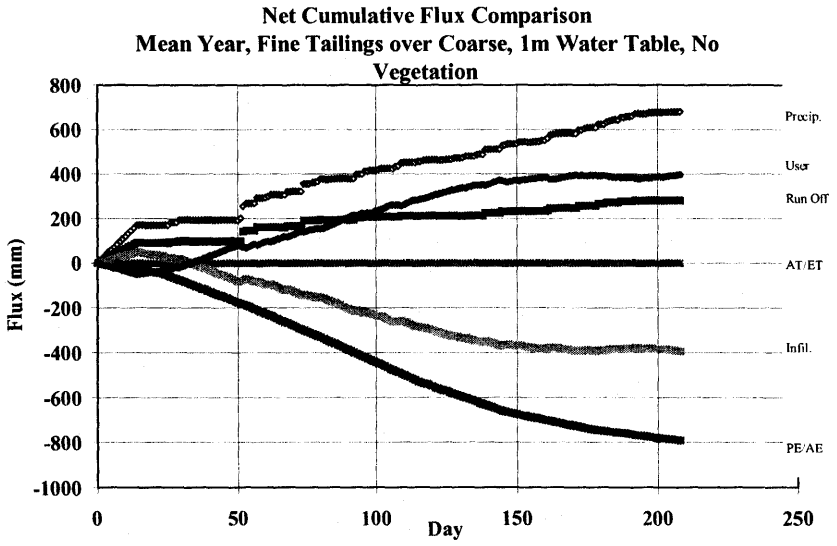
Net Cumulative Flux Comparison
Mean Year, Fine Tailings over Coarse, 1m Water Table, No Vegetation
Flux (mm)
Day
Precip.
User Run Off
AT/ET
Infil.
PE/AE

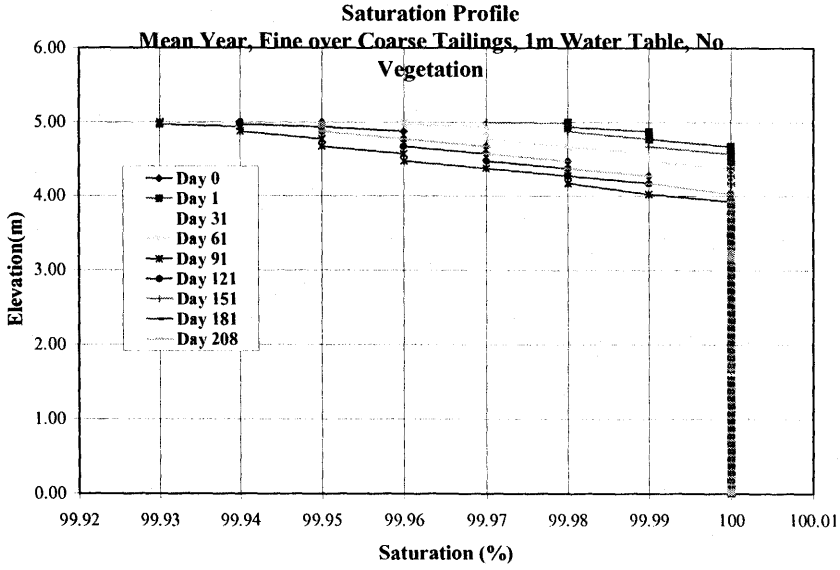
Saturation Profile
Mean Year, Fine over Coarse Tailings, 1m Water Table, No Vegetation
Elevation(m)
Saturation (%)
Day 0
Day 1
Day 31
Day 61
Day 91
Day 121
Day 151
Day 181
Day 208

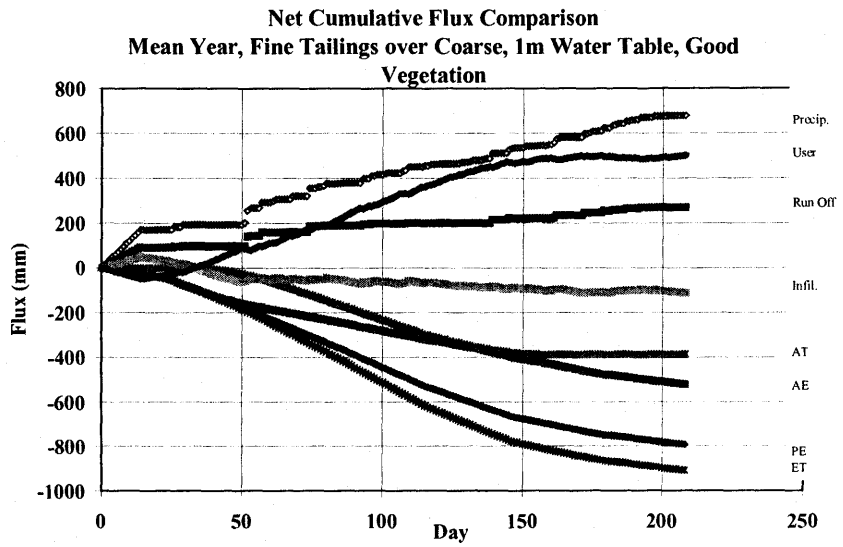
Net Cumulative Flux Comparison
Mean Year, Fine Tailings over Coarse, 1m Water Table, Good Vegetation
Flux (mm)
Day
Precip.
User
Run Off
Infil.
AT
AE
PE
ET

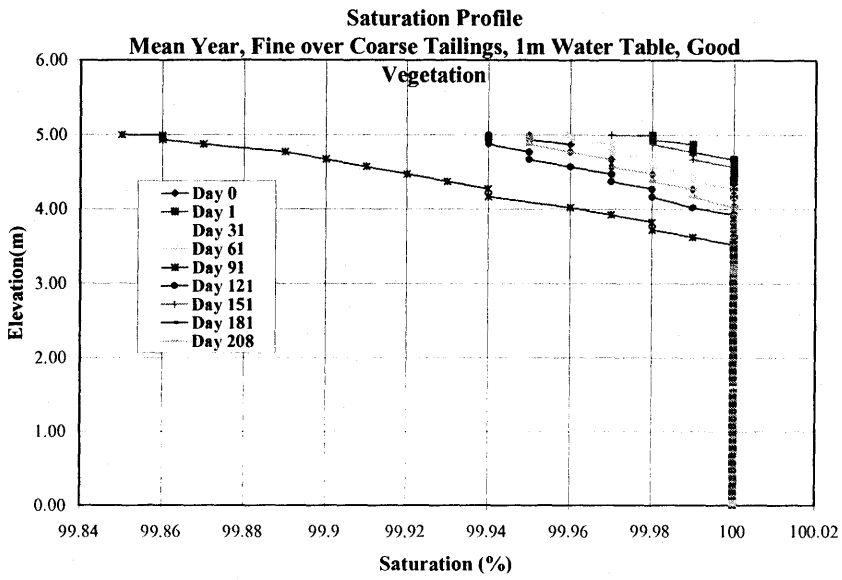
Saturation Profile
Mean Year, Fine over Coarse Tailings, 1m Water Table, Good Vegetation
Elevation(m)
Saturation (%)
Day 0
Day 1
Day 31
Day 61
Day 91
Day 121
Day 151
Day 181
Day 208

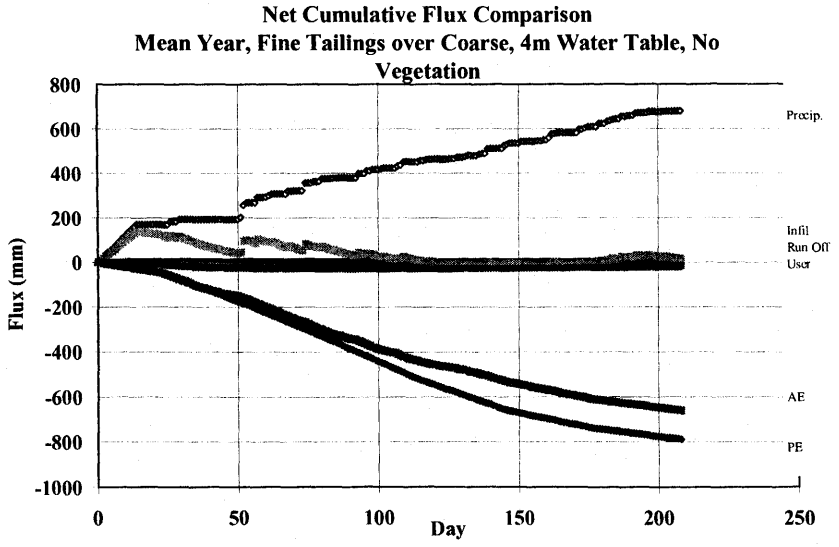
Net Cumulative Flux Comparison
Mean Year, Fine Tailings over Coarse, 4m Water Table, No Vegetation
Flux (mm)
Day
Precip.
Infil
Run Off
User
AE
PE

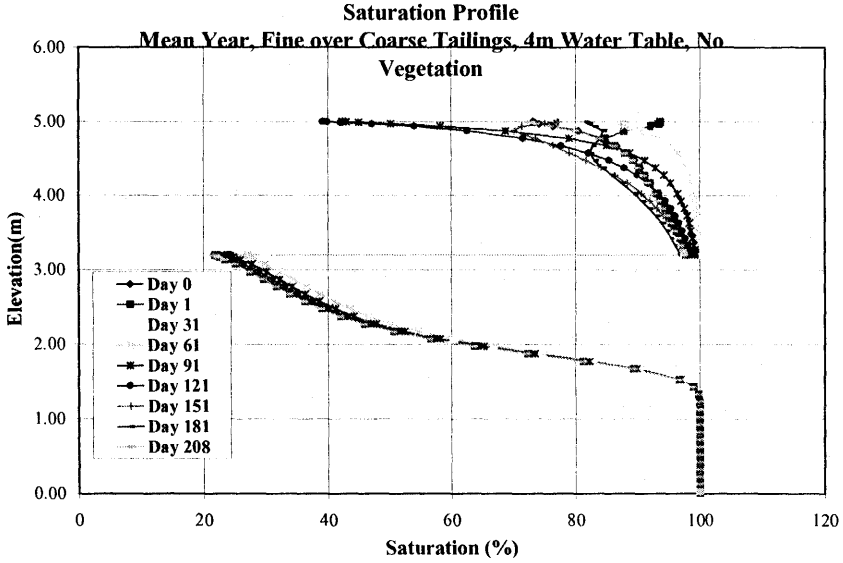
Saturation Profile
Mean Year, Fine over Coarse Tailings, 4m Water Table, No Vegetation
Elevation(m)
Saturation (%)
Day 0
Day 1
Day 31
Day 61
Day 91
Day 121
Day 151
Day 181
Day 208

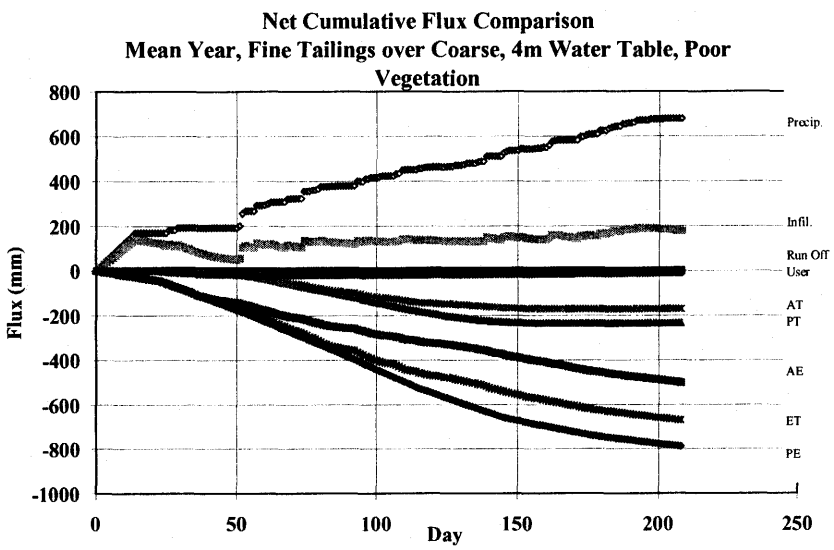
Net Cumulative Flux Comparison
Mean Year, Fine Tailings over Coarse, 4m Water Table, Poor Vegetation
Flux (mm)
Day
Precip.
Infil.
Run Off
User
AT
PT
AE
ET
PE

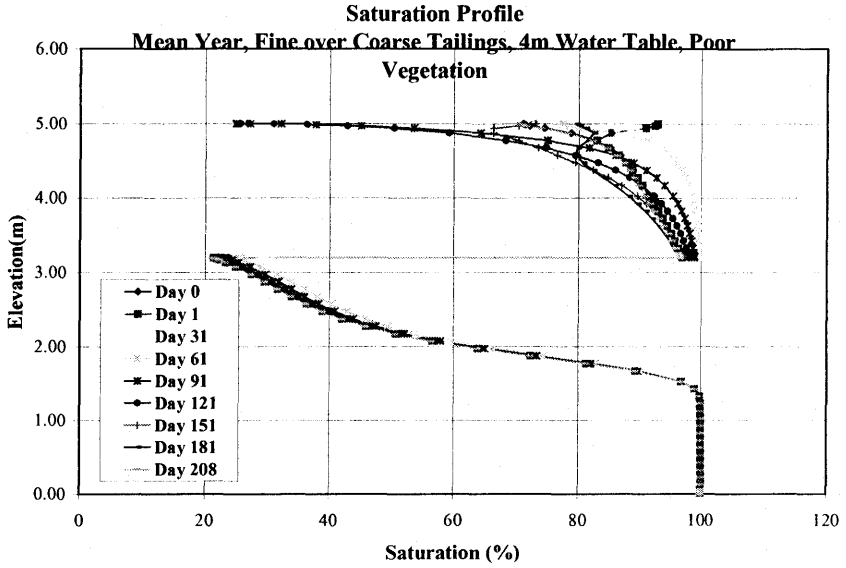
Saturation Profile
Mean Year, Fine over Coarse Tailings, 4m Water Table, Poor Vegetation
Elevation(m)
Saturation (%)
Day 0
Day 1
Day 31
Day 61
Day 91
Day 121
Day 151
Day 181
Day 208

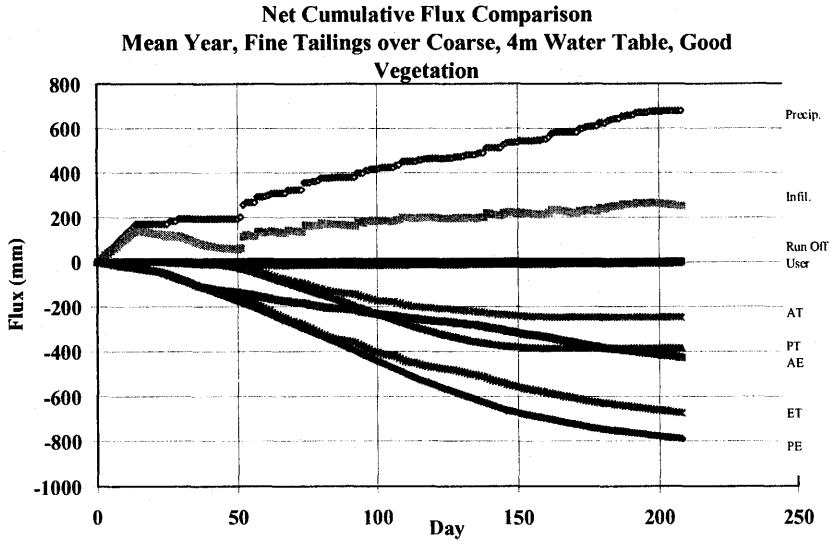
Net Cumulative Flux Comparison
Mean Year, Fine Tailings over Coarse, 4m Water Table, Good Vegetation
Flux (mm)
Day
Precip.
Infil.
Run Off
User
AT
PT
AE
ET
PE

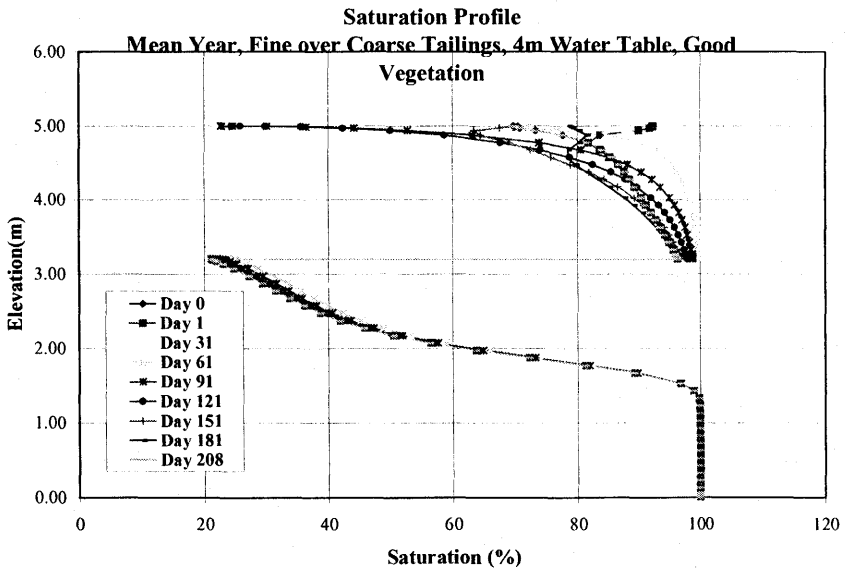
Saturation Profile
Mean Year, Fine over Coarse Tailings, 4m Water Table, Good Vegetation
Elevation(m)
Saturation (%)
Day 0
Day 1
Day 31
Day 61
Day 91
Day 121
Day 151
Day 181
Day 208

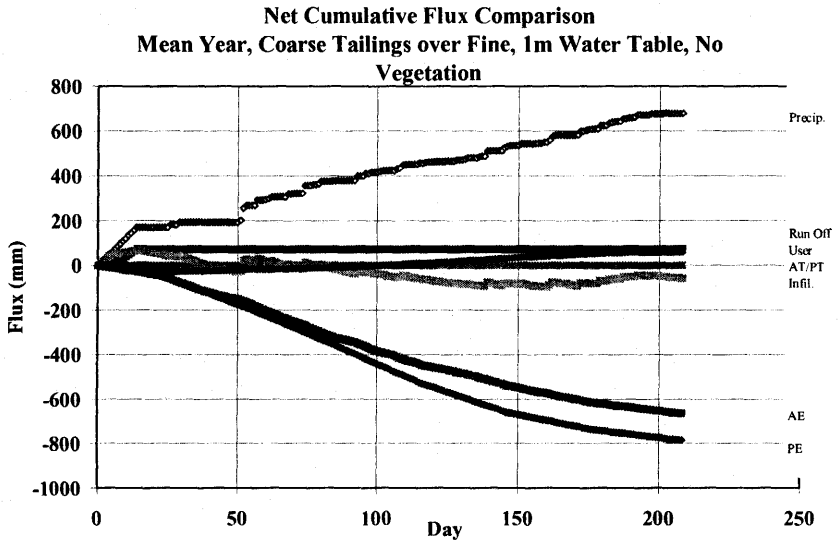
Net Cumulative Flux Comparison
Mean Year, Coarse Tailings over Fine, 1m Water Table, No Vegetation
Flux (mm)
Day
Precip.
Run Off
User
AT/PT
Infil.
AE
PE

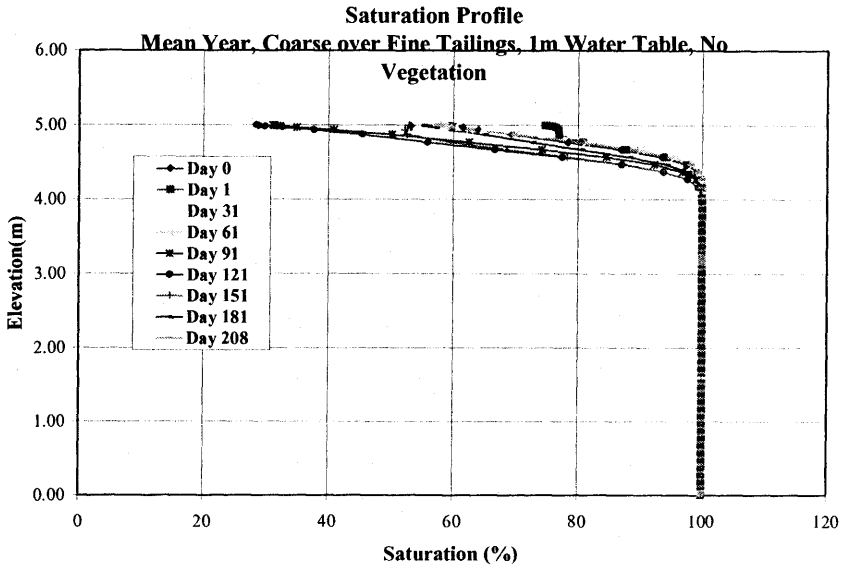
Saturation Profile
Mean Year, Coarse over Fine Tailings, 1m Water Table, No Vegetation
Elevation(m)
Saturation (%)
Day 0
Day 1
Day 31
Day 61
Day 91
Day 121
Day 151
Day 181
Day 208

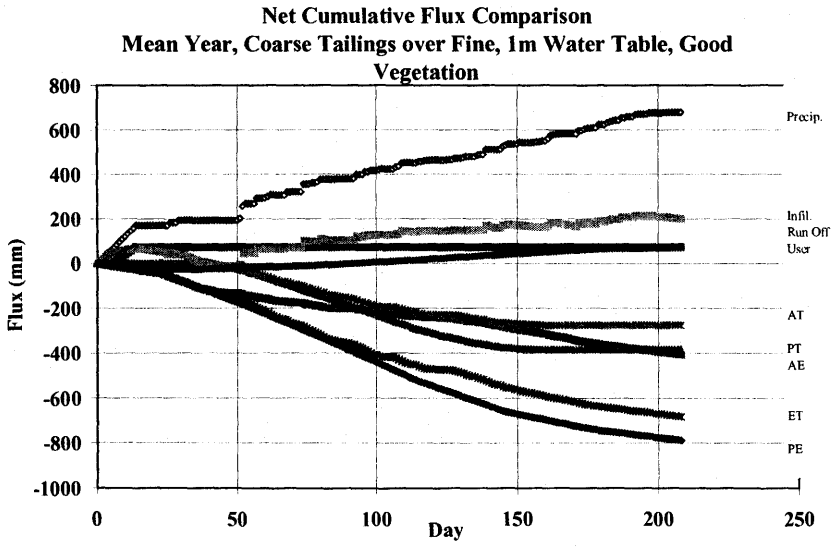
Net Cumulative Flux Comparison
Mean Year, Coarse Tailings over Fine, 1m Water Table, Good Vegetation
Flux (mm)
Day
Precip.
Infil.
Run Off
User
AT
PT
AE
ET
PE

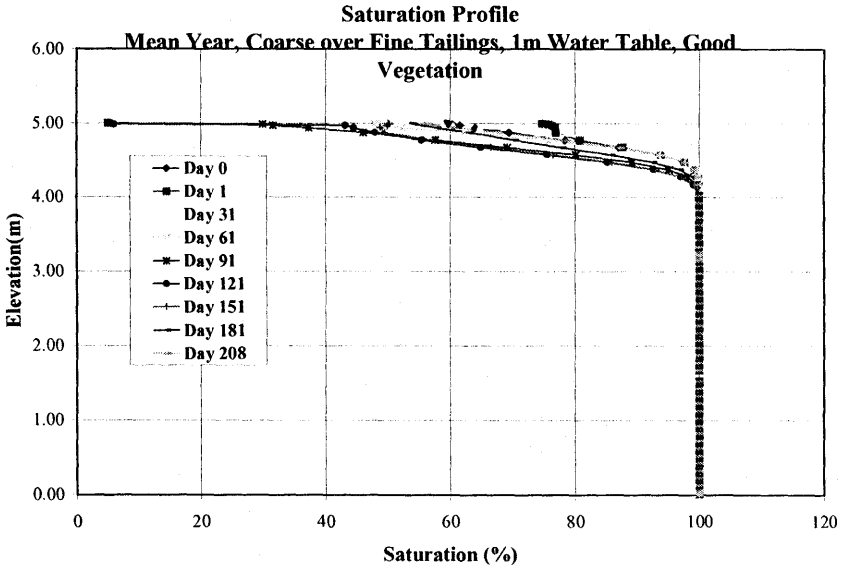
Saturation Profile
Mean Year, Coarse over Fine Tailings, 1m Water Table, Good Vegetation
Elevation(m)
Saturation (%)
Day 0
Day 1
Day 31
Day 61
Day 91
Day 121
Day 151
Day 181
Day 208

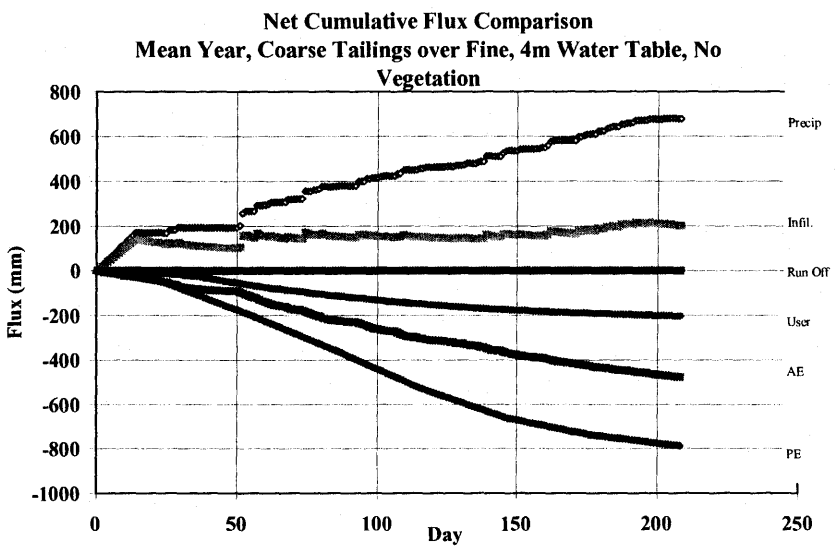
Net Cumulative Flux Comparison
Mean Year, Coarse Tailings over Fine, 4m Water Table, No Vegetation
Flux (mm)
Day
Precip
Infil.
Run Off
User
AE
PE

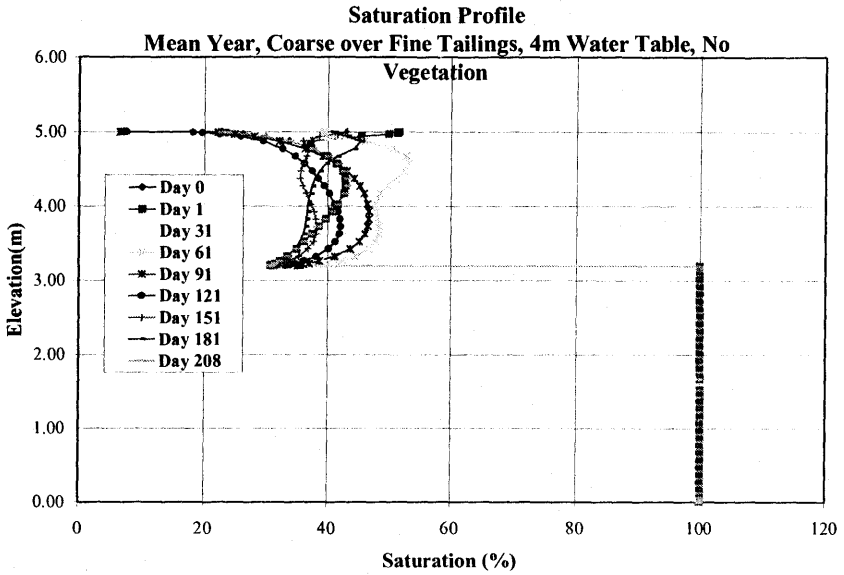
Saturation Profile
Mean Year, Coarse over Fine Tailings, 4m Water Table, No Vegetation
Elevation(m)
Saturation (%)
Day 0
Day 1
Day 31
Day 61
Day 91
Day 121
Day 151
Day 181
Day 208

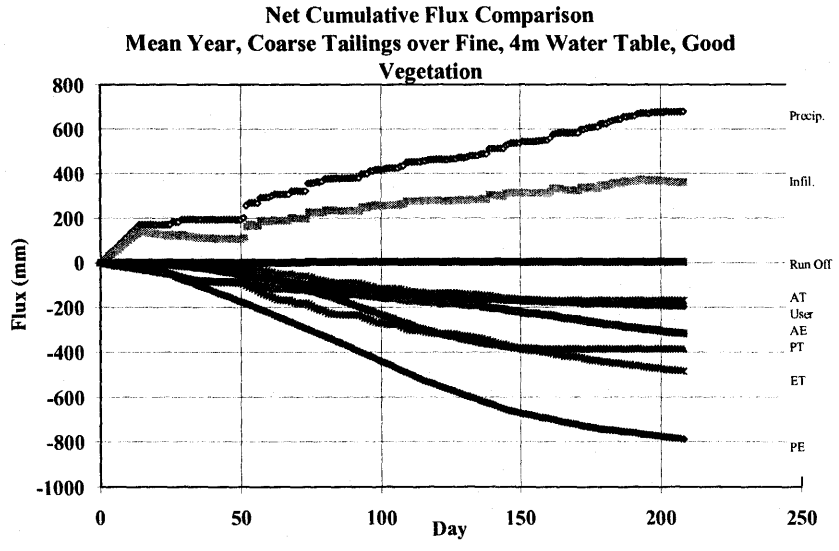
Net Cumulative Flux Comparison
Mean Year, Coarse Tailings over Fine, 4m Water Table, Good Vegetation
Flux (mm)
Day
Precip.
Infil.
Run Off
AT
User
AE
PT
ET
PE

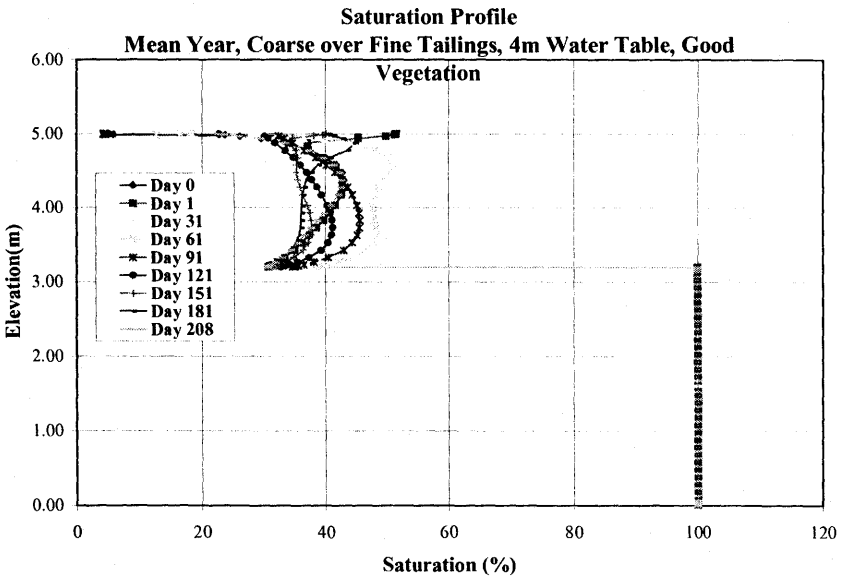
Saturation Profile
Mean Year, Coarse over Fine Tailings, 4m Water Table, Good Vegetation
Elevation(m)
Saturation (%)
Day 0
Day 1
Day 31
Day 61
Day 91
Day 121
Day 151
Day 181
Day 208

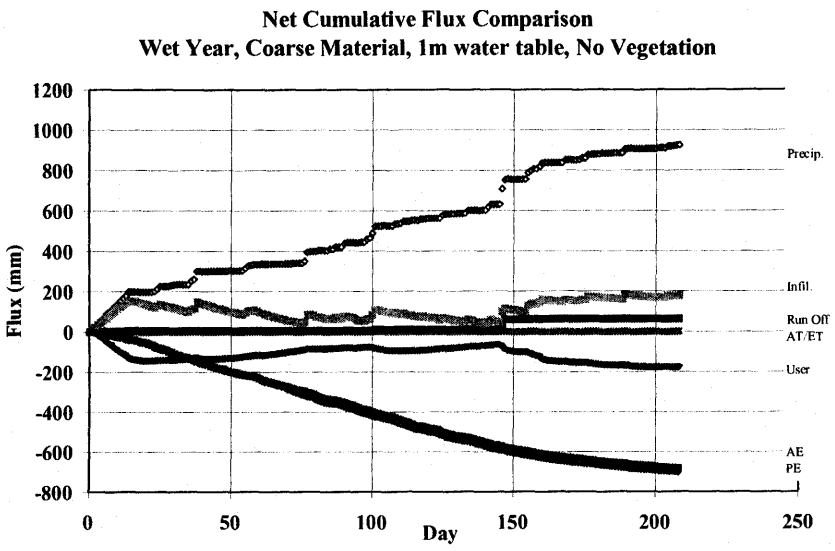
Net Cumulative Flux Comparison
Wet Year, Coarse Material, 1m water table, No Vegetation
Flux (mm)
Day
Precip.
Infil.
Run Off
AT/ET
User
AE
PE

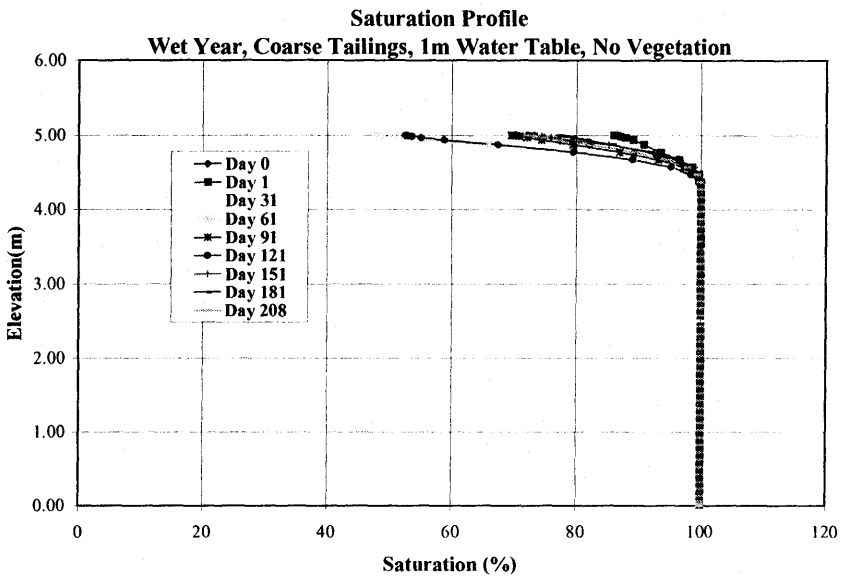
Saturation Profile
Wet Year, Coarse Tailings, 1m Water Table, No Vegetation
Elevation(m)
Saturation (%)
Day 0
Day 1
Day 31
Day 61
Day 91
Day 121
Day 151
Day 181
Day 208

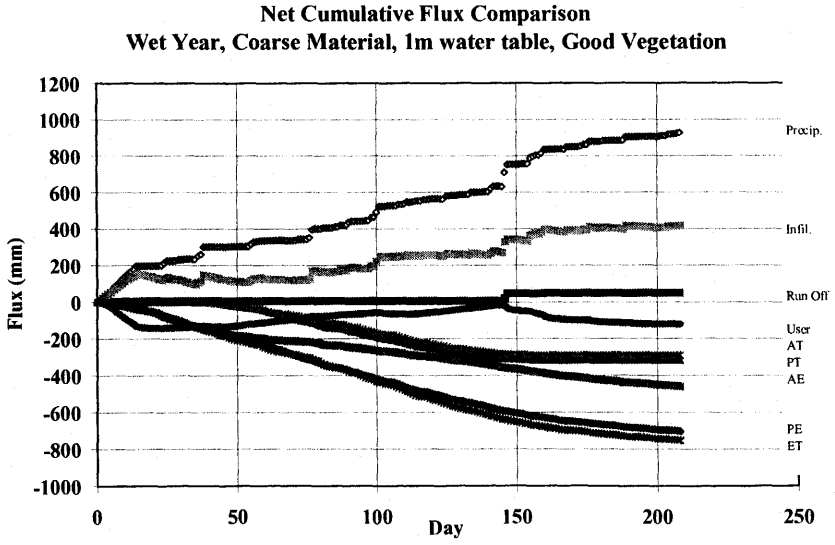
Net Cumulative Flux Comparison
Wet Year, Coarse Material, 1m water table, Good Vegetation
Flux (mm)
Day
Precip.
Infil.
Run Off
User
AT
PT
AE
PE
ET

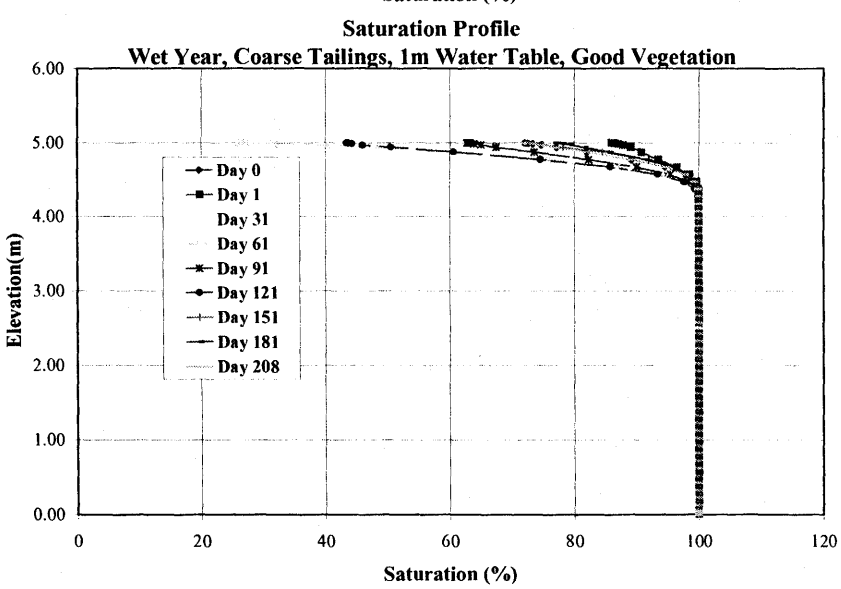
Saturation Profile
Wet Year, Coarse Tailings, 1m Water Table, Good Vegetation
Elevation(m)
Saturation (%)
Day 0
Day 1
Day 31
Day 61
Day 91
Day 121
Day 151
Day 181
Day 208

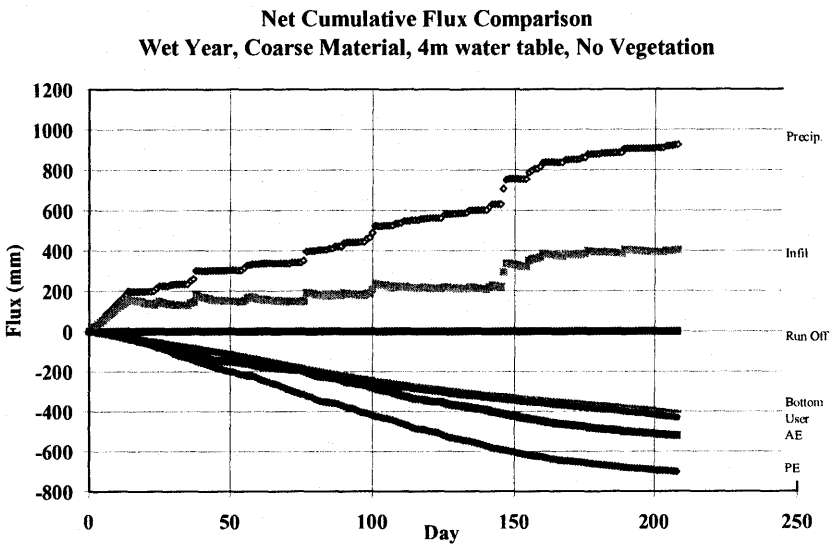
Net Cumulative Flux Comparison
Wet Year, Coarse Material, 4m water table, No Vegetation
Flux (mm)
Day
Precip.
Infil
Run Off
Bottom
User
AE
PE

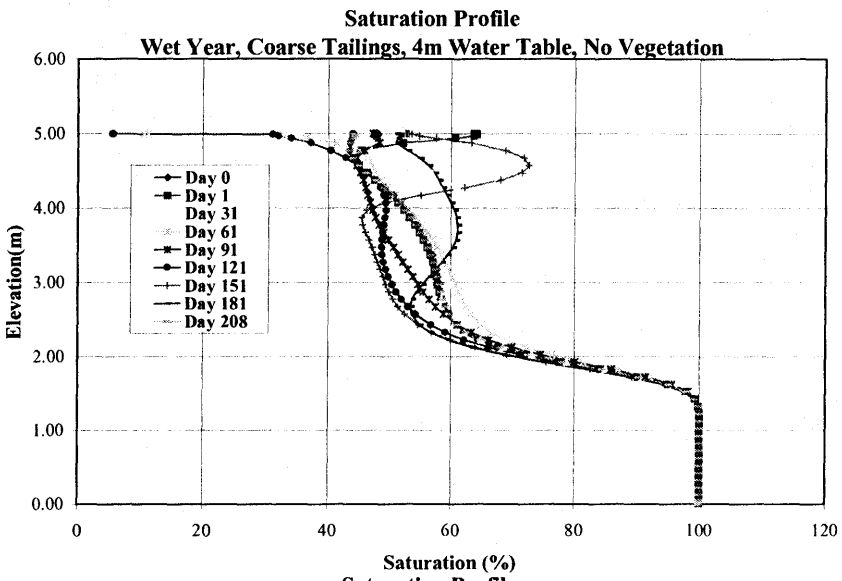
Saturation Profile
Wet Year, Coarse Tailings, 4m Water Table, No Vegetation
Elevation(m)
Saturation (%)
Day 0
Day 1
Day 31
Day 61
Day 91
Day 121
Day 151
Day 181
Day 208

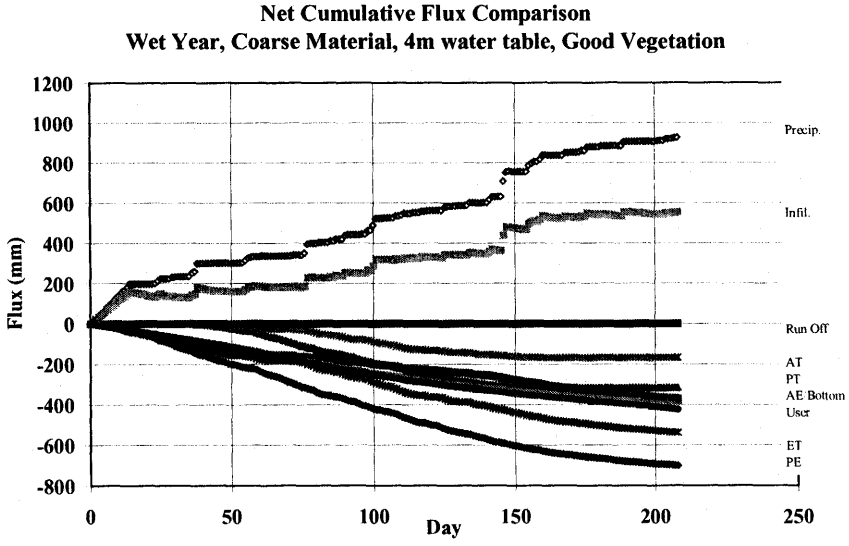
Net Cumulative Flux Comparison
Wet Year, Coarse Material, 4m water table, Good Vegetation
Flux (mm)
Day
Precip.
Infil.
Run Off
AT
PT
AE Bottom
User
ET
PE

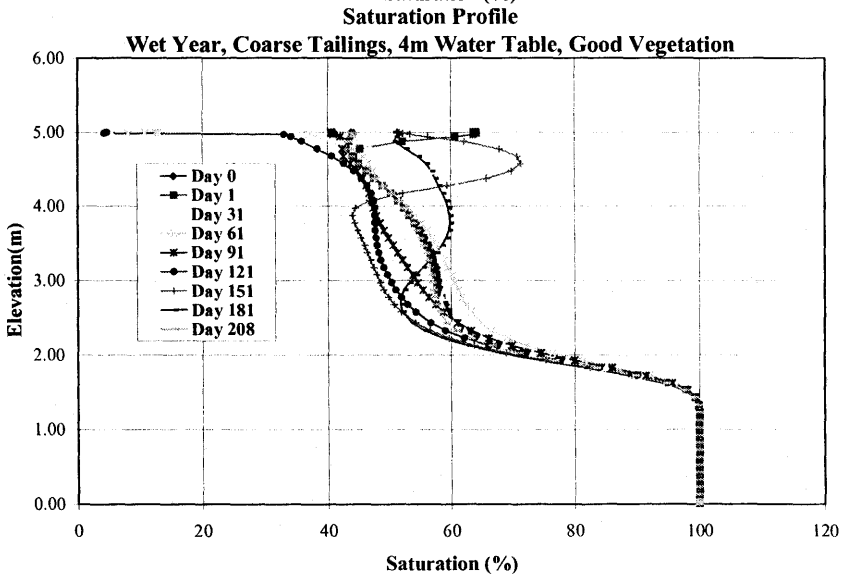
Saturation Profile
Wet Year, Coarse Tailings, 4m Water Table, Good Vegetation
Elevation(m)
Saturation (%)
Day 0
Day 1
Day 31
Day 61
Day 91
Day 121
Day 151
Day 181
Day 208

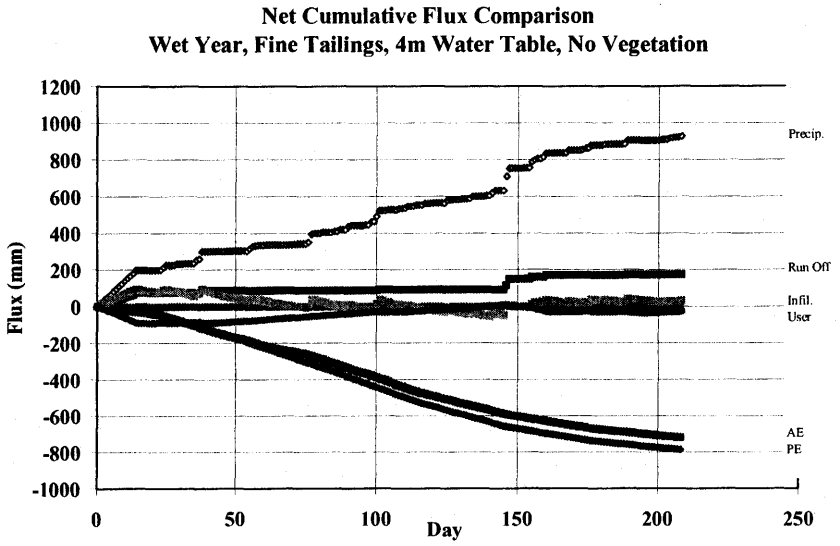
Net Cumulative Flux Comparison
Wet Year, Fine Tailings, 4m Water Table, No Vegetation
Flux (mm)
Day
Precip.
Run Off
Infil.
User
AE
PE

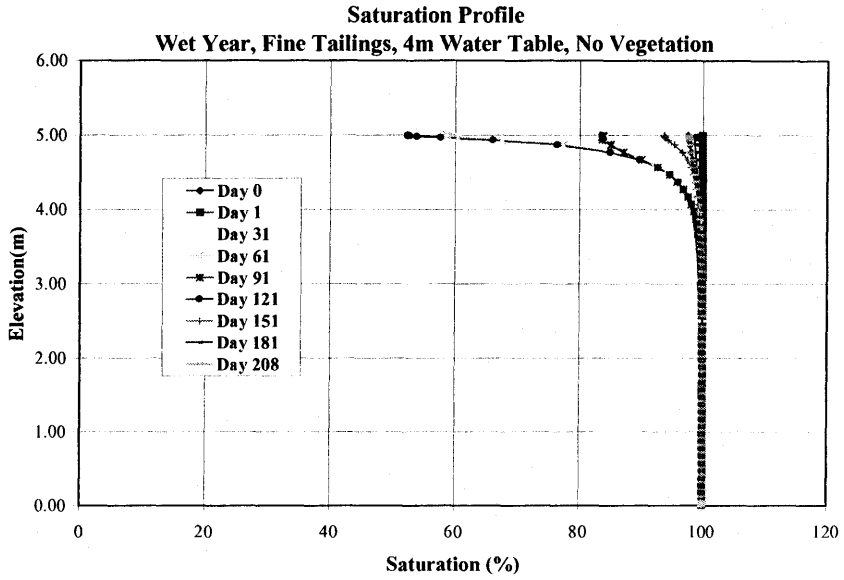
Saturation Profile
Wet Year, Fine Tailings, 4m Water Table, No Vegetation
Elevation(m)
Saturation (%)
Day 0
Day 1
Day 31
Day 61
Day 91
Day 121
Day 151
Day 181
Day 208

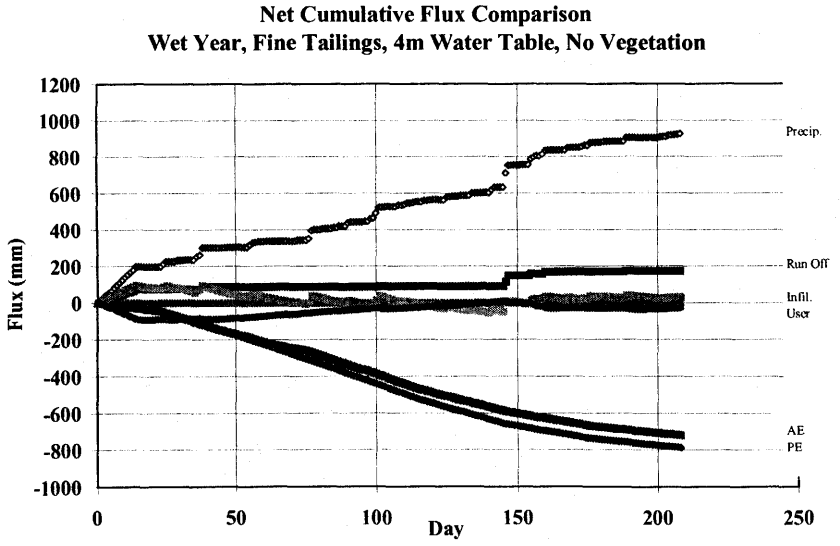
Net Cumulative Flux Comparison
Wet Year, Fine Tailings, 4m Water Table, No Vegetation
Flux (mm)
Day
Precip.
Run Off
Infil.
User
AE
PE

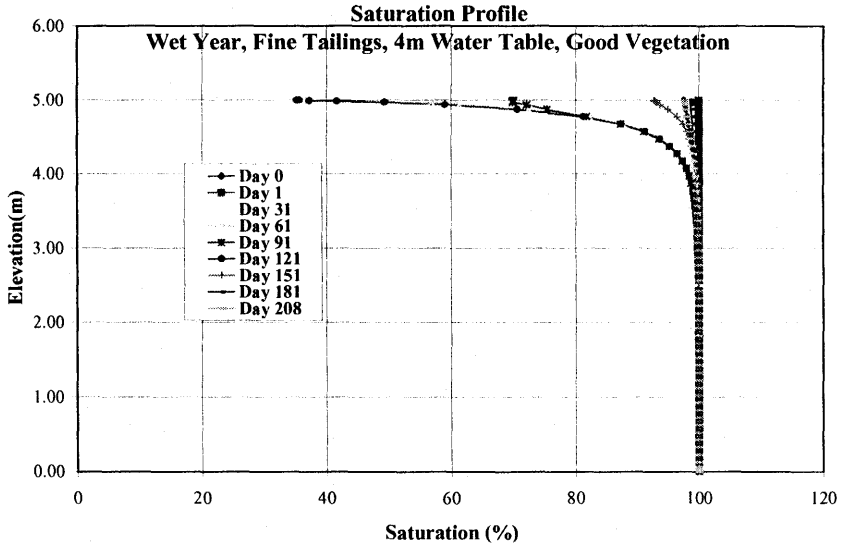
Saturation Profile
Wet Year, Fine Tailings, 4m Water Table, Good Vegetation
Elevation(m)
Saturation (%)
Day 0
Day 1
Day 31
Day 61
Day 91
Day 121
Day 151
Day 181
Day 208

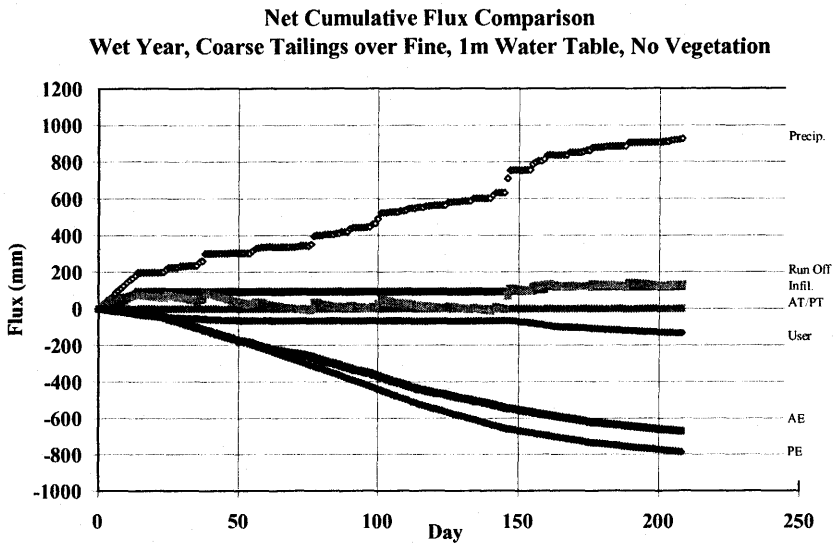
Net Cumulative Flux Comparison
Wet Year, Coarse Tailings over Fine, 1m Water Table, No Vegetation
Flux (mm)
Day
Precip.
Run Off
Infil.
AT/PT
User
AE
PE

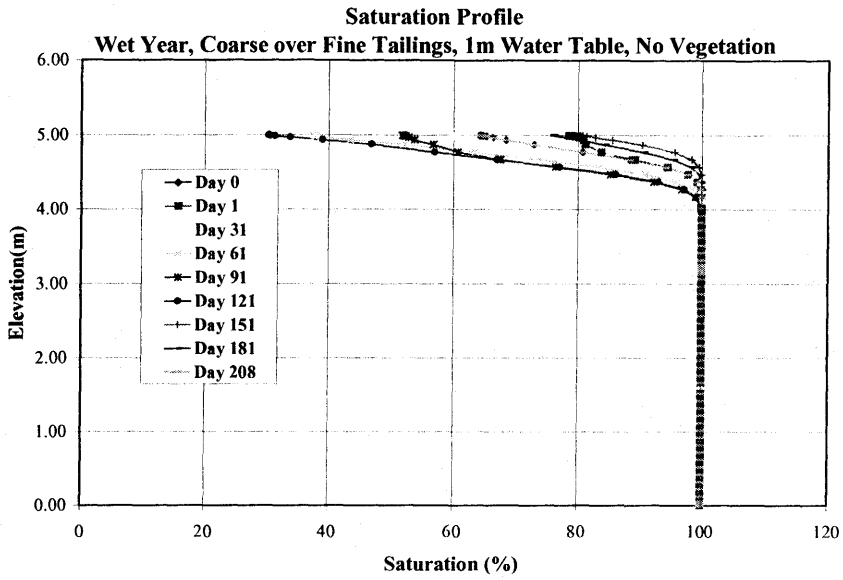
Saturation Profile
Wet Year, Coarse over Fine Tailings, 1m Water Table, No Vegetation
Elevation(m)
Saturation (%)
Day 0
Day 1
Day 31
Day 61
Day 91
Day 121
Day 151
Day 181
Day 208

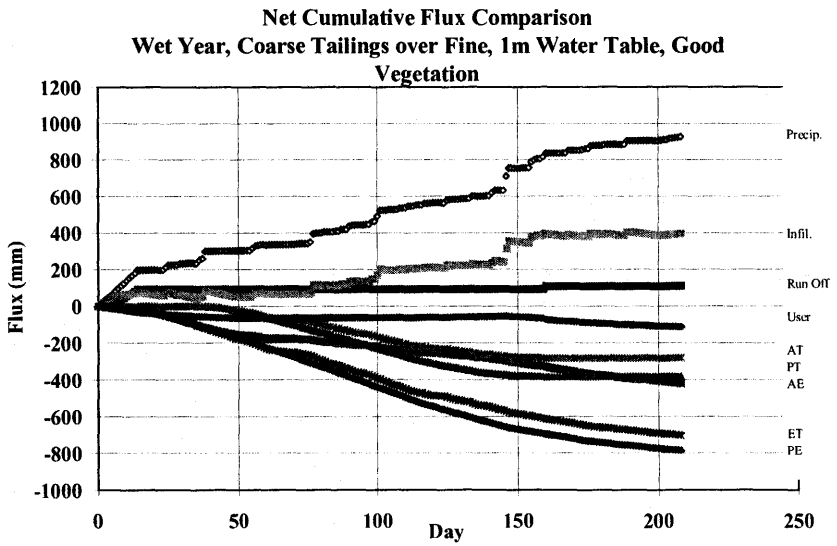
Net Cumulative Flux Comparison
Wet Year, Coarse Tailings over Fine, 1m Water Table, Good Vegetation
Flux (mm)
Day
Precip.
Infil.
Run Off
User
AT
PT
AE
ET
PE

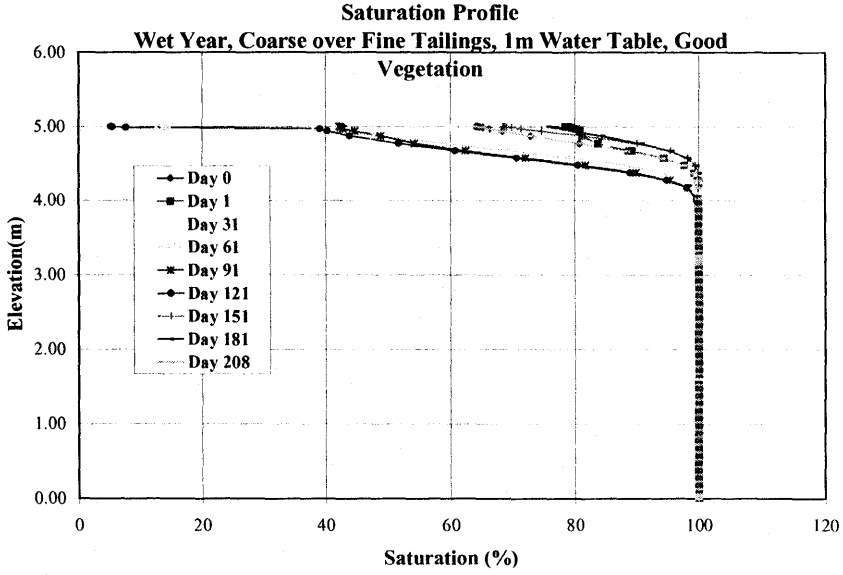
Saturation Profile
Wet Year, Coarse over Fine Tailings, 1m Water Table, Good Vegetation
Elevation(m)
Saturation (%)
Day 0
Day 1
Day 31
Day 61
Day 91
Day 121
Day 151
Day 181
Day 208

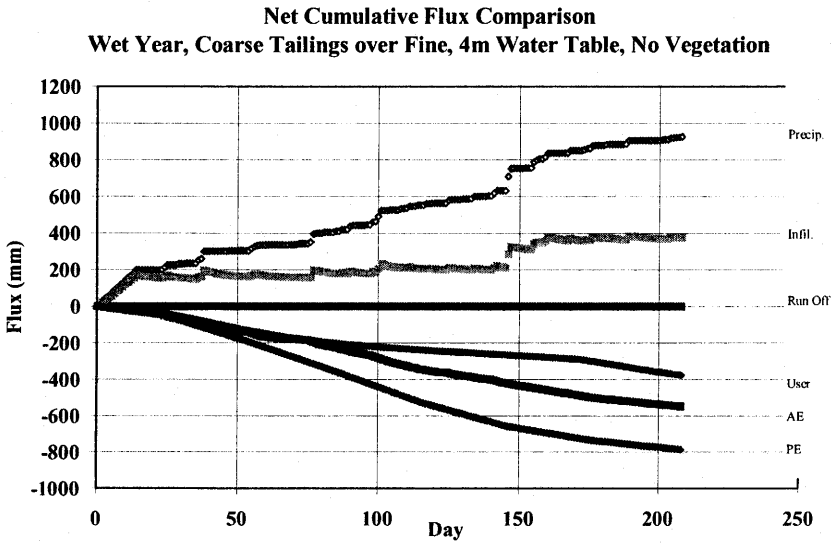
Net Cumulative Flux Comparison
Wet Year, Coarse Tailings over Fine, 4m Water Table, No Vegetation
Flux (mm)
Day
Precip.
Infil.
Run Off
User
AE
PE

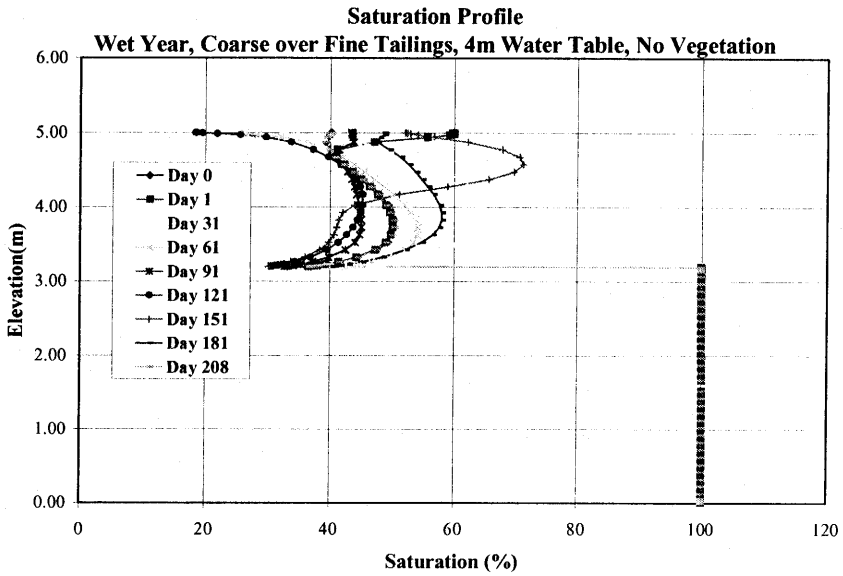
Saturation Profile
Wet Year, Coarse over Fine Tailings, 4m Water Table, No Vegetation
Elevation(m)
Saturation (%)
Day 0
Day 1
Day 31
Day 61
Day 91
Day 121
Day 151
Day 181
Day 208

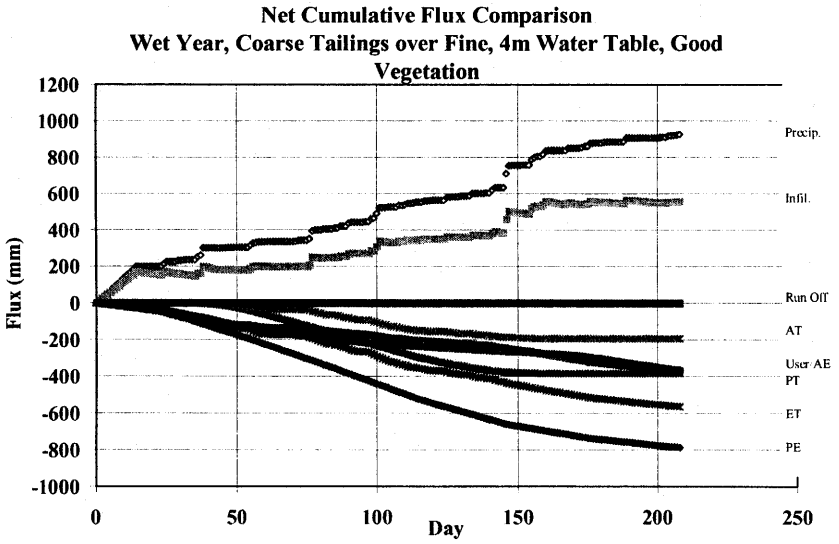
Net Cumulative Flux Comparison
Wet Year, Coarse Tailings over Fine, 4m Water Table, Good Vegetation
Flux (mm)
Day
Precip.
Infil.
Run Off
AT
User AE
PT
ET
PE

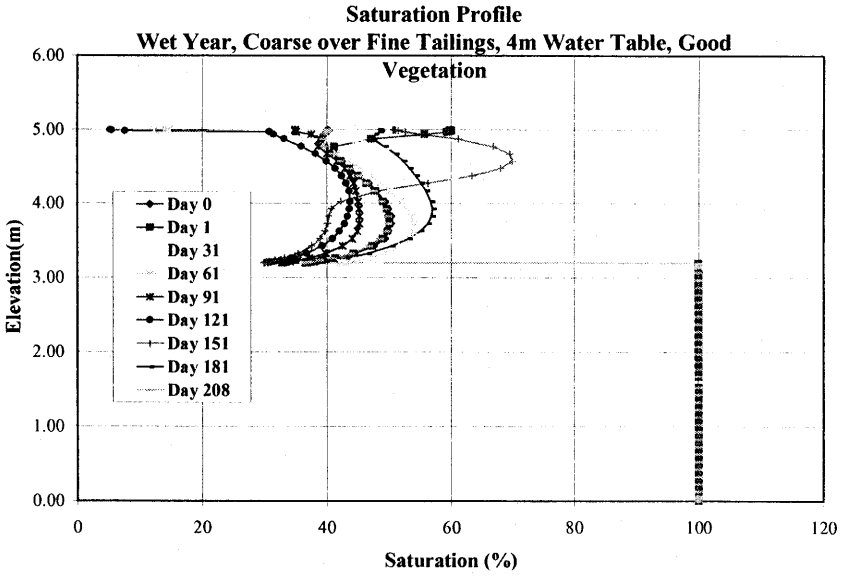
Saturation Profile
Wet Year, Coarse over Fine Tailings, 4m Water Table, Good Vegetation
Elevation(m)
Saturation (%)
Day 0
Day 1
Day 31
Day 61
Day 91
Day 121
Day 151
Day 181
Day 208

Appendix C: Oxygen Modeling

C1 OXYGEN CONCENTRATION PROFILES

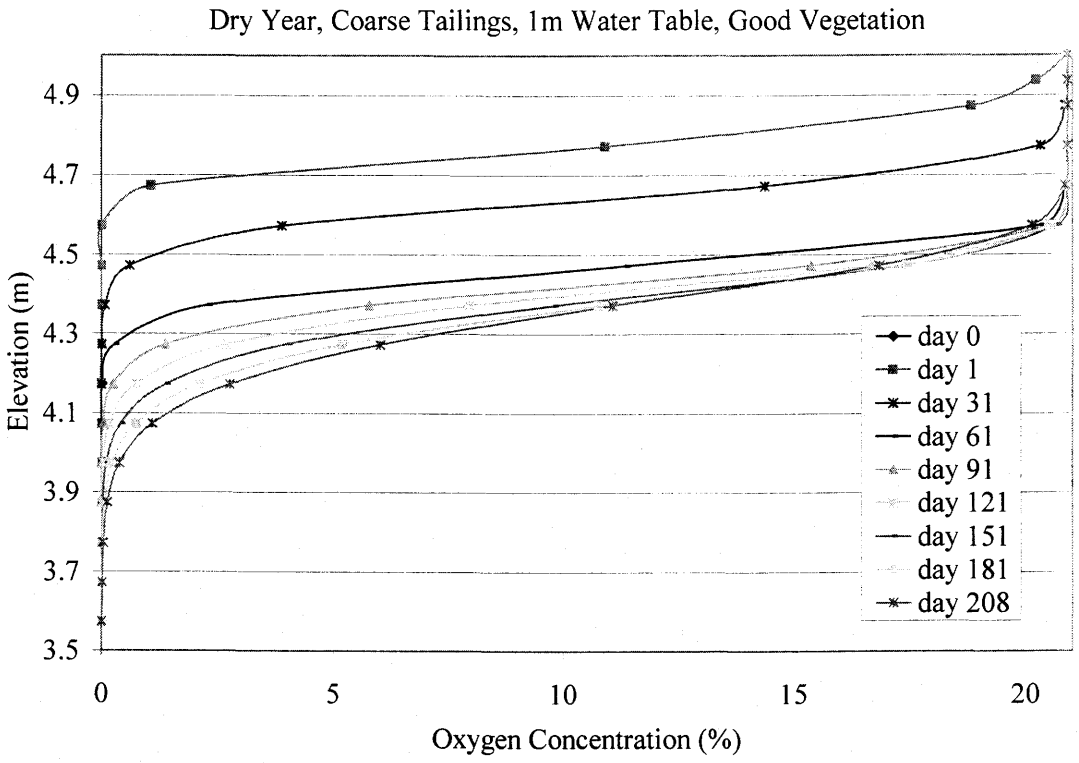

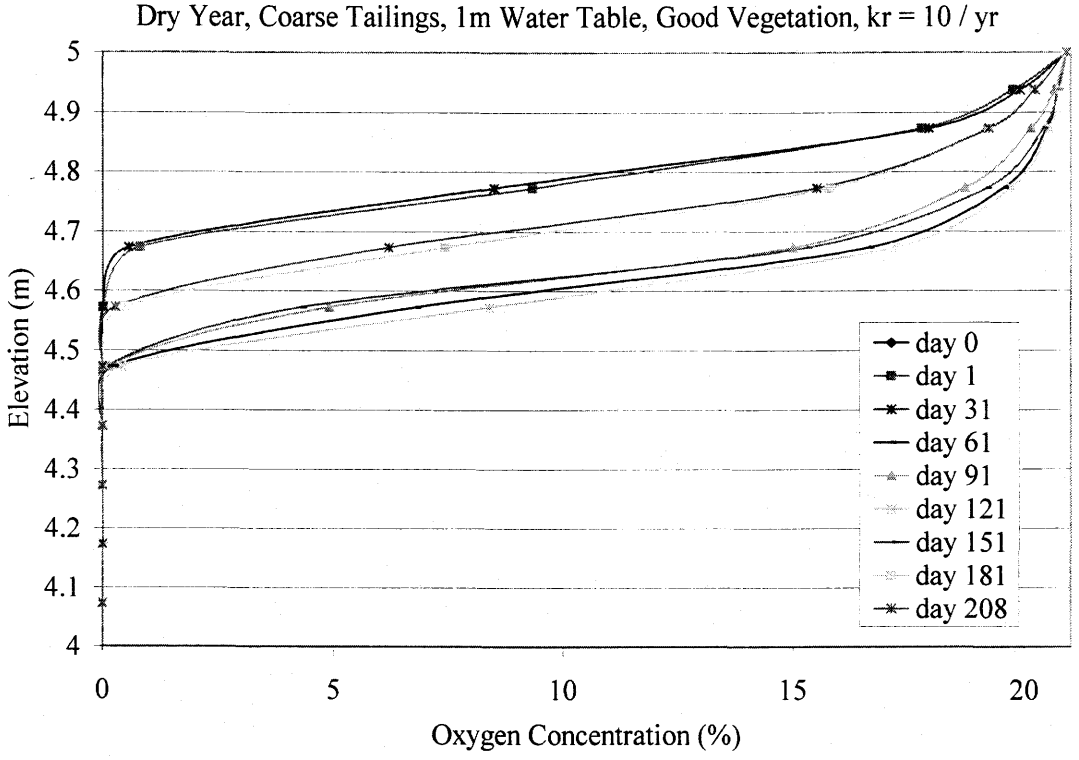

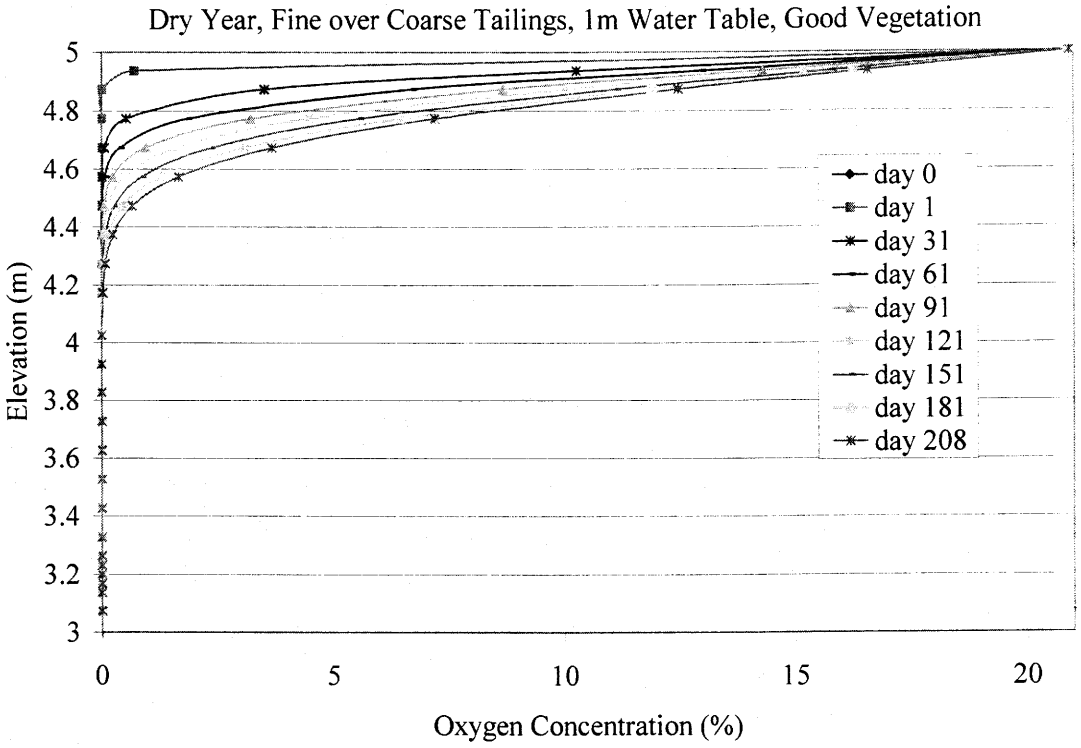
Dry Year, Fine over Coarse Tailings, 1m Water Table, Good Vegetation
Elevation (m)
5
4.8
4.6
4.4
4.2
4
3.8
3.6
3.4
3.2
3
0
5
10
15
20
Oxygen Concentration (%)
day 0
day 1
day 31
day 61
day 91
day 121
day 151
day 181
day 208

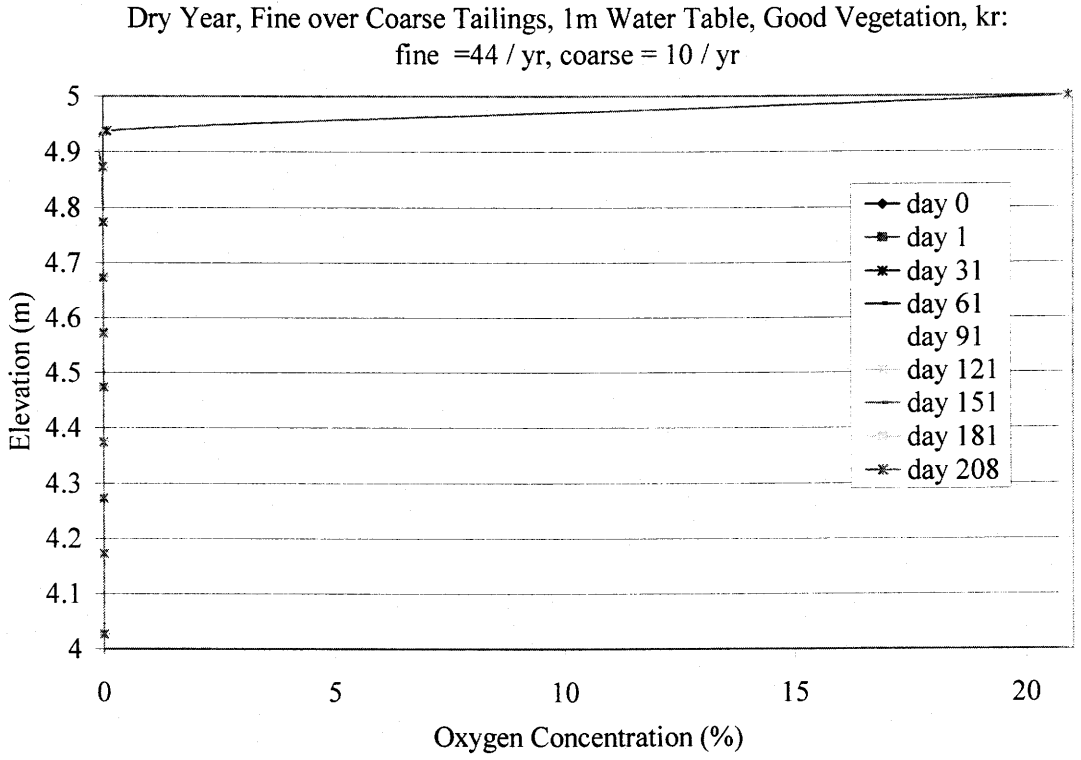
Dry Year, Fine over Coarse Tailings, 1m Water Table, Good Vegetation, kr:
fine =44 / yr, coarse = 10 / yr
Elevation (m)
5
4.9
4.8
4.7
4.6
4.5
4.4
4.3
4.2
4.1
4
0
5
10
15
20
Oxygen Concentration (%)
day 0
day 1
day 31
day 61
day 91
day 121
day 151
day 181
day 208

C2 ALTERED SATURATION PROFILES

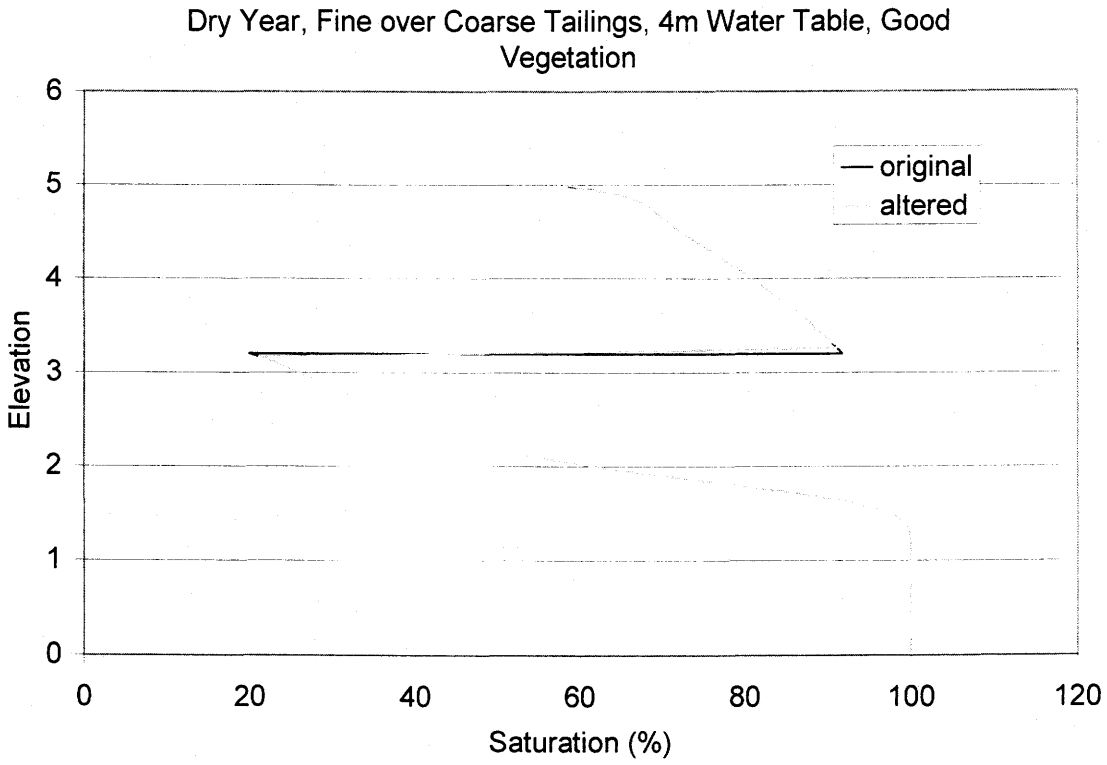

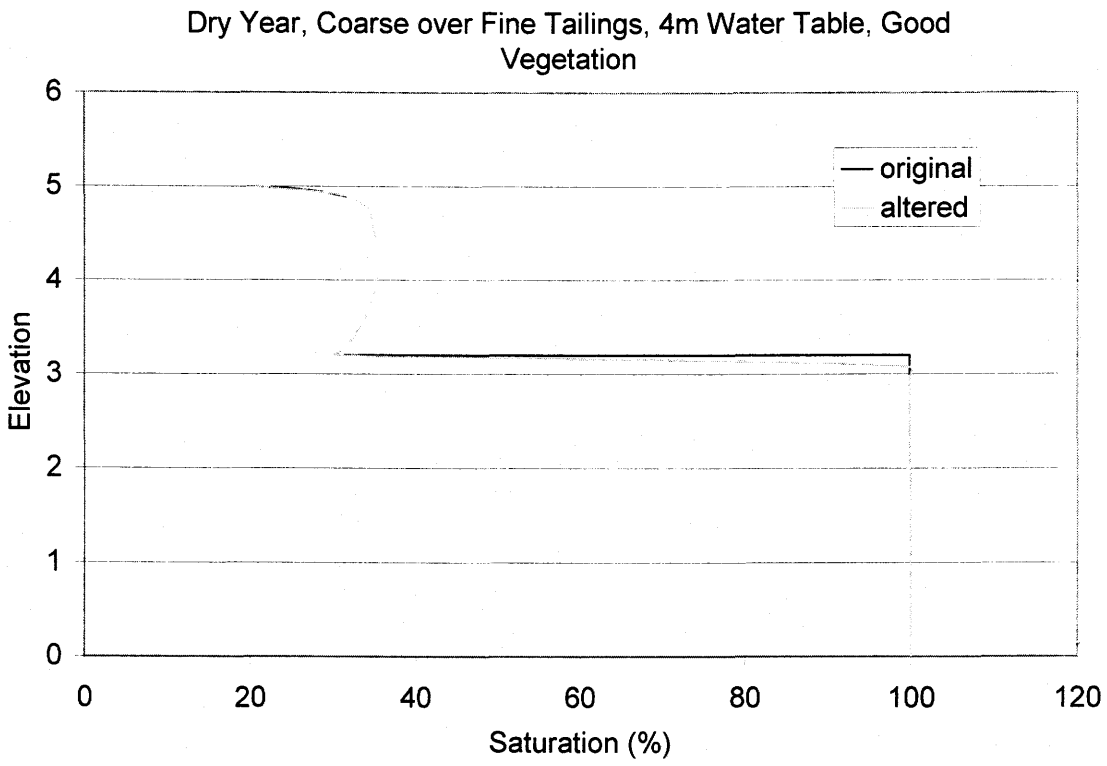

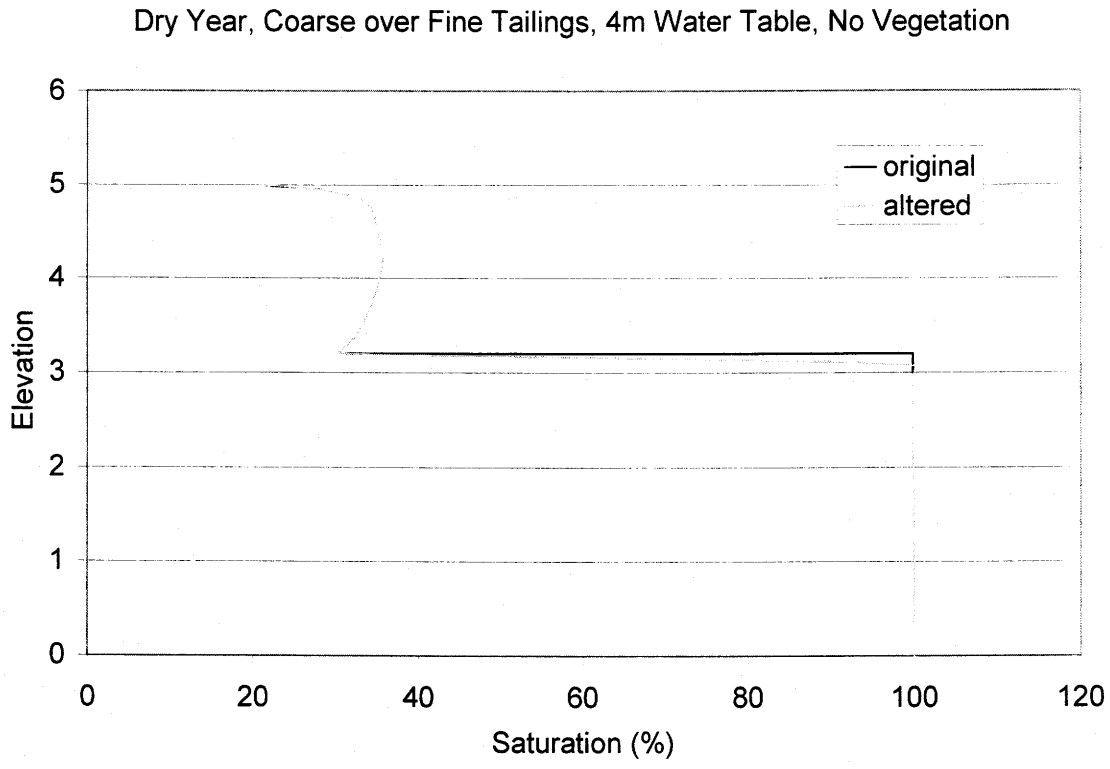
Dry Year, Coarse over Fine Tailings, 4m Water Table, No Vegetation
original
altered
Elevation
Saturation (%)
0
1
2
3
4
5
6
0
20
40
60
80
100
120

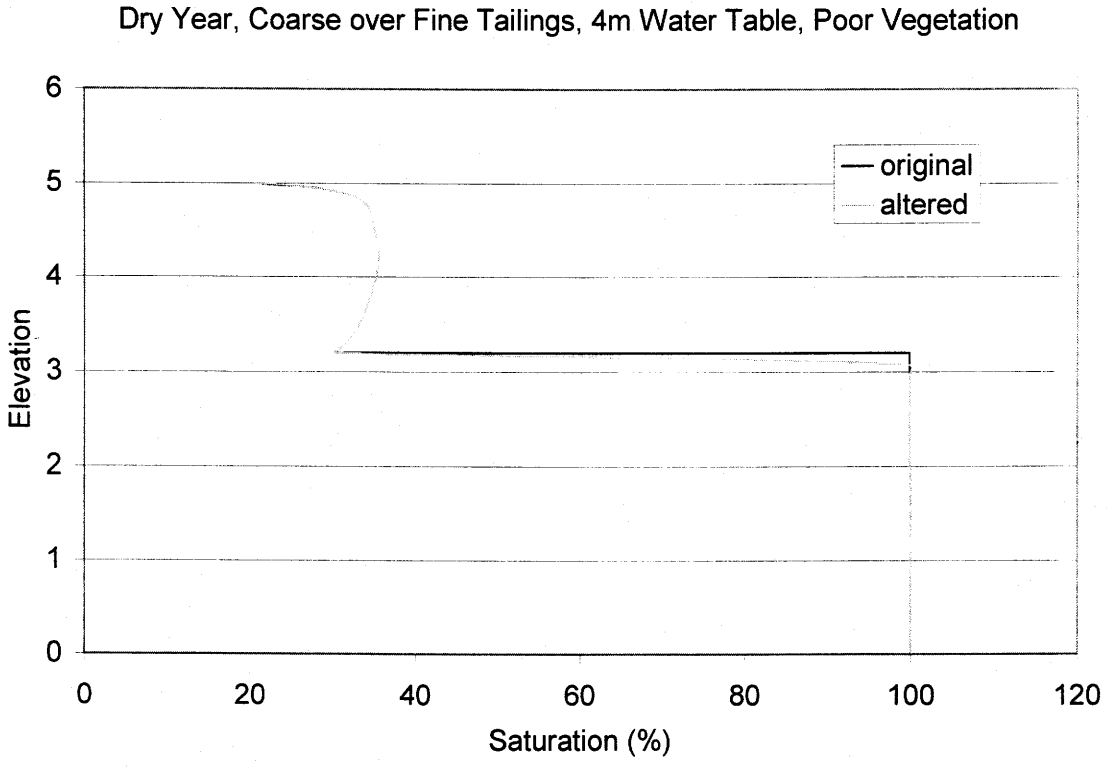
Dry Year, Coarse over Fine Tailings, 4m Water Table, Poor Vegetation
original
altered
Elevation
Saturation (%)
0
1
2
3
4
5
6
0
20
40
60
80
100
120

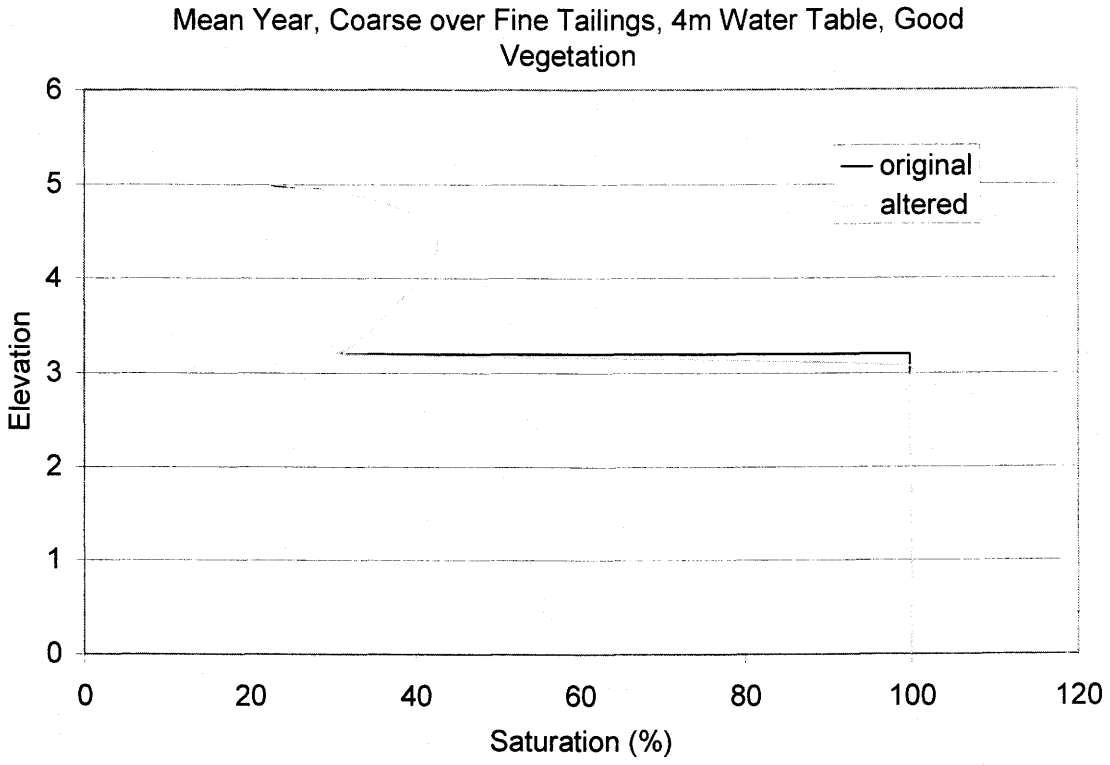
Mean Year, Coarse over Fine Tailings, 4m Water Table, Good Vegetation
original
altered
Elevation
Saturation (%)
0
1
2
3
4
5
6
0
20
40
60
80
100
120

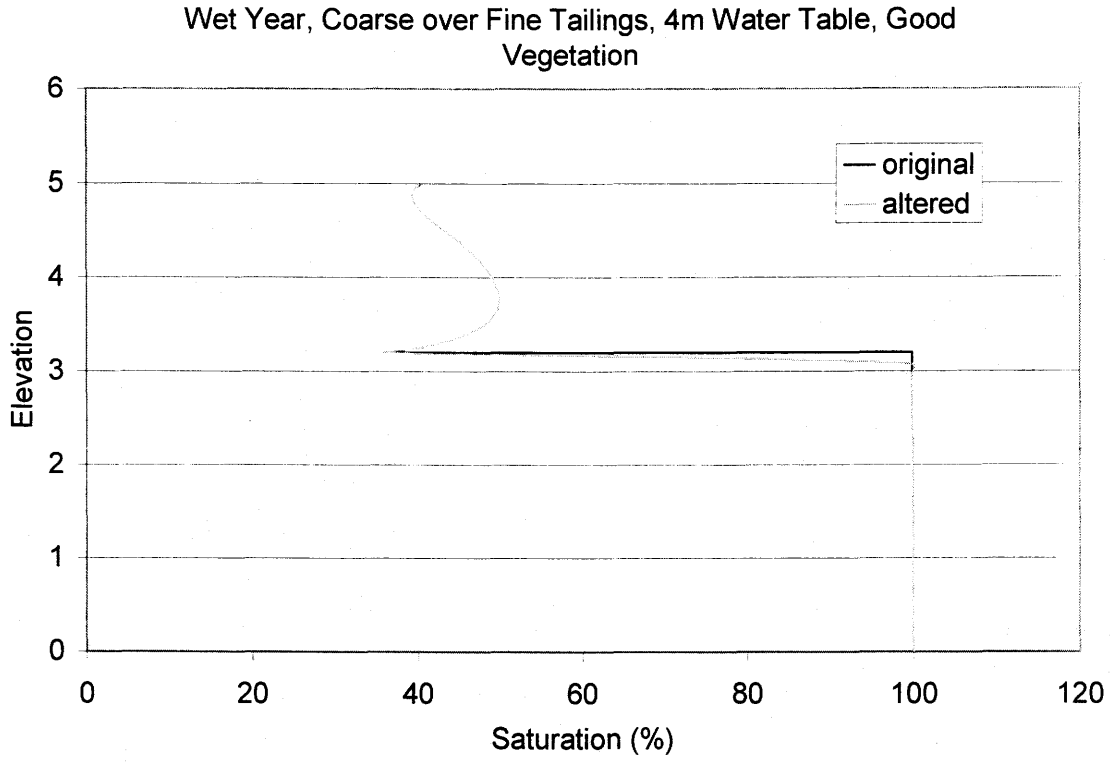
Wet Year, Coarse over Fine Tailings, 4m Water Table, Good Vegetation
original
altered
Elevation
Saturation (%)
0
1
2
3
4
5
6
0
20
40
60
80
100
120

Appendix D: Grain-size Distributions

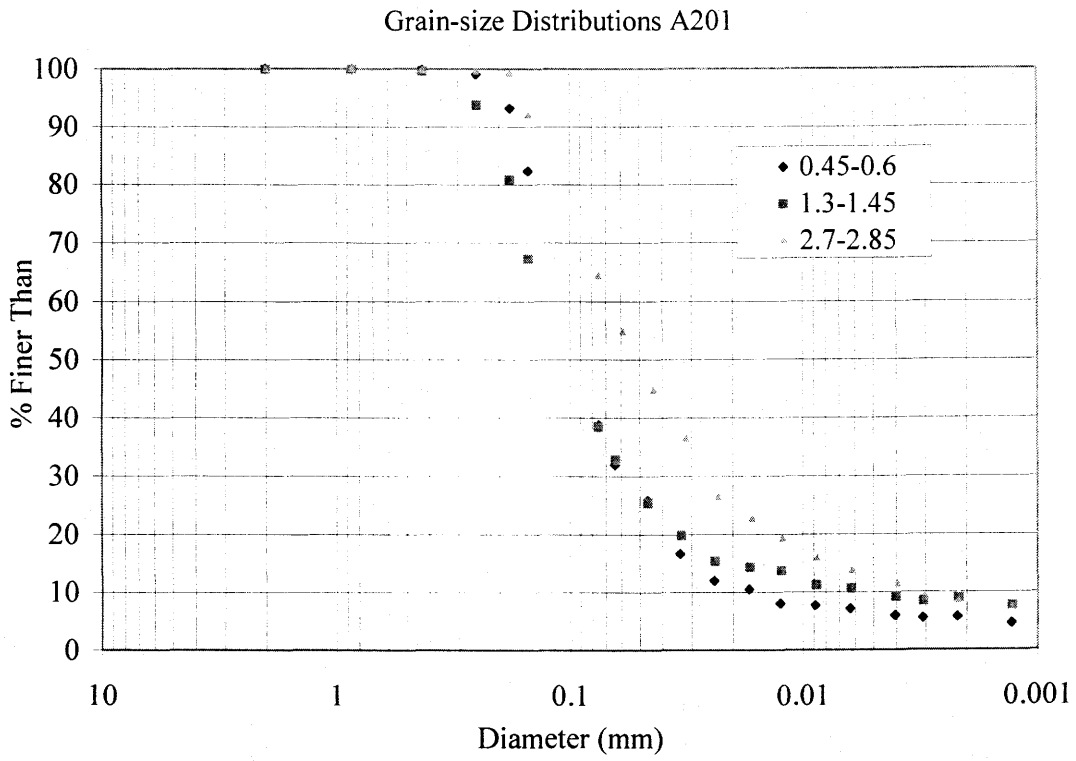

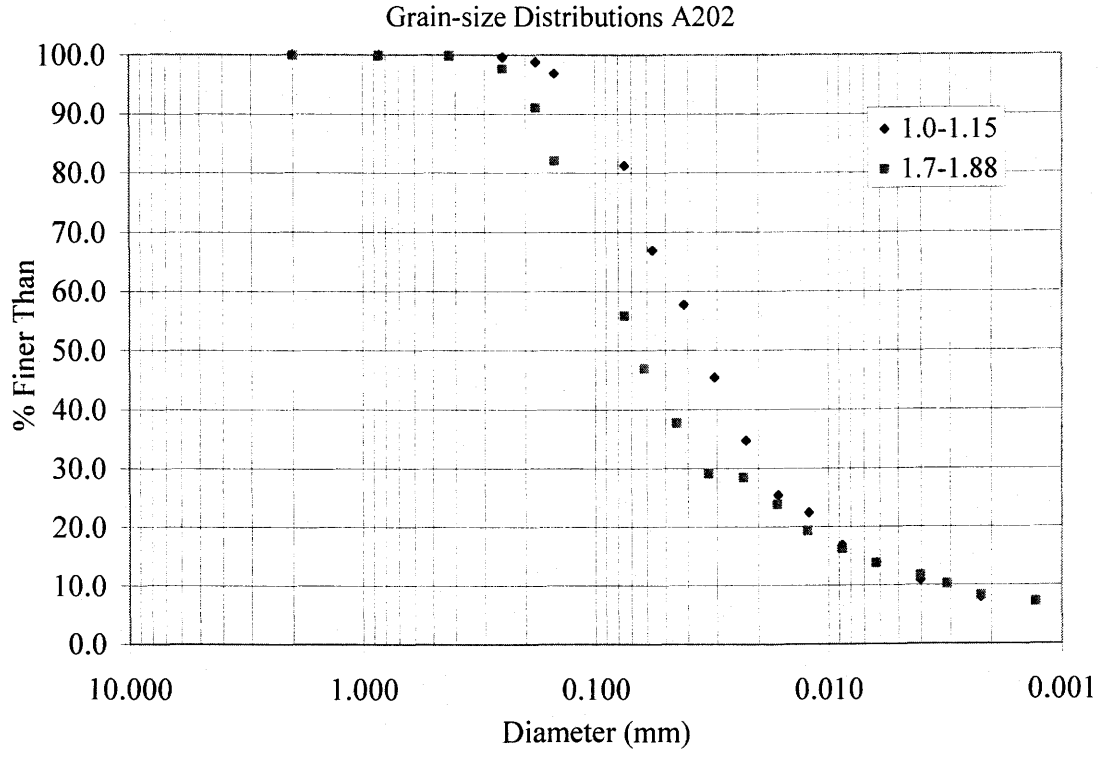

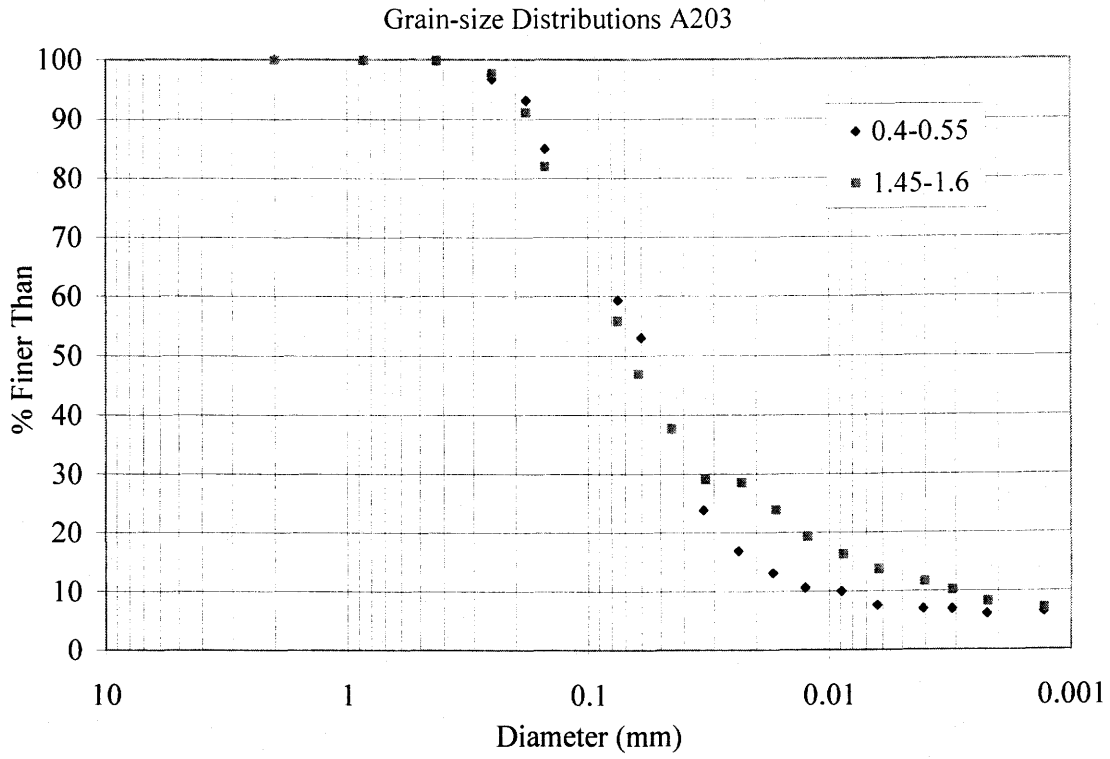
Grain-size Distributions A203
100
90
80
70
60
50
40
30
20
10
0
% Finer Than
0.4-0.55
1.45-1.6
10
1
0.1
0.01
0.001
Diameter (mm)

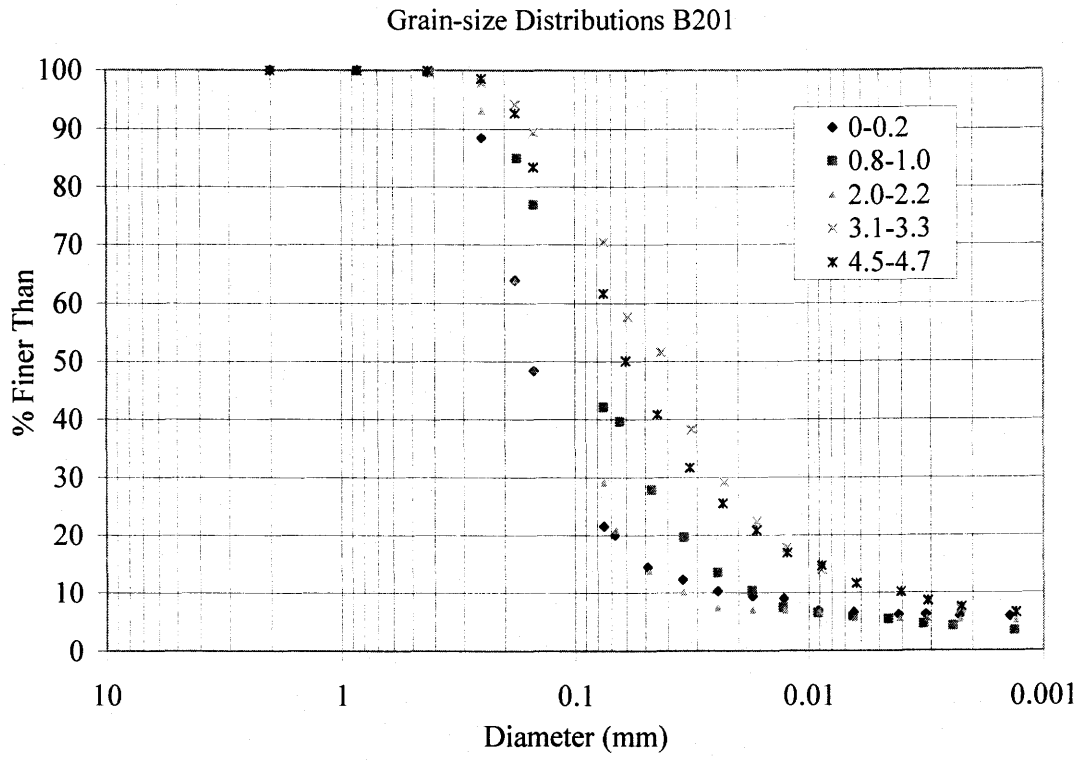
Grain-size Distributions B201
100
90
80
70
60
50
40
30
20
10
0
% Finer Than
0-0.2
0.8-1.0
2.0-2.2
3.1-3.3
4.5-4.7
10
1
0.1
0.01
0.001
Diameter (mm)

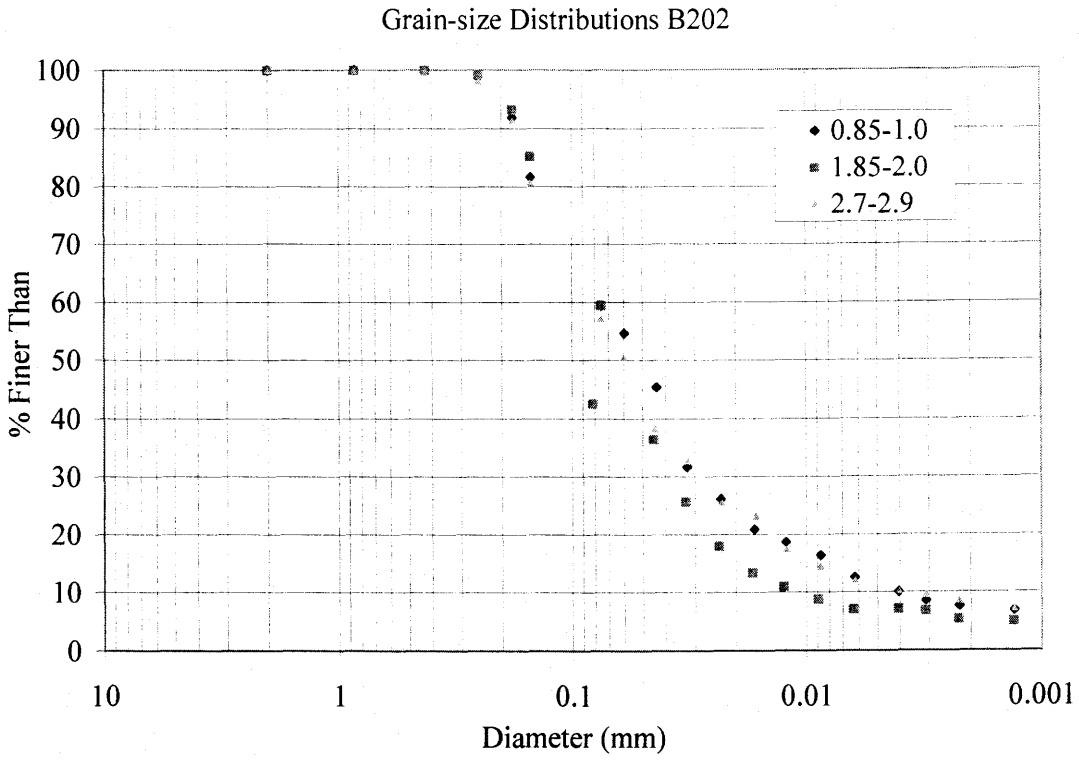
Grain-size Distributions B202
100
90
80
70
60
50
40
30
20
10
0
% Finer Than
0.85-1.0
1.85-2.0
2.7-2.9
10
1
0.1
0.01
0.001
Diameter (mm)

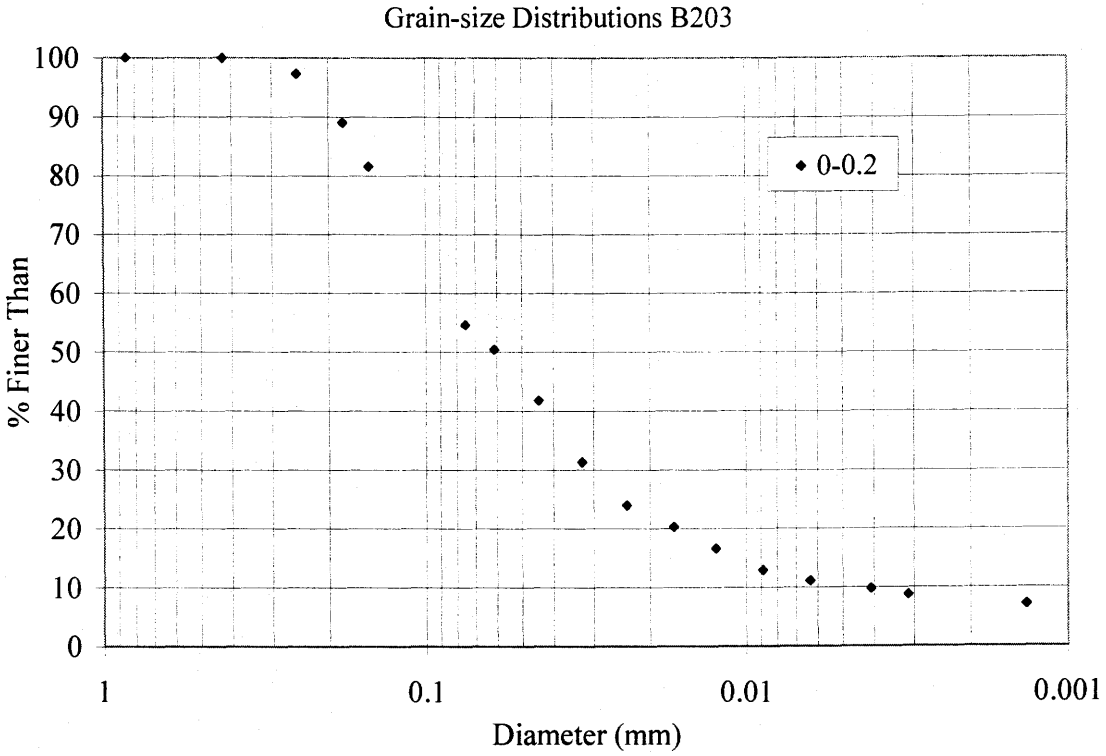
Grain-size Distributions B203
100
90
80
70
60
50
40
30
20
10
0
% Finer Than
0-0.2
1
0.1
0.01
0.001
Diameter (mm)

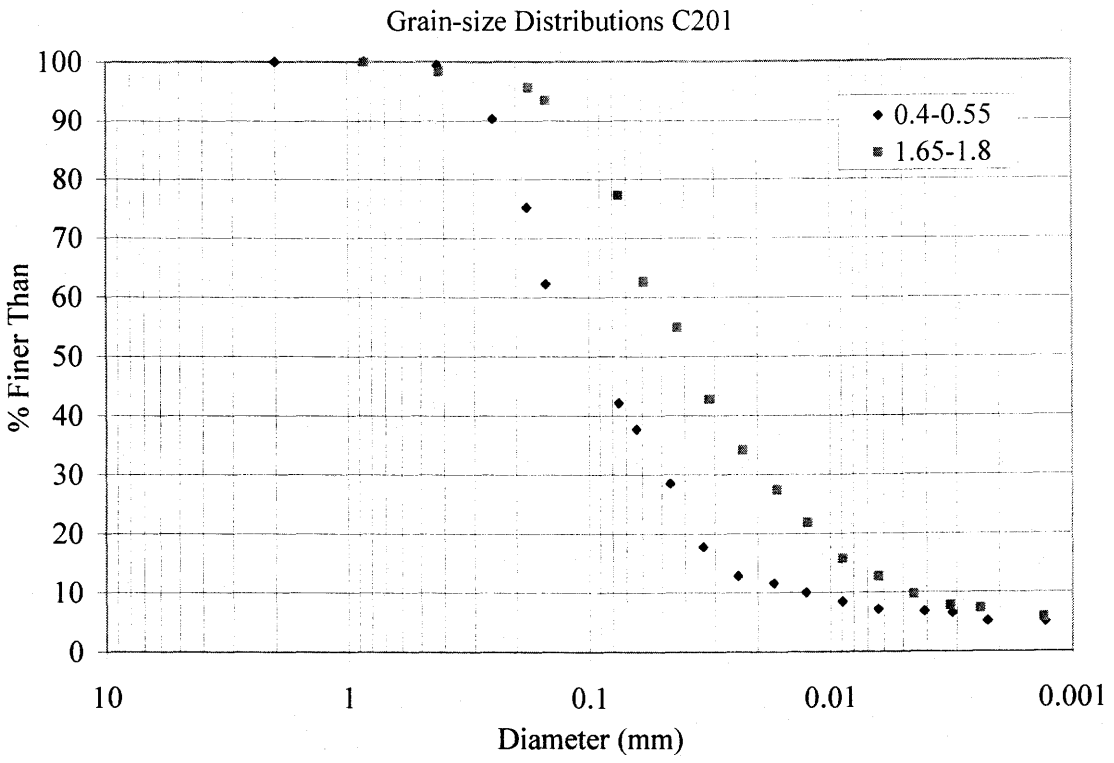
Grain-size Distributions C201
100
90
80
70
60
50
40
30
20
10
0
% Finer Than
0.4-0.55
1.65-1.8
10
1
0.1
0.01
0.001
Diameter (mm)

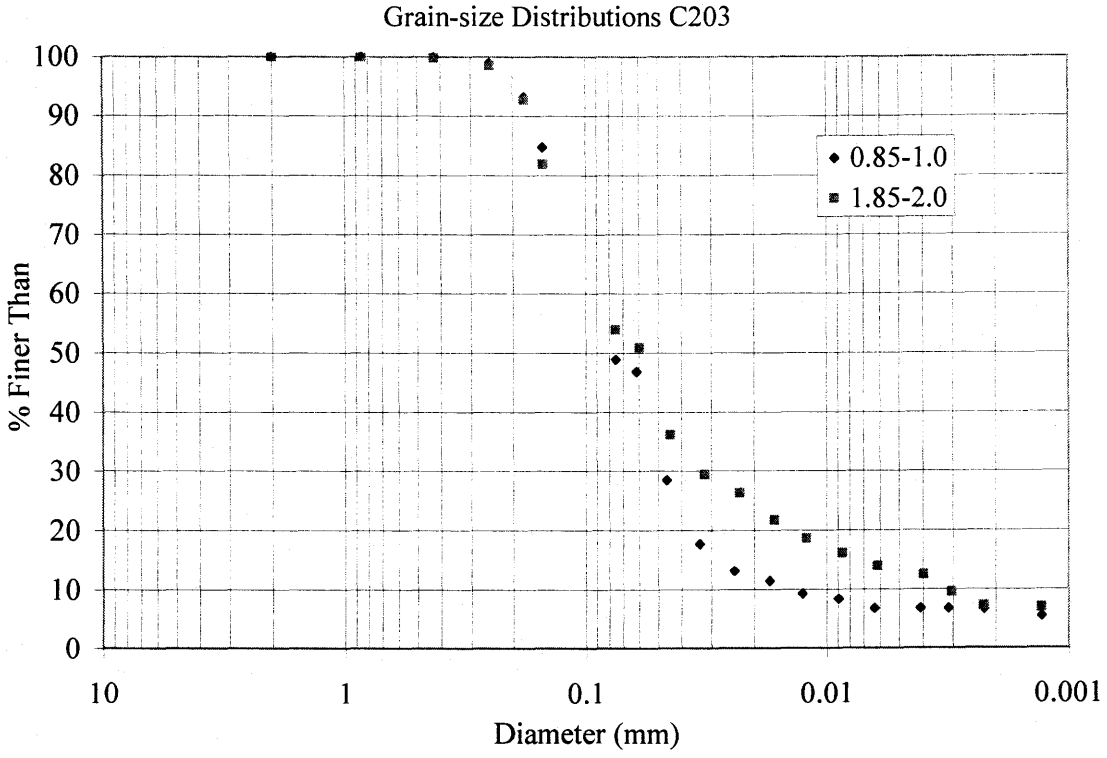
Grain-size Distributions C203
100
90
80
70
60
50
40
30
20
10
0
% Finer Than
0.85-1.0
1.85-2.0
10
1
0.1
0.01
0.001
Diameter (mm)

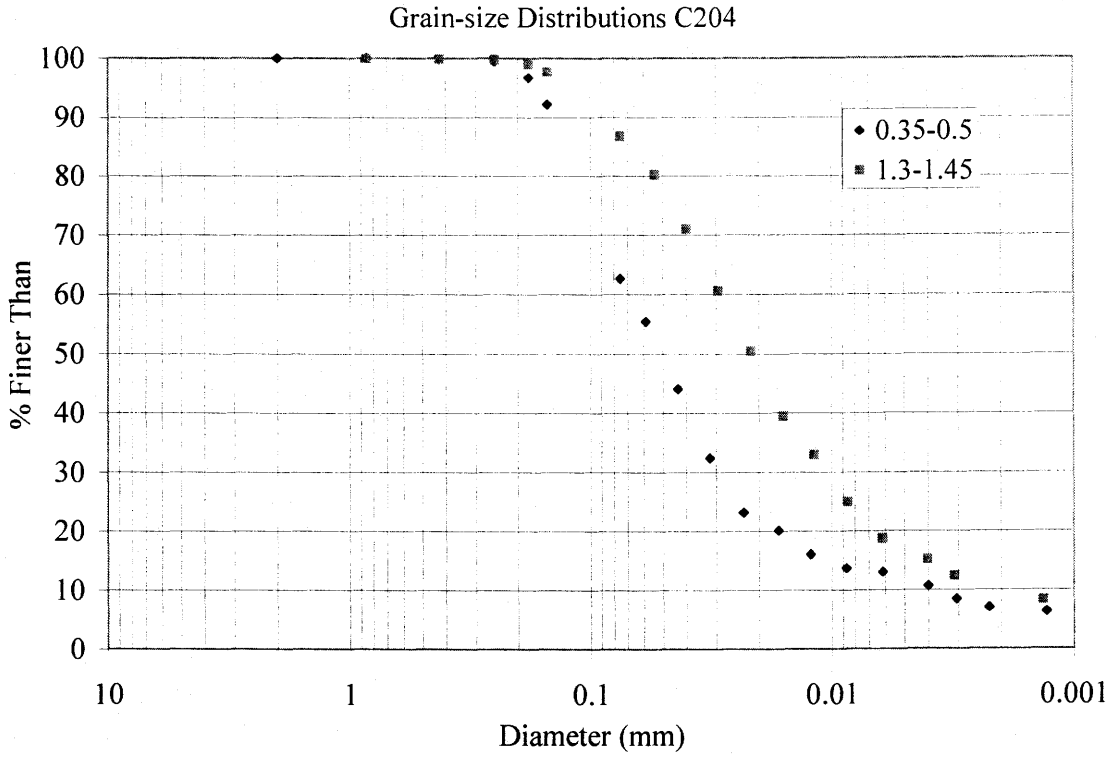
Grain-size Distributions C204
100
90
80
70
60
50
40
30
20
10
0
% Finer Than
10
1
0.1
0.01
0.001
Diameter (mm)
0.35-0.5
1.3-1.45